2017

Imaging Pain And Brain Plasticity: A Longitudinal Structural Imaging Study

James Hart Bishop
University of Vermont

IMAGING PAIN AND BRAIN PLASTICITY: A LONGITUDINAL STRUCTURAL IMAGING STUDY

A Dissertation Presented

by

James Hart Bishop

to

The Faculty of the Graduate College

of

The University of Vermont

In partial Fulfillment of the Requirements
For the Degree of Doctor of Philosophy
Specializing in Neuroscience

October, 2017

Defense Date: August 4, 2017
Dissertation Examination Committee:

Magdalena R. Naylor, M.D., Ph.D., Advisor
Helene M. Langevin, M.D., Co-Advisor
Donna M. Rizzo, Ph.D., Chairperson
Richard Watts, Ph.D.
Hugh Garavan, Ph.D.
Cynthia J. Forehand, Ph.D., Dean of the Graduate College

ABSTRACT

Chronic musculoskeletal pain is a leading cause of disability worldwide yet the mechanisms of chronification and neural responses to effective treatment remain elusive. Non-invasive imaging techniques are useful for investigating brain alterations associated with health and disease. Thus the overall goal of this dissertation was to investigate the white (WM) and grey matter (GM) structural differences in patients with musculoskeletal pain before and after psychotherapeutic intervention: cognitive behavioral therapy (CBT). To aid in the interpretation of clinical findings, we used a novel porcine model of low back pain-like pathophysiology and developed a post-mortem, *in situ*, neuroimaging approach to facilitate translational investigation.

The first objective of this dissertation (Chapter 2) was to identify structural brain alterations in chronic pain patients compared to healthy controls. To achieve this, we examined GM volume and diffusivity as well as WM metrics of complexity, density, and connectivity. Consistent with the literature, we observed robust differences in GM volume across a number of brain regions in chronic pain patients, however, findings of increased GM volume in several regions are in contrast to previous reports. We also identified WM changes, with pain patients exhibiting reduced WM density in tracts that project to descending pain modulatory regions as well as increased connectivity to default mode network structures, and bidirectional alterations in complexity. These findings may reflect network level dysfunction in patients with chronic pain.

The second aim (Chapter 3) was to investigate reversibility or neuroplasticity of structural alterations in the chronic pain brain following CBT compared to an active control group. Longitudinal evaluation was carried out at baseline, following 11-week intervention, and a four-month follow-up. Similarly, we conducted structural brain assessments including GM morphometry and WM complexity and connectivity. We did not observe GM volumetric or WM connectivity changes, but we did discover differences in WM complexity after therapy and at follow-up visits.

To facilitate mechanistic investigation of pain related brain changes, we used a novel porcine model of low back pain-like pathophysiology (Chapter 6). This model replicates hallmarks of chronic pain, such as soft tissue injury and movement alteration. We also developed a novel protocol to perform translational post-mortem, *in situ*, neuroimaging in our porcine model to reproduce WM and GM findings observed in humans, followed by a unique perfusion and immersion fixation protocol to enable histological assessment (Chapter 4).

In conclusion, our clinical data suggest robust structural brain alterations in patients with chronic pain as compared to healthy individuals and in response to therapeutic intervention. However, the mechanism of these brain changes remains unknown. Therefore, we propose to use a porcine model of musculoskeletal pain with a novel neuroimaging protocol to promote mechanistic investigation and expand our interpretation of clinical findings.

CITATIONS

Materials from this dissertation have been published in the following form:

Lichenstein S*, Bishop J*, Verstynen T, Yeh FC.. (2016). Diffusion capillary phantom vs. human data: outcomes for reconstruction methods depend on evaluation medium. Frontiers in Neuroscience, 10:407.
*Co-First Authors – Authors contributed equally to this manuscript

Bishop J, Fox J, Maple R, Loretan C, Badger G, Henry S, Vizzard M, Langevin H.. (2016). Ultrasound evaluation of the combined effects of thoracolumbar fascia injury and movement restriction in a porcine model. PLoS One, 11(1):e0147393.

DEDICATIONS

This dissertation is dedicated in loving memory to two of my grandparents for being tremendous role models in my life and inspiring me to follow my dreams and aspirations.

William ‘Bill’ Bishop

Roy ‘Nippy’ Provost

ACKNOWLEDGEMENTS

My path in science has been convoluted and not without a few bumps and bruises along the way. I have had tremendous support from my mother, Sherry Lavigne, and father, Bill Bishop, as well as from my step-father, Steve Lavigne, and step-mother Nancy Bishop. I attribute much of where I am today to their love, support, and guidance. I am also blessed to have wonderful grandparents: Capian Kelley, Roy 'Nippy' Provost, Ann Gay Bishop, William 'Bill' Bishop, Edward Lavigne, and Bonnie Lavigne. Each and every one of you have been pivotal in my success and have provided years of wisdom and guidance when I needed it the most.

I also owe a special tribute to my wonderful girlfriend, Estelle Spear, for spending countless hours helping me with challenging coursework, editing, and general scientific discussions over the years. Above all, she is a wonderful partner and together we have been privileged enough to share countless memories beyond science during our time in Vermont.

In addition to family, I am very fortunate for the wonderful mentors who have supported my training. I owe much of my interest in research to Drs. David Borsook and Lino Becerra at Harvard Medical School who have been instrumental in guiding me through the scientific career path. At the University of Vermont, my advisor, Dr. Magdalena Naylor has been a strong voice on my behalf since the time I applied to the program. I am thankful for her generosity and encouragement in my academic endeavors including additional coursework, intensive teaching roles, and lengthy fellowships that sometimes kept me away from the lab. I would also like to thank Dr. Helene Langevin at the University of Vermont, for her guidance and mentorship. I sincerely appreciate the trust she placed in me, and the opportunity that she afforded me to speak on her behalf at an international conference, in addition to the support she offered me throughout the years to facilitate my independent scientific inquiries. My dissertation committee, Drs. Donna Rizzo, Richard Watts, and Hugh Garavan have provided excellent feedback and recommendations while also encouraging me to explore an array of scientific interests.

I am grateful for all of the support and guidance over the years from Dr. Marina Shpaner. I would also like to thank the dedicated undergraduate researchers in the Naylor lab, namely Antoni Kubicki, Sarah Clements, and many others over the years for their help in all facets of the scientific process. I am grateful to the UVM NGP faculty and personnel for their support and desire to see that each and every student succeeds. Specifically, I would like to thank Carrie Perkins for tirelessly putting up with all of my questions and concerns. Thank you, Dr. Tony Morielli for promoting academic flexibility and facilitating academic interests well beyond UVM.

TABLE OF CONTENTS

LIST OF FIGURES

LIST OF TABLES

CHAPTER 1: COMPREHENSIVE LITERATURE REVIEW

Introduction

Musculoskeletal pain is a debilitating condition affecting as many as 13.5-47% of the population. In up to 24% of those patients, symptoms will persist for longer than three months, at which point the condition is termed chronic pain (Cimmino, Ferrone, & Cutolo, 2011). Pain disorders pose a substantial financial and economic burden globally and are attributed to the greatest decrease or loss of function in individuals less than 45 years of age (Frymoyer, 1988; Johannes, Le, Zhou, Johnston, & Dworkin, 2010). Moreover, chronic pain is a leading cause of physician visits annually (L. G. Hart, Deyo, & Cherkin, 1995).

Pain is comprised of complex components: sensory – nociception, emotional – affective, and cognitive – evaluative. The multifactorial nature of chronic pain conditions, not only affects peripheral tissues but also has profound influence on the central nervous system (CNS). Here, a broad review of the literature has been conducted to discuss chronic pain genesis, beginning with microscopic changes that influence neuronal excitability in the peripheral nervous system (PNS) and CNS that lead to potential macroscopic anatomical changes in brain structure. Next, a comprehensive introduction of pain neurocircuitry and endogenous gating systems is presented to expose the potential efficacy of mindfulness-based interventions such as cognitive behavioral therapy (CBT) to treat clinical chronic pain conditions.

The complexity of pain and diversity of systems involved are likely reasons why modern medical techniques, such as surgery and pharmacological therapies, have remained insufficient. Pharmaceutics such as opioids, simply mask pain symptoms while posing a

significant risk of dependency through prolonged usage. The risk of addiction coupled with the lack of long term-efficacy makes these medications less than ideal for chronic pain applications. Behavioral approaches, such as CBT, are encouraging alternatives that provide longstanding, cost effective treatment without inherent risks or side effects. Several published studies exhibit the effectiveness of CBT to treat and reduce pain symptoms, improve quality of life, and enhance global functioning of chronic pain patients (as reviewed by (Hatchard, Lepage, Hutton, Skidmore, & Poulin, 2014)). The mechanisms and potential neural plasticity underlying the effectiveness of CBT remain elusive, however, it has been speculated that top-down circuitry under cognitive control may play a critical role. Non-invasive neuroimaging methods such as magnetic resonance imaging (MRI) provide the ideal toolbox to longitudinally evaluate pain patients before and after therapy.

Functional changes in the chronic pain brain have been reported extensively throughout the literature (Kregel et al., 2015; Malfliet et al., 2017; Martucci, Ng, & Mackey, 2014) yet there are conflicting reports of the grey matter (GM) structural alterations, and those in the white matter (WM) remain understudied and poorly understood. The research described in this dissertation is broadly relevant to the chronic pain field because it expands upon our understanding of structural changes in the chronic pain brain and potential neuroplasticity associated with successful CBT intervention.

While pain attenuation and alleviation of pain is the ultimate clinical objective, the use of MRI to evaluate patients provides minimal insight into the cellular mechanisms associated with the condition. These limitations can be mediated to some extent by advanced neuroimaging techniques that allow for investigation of GM and WM microstructural changes. However, better understanding of pain pathophysiology could

define the usefulness of currently available therapies and improve treatment through the development of novel ones. Because the location, duration, and intensity of pain in clinical populations are heterogeneous, translational animal models of pain are essential for true mechanistic understanding of chronic pain genesis, brain alterations, and plasticity following treatment.

When possible, parallel pre-clinical experiments add to the interpretability of clinical results. Complementary to clinical experiments presented in this dissertation, a novel porcine model of musculoskeletal pain pathophysiology is introduced. Moreover, we define a framework to conduct neuroimaging experiments in this animal model that are analogous to our clinical MRI. This translational model not only reproduces the peripheral pathophysiology observed in clinical low back pain patients, but it also enables histological investigation of altered brain structure reported in chronic pain populations.

Overview of Pain Systems

Chronic musculoskeletal pain (CMP) may originate from insult to anatomical structures including muscle, bone, tendons, ligaments, fascia and nerves (Bishop et al., 2016; Dieppe, 2013; Langevin et al., 2011; Ren & Dubner, 2008) although many sufferers present with pain of unknown etiology. Pain receptors, termed nociceptors, that are located throughout the body transmit pain signals to the spinal cord via peripheral pain fibers. These fibers synapse with ascending corticobulbar and corticospinal tracts that directly relay the incoming information to the thalamus, hypothalamus, and amygdala. Endogenous mechanisms regulate afferent pain signaling at various levels via descending pathways that originate throughout the brain and brainstem. Ultimately, the consciousness of pain is

mediated by a neural network of higher order brain areas, termed the pain matrix, that facilitates the cognition, emotion, and appraisal of painful experiences. The pathogenesis of CMP is thought to occur following maladaptive potentiation of a positive feedback loop of inflammation and sensitization that culminates in altered neuronal excitability and ultimately, CNS structure (Figure 1.1). This cycle of chronic pain initiates with peripheral and central sensitization, leading to neurogenic neuroinflammation, and CNS gliopathy. Below, we more thoroughly describe pain pathogenesis from the periphery to the CNS including the specific brain networks and pathways involved.

Figure 1.1 Cycle of Chronic Pain

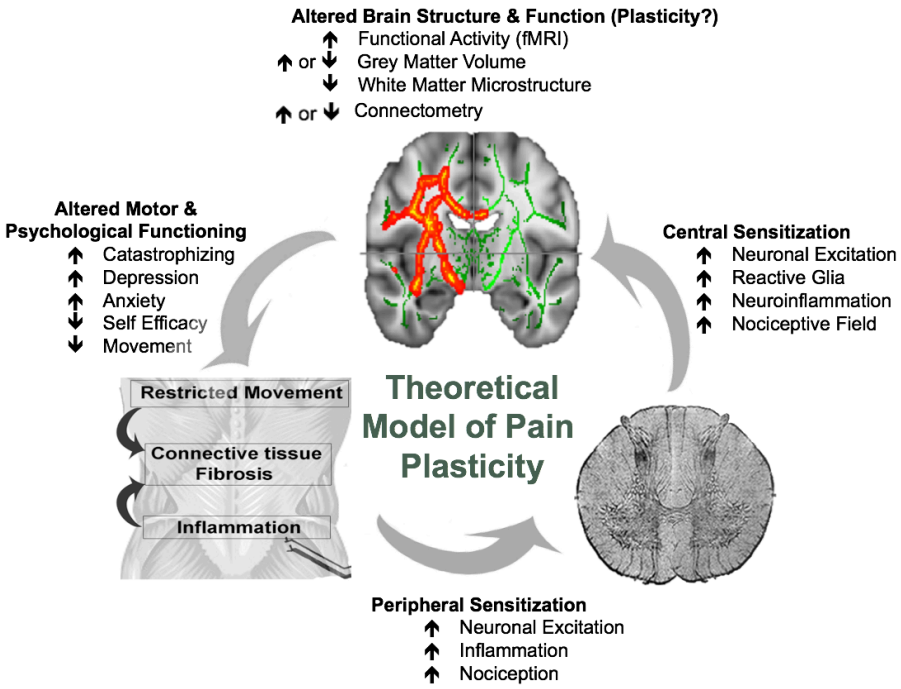

Figure 1.1. Cycle of Chronic Pain. Injury or pathology propagates sensitization changes, both peripherally and centrally, that elicit increases in neuronal excitability, glial reactivity, and inflammation that can lead to increased nociception and a broadening of the nociceptive field. Over time these hallmarks of chronic pain can potentiate structural and functional brain plasticity as well as alterations in motor functioning and maladaptive behaviors. These maladaptive traits can further manifest as increased peripheral inflammation and alterations in musculoskeletal tissues such as connective tissue fibrosis, perpetuating a vicious cycle of chronic pain. Interventions that break this cycle and diminish behavioral or cellular features of chronic pain may perpetuate dynamic changes in the brain suggestive of neuroplasticity.

Peripheral Catalysts of Altered CNS Circuitry

Under normal circumstances, tissue injury results in the recruitment, extravasation, and infiltration of innate immune cells including T cells, neutrophils, mast cells, and macrophages. This acute inflammation is a protective response following injury to aid in healing and prevent further damage. Tissue inflammation also causes a local increase of pain signaling, serving a physiologically protective function that is critical for survival. Increased sensitivity to painful stimuli is called hyperalgesia, and a painful response to normally non-painful stimuli is termed allodynia. These processes are generally resolved by an innate anti-inflammatory response, returning the system to a homeostatic state. In the case of chronic pain, a pro-inflammatory state may persist in peripheral tissues via a series of cellular cascades and signaling events (Figure 1.2).

Pro-inflammatory compounds, such as histamine and inflammatory cytokines, are released during mast cell degranulation, consequently triggering vasodilation, increased vascular permeability and stimulation of nociceptors. Primary afferent neurons are equipped with metabotropic and ionotropic receptors that respond to histamines and other inflammatory mediators. Activation of these receptors induces an intracellular release of Ca^{2+} and cyclic adenosine monophosphate (cAMP) resulting in activation of second messenger signaling factors such as kinases. Consequent nociception is caused by kinase phosphorylation and stimulation of nociceptors including the transient receptor potential cation channels (TRPV, TRPA) leading to peripheral afferent hyperexcitability and hypersensitivity: this is known as peripheral sensitization.

Peripheral sensitization results in a persistent state of inflammation and nociception, and is a catalyst of chronic pain pathology. This pain response may contribute

to prolonged hyperalgesia and allodynia through dysregulation of primary afferent neurons. In response to stimulation, the peripheral terminus of pain fibers potentiates hyperexcitability and propagates neurogenic inflammation by releasing neuropeptides such as substance P, calcitonin gene-related peptide (CGRP) and brain-derived neurotrophic factor (BDNF). The release of inflammatory mediators in turn produces adjacent vasodilation, ensuing an infiltration of mast cells, and release of histamine. This can lead to broadening of the nociceptive field, termed secondary hyperalgesia, that further propagating pain signaling.

Other factors such as post-transcriptional and translational modifications can lead to upregulation and transport of peripheral nociceptors (Woolf & Costigan, 1999). These molecular processes affect channel kinetics by lowering excitability thresholds. For example, TRPV1, a nociceptor responsible for heat pain sensation, is typically activated by a stimulus of >42°C, however, following peripheral sensitization, stimuli of <40°C can elicit activation (Andrew & Greenspan, 1999; Woolf & Salter, 2000). As a result of increased nociception, prolonged glutamate release in the dorsal horn of the spinal cord mediates AMPA and NMDA receptor activity leading to central sensitization (Xanthos & Sandkuhler, 2014).

Central Sensitization and Neuroinflammation: A Gateway to Altered CNS Activity

Central sensitization is a phenomenon underlying synaptic plasticity and pain hypersensitivity. Action-potential dependent activity (Ji, Kohno, Moore, & Woolf, 2003) and inflammation (Ji, Berta, & Nedergaard, 2013; Xanthos & Sandkuhler, 2014) each contribute to central sensitization independently, however increasing literature supports a

combination of these factors in chronic pain states. Activity-dependent central sensitization is a result of neuronal processes termed windup and long-term potentiation (LTP). In windup, multiple subthreshold stimuli summate on a neuron to produce extended suprathreshold events, exacerbated by additional repetitive stimuli. In this process, normally innocuous stimuli may become noxious. LTP-like central sensitization shares many similarities to LTP responsible for memory consolidation. In chronic pain states, LTP occurs when an increase in primary afferent signaling stimulates heightened glutamate neurotransmitter release in the dorsal horn of the spinal cord. Glutamate binds and activates a variety of receptor subtypes on the dorsal horn neurons such as AMPA, mglu, and NMDA. Receptor stimulation causes intracellular Ca^{2+} release that further activates protein messengers including phospholipid-dependent protein kinase C (PKC). PKC is important for initiating multiple intra-neuronal cascades such as recruitment of AMPA receptors to the synapse, phosphorylation of the NMDA receptor to remove the Mg^{2+} block, and stimulation of extracellular-signal-regulating kinase (ERK) to phosphorylate and activate K^{+} channels. This increased glutamate signaling stimulates an upregulation of AMPA receptors, further increasing neuronal excitability in the spinal cord (Latremoliere & Woolf, 2009).

Figure 1.2 Peripheral Sensitization and Neurogenic Inflammation Following Injury

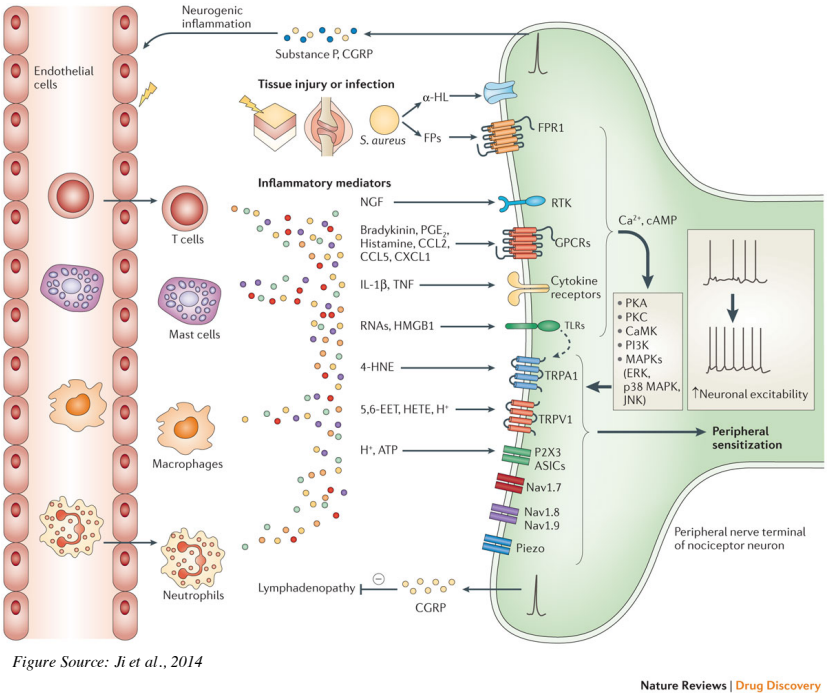

Figure 1.2. Peripheral Sensitization and Neurogenic Inflammation Following Injury. Inflammatory mediators activate numerous channels on the peripheral neuron. Intracellular signaling cascades lead to increased neuronal excitability, ensuing efferent flux of neuropeptides.

Central sensitization may also result from transient cytokine signaling in the CNS (Samad et al., 2001). Inflammatory cytokines are released into humoral circulation at the site of an injury following the cascade of peripheral sensitization and neurogenic inflammation (Ji, Xu, & Gao, 2014). These molecules can travel systemically and may act on endothelial cells in the cerebrovasculature. Cytokine-endothelial interactions induce pro-inflammatory interleukin-1β (IL-1β) release in the CNS, and can activate astrocytes and microglia (DeLeo & Yezierski, 2001). These signaling events can affect numerous genes encoding for receptor expression, neuronal excitability, and signal transduction, further contributing to pain pathology (Costigan & Woolf, 2002). The primary nociceptive fibers themselves secrete inflammatory neuropeptides (substance P, CGRP, BDNF) from

their central terminus directly into the spinal cord. This process is termed neurogenic neuroinflammation and is homologus to the release of neuropeptides in the periphery.

It is out of the scope of this dissertation to investigate the specific mechanisms driving peripheral and central sensitization. However, the importance of understanding these is to provide a cellular and molecular groundwork that summates to induce morphological and functional changes in the chronic pain brain that are detectable with MRI. In summary, chronic pain genesis results in altered excitability of peripheral and central neurons, respectively termed peripheral and central sensitization. Sensitization subsequently facilitates changes in the CNS glial cells that further influence neural circuitry and architecture.

Pain Related Changes in Neuroglia: Gliopathy

Non-neuronal cells, termed neuroglia, which include microglia, astrocytes, and oligodendrocytes in the CNS, have been implicated in chronic pain sensitization and maintenance. Microglia and astrocytes communicate directly with neurons and may influence neuronal activity and pain hypersensitivity by modulating synaptic strength (Ren & Dubner, 2008), promoting inflammation (Skaper, Facci, & Giusti, 2014), regulating the extracellular environment (Haroon, Miller, & Sanacora, 2017), modulating chemokine signaling (Gao & Ji, 2010) and influencing myelination (Ishibashi et al., 2006). Glial abnormalities have also been identified as key players in mood disorders (Ongur, Bechtholt, Carlezon, & Cohen, 2014; Schroeter et al., 2010) and cognitive impairment (Chung, Welsh, Barres, & Stevens, 2015). Oligodendrocytes are the major myelinating cells of the CNS and are thought to maintain malleability throughout adulthood and are

affected by action-potential signaling (Chang, Redmond, & Chan, 2016; Fields, 2008a, 2008b; Pajevic, Basser, & Fields, 2014). Due to their potential role in GM and WM neuroplasticity; microglia, astrocytes, and oligodendrocytes will be addressed in depth in the following sections.

Microglia

Under non-pathological conditions, microglia, the macrophage-like cells of the CNS, are found throughout the brain and spinal cord in a quiescent state where they continually monitor their environment. Chronic pain-induced peripheral and central sensitization initiates a prolonged depolarization in the dorsal horn of the spinal cord that stimulates these cells to become reactive or non-quiescent. Consequently, expression and release of chemoattractants from the central process of the primary afferents propagates microglia proliferation, chemotaxis, and cytokine release (Ellis & Bennett, 2013). Reactive microglia undergo morphological changes, in addition to evoking numerous pro- and anti-inflammatory signaling pathways. Pro-inflammatory signaling factors regulated by reactive microglia are particularly important to pain induction: these include cathepsin S, involved in downstream cleavage and release of fractalkine, BDNF, and IL-1β. Willemen and colleagues demonstrate that persistent inflammation downregulates G-protein-coupled receptor kinase (GRK2) in microglia. This prevents microglia inactivation and facilitates transition from acute to chronic inflammatory pain by prolonging the release of inflammatory molecules (Willemen et al., 2010).

Pharmacological studies show that inhibiting microglia activity sufficiently diminishes inflammatory, neuropathic, and postoperative pain, providing additional

evidence that chronic pain states may result from gliopathy (Beggs, Currie, Salter, Fitzgerald, & Walker, 2012; Hains & Waxman, 2006; Hua et al., 2005; Ji et al., 2013). Reactive microglia also alter neural structure and function by engulfing dysfunctional synapses (Kettenmann, Kirchhoff, & Verkhratsky, 2013; Tremblay et al., 2011). Microglia activation provides a significant marker of pathology, leading to changes in cell morphology and alterations in synaptic density. These influences serve a potential mechanism that could lead to the changes in GM structure observed in chronic pain populations. Furthermore, activated microglia change morphologically, by increasing in volume and quantity and may facilitate changes in WM microstructure by altering the packing density of the tracts.

Astrocytes

Astrocytes maintain an important role in neuron-glia communication by surrounding both synapses and nodes of Ranvier (Ji et al., 2013). Other important homeostatic functions of astrocytes include synaptic regulation such as formation, elimination, and plasticity (Eroglu & Barres, 2010). These connections facilitate intercellular signaling of ions such as Ca^{2+} and regulate neuronal environment following synaptic transmission. Intracellular Ca^{2+} signaling feedback can promote release of glial transmitters, affecting neuronal activity and synaptic strength. It is known that astrocytes are important for potassium (K^+) homeostasis, suggesting that alterations in K^+ regulation could influence network excitability by changing resting membrane potentials.

Astrocytes are dispersed widely throughout the brain and when activated, they increase in size, number, and protein expression. Studies have shown that astrocyte

proliferation, particularly within the spinal cord, is associated with increased pain (G. Chen et al., 2014). Further research in a rat model revealed that reactive astrocytes in both the brainstem and anterior cingulate cortex (ACC) contributed to affective pain symptoms. Administration of an astrocytic toxin attenuated affective pain behavior (F. L. Chen et al., 2012). This suggests that reactive astrocytosis could account for global morphological and functional changes in the pain matrix.

In summary, astrocytes maintain a critical role in CNS structure and function via synaptic regulation. Due to the profound increase in neuronal excitability that occurs in chronic pain states, reactive astrocytes proliferate and change morphologically, yielding a potential mechanism leading to altered GM volume and density in pain matrix structures. These morphological changes may also be responsible for the observed WM neuroimaging findings often reported in the literature by altering the organization and packing density of WM tracts. Furthermore, astrocytes may influence WM myelination properties by releasing signaling factors onto oligodendrocytes in an action-potential dependent manner (Ishibashi et al., 2006; Lee & Fields, 2009).

Oligodendrocytes / Oligodendrocyte Precursor Cells

Specialized neuroglia in the CNS known as oligodendrocytes are responsible for axon myelination. Myelin is a dielectric material primarily composed of lipids and proteins that ensheathe axons, constituting the CNS WM. It facilitates rapid neuronal communication by increasing the membrane resistance to permeable ions, allowing electrical signals to propagate via rapid saltatory conduction. In humans, myelination continues from fetal development into adulthood. Recent literature suggests that myelin

structure is far from static in the adult brain, and instead undergoes dynamic remodeling and turnover (Liu et al., 2012). Remodeling is the process of altering myelin structure without replacing the oligodendrocyte, whereas turnover occurs when oligodendrocyte precursor cells (OPC) form and replace mature oligodendrocytes. There is increasing evidence that electrical activity drives myelination by synergistic signaling events between axons, astrocytes and oligodendrocytes (Chang et al., 2016; Ishibashi et al., 2006).

In brief, one mechanism of oligodendrocyte plasticity occurs when adenosine triphosphate (ATP) escapes from axons at the nodes of Ranvier following synaptic transmission and binds to astrocyte purinergic receptors (Figure 1.3). In response, astrocytes secrete Leukemia inhibitory factor (LIF), a cytokine that has been linked to myelination changes in oligodendrocytes (Lee & Fields, 2009). In one experiment, electrical stimulation applied to axons in co-culture with mature oligodendrocytes and astrocytes resulted in increased myelination and LIF secretion. However, blockade of LIF or purinergic receptors prevented pro-myelinating effects of electrical activity (Ishibashi et al., 2006). Contradictory to the previous study, Park and colleagues illustrate that LIF inhibited myelination (Park, Solomon, & Vartanian, 2001). The discrepancy was resolved in a set of experiments by Ishibashi and colleagues in 2006. Incremental administration of LIF in co-cultured dorsal root ganglion (DRG) neurons demonstrated that high concentrations of LIF contribute to demyelination while lower levels increase myelination. To summarize, chronic pain states alter neuronal excitability that subsequently activates astrocytes and oligodendrocytes, leading to dynamic changes in myelination. This provides a mechanism by which neural activity could modify somatosensory, cognitive, motor, and emotional WM network structure in chronic pain patients.

Figure 1.3 Activity-Dependent Myelination in Mature Oligodendrocytes

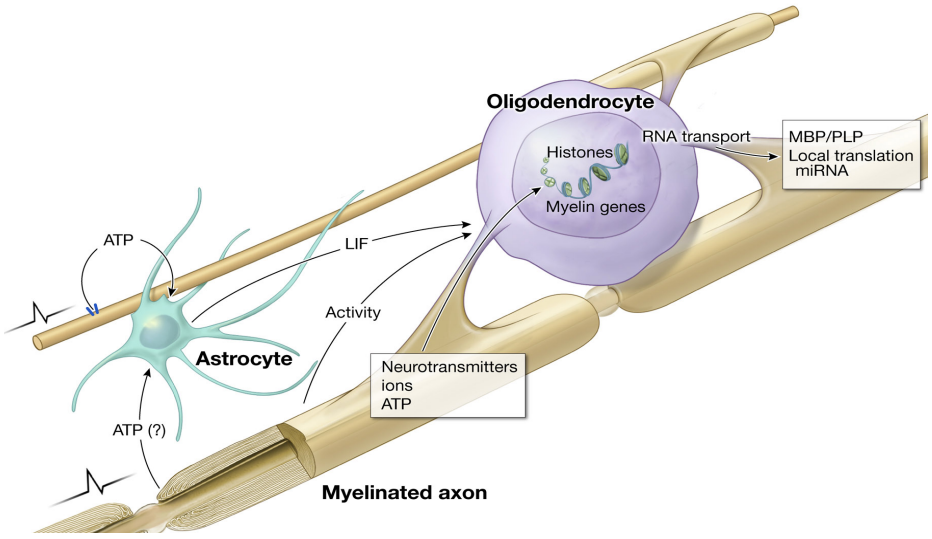

Figure Source: Adapted from Lee & Fields, 2009

Figure 1.3. Activity-Dependent Myelination in Mature Oligodendrocytes. Astrocytes uptake ATP which is released at the nodes, facilitating LIF signaling and promoting myelin alterations.

Neural Activity Induced White Matter Neuroplasticity

Dynamic changes in myelination occur in response to neural activity including motor learning, emotional, and cognitive processes (Gibson et al., 2014; Liu et al., 2012; McKenzie et al., 2014). Here, we discuss previous literature that investigates the role of each process in WM neuroplasticity.

Motor Learning

One of the first studies to demonstrate WM neuroplasticity in a healthy human brain found that juggling increased WM volume (Scholz, Klein, Behrens, & Johansen-Berg, 2009). A more eloquent study conducted in a murine model used optogenetic technology to illustrate the potential of electrical signaling to initiate changes in oligodendrocyte and OPC activation states (Gibson et al., 2014). In this study, the authors utilized optical

approaches to drive activation of premotor cortex (M2) neurons *in vivo*, at a rate representative of learning a complex motor task. Subsequent excitation increased cortical and subcortical myelination and the animals exhibited increased behavioral performance during a limb function task. To confirm that OPC proliferation and differentiation was responsible for the observed myelin changes, oligodendrogenesis was inhibited by pharmacological blockade with trichostatin A (TSA). Stimulation of M2 in the presence of TSA prevented myelin plasticity and diminished the behavioral enhancement of the limb task (Gibson et al., 2014). While these studies support the role of motor activity in WM neuroplasticity, it is well documented that pain patients have altered movement and motor function. Several theories of pain-related motor changes have been proposed, and these could ultimately influence neural architecture (Hodges & Tucker, 2011).

Emotional

Investigators have also shown maladaptive transformations in myelination associated with behavioral abnormalities. Liu and colleagues demonstrated hypomyelination in the adult mouse prefrontal cortex, an important center for emotional and cognitive regulation, in response to protracted social isolation (Liu et al., 2012), which could be rescued using pharmacological agents that promote oligodendrocyte differentiation (J. Liu et al., 2016). The researchers found a significant decrease in myelin thickness and gene transcripts compared to healthy control animals. These results were attenuated and reversed upon social reintegration, exemplifying epigenetic WM neuroplasticity. This study illustrates the malleability of WM continuing into adulthood and emphasizes the role of environment and behavior to drive cellular changes affecting

WM. Environmental factors and maladaptive behavioral traits are both major constituents of chronic pain. Therefore, alienation from social interactions as opposed to an enriched environment, and elevated levels of depression, anxiety, and catastrophizing could potentiate WM structural alterations in chronic pain populations.

Cognition

Cognitive impairment is frequently reported across chronic pain conditions (Moriarty, McGuire, & Finn, 2011). Factors such as stress, anxiety, mood change, sleep disturbance, and fatigue contribute to disrupted cognition in these populations (R. P. Hart, Wade, & Martelli, 2003). A number of studies have reported adverse WM alterations following cognitive impairment in the context of traumatic brain injury (Kinnunen et al., 2011), Alzheimer's Disease (Medina et al., 2006), and normal aging (Charlton et al., 2006). Few investigations have examined whether cognitive-based therapies or cognitive training has the potential to modify WM. Mackey and colleagues performed diffusion weighted imaging on students preparing for the LSAT and showed that WM tracts connecting the frontal cortices had decreased radial diffusivity (Mackey, Whitaker, & Bunge, 2012). Additionally, mindfulness meditation, a form of integrative body-mind training, showed an increase in fractional anisotropy in the superior longitudinal fasciculus, corona radiata (superior and anterior), corpus callosum and the ACC after a 4-week training period (Tang, Lu, Fan, Yang, & Posner, 2012; Tang et al., 2010). Decreased radial diffusivity and increased fractional anisotropy are metrics that are often favorably interpreted as increases in WM tract integrity. These studies suggest that cognitive-based therapies such as CBT

could be beneficial to treat WM pathologies by targeting maladaptive traits, such as anxiety and stress that are commonly associated with chronic pain conditions.

Pain Networks

The complex networks that comprise pain: sensory – nociception, emotional – affective, and cognitive – evaluative – have been shown to induce neuroplasticity in an activity dependent manner. To this point, a broad synopsis of the cellular underpinnings contributing to chronic pain genesis has been identified, that progressively encompasses the major factors that promote structural brain plasticity. Higher order pain processing involves a magnitude of functional GM regions that are intricately connected via WM tracts; together these CNS regions are termed the pain matrix. Here we highlight the anatomy of pain processing, beginning with afferent signaling into the spinal cord, continuing into higher order CNS pain matrix structures, and finally efferent signaling to the spinal cord through an endogenous descending gating system that modulates incoming nociceptive signaling. This feed-forward loop is an integral component to pain processing that can be influenced by cognitive processes and ultimately provides a non-pharmacological mechanism for behavioral interventions to treat and diminish chronic pain in clinical populations.

Ascending Pain Pathways

In the periphery, noxious stimuli or tissue damage results in the transformation of chemical or mechanical inputs into electrical signals that are primarily propagated along myelinated Aδ and unmyelinated C fibers that project to the ipsilateral dorsal horn of the

spinal cord. They are then relayed contralaterally before ascending in the anterolateral spinothalamic and spinobulbar WM tracts. The terminal projections are slightly different between these ascending pain pathways. For example, the spinothalamic tract relays nociceptive inputs to the cortex and is important for pain perception. In this tract, second-order neurons ascend in the spinal cord contralateral to the stimulus, where they synapse in thalamic nuclei. Tertiary afferent neurons that originate in the thalamus project to the anterior cingulate cortex, somatosensory, and insular cortices. Conversely, the spinobulbar tract is important for affective and intensity coding of pain. It sends ascending second-order neurons to several brainstem nuclei, including the locus coeruleus, periaqueductal grey (PAG), and parabrachial nucleus. Tertiary neurons in the parabrachial nucleus project to both the amygdala and hypothalamic subcortical structures.

The Pain Matrix

The experience and perception of pain was originally believed to reside in a single pain 'center' of the brain, but the modern consensus is that pain is a multidimensional process involving cognitive, affective, and sensory brain regions. Evolving from what was originally termed the neuromatrix, the 'pain matrix' we refer to today consists of three orders of networks.

The primary nociceptive matrix includes neural structures that receive direct innervation from the spinothalamic pathway. Its afferent innervation arises from third-order neurons that originated in posterior thalamic nuclei such as the ventral posterior, centrolateral, mediodorsal, and the posterior group nuclei (Garcia-Larrea & Peyron, 2013). These tertiary neurons project from the thalamus to the posterior insula, medial parietal operculum, and the mid-cingulate cortex. Interestingly, indirect stimulation of thalamic

nuclei projections or direct stimulation of the inner operculum or posterior insula is sufficient to elicit pain, the only known brain structures to have this effect (Mazzola, Isnard, & Mauguiere, 2006; Mazzola, Isnard, Peyron, & Mauguiere, 2012).

The transition from noxious input to pain consciousness requires additional neural networks which has been demonstrated by studies in patient populations with unresponsive wakefulness syndrome or vegetative state (Schnakers, Chatelle, Demertzi, Majerus, & Laureys, 2012). These structures include the mid and anterior insula, the anterior cingulate cortex (ACC), prefrontal cortex, posterior parietal areas, as well as the striatum, supplementary motor area, hippocampus, and temporoparietal junction. A defining feature of the second-order pain matrix in contrast to the primary, is that the former are not directly connected to afferent pain pathways. Moreover, within the second-order matrix, distinct activation patterns can be generated by context-dependent nociception. Within the brain there is substantial overlap between networks, structure, and function. This is apparent within the pain matrix as many of the second-order structures are implicated in non-noxious events, including pleasure and reward.

Additional pain matrix structures are involved in reinterpretation of pain by reappraisal, affective and emotional regulation. These structures include the perigenual cingulate cortex, orbitofrontal cortex, temporal pole, and anterolateral and dorsolateral prefrontal areas. It is postulated that these regions are the source of pain control in psychotherapies such as CBT, the placebo effect, and meditation (Bushnell, Ceko, & Low, 2013).

Descending Pain Pathways

The CNS is equipped with endogenous descending inhibitory pathways to modulate afferent spinothalamic and spinobulbar signaling. Several limbic and cognitive structures summate on brainstem nuclei that directly control descending inhibition. These brainstem nuclei include the PAG, the rostroventral medulla (RVM), and the parabrachial nucleus (PBN) (Millan, 2002). Projections travel from the brainstem via the dorsolateral funiculus of the spinal cord to the dorsal horn. Brainstem nuclei such as the RVM have dimorphic functionality including both nociceptive and anti-nociceptive capabilities (Porreca, Ossipov, & Gebhart, 2002). Studies have shown that direct stimulation of the PAG produces analgesic effects (Beitz & Buggy, 1981). The loss of either inhibitory interneurons or descending inhibition contributes to chronic pain conditions.

The loss of descending modulation could further potentiate maladaptive afferent signaling and increase nociception, subsequently promoting alterations of brain structure and function within the pain matrix. This cycle may also be exacerbated by motor, behavioral, and emotional dysregulation. Thus, interventions that are rooted in the contemporary theories that pain is a complex phenomenon are pivotal for long-lasting treatment and alleviation of symptoms in chronic pain populations.

The Gate Control Theory of Chronic Pain

Melzack and Wall's inception of the Gate Control Theory of pain in 1965 was the first to introduce multi-dimensionality to the condition (Melzack, 1999; Melzack & Wall, 1965). The Gate Control Theory postulates that significant psychological factors contribute to pain experience and perception, indicating a substantial involvement of the central

nervous system (CNS). Endogenous gating systems at the dorsal horn of the spinal cord mitigate afferent nociceptive signals, illustrating a dynamic pain network. Since Melzack and colleagues' seminal work, the consensus among the field remains fixed on pain as a multifactorial condition.

Complex Pathology Requires Multifaceted Therapies

Opioid Pharmacotherapy

Opioid medications have become the most abundantly prescribed class of drug in the United States (The Centers for Disease Control and Prevention, 2014) and it has been speculated that as much as 3% of the U.S. general population, excluding those with cancer pain, use opioids for greater than one month per year (M. D. Sullivan et al., 2008; M. D. Sullivan, Edlund, Steffick, & Unutzer, 2005). Physicians have increasingly prescribed opioid pharmaceutics and their derivatives to treat chronic pain despite considerable debate surrounding the benefits of prolonged use (Chou et al., 2015). In fact, sustained use in chronic pain patients has been shown to result in increased pain sensitivity known as hyperalgesia (Arout, Edens, Petrakis, & Sofuoglu, 2015; S. H. Kim, Stoicea, Soghomonyan, & Bergese, 2014). The mechanism underlying the resulting hyperalgesia has long been thought to be micgroglia-mediated (Ferrini et al., 2013), although recent evidence contests these findings and proposes that a loss of μ opioid receptor signaling in nociceptors is the culprit (Corder et al., 2017). Regardless of the mechanism of action, opioid use has been exhibited to profoundly influence brain structure. Younger and colleagues demonstrated in two separate studies that a one-month regimen of oral morphine to treat chronic low back pain was sufficient to alter GM volume, specifically showing a

volumetric decrease in reward and pain-related regions (Lin et al., 2016; Younger et al., 2011). Despite these caveats, 50% of opioid prescriptions are for greater than six months in duration (M. D. Sullivan et al., 2008).

Aside from the controversial evidence around their long-term efficacy and known association with volumetric brain changes, opioids pose a substantial risk of tolerance and addiction. Currently, there are no diagnostic criteria that predict which individuals are most prone to developing an opioid addiction, although genetic vulnerability is thought to account for up to 40% of the risk (Mistry, Bawor, Desai, Marsh, & Samaan, 2014; Tsuang et al., 1998; Xian et al., 2000). The pitfalls associated with opioid use are apparent and become further exacerbated in chronic conditions such as pain. As such, non-pharmacological interventions may diminish the reliance on opioid medications in chronic pain populations and provide long-lasting relief to treat an array of pain disorders without inherent risk.

Cognitive Behavioral Therapy (CBT)

Mind-body therapies such as CBT, yoga, meditation, and hypnosis provide safer, non-pharmacological alternatives to manage chronic pain and increase physical functioning. CBT is one such approach that has become increasingly popular to treat not only pain but a variety of psychological conditions such as depression (Hawley et al., 2017) and anxiety (Hofmann & Smits, 2008). CBT is a psychotherapeutic approach aimed at modifying dysfunctional emotions, maladaptive behaviors, and cognitive processes through goal oriented, 'problem focused' treatment. These social and environmental factors as well as aberrant psychological traits such as depression, anxiety, and

catastrophizing are associated with increased pain experiences and psychosocial dysfunction in chronic pain populations (Ehde, Dillworth, & Turner, 2014). Not surprisingly, chronic pain patients often exhibit fear avoidance behavior that inhibits social, physical, and even professional activities. This can further exacerbate the condition since physical activity and exercise have long been shown to reduce pain and disability in musculoskeletal pain patients (Booth et al., 2017). Taken together these influences propagate the cycle of chronic pain described previously (Figure 1.1) and may perpetuate disease chronification.

Large randomized clinical trials assessing various behavioral metrics have established the effectiveness of behavioral therapies such as CBT and mindfulness-based approaches to manage chronic pain (Cherkin, Sherman, Balderson, et al., 2016; Cherkin, Sherman, & Turner, 2016). For recent reviews see (Ehde et al., 2014; Hanscom, Brox, & Bunnage, 2015; Knoerl, Lavoie Smith, & Weisberg, 2016), and a complete meta-analysis by Hofmann and colleagues (Hofmann & Smits, 2008). However, the underlying cellular mechanisms and neural circuitry responsible for the therapeutic effects of CBT remain unknown. In a small heterogeneous chronic pain cohort, Seminowicz and colleagues demonstrated that 11-week group CBT intervention reversed volumetric brain alterations and reduced catastrophizing in pain patients (Seminowicz et al., 2013). Interestingly, these volumetric changes were observed in regions that are known to be involved in top-down cognitive control such as the prefrontal cortices. To briefly recap the neurocircuitry, WM connections between cognitive, limbic, and emotional centers of the pain matrix project to brain stem nuclei and ultimately the spinal cord, creating a descending inhibitory pathway through which afferent pain signaling can be mediated. In summary, it is believed that

regulation of emotion and cognition associated with chronic pain can regulate descending inhibitory pathways, potentially through endogenous opioidergic systems, clinically improving the quality of life by reducing pain symptoms and disability.

The study reported by Seminowicz and colleagues is one of the few experiments to show structural GM plasticity associated with CBT in chronic pain patients. Further investigation of structural plasticity associated with CBT is warranted in larger homogenous patient populations with relevant active patient control groups. Because of the array of systems on which CBT acts, it is plausible that successful intervention in pain populations will elicit structural changes in both the grey and white matter that could be exploited through non-invasive imaging technologies.

Imaging Chronic Pain & Plasticity

Imaging Overview

Technological advances have significantly expanded our capabilities of non-invasive, *in vivo* imaging. These developments support longitudinal evaluation in clinical populations that is pertinent for investigating disease progression and/or chronification, as well as plasticity associated with behavioral interventions. Safe and repeatable imaging procedures such as MRI and ultrasound can be applied to image a host of structures - for example the brain and the musculoskeletal system. The field of brain imaging, more generally referred to as neuroimaging, has undergone exponential growth in recent years and is a well-established tool among neuroscientists. Branching from this more general field, pain neuroimaging has been paramount in our understanding of the neurocircuitry involved in pain processing, helping to identify subtleties and similarities within chronic

pain subtypes. Borsook and colleagues suggest that neuroimaging has revolutionized the field of pain and its therapy, describing structural, functional, and neurochemical findings detected by MRI (Borsook, Moulton, Schmidt, & Becerra, 2007). One of the strengths of MRI, particularly in clinical populations such as chronic pain, is the ability to obtain several disparate measures in a single visit. For example, an investigator can collect a tremendous amount of data relevant to multiple hypotheses by acquiring several MRI acquisitions over the course of one procedure - brain function (fMRI), structure (diffusion weighted imaging and anatomical imaging), as well as chemistry and metabolism (MRI Spectroscopy).

Task-based fMRI studies have been designed to tease apart how the chronic pain brain differs from the healthy brain in reference to pain processing, appraisal, emotion, and cognition (Kregel et al., 2015; Malfliet et al., 2017; Martucci et al., 2014). Alterations in passive resting brain activity not associated with a task, termed resting state fMRI, have also been documented in chronic pain populations (Martucci & Mackey, 2016). Given that differences observed in function largely reflect metabolic demands of neuronal cell bodies, many investigators have reported alterations in the GM structure itself utilizing structural neuroimaging. Though numerous GM volumetric and density studies exist across pain subtypes there is still substantial discrepancy throughout the literature regarding the directionality of results – i.e. increase or decrease in GM volume, density and thickness (Cauda et al., 2014; Moayedi, Desouza, & Erpelding, 2011; Smallwood et al., 2013). One plausible reason for the discrepancy in results is the comparatively low sample sizes examined in many of the reports, warranting additional follow-up investigations in larger patient samples and reproducibility studies.

Conversely, fewer pain imaging studies have examined WM abnormalities in pain conditions, and most are largely based on rudimentary diffusion tensor imaging (DTI) metrics. DTI analysis has proven to be a powerful tool to define WM pathology and plasticity, however it has come under scrutiny because it drastically oversimplifies the underlying WM architecture and may ultimately render findings unreliable. Fortunately, once again, expansion in imaging capabilities provide better, more time-efficient diffusion acquisitions and analysis tools that allow us to overcome some of the previously stated limitations.

In summary, large cohort structural imaging studies need to be conducted to further extrapolate potential GM alterations associated with chronic pain. Also, WM investigations must move past oversimplified models to delineate tract differences associated with pain pathology. A specific pain imaging literature review for each imaging modality is covered in greater depth below, further highlighting our progress in functional brain states and identifying the gaps in our understanding of GM and WM pathology.

Functional Magnetic Resonance Imaging (fMRI) of Chronic Pain

FMRI has become a powerful tool for researchers to measure brain activity. The vascular hemodynamic response known as the BOLD (blood oxygen level dependent) effect provides an indirect measurement of neuronal activity and metabolism via neurovascular coupling. Signal is obtained in fMRI by fluctuations in deoxyhemoglobin driven by changes in brain blood flow and oxygenation. FMRI has been applied across numerous chronic pain conditions in a variety of resting and task-based experimental paradigms. For an extensive review and meta analysis of fMRI studies conducted in clinical

pain populations and acute pain paradigms see (Apkarian, Bushnell, Treede, & Zubieta, 2005) and more recently (Martucci & Mackey, 2016). Given the multitude of networks involved in pain processing, consistent findings in the literature report increased neural activity in the ACC, somatosensory cortices, insula, and prefrontal cortices across pain conditions. Interestingly, the thalamus, a known relay station for nociceptive transmission, demonstrates functional discrepancy between pain conditions. In neuropathic pain, it is consistently shown to be hypoactive (Garcia-Larrea & Peyron, 2013), however in chronic low back pain a hyperactivation is predominately reported (Baliki et al., 2008; Tracey & Bushnell, 2009). Advanced fMRI analysis techniques contribute to our understanding of the 'chronic pain brain.' For example, resting state MRI (rsMRI) measures low frequency neural oscillations that are constitutively active, this is known as the default mode network (DMN). The DMN has been implicated as a potential biomarker in many chronic pain subtypes. In low back pain, an increase in high frequency BOLD oscillations has been measured in the DLPFC, an important structure for descending modulation of pain (Baliki, Baria, & Apkarian, 2011). This result suggests that chronic pain states require increased deactivation of the DMN to activate task-driven networks, including descending modulatory pathways.

This literature supports a rich understanding of the GM neural structures involved functionally across chronic pain conditions. Alterations in brain function provide ample motive to investigate the possible structural deviations in GM and even WM, given the literature to support activity-dependent WM plasticity (Gibson et al., 2014; Ishibashi et al., 2006; Liu et al., 2012; J. Liu et al., 2016) Together with our previously reported longitudinal fMRI findings following CBT (Shpaner et al., 2014), the addition of our

structural investigation will provide greater insight into the efficacy of behavioral intervention.

Grey Matter (GM) Structural Imaging of Chronic Pain

In the CNS, GM is predominately comprised of neuronal cell bodies, glia, and unmyelinated axons. GM structure is typically assessed by various analysis pipelines of T_1-weighted images such as surface-based, voxel-based, and tensor-based morphometry. Depending on the specific approach, primary outcome measures include cortical and subcortical thickness and surface area as well as density and volume. While most of these measures are self-explanatory in nature, others can be deceivably counterintuitive. For example, the output of voxel-based morphometry includes GM density and volume, which are sometimes used synonymously in the literature. In actuality, the subtle differences in meaning arise from the modulation step in the analysis. Modulation, in GM analysis terms, is the mathematical operation of scaling based on stretching and compression in a voxel (Greve, 2011). GM density refers to results obtained without a modulation step, and, conversely, results where a modulation step was applied are referred to as GM volume. Semantics aside, alterations in these measures may reflect a variety of changes in the underlying microstructure: remodeling, neuronal loss or genesis, synaptic regulation, neurovasculature alterations, dendritic pruning and arborization, as well as changes in glia reactivity, morphology and number (Zatorre, Fields, & Johansen-Berg, 2012).

GM morphometry methods have been applied extensively to pain cohorts, however, many studies suffer from small sample sizes, possibly contributing to the discrepancy of results in the literature. Neural regions consistently reported in chronic pain pathology

include the ACC, insular cortex, operculum, DLPFC, limbic regions such as amygdala, and brain stem structures. Diminished GM volume has been predominately reported across pain conditions, including fibromyalgia and migraine (See meta analysis for a complete review of pain types and systems involved) (Cauda et al., 2014). Research involving other pain subtypes report increases in GM metrics such as chronic pelvic pain (Bagarinao et al., 2014) and trigeminal neuralgia (Desouza, Moayedi, Chen, Davis, & Hodaie, 2013). Investigations in low back pain populations report mixed results suggesting volumetric increases in some GM regions, for example the somatosensory cortex, precuneus, and the dorsal ACC (Kong et al., 2013; Luchtmann et al., 2015) while other regions involved in nociceptive processing exhibit a consistent decrease in GM metrics. Interestingly, Mao and colleagues conducted a study comparing low back pain patients and upper back pain patients to healthy controls with intriguing results. They showed that low back pain patients, but not upper back pain patients, had decreased GM volume in the postcentral gyrus, precuneus, and cuneal cortices (Mao et al., 2013). Substantial evidence suggests bidirectional GM morphometric differences in chronic pain conditions, however, additional investigations are warranted to substantiate the directionality of outcome measures and pinpoint the key neural structures involved.

Though MRI lacks the spatial resolution to infer the specific mechanisms leading to changes in GM structure, longitudinal evaluation in patient populations provides some critical insight. For example, a reversal of GM morphometric alterations has been demonstrated following successful surgical intervention and subsequent alleviation of pain symptoms (Ceko et al., 2015; Rodriguez-Raecke, Niemeier, Ihle, Ruether, & May, 2013; Seminowicz et al., 2011). This suggests that GM changes in chronic pain cohorts are not

reflective of neuronal cell death or atrophy, nor are they predisposing factors, but instead may be secondary to the onset of chronic pain. Behavioral interventions have also exhibited neuroplasticity associated with behavioral modification and pain relief. In a study by Seminowicz and colleagues, it was shown that following an 11-week CBT treatment for chronic pain, patients exhibited an increase in GM volume in the DLPFC, ACC, orbitofrontal cortex, sensorimotor cortices, and the hippocampus (Seminowicz et al., 2013). A pitfall in this study, however, was the lack of an adequate active control group. This evidence suggests that GM alterations associated with chronic pain are reversible with therapy, demonstrating GM neuroplasticity.

Combining GM morphometry metrics with other imaging techniques such as diffusion weighted imaging and spectroscopy may add to our understanding of the significance of these findings *in vivo* and may help delineate the specific cellular influences responsible in chronic pain conditions. For example, GM diffusion alterations would provide an indication of membrane and cell packing density while spectroscopy would yield insight into neurochemical changes that could influence brain metabolism and receptor up- or downregulation. Overall the alterations in GM morphometry are robust in chronic pain populations, most notably in regions involved in pain processing. Furthermore, these hubs of functional activity form complex networks that are interconnected by axons that comprise the brain's WM. While sufficient literature exists to support GM changes, WM remains significantly understudied across chronic pain states. Fortunately, diffusion MRI can be acquired in parallel to GM (T_1-Weighted) acquisitions and can be utilized in parallel to study potential WM alterations in the chronic pain brain.

Diffusion Weighted Imaging

Principles of Diffusion Imaging

Diffusion weighted imaging (DWI) is a technique that exploits water to generate a signal or contrast and relies heavily on the principles of Brownian motion; the random diffusion of molecules that can be influenced by thermodynamic qualities (Andre & Bammer, 2010). DWI is adept for *in vivo* study of WM, because diffusion within the brain is restricted by macromolecules, cell membranes, and myelin. By measuring the direction of diffusion, DWI provides measures of magnitude, anisotropy, and orientation (Alexander, Lee, Lazar, & Field, 2007). Mathematical techniques used to model diffusion vary in complexity and offer an array of diffusion indices. The most prevalent and simple model of diffusion used to assess brain imaging data is the single-tensor or diffusion tensor imaging (DTI) model. This method calculates and estimates a single axial vector of diffusion (λ_1) and two vectors of radial diffusion (λ_2, λ_3). From these vectors, a number of scalars can be generated including: axial diffusivity (AD) - λ_1, radial diffusivity (RD) – $(\lambda_2+\lambda_3)/2$, mean diffusivity (MD) or the average diffusion in each voxel $(\lambda_1+\lambda_2+\lambda_3)/3$, and fractional anisotropy (FA) - a measure of linearity from zero (isotropic diffusion) to one (anisotropic diffusion) (Hagmann et al., 2006). DWI metrics can be utilized to measure a host of WM microstructural attributes including 'integrity,' volume, density, cross-section, and connectivity. Similarly, diffusion MRI can also be used to probe GM properties. For example, MD has been applied to investigate microstructural alterations associated with changes in GM morphometry (Kang, Herron, Turken, & Woods, 2012; Kwon, Park, Seo, Na, & Lee, 2015).

Diffusion Imaging of Microstructure in Chronic Pain

It has been well characterized that chronic pain results in a dysregulation of cellular and molecular signaling that influences neuronal excitability theoretically ensuing dynamic alterations in CNS WM. Altered behavior and social interactions also influence myelination states (Liu et al., 2012; J. Liu et al., 2016). Although the cellular literature supports that peripheral mechanisms could lead to structural WM alterations, the effect of chronic pain on WM is not well characterized, neither in humans nor in animal models. Further, the underlying significance of described WM changes observed using neuroimaging is unknown. With the advent of *in vivo* diffusion MRI, DTI methodology has emerged as the frontrunner to assess tissue microstructure. Several studies have assessed WM alterations in chronic pain states such as fibromyalgia (D. J. Kim et al., 2014; Lutz et al., 2008), temporomandibular disorder (Moayedi et al., 2012b), complex regional pain syndrome (Geha et al., 2008), neuropathic pain (Gustin, Wrigley, Siddall, & Henderson, 2010), migraine with aura (Yu et al., 2013), urological chronic pelvic pain (Woodworth et al., 2015), and irritable bowel syndrome (J. Y. Chen, Blankstein, Diamant, & Davis, 2011; Ellingson et al., 2013). Our lab also reported WM microstructural alterations in chronic musculoskeletal pain patients with observed decreases in FA found in the corpus callosum (CC) and cingulum as well as increased RD in the CC, internal capsule, external capsule, SLF, and the cerebral peduncle (Lieberman et al., 2014). In general, a reduction in FA (Moayedi et al., 2011; Szabo et al., 2012; Yuan et al., 2012) has been reported in a range of WM tracts projecting to pain matrix GM regions such as the somatosensory cortex, amygdala, hippocampus, ACC, thalamus, and insula, however, increases in axial diffusivity have been reported as well (Rayhan et al., 2013). Interestingly,

Mansour and colleagues found that DTI metrics, specifically FA, correlated with GM functional connectivity in the medial and lateral prefrontal cortices in patients experiencing sub-acute low back pain (Mansour et al., 2013). These WM indices accurately predicted which participants progressed to develop persistent low back pain, which they suggest as a possible biomarker of chronic pain. Remarkably, WM plasticity has been demonstrated following therapeutic intervention. Successful relinquishment of pain in surgically treatable chronic pain conditions has been associated with reversal of abnormal diffusion microstructural metrics. Specifically, Wu and colleagues longitudinally investigated radiculopathy patients that underwent surgery to alleviate compressed nerve roots and showed that FA was increased one month post-surgery (W. Wu et al., 2017). Together, the evidence provided strongly supports WM involvement across pain conditions and indicates that diffusion metrics could be used as a prospective marker of intervention efficacy.

Although the current approaches hold tremendous potential for biomarker development, distinction between pain conditions, and therapeutic outcomes, it is important to identify and understand several methodological limitations. First, DTI assumes a normative, or Gaussian, distribution of the diffusion of water molecules in the brain. We know that water in the brain does not follow a Gaussian distribution based on microstructural barriers such as cell membranes and organelles that dictate the direction in which water freely moves. Additionally, of the studies described above, only one implemented analysis techniques that are sensitive for resolving complex fiber geometry. This is a significant drawback because it has been postulated that up to 90% of WM voxels contain more than one fiber orientation (Jeurissen, Leemans, Tournier, Jones, & Sijbers, 2013). Moreover, single tensor diffusion reconstructions such as DTI enable only the

principal diffusion direction in each voxel to be modeled. Unfortunately, this method breaks down in areas of complex fiber geometry such as crossing, touching, or kissing fibers. For example, if two similarly sized WM tracts cross orthogonally in a voxel, the resulting FA may inaccurately yield an isotropic value rather than the true anisotropy present from the respective tracts. Thus, it is imperative that the current literature is complemented by diffusion methods with greater sensitivity and accuracy in complex neural architecture.

The breakdown of common single tensor metrics in complex fiber geometry may also influence the interpretability of the current findings. The literature often concedes that a diminished FA indicates loss of tract integrity, but this interpretation is largely based on decreased FA in multiple sclerosis; a disease characterized by loss of CNS myelin, allowing for water to diffuse radially from the affected WM tracts. Whether decreased FA represents tract integrity in pain states has not been confirmed, and in many instances, this interpretation may be incorrect. However, as the use of diffusion weighted imaging has become more popular, reports of WM deviations in psychiatric conditions and non-neurodegenerative disease states have surfaced with little mechanistic data to support the presumed loss of tract integrity. This is also true in chronic pain conditions where there is negligible evidence to suggest neurodegenerative pathology, either via excitotoxicity or otherwise. Interpretations often fail to acknowledge the role of glial morphology on WM diffusion metrics.

In addition to potential errors pertaining to complex fiber geometry, non-neuronal influences on the diffusion signal have largely been ignored. It has been postulated that glia comprise up to ~48% of the volume of a $100\mu m^3$ voxel in rats, which, when scaled to

human equivalence, equates to approximately 880,000 oligodendrocytes and astrocytes in a typical $2mm^3$ isotropic voxel – a tissue volume considered standard to high resolution in diffusion weighted imaging protocols (Walhovd, Johansen-Berg, & Karadottir, 2014). Further, gliosis has been shown to influence both AD and RD diffusion metrics (Alexander et al., 2007; Aojula et al., 2016; Hoza, Vlasak, Horinek, Sames, & Alfieri, 2015). Neurochemical alterations of myo-inositol, used for identification of glial cells in proton magnetic resonance spectroscopy (^{1}H-MRS) that is interpreted as a marker of neuroinflammation, is negatively associated with changes in FA in schizophrenia patients (Chiappelli et al., 2015). In an animal model of traumatic brain injury, gliosis was also demonstrated to contribute to anisotropy and tractography alterations with subsequent histological validation (Budde, Janes, Gold, Turtzo, & Frank, 2011). These cells likely alter diffusion properties in a voxel, because cell bodies and glia are largely isotropic in nature. The influence of these cells provide additional mechanisms that could lead to alterations in single tensor metrics or fiber density, the significance of which is largely overlooked in interpretation of diffusion imaging.

The influence of glial cells on diffusion metrics may be of particular importance in chronic pain, a condition that has known effects on the morphology of CNS glia. Brain imaging techniques such as positron emission tomography have confirmed that chronic pain contributes to glia reactivity, ultimately influencing their quantity and morphology. Utilizing a translocator protein (TSPO) radioligand sensitive to reactive astrocytes and microglia, Loggia and colleagues demonstrated that chronic musculoskeletal pain patients had increased reactive glia compared to healthy controls (Loggia et al., 2015). This further

exemplifies the relevance of non-neuronal contributions to the diffusion signal in chronic pain conditions.

Nonetheless, the interpretation of diffusion metrics as an indicator of tract integrity persists in many investigations of WM microstructure even as mounting literature is beginning to divulge the fundamental flaws in single tensor metrics. This evidence demonstrates the necessity of implementing diffusion modeling techniques that account for complex fiber geometry or multiple compartments (isotropic and anisotropic) within each voxel. Furthermore, translational studies involving animal models of chronic pain will undoubtedly be required to facilitate our understanding of the underlying mechanisms leading to WM microstructural alterations and plasticity. As a supplement to the clinical framework presented in this dissertation, a novel animal model of low-back pain pathophysiology was developed based on the foundations of injury and movement restriction presented in the vicious cycle of chronic pain (Supplemental Chapter 6). Furthermore, a protocol describing a unique post mortem, *in situ,* translational DWI method is outlined. This pipeline enables parallel WM microstructural assessment along with the ability to conduct mechanistic investigation necessary to strengthen the interpretations of WM alterations in chronic pain conditions (Chapter 4).

Advanced Diffusion Acquisition and Analysis

The brain is a complex system that requires advanced computational modeling to ensure acurate assessment of the underlying WM tissue complexity and architecture. WM tracts are known to cross and interdigitate throughout the brain; these patterns are poorly represented using DTI reconstruction techniques that only model a single intravoxel fiber

orientation. The application of modeling techniques is largely predicated on model-based or model-free diffusion hypotheses and imaging parameters such as acquisition scheme and mathematical reconstruction of the diffusion signal. Acquisition factors such as the gradient strength of the magnet and number of gradient directions can dramatically influence the downstream processing steps and outcome measures. For example, a single b value of 1000 may be sufficient for microstructural analysis in human data, however, it provides suboptimal angular resolution desired for tractography and connectometry applications. In some instances the aquisiton scheme dictates the specific reconstruction technique that can be applied. For example, diffusion spectrum imaging (DSI) thoroughly samples q-space in a grid-like fashion utilizing multiple varying b values and requiring hundreds of images (Wedeen, Hagmann, Tseng, Reese, & Weisskoff, 2005; Wedeen et al., 2008). As such, DSI reconstructions typically are only applied to data that was acquired using a DSI sequence. Fortunately, novel reconstruction approaches have been developed that enable reconstruction of complex WM geometry from diffusion acquisitions with sparse q-space sampling. Ball & sticks multi-compartment method (BAS) (Behrens et al., 2003) and generalized q-sampling imaging (GQI) (Yeh, Wedeen, & Tseng, 2010) are two such methods that are more flexible and can be applied to a broad range of diffusion acquistions including DTI. Even still, reconstruction of the fiber orientation distribution function (ODF) from the diffusion signal can be carried out in countless ways with each providing unique solutions to an unknown ground truth in the human brain. Here we focus on both BAS and GQI because of their application in the preceding chapters.

Multi-compartment BAS reconstruction fits multiple fiber orientations within each voxel and provides more robust scalar calculations. BAS is a model-based diffusion

reconstruction that uses a multi-compartment approach to parameterize the diffusion signal. The multi-compartment method is premised on a Bayesian partial volume fraction model of the diffusion signal within each voxel. The sticks represent the anisotropic diffusion of water constrained within or along the tracts and the ball symbolizes the isotropic diffusion of water that is not constrained within axons. Conversely, GQI is a model-free based approach that implements non-parametric modeling to estimate the ODF. Both the model free GQI, and the multi-compartment BAS approaches, aim to minimize crossing and kissing fiber errors that are characteristic of complex fiber geometry. With the anticipation of investigating WM microstructural and connectivity differences in pain populations, we carried out a methodological assessment of diffusion reconstruction algorithms. This comparison was conducted in lieu of arbitrarily selecting a random method and provided valuable insight into the translatability of reconstruction methods from phantom to human data sets.

Phantoms are typically engineered vessels that contain fluid and 'neuron-like' fibers made of polyester (Pullens, Roebroeck, & Goebel, 2010) or capillary tubes (A. Krzyzak, Klodowski, & Raszewski, 2015; A. T. Krzyzak & Klodowski, 2015; Yanasak & Allison, 2006). They provide geometry similar to what is found in the human brain with the added importance of a known number of fibers and angular crossings. These systems are then used to test the performance of diffusion acquisitions and reconstruction algorithms. There have been exhaustive studies and even competitions conducted in phantoms to develop accurate reconstruction techniques (Daducci, Dal Palu, Lemkaddem, & Thiran, 2015). While this is often thought of as the gold standard of methodological

development, few studies complement phantom results with *in vivo* human data to test whether these findings hold true.

Thus, we demonstrated the effects of multiple reconstruction algorithms on a single acquisition scheme in both a diffusion phantom and human data (Lichenstein, Bishop, Verstynen, & Yeh, 2016). In brief, this was completed prior to selecting a diffusion model for the clinical connectivity experiments discussed in this dissertation. The centrum semiovale was chosen as the region of interest based on the known complexity of the fiber orientations. Model-free (GQI and DSI) and multi-compartment (BAS) reconstructions more accurately represented the complex geometry than the single-tensor model in both the human and phantom data. Ultimately, reliable measures of intra-voxular diffusion provide the foundation for advanced analysis of connectivity which we felt was imperative before proceeding with clinical comparisons. The outcomes of this study have been published and are presented as supplemental chapter (Supplemental Chapter 7).

In summary, accurate reconstruction methods are crtical for robust WM characterization and evaluation of brain data. Anisotropy metrics such as FA or generalized fractional anisotropy (GFA) are often utilized to perform tractography and thus reconstruction choice can substantially impact study results. This undermines scalar metrics and tractography results, and leads to inconsistency between imaging studies. To combat these challenges, model free reconstruction algorithms exploit the increased angular resolution provided by increased Q-space sampling. Q-space is somewhat analogous to k-space encoding, however, instead of being defined by the readout gradient, q-space is defined by the diffusion gradient. This ultimately enables characterization of a 3-deminsional probability distribution function of the diffusion distribution by first

estimating the ensemble average propagator. A drawback to model-free approaches includes long acquisition times that are usually not suitable for patient populations. Alternatively, multi-compartment methods often require sizeable computational power required for reconstruction and analysis. Fortunately, advances in MRI hardware technology and computing now allow for simultaneous slice acquisition, termed multi-band imaging, dramatically reducing scan times and facilitating higher resolution diffusion imaging.

Tractography and Connectometry

Connectomics is a rapidly evolving field where diffusion weighted imaging approaches are implemented to establish the WM connections between GM regions in the brain, ultimately delineating a global connectivity pattern between adjacent voxels. Classically, this connectivity profile is assessed by first performing tractography to render and obtain the WM connections that pass through, or terminate within specified GM anatomical structures. The basis of tractography analysis often begins with the selection of acquisition parameters and reconstruction approaches. Two fundamental divergences in methodology arise in the choice of tractography - either deterministic or probabilistic. Deterministic tractography provides an estimate of the model parameters in each voxel whereas probabilistic tractography provides the uncertainty. Additionally, tractography outcomes can vary depending on the seed region and ambiguous tracking constraints provided prior to implementation. Fortunately, several software packages have developed pipelines that bypass some of the pitfalls and limitations described and allow for between-group and longitudinal comparison of large brain networks.

One alternative to tractography-based connectometry is analysis of spin distribution functions (Yeh, Tang, & Tseng, 2013). An advantage of this technique over traditional tractography is that it bypasses the initial tracking step and defines regions that have significantly different diffusion properties. This is statistically calculated by group mean difference, multiple regression, or statistical rank, so that only the significant regions are used for tractography. Elucidating tract differences between disease states may offer biological clues pertaining to disease susceptibility, progression, and treatment response.

Previously, pathology or lesion studies were the only available means to assess network and structural functionality. WM connectivity has been shown to play an important role in diverse cognitive and psychological conditions such as major depressive disorder (Olvet et al., 2016), autism (Billeci, Calderoni, Tosetti, Catani, & Muratori, 2012), Alzheimer's disease (T. Wang et al., 2016), schizophrenia (Di Biase et al., 2017) and even pain conditions such as complex regional pain syndrome (Geha et al., 2008). One longitudinal study followed sub-acute back pain patients from onset through either recovery or transition to chronic pain, and demonstrated that structural connectivity differences in the medial and lateral prefrontal cortices may predispose and predict the transition to back pain chronification (Mansour et al., 2013). Combining WM and GM structural information may better inform investigators pertaining to network deviations in chronic pain conditions. Furthermore, it is important to investigate the generalizability of these findings to more broadly encompass other types of musculoskeletal pain.

References for Chapter 1

Alexander, A. L., Lee, J. E., Lazar, M., & Field, A. S. (2007). Diffusion tensor imaging of the brain. *Neurotherapeutics, 4*(3), 316-329. doi:10.1016/j.nurt.2007.05.011

Andre, J. B., & Bammer, R. (2010). Advanced diffusion-weighted magnetic resonance imaging techniques of the human spinal cord. *Top Magn Reson Imaging, 21*(6), 367-378. doi:10.1097/RMR.0b013e31823e65a1

Andrew, D., & Greenspan, J. D. (1999). Mechanical and heat sensitization of cutaneous nociceptors after peripheral inflammation in the rat. *J Neurophysiol, 82*(5), 2649-2656.

Aojula, A., Botfield, H., McAllister, J. P., 2nd, Gonzalez, A. M., Abdullah, O., Logan, A., & Sinclair, A. (2016). Diffusion tensor imaging with direct cytopathological validation: characterisation of decorin treatment in experimental juvenile communicating hydrocephalus. *Fluids Barriers CNS, 13*(1), 9. doi:10.1186/s12987-016-0033-2

Apkarian, A. V., Bushnell, M. C., Treede, R. D., & Zubieta, J. K. (2005). Human brain mechanisms of pain perception and regulation in health and disease. *Eur J Pain, 9*(4), 463-484. doi:10.1016/j.ejpain.2004.11.001

Arout, C. A., Edens, E., Petrakis, I. L., & Sofuoglu, M. (2015). Targeting Opioid-Induced Hyperalgesia in Clinical Treatment: Neurobiological Considerations. *CNS Drugs, 29*(6), 465-486. doi:10.1007/s40263-015-0255-x

Bagarinao, E., Johnson, K. A., Martucci, K. T., Ichesco, E., Farmer, M. A., Labus, J., . . . Mackey, S. (2014). Preliminary structural MRI based brain classification of chronic pelvic pain: A MAPP network study. *Pain, 155*(12), 2502-2509. doi:10.1016/j.pain.2014.09.002

Baliki, M. N., Baria, A. T., & Apkarian, A. V. (2011). The cortical rhythms of chronic back pain. *J Neurosci, 31*(39), 13981-13990. doi:10.1523/JNEUROSCI.1984-11.2011

Baliki, M. N., Geha, P. Y., Jabakhanji, R., Harden, N., Schnitzer, T. J., & Apkarian, A. V. (2008). A preliminary fMRI study of analgesic treatment in chronic back pain and knee osteoarthritis. *Mol Pain, 4*, 47. doi:10.1186/1744-8069-4-47

Beggs, S., Currie, G., Salter, M. W., Fitzgerald, M., & Walker, S. M. (2012). Priming of adult pain responses by neonatal pain experience: maintenance by central neuroimmune activity. *Brain, 135*(Pt 2), 404-417. doi:10.1093/brain/awr288

Behrens, T. E., Woolrich, M. W., Jenkinson, M., Johansen-Berg, H., Nunes, R. G., Clare, S., . . . Smith, S. M. (2003). Characterization and propagation of uncertainty in diffusion-weighted MR imaging. *Magn Reson Med, 50*(5), 1077-1088. doi:10.1002/mrm.10609

Beitz, A. J., & Buggy, J. (1981). Brain functional activity during PAG stimulation-produced analgesia: a 2-DG study. *Brain Res Bull, 6*(6), 487-494.

Billeci, L., Calderoni, S., Tosetti, M., Catani, M., & Muratori, F. (2012). White matter connectivity in children with autism spectrum disorders: a tract-based spatial statistics study. *BMC Neurol, 12*, 148. doi:10.1186/1471-2377-12-148

Bishop, J. H., Fox, J. R., Maple, R., Loretan, C., Badger, G. J., Henry, S. M., . . . Langevin, H. M. (2016). Ultrasound Evaluation of the Combined Effects of

Thoracolumbar Fascia Injury and Movement Restriction in a Porcine Model. *PLoS One, 11*(1), e0147393. doi:10.1371/journal.pone.0147393

Booth, J., Moseley, G. L., Schiltenwolf, M., Cashin, A., Davies, M., & Hubscher, M. (2017). Exercise for chronic musculoskeletal pain: A biopsychosocial approach. *Musculoskeletal Care*. doi:10.1002/msc.1191

Borsook, D., Moulton, E. A., Schmidt, K. F., & Becerra, L. R. (2007). Neuroimaging revolutionizes therapeutic approaches to chronic pain. *Mol Pain, 3*, 25. doi:10.1186/1744-8069-3-25

Budde, M. D., Janes, L., Gold, E., Turtzo, L. C., & Frank, J. A. (2011). The contribution of gliosis to diffusion tensor anisotropy and tractography following traumatic brain injury: validation in the rat using Fourier analysis of stained tissue sections. *Brain, 134*(Pt 8), 2248-2260. doi:10.1093/brain/awr161

Bushnell, M. C., Ceko, M., & Low, L. A. (2013). Cognitive and emotional control of pain and its disruption in chronic pain. *Nat Rev Neurosci, 14*(7), 502-511. doi:10.1038/nrn3516

Cauda, F., Palermo, S., Costa, T., Torta, R., Duca, S., Vercelli, U., . . . Torta, D. M. (2014). Gray matter alterations in chronic pain: A network-oriented meta-analytic approach. *Neuroimage Clin, 4*, 676-686. doi:10.1016/j.nicl.2014.04.007

Ceko, M., Shir, Y., Ouellet, J. A., Ware, M. A., Stone, L. S., & Seminowicz, D. A. (2015). Partial recovery of abnormal insula and dorsolateral prefrontal connectivity to cognitive networks in chronic low back pain after treatment. *Hum Brain Mapp, 36*(6), 2075-2092. doi:10.1002/hbm.22757

Chang, K. J., Redmond, S. A., & Chan, J. R. (2016). Remodeling myelination: implications for mechanisms of neural plasticity. *Nat Neurosci, 19*(2), 190-197. doi:10.1038/nn.4200

Charlton, R. A., Barrick, T. R., McIntyre, D. J., Shen, Y., O'Sullivan, M., Howe, F. A., . . . Markus, H. S. (2006). White matter damage on diffusion tensor imaging correlates with age-related cognitive decline. *Neurology, 66*(2), 217-222. doi:10.1212/01.wnl.0000194256.15247.83

Chen, F. L., Dong, Y. L., Zhang, Z. J., Cao, D. L., Xu, J., Hui, J., . . . Gao, Y. J. (2012). Activation of astrocytes in the anterior cingulate cortex contributes to the affective component of pain in an inflammatory pain model. *Brain Res Bull, 87*(1), 60-66. doi:10.1016/j.brainresbull.2011.09.022

Chen, G., Park, C. K., Xie, R. G., Berta, T., Nedergaard, M., & Ji, R. R. (2014). Connexin-43 induces chemokine release from spinal cord astrocytes to maintain late-phase neuropathic pain in mice. *Brain, 137*(Pt 8), 2193-2209. doi:10.1093/brain/awu140

Chen, J. Y., Blankstein, U., Diamant, N. E., & Davis, K. D. (2011). White matter abnormalities in irritable bowel syndrome and relation to individual factors. *Brain Res, 1392*, 121-131. doi:10.1016/j.brainres.2011.03.069

Cherkin, D. C., Sherman, K. J., Balderson, B. H., Cook, A. J., Anderson, M. L., Hawkes, R. J., . . . Turner, J. A. (2016). Effect of Mindfulness-Based Stress Reduction vs Cognitive Behavioral Therapy or Usual Care on Back Pain and Functional Limitations in Adults With Chronic Low Back Pain: A Randomized Clinical Trial. *JAMA, 315*(12), 1240-1249. doi:10.1001/jama.2016.2323

Cherkin, D. C., Sherman, K. J., & Turner, J. A. (2016). Mindfulness-Based Stress Reduction vs Cognitive Behavioral Therapy for Chronic Low Back Pain--Reply. *JAMA, 316*(6), 663-664. doi:10.1001/jama.2016.7951

Chiappelli, J., Hong, L. E., Wijtenburg, S. A., Du, X., Gaston, F., Kochunov, P., & Rowland, L. M. (2015). Alterations in frontal white matter neurochemistry and microstructure in schizophrenia: implications for neuroinflammation. *Transl Psychiatry, 5*, e548. doi:10.1038/tp.2015.43

Chou, R., Turner, J. A., Devine, E. B., Hansen, R. N., Sullivan, S. D., Blazina, I., . . . Deyo, R. A. (2015). The effectiveness and risks of long-term opioid therapy for chronic pain: a systematic review for a National Institutes of Health Pathways to Prevention Workshop. *Ann Intern Med, 162*(4), 276-286. doi:10.7326/M14-2559

Chung, W. S., Welsh, C. A., Barres, B. A., & Stevens, B. (2015). Do glia drive synaptic and cognitive impairment in disease? *Nat Neurosci, 18*(11), 1539-1545. doi:10.1038/nn.4142

Cimmino, M. A., Ferrone, C., & Cutolo, M. (2011). Epidemiology of chronic musculoskeletal pain. *Best Pract Res Clin Rheumatol, 25*(2), 173-183. doi:10.1016/j.berh.2010.01.012

Corder, G., Tawfik, V. L., Wang, D., Sypek, E. I., Low, S. A., Dickinson, J. R., . . . Scherrer, G. (2017). Loss of mu opioid receptor signaling in nociceptors, but not microglia, abrogates morphine tolerance without disrupting analgesia. *Nat Med, 23*(2), 164-173. doi:10.1038/nm.4262

Costigan, M., & Woolf, C. J. (2002). No DREAM, No pain. Closing the spinal gate. *Cell, 108*(3), 297-300.

Daducci, A., Dal Palu, A., Lemkaddem, A., & Thiran, J. P. (2015). COMMIT: Convex optimization modeling for microstructure informed tractography. *IEEE Trans Med Imaging, 34*(1), 246-257. doi:10.1109/TMI.2014.2352414

DeLeo, J. A., & Yezierski, R. P. (2001). The role of neuroinflammation and neuroimmune activation in persistent pain. *Pain, 90*(1-2), 1-6.

Desouza, D. D., Moayedi, M., Chen, D. Q., Davis, K. D., & Hodaie, M. (2013). Sensorimotor and Pain Modulation Brain Abnormalities in Trigeminal Neuralgia: A Paroxysmal, Sensory-Triggered Neuropathic Pain. *PLoS One, 8*(6), e66340. doi:10.1371/journal.pone.0066340

Di Biase, M. A., Cropley, V. L., Baune, B. T., Olver, J., Amminger, G. P., Phassouliotis, C., . . . Zalesky, A. (2017). White matter connectivity disruptions in early and chronic schizophrenia. *Psychol Med*, 1-14. doi:10.1017/S0033291717001313

Dieppe, P. (2013). Chronic musculoskeletal pain. *BMJ, 346*, f3146. doi:10.1136/bmj.f3146

Ehde, D. M., Dillworth, T. M., & Turner, J. A. (2014). Cognitive-behavioral therapy for individuals with chronic pain: efficacy, innovations, and directions for research. *Am Psychol, 69*(2), 153-166. doi:10.1037/a0035747

Ellingson, B. M., Mayer, E., Harris, R. J., Ashe-McNally, C., Naliboff, B. D., Labus, J. S., & Tillisch, K. (2013). Diffusion tensor imaging detects microstructural reorganization in the brain associated with chronic irritable bowel syndrome. *Pain, 154*(9), 1528-1541. doi:10.1016/j.pain.2013.04.010

Ellis, A., & Bennett, D. L. (2013). Neuroinflammation and the generation of neuropathic pain. *Br J Anaesth, 111*(1), 26-37. doi:10.1093/bja/aet128

Eroglu, C., & Barres, B. A. (2010). Regulation of synaptic connectivity by glia. *Nature, 468*(7321), 223-231. doi:10.1038/nature09612

Ferrini, F., Trang, T., Mattioli, T. A., Laffray, S., Del'Guidice, T., Lorenzo, L. E., . . . De Koninck, Y. (2013). Morphine hyperalgesia gated through microglia-mediated disruption of neuronal Cl(-) homeostasis. *Nat Neurosci, 16*(2), 183-192. doi:10.1038/nn.3295

Fields, R. D. (2008a). Oligodendrocytes changing the rules: action potentials in glia and oligodendrocytes controlling action potentials. *Neuroscientist, 14*(6), 540-543. doi:10.1177/1073858408320294

Fields, R. D. (2008b). White matter in learning, cognition and psychiatric disorders. *Trends Neurosci, 31*(7), 361-370. doi:10.1016/j.tins.2008.04.001

Frymoyer, J. W. (1988). Back pain and sciatica. *N Engl J Med, 318*(5), 291-300. doi:10.1056/NEJM198802043180506

Gao, Y. J., & Ji, R. R. (2010). Targeting astrocyte signaling for chronic pain. *Neurotherapeutics, 7*(4), 482-493. doi:10.1016/j.nurt.2010.05.016

Garcia-Larrea, L., & Peyron, R. (2013). Pain matrices and neuropathic pain matrices: a review. *Pain, 154 Suppl 1*, S29-43. doi:10.1016/j.pain.2013.09.001

Geha, P. Y., Baliki, M. N., Harden, R. N., Bauer, W. R., Parrish, T. B., & Apkarian, A. V. (2008). The brain in chronic CRPS pain: abnormal gray-white matter interactions in emotional and autonomic regions. *Neuron, 60*(4), 570-581. doi:10.1016/j.neuron.2008.08.022

Gibson, E. M., Purger, D., Mount, C. W., Goldstein, A. K., Lin, G. L., Wood, L. S., . . . Monje, M. (2014). Neuronal activity promotes oligodendrogenesis and adaptive myelination in the mammalian brain. *Science, 344*(6183), 1252304. doi:10.1126/science.1252304

Greve, D. N. (2011). *An absolute beginner's guide to surface- and voxel- based morphometric analysis.* Paper presented at the Proceedings of the International Society for Magnetic Resonance in Medicine.

Gustin, S. M., Wrigley, P. J., Siddall, P. J., & Henderson, L. A. (2010). Brain anatomy changes associated with persistent neuropathic pain following spinal cord injury. *Cereb Cortex, 20*(6), 1409-1419. doi:10.1093/cercor/bhp205

Hagmann, P., Jonasson, L., Maeder, P., Thiran, J. P., Wedeen, V. J., & Meuli, R. (2006). Understanding diffusion MR imaging techniques: from scalar diffusion-weighted imaging to diffusion tensor imaging and beyond. *Radiographics, 26 Suppl 1*, S205-223. doi:10.1148/rg.26si065510

Hains, B. C., & Waxman, S. G. (2006). Activated microglia contribute to the maintenance of chronic pain after spinal cord injury. *J Neurosci, 26*(16), 4308-4317. doi:10.1523/JNEUROSCI.0003-06.2006

Hanscom, D. A., Brox, J. I., & Bunnage, R. (2015). Defining the Role of Cognitive Behavioral Therapy in Treating Chronic Low Back Pain: An Overview. *Global Spine J, 5*(6), 496-504. doi:10.1055/s-0035-1567836

Haroon, E., Miller, A. H., & Sanacora, G. (2017). Inflammation, Glutamate, and Glia: A Trio of Trouble in Mood Disorders. *Neuropsychopharmacology, 42*(1), 193-215. doi:10.1038/npp.2016.199

Hart, L. G., Deyo, R. A., & Cherkin, D. C. (1995). Physician office visits for low back pain. Frequency, clinical evaluation, and treatment patterns from a U.S. national survey. *Spine (Phila Pa 1976), 20*(1), 11-19.

Hart, R. P., Wade, J. B., & Martelli, M. F. (2003). Cognitive impairment in patients with chronic pain: the significance of stress. *Curr Pain Headache Rep, 7*(2), 116-126.

Hatchard, T., Lepage, C., Hutton, B., Skidmore, B., & Poulin, P. A. (2014). Comparative evaluation of group-based mindfulness-based stress reduction and cognitive behavioral therapy for the treatment and management of chronic pain disorders: protocol for a systematic review and meta-analysis with indirect comparisons. *Syst Rev, 3*(1), 134. doi:10.1186/2046-4053-3-134

Hawley, L. L., Padesky, C. A., Hollon, S. D., Mancuso, E., Laposa, J. M., Brozina, K., & Segal, Z. V. (2017). Cognitive-Behavioral Therapy for Depression Using Mind Over Mood: CBT Skill Use and Differential Symptom Alleviation. *Behav Ther, 48*(1), 29-44. doi:10.1016/j.beth.2016.09.003

Hodges, P. W., & Tucker, K. (2011). Moving differently in pain: a new theory to explain the adaptation to pain. *Pain, 152*(3 Suppl), S90-98. doi:10.1016/j.pain.2010.10.020

Hofmann, S. G., & Smits, J. A. (2008). Cognitive-behavioral therapy for adult anxiety disorders: a meta-analysis of randomized placebo-controlled trials. *J Clin Psychiatry, 69*(4), 621-632.

Hoza, D., Vlasak, A., Horinek, D., Sames, M., & Alfieri, A. (2015). DTI-MRI biomarkers in the search for normal pressure hydrocephalus aetiology: a review. *Neurosurg Rev, 38*(2), 239-244; discussion 244. doi:10.1007/s10143-014-0584-0

Hua, X. Y., Svensson, C. I., Matsui, T., Fitzsimmons, B., Yaksh, T. L., & Webb, M. (2005). Intrathecal minocycline attenuates peripheral inflammation-induced hyperalgesia by inhibiting p38 MAPK in spinal microglia. *Eur J Neurosci, 22*(10), 2431-2440. doi:10.1111/j.1460-9568.2005.04451.x

Ishibashi, T., Dakin, K. A., Stevens, B., Lee, P. R., Kozlov, S. V., Stewart, C. L., & Fields, R. D. (2006). Astrocytes promote myelination in response to electrical impulses. *Neuron, 49*(6), 823-832. doi:10.1016/j.neuron.2006.02.006

Jeurissen, B., Leemans, A., Tournier, J. D., Jones, D. K., & Sijbers, J. (2013). Investigating the prevalence of complex fiber configurations in white matter tissue with diffusion magnetic resonance imaging. *Hum Brain Mapp, 34*(11), 2747-2766. doi:10.1002/hbm.22099

Ji, R. R., Berta, T., & Nedergaard, M. (2013). Glia and pain: is chronic pain a gliopathy? *Pain, 154 Suppl 1*, S10-28. doi:10.1016/j.pain.2013.06.022

Ji, R. R., Kohno, T., Moore, K. A., & Woolf, C. J. (2003). Central sensitization and LTP: do pain and memory share similar mechanisms? *Trends Neurosci, 26*(12), 696-705. doi:10.1016/j.tins.2003.09.017

Ji, R. R., Xu, Z. Z., & Gao, Y. J. (2014). Emerging targets in neuroinflammation-driven chronic pain. *Nat Rev Drug Discov, 13*(7), 533-548. doi:10.1038/nrd4334

Johannes, C. B., Le, T. K., Zhou, X., Johnston, J. A., & Dworkin, R. H. (2010). The prevalence of chronic pain in United States adults: results of an Internet-based survey. *J Pain, 11*(11), 1230-1239. doi:10.1016/j.jpain.2010.07.002

Kang, X., Herron, T. J., Turken, A. U., & Woods, D. L. (2012). Diffusion properties of cortical and pericortical tissue: regional variations, reliability and methodological issues. *Magn Reson Imaging, 30*(8), 1111-1122. doi:10.1016/j.mri.2012.04.004

Kettenmann, H., Kirchhoff, F., & Verkhratsky, A. (2013). Microglia: new roles for the synaptic stripper. *Neuron, 77*(1), 10-18. doi:10.1016/j.neuron.2012.12.023

Kim, D. J., Lim, M., Kim, J. S., Son, K. M., Kim, H. A., & Chung, C. K. (2014). Altered white matter integrity in the corpus callosum in fibromyalgia patients identified by tract-based spatial statistical analysis. *Arthritis Rheumatol, 66*(11), 3190-3199. doi:10.1002/art.38771

Kim, S. H., Stoicea, N., Soghomonyan, S., & Bergese, S. D. (2014). Intraoperative use of remifentanil and opioid induced hyperalgesia/acute opioid tolerance: systematic review. *Front Pharmacol, 5*, 108. doi:10.3389/fphar.2014.00108

Kinnunen, K. M., Greenwood, R., Powell, J. H., Leech, R., Hawkins, P. C., Bonnelle, V., . . . Sharp, D. J. (2011). White matter damage and cognitive impairment after traumatic brain injury. *Brain, 134*(Pt 2), 449-463. doi:10.1093/brain/awq347

Knoerl, R., Lavoie Smith, E. M., & Weisberg, J. (2016). Chronic Pain and Cognitive Behavioral Therapy: An Integrative Review. *West J Nurs Res, 38*(5), 596-628. doi:10.1177/0193945915615869

Kong, J., Spaeth, R. B., Wey, H. Y., Cheetham, A., Cook, A. H., Jensen, K., . . . Gollub, R. L. (2013). S1 is associated with chronic low back pain: a functional and structural MRI study. *Mol Pain, 9*, 43. doi:10.1186/1744-8069-9-43

Kregel, J., Meeus, M., Malfliet, A., Dolphens, M., Danneels, L., Nijs, J., & Cagnie, B. (2015). Structural and functional brain abnormalities in chronic low back pain: A systematic review. *Semin Arthritis Rheum, 45*(2), 229-237. doi:10.1016/j.semarthrit.2015.05.002

Krzyzak, A., Klodowski, K., & Raszewski, Z. (2015). Anisotropic phantoms in Magnetic Resonance Imaging. *Conf Proc IEEE Eng Med Biol Soc, 2015*, 414-417. doi:10.1109/EMBC.2015.7318387

Krzyzak, A. T., & Klodowski, K. (2015). The b matrix calculation using the anisotropic phantoms for DWI and DTI experiments. *Conf Proc IEEE Eng Med Biol Soc, 2015*, 418-421. doi:10.1109/EMBC.2015.7318388

Kwon, O. H., Park, H., Seo, S. W., Na, D. L., & Lee, J. M. (2015). A framework to analyze cerebral mean diffusivity using surface guided diffusion mapping in diffusion tensor imaging. *Front Neurosci, 9*, 236. doi:10.3389/fnins.2015.00236

Langevin, H. M., Fox, J. R., Koptiuch, C., Badger, G. J., Greenan-Naumann, A. C., Bouffard, N. A., . . . Henry, S. M. (2011). Reduced thoracolumbar fascia shear strain in human chronic low back pain. *BMC Musculoskelet Disord, 12*, 203. doi:10.1186/1471-2474-12-203

Latremoliere, A., & Woolf, C. J. (2009). Central sensitization: a generator of pain hypersensitivity by central neural plasticity. *J Pain, 10*(9), 895-926. doi:10.1016/j.jpain.2009.06.012

Lee, P. R., & Fields, R. D. (2009). Regulation of myelin genes implicated in psychiatric disorders by functional activity in axons. *Front Neuroanat, 3*, 4. doi:10.3389/neuro.05.004.2009

Lichenstein, S. D., Bishop, J. H., Verstynen, T. D., & Yeh, F. C. (2016). Diffusion Capillary Phantom vs. Human Data: Outcomes for Reconstruction Methods

Depend on Evaluation Medium. *Front Neurosci, 10*, 407. doi:10.3389/fnins.2016.00407
Lieberman, G., Shpaner, M., Watts, R., Andrews, T., Filippi, C. G., Davis, M., & Naylor, M. R. (2014). White matter involvement in chronic musculoskeletal pain. *J Pain*. doi:10.1016/j.jpain.2014.08.002
Lin, J. C., Chu, L. F., Stringer, E. A., Baker, K. S., Sayyid, Z. N., Sun, J., . . . Younger, J. W. (2016). One Month of Oral Morphine Decreases Gray Matter Volume in the Right Amygdala of Individuals with Low Back Pain: Confirmation of Previously Reported Magnetic Resonance Imaging Results. *Pain Med, 17*(8), 1497-1504. doi:10.1093/pm/pnv047
Liu, J., Dietz, K., DeLoyht, J. M., Pedre, X., Kelkar, D., Kaur, J., . . . Casaccia, P. (2012). Impaired adult myelination in the prefrontal cortex of socially isolated mice. *Nat Neurosci, 15*(12), 1621-1623. doi:10.1038/nn.3263
Liu, J., Dupree, J. L., Gacias, M., Frawley, R., Sikder, T., Naik, P., & Casaccia, P. (2016). Clemastine Enhances Myelination in the Prefrontal Cortex and Rescues Behavioral Changes in Socially Isolated Mice. *J Neurosci, 36*(3), 957-962. doi:10.1523/JNEUROSCI.3608-15.2016
Loggia, M. L., Chonde, D. B., Akeju, O., Arabasz, G., Catana, C., Edwards, R. R., . . . Hooker, J. M. (2015). Evidence for brain glial activation in chronic pain patients. *Brain, 138*(Pt 3), 604-615. doi:10.1093/brain/awu377
Luchtmann, M., Baecke, S., Steinecke, Y., Bernarding, J., Tempelmann, C., Ragert, P., & Firsching, R. (2015). Changes in gray matter volume after microsurgical lumbar discectomy: a longitudinal analysis. *Front Hum Neurosci, 9*, 12. doi:10.3389/fnhum.2015.00012
Lutz, J., Jager, L., de Quervain, D., Krauseneck, T., Padberg, F., Wichnalek, M., . . . Schelling, G. (2008). White and gray matter abnormalities in the brain of patients with fibromyalgia: a diffusion-tensor and volumetric imaging study. *Arthritis Rheum, 58*(12), 3960-3969. doi:10.1002/art.24070
Mackey, A. P., Whitaker, K. J., & Bunge, S. A. (2012). Experience-dependent plasticity in white matter microstructure: reasoning training alters structural connectivity. *Front Neuroanat, 6*, 32. doi:10.3389/fnana.2012.00032
Malfliet, A., Coppieters, I., Van Wilgen, P., Kregel, J., De Pauw, R., Dolphens, M., & Ickmans, K. (2017). Brain changes associated with cognitive and emotional factors in chronic pain: A systematic review. *Eur J Pain, 21*(5), 769-786. doi:10.1002/ejp.1003
Mansour, A. R., Baliki, M. N., Huang, L., Torbey, S., Herrmann, K. M., Schnitzer, T. J., & Apkarian, A. V. (2013). Brain white matter structural properties predict transition to chronic pain. *Pain, 154*(10), 2160-2168. doi:10.1016/j.pain.2013.06.044
Mao, C., Wei, L., Zhang, Q., Liao, X., Yang, X., & Zhang, M. (2013). Differences in brain structure in patients with distinct sites of chronic pain: A voxel-based morphometric analysis. *Neural Regen Res, 8*(32), 2981-2990. doi:10.3969/j.issn.1673-5374.2013.32.001
Martucci, K. T., & Mackey, S. C. (2016). Imaging Pain. *Anesthesiol Clin, 34*(2), 255-269. doi:10.1016/j.anclin.2016.01.001

Martucci, K. T., Ng, P., & Mackey, S. (2014). Neuroimaging chronic pain: what have we learned and where are we going? *Future Neurol, 9*(6), 615-626. doi:10.2217/FNL.14.57

Mazzola, L., Isnard, J., & Mauguiere, F. (2006). Somatosensory and pain responses to stimulation of the second somatosensory area (SII) in humans. A comparison with SI and insular responses. *Cereb Cortex, 16*(7), 960-968. doi:10.1093/cercor/bhj038

Mazzola, L., Isnard, J., Peyron, R., & Mauguiere, F. (2012). Stimulation of the human cortex and the experience of pain: Wilder Penfield's observations revisited. *Brain, 135*(Pt 2), 631-640. doi:10.1093/brain/awr265

McKenzie, I. A., Ohayon, D., Li, H., de Faria, J. P., Emery, B., Tohyama, K., & Richardson, W. D. (2014). Motor skill learning requires active central myelination. *Science, 346*(6207), 318-322. doi:10.1126/science.1254960

Medina, D., DeToledo-Morrell, L., Urresta, F., Gabrieli, J. D., Moseley, M., Fleischman, D., . . . Stebbins, G. T. (2006). White matter changes in mild cognitive impairment and AD: A diffusion tensor imaging study. *Neurobiol Aging, 27*(5), 663-672. doi:10.1016/j.neurobiolaging.2005.03.026

Melzack, R. (1999). From the gate to the neuromatrix. *Pain, Suppl 6*, S121-126.

Melzack, R., & Wall, P. D. (1965). Pain mechanisms: a new theory. *Science, 150*(3699), 971-979.

Millan, M. J. (2002). Descending control of pain. *Prog Neurobiol, 66*(6), 355-474.

Mistry, C. J., Bawor, M., Desai, D., Marsh, D. C., & Samaan, Z. (2014). Genetics of Opioid Dependence: A Review of the Genetic Contribution to Opioid Dependence. *Curr Psychiatry Rev, 10*(2), 156-167. doi:10.2174/1573400510666140320000928

Moayedi, M., Desouza, D., & Erpelding, N. (2011). Making sense of gray matter abnormalities in chronic orofacial pain--synthesizing divergent findings. *J Neurosci, 31*(35), 12396-12397. doi:10.1523/JNEUROSCI.3103-11.2011

Moayedi, M., Weissman-Fogel, I., Salomons, T. V., Crawley, A. P., Goldberg, M. B., Freeman, B. V., . . . Davis, K. D. (2012b). White matter brain and trigeminal nerve abnormalities in temporomandibular disorder. *Pain, 153*(7), 1467-1477. doi:10.1016/j.pain.2012.04.003

Moriarty, O., McGuire, B. E., & Finn, D. P. (2011). The effect of pain on cognitive function: a review of clinical and preclinical research. *Prog Neurobiol, 93*(3), 385-404. doi:10.1016/j.pneurobio.2011.01.002

Olvet, D. M., Delaparte, L., Yeh, F. C., DeLorenzo, C., McGrath, P. J., Weissman, M. M., . . . Parsey, R. V. (2016). A Comprehensive Examination of White Matter Tracts and Connectometry in Major Depressive Disorder. *Depress Anxiety, 33*(1), 56-65. doi:10.1002/da.22445

Ongur, D., Bechtholt, A. J., Carlezon, W. A., Jr., & Cohen, B. M. (2014). Glial abnormalities in mood disorders. *Harv Rev Psychiatry, 22*(6), 334-337. doi:10.1097/HRP.0000000000000060

Pajevic, S., Basser, P. J., & Fields, R. D. (2014). Role of myelin plasticity in oscillations and synchrony of neuronal activity. *Neuroscience, 276*, 135-147. doi:10.1016/j.neuroscience.2013.11.007

Park, S. K., Solomon, D., & Vartanian, T. (2001). Growth factor control of CNS myelination. *Dev Neurosci, 23*(4-5), 327-337.

Porreca, F., Ossipov, M. H., & Gebhart, G. F. (2002). Chronic pain and medullary descending facilitation. *Trends Neurosci, 25*(6), 319-325.

Pullens, P., Roebroeck, A., & Goebel, R. (2010). Ground truth hardware phantoms for validation of diffusion-weighted MRI applications. *J Magn Reson Imaging, 32*(2), 482-488. doi:10.1002/jmri.22243

Rayhan, R. U., Stevens, B. W., Timbol, C. R., Adewuyi, O., Walitt, B., VanMeter, J. W., & Baraniuk, J. N. (2013). Increased brain white matter axial diffusivity associated with fatigue, pain and hyperalgesia in Gulf War illness. *PLoS One, 8*(3), e58493. doi:10.1371/journal.pone.0058493

Ren, K., & Dubner, R. (2008). Neuron-glia crosstalk gets serious: role in pain hypersensitivity. *Curr Opin Anaesthesiol, 21*(5), 570-579. doi:10.1097/ACO.0b013e32830edbdf

Rodriguez-Raecke, R., Niemeier, A., Ihle, K., Ruether, W., & May, A. (2013). Structural brain changes in chronic pain reflect probably neither damage nor atrophy. *PLoS One, 8*(2), e54475. doi:10.1371/journal.pone.0054475

Samad, T. A., Moore, K. A., Sapirstein, A., Billet, S., Allchorne, A., Poole, S., . . . Woolf, C. J. (2001). Interleukin-1beta-mediated induction of Cox-2 in the CNS contributes to inflammatory pain hypersensitivity. *Nature, 410*(6827), 471-475. doi:10.1038/35068566

Schnakers, C., Chatelle, C., Demertzi, A., Majerus, S., & Laureys, S. (2012). What about pain in disorders of consciousness? *AAPS J, 14*(3), 437-444. doi:10.1208/s12248-012-9346-5

Scholz, J., Klein, M. C., Behrens, T. E., & Johansen-Berg, H. (2009). Training induces changes in white-matter architecture. *Nat Neurosci, 12*(11), 1370-1371. doi:10.1038/nn.2412

Schroeter, M. L., Abdul-Khaliq, H., Sacher, J., Steiner, J., Blasig, I. E., & Mueller, K. (2010). Mood disorders are glial disorders: evidence from in vivo studies. *Cardiovasc Psychiatry Neurol, 2010*, 780645. doi:10.1155/2010/780645

Seminowicz, D. A., Shpaner, M., Keaser, M. L., Krauthamer, G. M., Mantegna, J., Dumas, J. A., . . . Naylor, M. R. (2013). Cognitive-behavioral therapy increases prefrontal cortex gray matter in patients with chronic pain. *J Pain, 14*(12), 1573-1584. doi:10.1016/j.jpain.2013.07.020

Seminowicz, D. A., Wideman, T. H., Naso, L., Hatami-Khoroushahi, Z., Fallatah, S., Ware, M. A., . . . Stone, L. S. (2011). Effective treatment of chronic low back pain in humans reverses abnormal brain anatomy and function. *J Neurosci, 31*(20), 7540-7550. doi:10.1523/JNEUROSCI.5280-10.2011

Shpaner, M., Kelly, C., Lieberman, G., Perelman, H., Davis, M., Keefe, F. J., & Naylor, M. R. (2014). Unlearning chronic pain: A randomized controlled trial to investigate changes in intrinsic brain connectivity following Cognitive Behavioral Therapy. *Neuroimage Clin, 5*, 365-376. doi:10.1016/j.nicl.2014.07.008

Skaper, S. D., Facci, L., & Giusti, P. (2014). Neuroinflammation, microglia and mast cells in the pathophysiology of neurocognitive disorders: a review. *CNS Neurol Disord Drug Targets, 13*(10), 1654-1666.

Smallwood, R. F., Laird, A. R., Ramage, A. E., Parkinson, A. L., Lewis, J., Clauw, D. J., . . . Robin, D. A. (2013). Structural brain anomalies and chronic pain: a quantitative meta-analysis of gray matter volume. *J Pain, 14*(7), 663-675. doi:10.1016/j.jpain.2013.03.001

Sullivan, M. D., Edlund, M. J., Fan, M. Y., Devries, A., Brennan Braden, J., & Martin, B. C. (2008). Trends in use of opioids for non-cancer pain conditions 2000-2005 in commercial and Medicaid insurance plans: the TROUP study. *Pain, 138*(2), 440-449. doi:10.1016/j.pain.2008.04.027

Sullivan, M. D., Edlund, M. J., Steffick, D., & Unutzer, J. (2005). Regular use of prescribed opioids: association with common psychiatric disorders. *Pain, 119*(1-3), 95-103. doi:10.1016/j.pain.2005.09.020

Szabo, N., Kincses, Z. T., Pardutz, A., Tajti, J., Szok, D., Tuka, B., . . . Vecsei, L. (2012). White matter microstructural alterations in migraine: a diffusion-weighted MRI study. *Pain, 153*(3), 651-656. doi:10.1016/j.pain.2011.11.029

Tang, Y. Y., Lu, Q., Fan, M., Yang, Y., & Posner, M. I. (2012). Mechanisms of white matter changes induced by meditation. *Proc Natl Acad Sci U S A, 109*(26), 10570-10574. doi:10.1073/pnas.1207817109

Tang, Y. Y., Lu, Q., Geng, X., Stein, E. A., Yang, Y., & Posner, M. I. (2010). Short-term meditation induces white matter changes in the anterior cingulate. *Proc Natl Acad Sci U S A, 107*(35), 15649-15652. doi:10.1073/pnas.1011043107

The Centers for Disease Control and Prevention. (2014). Therapeutic Drug Use. https://www.cdc.gov/nchs/fastats/drug-use-therapeutic.htm

Tracey, I., & Bushnell, M. C. (2009). How neuroimaging studies have challenged us to rethink: is chronic pain a disease? *J Pain, 10*(11), 1113-1120. doi:10.1016/j.jpain.2009.09.001

Tremblay, M. E., Stevens, B., Sierra, A., Wake, H., Bessis, A., & Nimmerjahn, A. (2011). The role of microglia in the healthy brain. *J Neurosci, 31*(45), 16064-16069. doi:10.1523/JNEUROSCI.4158-11.2011

Tsuang, M. T., Lyons, M. J., Meyer, J. M., Doyle, T., Eisen, S. A., Goldberg, J., . . . Eaves, L. (1998). Co-occurrence of abuse of different drugs in men: the role of drug-specific and shared vulnerabilities. *Arch Gen Psychiatry, 55*(11), 967-972.

Walhovd, K. B., Johansen-Berg, H., & Karadottir, R. T. (2014). Unraveling the secrets of white matter--bridging the gap between cellular, animal and human imaging studies. *Neuroscience, 276*, 2-13. doi:10.1016/j.neuroscience.2014.06.058

Wang, T., Shi, F., Jin, Y., Yap, P. T., Wee, C. Y., Zhang, J., . . . Shen, D. (2016). Multilevel Deficiency of White Matter Connectivity Networks in Alzheimer's Disease: A Diffusion MRI Study with DTI and HARDI Models. *Neural Plast, 2016*, 2947136. doi:10.1155/2016/2947136

Wedeen, V. J., Hagmann, P., Tseng, W. Y., Reese, T. G., & Weisskoff, R. M. (2005). Mapping complex tissue architecture with diffusion spectrum magnetic resonance imaging. *Magn Reson Med, 54*(6), 1377-1386. doi:10.1002/mrm.20642

Wedeen, V. J., Wang, R. P., Schmahmann, J. D., Benner, T., Tseng, W. Y., Dai, G., . . . de Crespigny, A. J. (2008). Diffusion spectrum magnetic resonance imaging (DSI) tractography of crossing fibers. *Neuroimage, 41*(4), 1267-1277. doi:10.1016/j.neuroimage.2008.03.036

Willemen, H. L., Eijkelkamp, N., Wang, H., Dantzer, R., Dorn, G. W., 2nd, Kelley, K. W., . . . Kavelaars, A. (2010). Microglial/macrophage GRK2 determines duration of peripheral IL-1beta-induced hyperalgesia: contribution of spinal cord CX3CR1, p38 and IL-1 signaling. *Pain, 150*(3), 550-560. doi:10.1016/j.pain.2010.06.015

Woodworth, D., Mayer, E., Leu, K., Ashe-McNalley, C., Naliboff, B. D., Labus, J. S., . . . Network, M. R. (2015). Unique Microstructural Changes in the Brain Associated with Urological Chronic Pelvic Pain Syndrome (UCPPS) Revealed by Diffusion Tensor MRI, Super-Resolution Track Density Imaging, and Statistical Parameter Mapping: A MAPP Network Neuroimaging Study. *PLoS One, 10*(10), e0140250. doi:10.1371/journal.pone.0140250

Woolf, C. J., & Costigan, M. (1999). Transcriptional and posttranslational plasticity and the generation of inflammatory pain. *Proc Natl Acad Sci U S A, 96*(14), 7723-7730.

Woolf, C. J., & Salter, M. W. (2000). Neuronal plasticity: increasing the gain in pain. *Science, 288*(5472), 1765-1769.

Wu, W., Liang, J., Chen, Y., Chen, A., Wu, Y., & Yang, Z. (2017). Microstructural changes are coincident with the improvement of clinical symptoms in surgically treated compressed nerve roots. *Sci Rep, 7*, 44678. doi:10.1038/srep44678

Xanthos, D. N., & Sandkuhler, J. (2014). Neurogenic neuroinflammation: inflammatory CNS reactions in response to neuronal activity. *Nat Rev Neurosci, 15*(1), 43-53. doi:10.1038/nrn3617

Xian, H., Chantarujikapong, S. I., Scherrer, J. F., Eisen, S. A., Lyons, M. J., Goldberg, J., . . . True, W. R. (2000). Genetic and environmental influences on posttraumatic stress disorder, alcohol and drug dependence in twin pairs. *Drug Alcohol Depend, 61*(1), 95-102.

Yanasak, N., & Allison, J. (2006). Use of capillaries in the construction of an MRI phantom for the assessment of diffusion tensor imaging: demonstration of performance. *Magn Reson Imaging, 24*(10), 1349-1361. doi:10.1016/j.mri.2006.08.001

Yeh, F. C., Tang, P. F., & Tseng, W. Y. (2013). Diffusion MRI connectometry automatically reveals affected fiber pathways in individuals with chronic stroke. *Neuroimage Clin, 2*, 912-921. doi:10.1016/j.nicl.2013.06.014

Yeh, F. C., Wedeen, V. J., & Tseng, W. Y. (2010). Generalized q-sampling imaging. *IEEE Trans Med Imaging, 29*(9), 1626-1635. doi:10.1109/TMI.2010.2045126

Younger, J. W., Chu, L. F., D'Arcy, N. T., Trott, K. E., Jastrzab, L. E., & Mackey, S. C. (2011). Prescription opioid analgesics rapidly change the human brain. *Pain, 152*(8), 1803-1810. doi:10.1016/j.pain.2011.03.028

Yu, D., Yuan, K., Qin, W., Zhao, L., Dong, M., Liu, P., . . . Tian, J. (2013). Axonal loss of white matter in migraine without aura: a tract-based spatial statistics study. *Cephalalgia, 33*(1), 34-42. doi:10.1177/0333102412466964

Yuan, K., Qin, W., Liu, P., Zhao, L., Yu, D., Zhao, L., . . . Tian, J. (2012). Reduced fractional anisotropy of corpus callosum modulates inter-hemispheric resting state functional connectivity in migraine patients without aura. *PLoS One, 7*(9), e45476. doi:10.1371/journal.pone.0045476

Zatorre, R. J., Fields, R. D., & Johansen-Berg, H. (2012). Plasticity in gray and white: neuroimaging changes in brain structure during learning. *Nat Neurosci, 15*(4), 528-536. doi:10.1038/nn.3045

CHAPTER 2: STRUCTURAL NETWORK ALTERATIONS IN CHRONIC MUSCULOSKELETAL PAIN: BEYOND FRACTIONAL ANISOTROPY

Abstract

Chronic pain is a multifactorial condition that is thought to have profound influence on central nervous system structure. In this study, we characterized brain grey (GM) and white matter (WM) alterations in 74 chronic pain participants compared to 31 pain-free controls utilizing neuroimaging techniques. We identified significant volumetric increases in subcortical GM structures as well an increase and decrease in cortical volume in the pain cohort. WM microstructural metrics of complexity and density were shown to be altered in chronic musculoskeletal pain patients across the dorsal attention, sensorimotor, and salience networks. Structural connectivity analysis also yielded increased connectivity from the superior parietal lobule to the hippocampus in pain patients. We propose that these structural changes may reflect dynamic alterations in aberrant signaling that manifest as a result of pain chronification. Specifically, signaling alterations may potentiate neurogenic neuroinflammation which can influence glia reactivity and ultimately affect GM volume and WM diffusion properties. Chronic pain may also alter WM tract properties via myelin remodeling in an activity-dependent manner. Aside from the underlying cellular likelihoods, physical and behavioral dysregulation may also contribute to brain changes. This study encompasses well-documented metrics of GM volume and is the first to delineate altered WM measures of complexity and density in a chronic pain population.

Introduction

Chronic musculoskeletal pain syndrome is a widespread condition affecting both specialized and non-specialized tissue types including muscles, joints, fascia, and bone (Bishop et al., 2016; Dieppe, 2013; Langevin et al., 2011). Unfortunately, the progression and genesis of pain chronicity are still poorly understood phenomena: a subset of patients present with defined trauma or pathology, while others experience symptoms of unknown etiology. In addition to the effects on peripheral tissues, chronic pain has been shown to influence the structure and function of the central nervous system (CNS), including the brain and spinal cord. Given the complexity of pain perception, which relies on sensory, motor, emotional, and cognitive neural networks, investigations have moved beyond the periphery to examining potential CNS contributions to pain pathophysiology.

Through advances in non-invasive magnetic resonance imaging (MRI) technology and statistical approaches, scientists have attempted to delineate pain-related changes in brain structure and function across a variety of chronic pain conditions. Functional neuroimaging studies, utilizing resting state, functional connectivity, and task-based functional magnetic resonance imaging (fMRI), have revealed dynamic changes in chronic pain neurocircuitry (please see Martucci and Mackey (2016) for a current overview of functional brain alterations in chronic pain). In addition, investigators have implemented structural imaging approaches to examine alterations in brain grey matter (GM) volume, thickness, and density in musculoskeletal and other chronic pain subtypes, including neuropathic and visceral conditions (Apkarian et al., 2004; Baliki, Schnitzer, Bauer, & Apkarian, 2011; Buckalew, Haut, Morrow, & Weiner, 2008; Burgmer et al., 2009; Gwilym, Filippini, Douaud, Carr, & Tracey, 2010; Kuchinad et al., 2007; Lutz et al., 2008;

Moayedi et al., 2012a, 2012b; Rodriguez-Raecke, Niemeier, Ihle, Ruether, & May, 2009; Schmidt-Wilcke et al., 2006; Schmidt-Wilcke et al., 2005; Schmidt-Wilcke et al., 2007; Seminowicz et al., 2013; Seminowicz et al., 2011). The directionality of reported outcome measures within cortical structures varies somewhat across the literature, with most reporting diminished GM metrics (Kairys et al., 2015; Kong et al., 2013). Subcortical GM results are not as consistent, and studies report both increases and decreases in GM structural metrics (Kregel et al., 2015). Collectively, most studies document diminished GM metrics across the brain; however, several chronic pain studies have reported increased GM density within cortical regions including the somatosensory cortex and pre-supplementary motor area. Increased subcortical GM has been observed within the amygdala, hippocampus, thalamus, and periaqueductal gray (Bagarinao et al., 2014; Desouza et al., 2013; Mao et al., 2013; Schmidt-Wilcke et al., 2006). Together, these inconsistencies require further investigation in large homogenous pain cohorts.

While standard GM imaging methodologies have proven useful for defining morphometric differences between the chronic pain brain and the healthy brain, substantial debate has been generated regarding the underlying microstructural mechanisms of the observed changes. Fortunately, quantitative diffusion weighted imaging (DWI) can be implemented in conjunction with standard GM (T_1) analyses techniques to investigate GM microstructural changes *in vivo*. This approach is well-established in disease states, such as Schizophrenia (Chiapponi et al., 2013), Alzheimer's disease (Weston, Simpson, Ryan, Ourselin, & Fox, 2015), multiple sclerosis (Deppe et al., 2013), and Creutzfeldt-Jakob disease (Demaerel, Heiner, Robberecht, Sciot, & Wilms, 1999; Zerr et al., 2009), as well as in normal aging (Salminen et al., 2016). Furthermore, several chronic pain studies have

examined GM diffusivity changes in irritable bowel syndrome (Ellingson et al., 2013) and fibromyalgia cohorts (Lutz et al., 2008). These investigations define alterations in GM diffusivity metrics, such as mean diffusivity (MD) and fractional anisotropy (FA), within pain matrix GM regions, including the thalamus, anterior cingulate gyrus, postcentral gyrus, and superior frontal gyrus. Changes in GM diffusion may be reflective of a host of cellular mechanisms. In general, a decrease in mean diffusivity (MD) indicates increased tissue density or cellular crowding and, conversely, an increase in MD suggests diminished cell density. Increased FA in the GM suggests hindrance and linearity of diffusion—potentially, indicating an increase in cell density. Thus, measuring GM diffusivity complements volumetric approaches.

While DWI can be expanded to probe GM microstructure, it is primarily used to investigate WM microstructure and connectivity. The limited existing studies of WM in chronic pain rely on diffusion tensor imaging (DTI) and report microstructural differences in various chronic pain conditions. In a previous study comparing chronic musculoskeletal pain patients to healthy controls, our lab demonstrated global increases in the DTI WM metric, radial diffusivity (RD), across a number of pain-related tracts in a chronic musculoskeletal pain cohort (Lieberman et al., 2014). Findings in other chronic pain subtypes also report changes in DTI indices, including reduced FA (Moayedi et al., 2012b; Szabo et al., 2012; Yuan et al., 2011) and axial diffusivity (AD)(D. J. Kim et al., 2014), as well as increased RD (Farmer et al., 2015) and MD (Hotta, Zhou, Harno, Forss, & Hari, 2017). These WM microstructural alterations often extend throughout the pain matrix to include tracts that relay sensory, motor, affective, and cognitive information.

Over the past several years, the expansive WM DTI literature has come under scrutiny for oversimplifying the complexity of structure within most voxels. The interpretation of single tensor (DTI) findings as proxies of 'tract integrity' may mistakenly imply that changes in diffusion metrics are attributable to neuronal degeneration, loss of myelin, or remodeling. Potential contributions of glia, including microglia and astrocytes, are largely ignored in the interpretation of findings despite the fact that gliosis has been demonstrated to impact tensor derived WM metrics (Alexander et al., 2007; Aojula et al., 2016; Budde et al., 2011; Hoza et al., 2015). Interestingly, positron emission tomography reveals that reactive glia are elevated in chronic low back pain (Loggia et al., 2015), which suggests their particular relevance to microstructural changes observed in pain populations. During reactive gliosis, astrocytes and microglia become morphologically larger, potentially explaining changes in GM volume and diffusivity in chronic pain (Sofroniew & Vinters, 2010; Torres-Platas et al., 2014). Additionally, in the WM, astrocytes regulate the extra-axonal environment at the nodes of Ranvier, which can be impacted by aberrant signaling in chronic pain conditions, leading to oligodendrocyte remodeling, and, ultimately, to glial reactivity. These microstructural changes negatively impact the reliability of single tensor metrics, irrespective of complex fiber geometry, and challenge the broadly used interpretations of tensor changes as reflecting general 'tract integrity.' Despite these important mechanistic considerations for the involvement of glia in chronic pain, very few available studies have utilized advanced DWI analyses approaches, and none have investigated tract-specific differences in the underlying complexity of the WM. Complexity measures may be reflective of alterations in the respective fiber tracts (Figure 2.2). Measuring fiber density and complexity will allow us to disambiguate the origin of

observed neuroplasticity in existing RD studies. Specifically, complexity changes in the absence of density changes support neuronal etiology (e.g., fiber remodeling) and density changes in the absence of complexity changes argue for non-neuronal etiology (e.g., reactive gliosis) (Figure 2.3).

The objectives of this study were, therefore, to 1) reproduce GM morphometric findings reported in the literature in a larger chronic musculoskeletal pain cohort, 2) assess GM MD to inform the interpretation of volumetric changes, specifically as related to GM cell density, 3) investigate WM microstructure to disambiguate RD changes of neuronal and non-neuronal origin, and 4) investigate whether changes in fiber complexity affect WM connectivity between regions, using deterministic tractography.

Materials and Methods

Participant Recruitment and Evaluation

The study was approved by the University of Vermont Institutional Review Board (IRB). All procedures were in compliance with the Declaration of Helsinki. Seventy-four chronic pain patients with a primary diagnosis of musculoskeletal pain and 31 healthy controls were analyzed for this study. Participants with chronic musculoskeletal pain and pain-free healthy controls underwent a baseline (TP1) MRI evaluation to examine structural brain differences which is the focus of this chapter (Figure 2.1). The chronic pain cohort underwent two additional MRI evaluations following behavioral treatment which were analyzed and reported in chapter 3 of this dissertation (Figure 2.1). Prior to imaging, participants were evaluated in-person by a study physician and provided informed consent. Healthy control volunteers completed screening questionnaires and provided informed

consent. Inclusion criteria for chronic pain participants were as follows: a primary diagnosis of musculoskeletal pain, symptoms of pain for at least one year in duration as indicated by self-reports, and a minimum of 4 out of 10 score on a pain likert scale. Exclusion criteria for pain participants were standard MRI contraindications, current daily opioid regimens, a history of traumatic brain injury, unmanaged hypertension or diabetes, and psychiatric disorders including major depression, schizophrenia, and bipolar disorder. Healthy volunteers met similar exclusion criteria and, additionally, could not have a present or past history of chronic pain.

Eligible participants underwent an MRI evaluation consisting of structural (T_1-weighted and diffusion weighted imaging) and functional (resting state, task-based, and evoked) acquisitions. However, for this manuscript, only structural images were analyzed and interpreted.

Magnetic Resonance Imaging Data Acquisition

All data were collected using a Philips 3T Achieva MRI scanner (Philips Healthcare, Best, Netherlands). The scanner underwent an upgrade in the course of the study and an 8-channel sensitivity encoding (SENSE) head coil was replaced with a 15-channel SENSE digital head coil. The same pulse sequences were used before and after the upgrade: T_1-weighted structural imaging data were acquired using a spoiled gradient volumetric sequence oriented perpendicular to the anterior commissure-posterior commissure with 9.9ms TR, 4.6ms TE, 8º flip angle, 256mm FOV, 1.0 NSA, 256 X 256 matrix, and 1.0mm slice thickness with no gap for 140 contiguous slices as well as an axial T2-weighted gradient spin echo sequence using 28 contiguous 5mm slices, 2466ms TR,

80ms TE, 3.0 NSA, and 230mm FOV. Diffusion weighted imaging data were acquired using an axial 2-dimensional spin echo echo planar imaging (EPI) sequence with 46 diffusion directions and the following specifications: 59 slices, 2mm slice thickness, 10,000ms TR, 68ms TE, 2x2mm in-plane resolution, 1000 s/mm^2 B-value, and 63 EPI factor.

Grey Matter (GM) Analyses

1. *GM Morphometry Preprocessing & Analysis*

T_1-weighted images were analyzed with the FSLVBM pipeline (Douaud et al., 2007; Good et al., 2001; S. M. Smith et al., 2004), part of the FSL toolbox. In brief, structural images were first brain extracted, segmented into GM, WM, and cerebral spinal fluid, and non-linearly registered to 2x2x2mm^3 MNI152 standard space. A study specific GM template was generated from the segmented (GM) images with equal pain and control participants selected at random. To achieve this, the resulting images were averaged and flipped along the x-axis to create left-right symmetry. Next, native T_1 images were non-linearly registered to the study-specific template. Modulation was then implemented to correct for local expansion (or contraction) due to the non-linear component of the spatial transformation. An isotropic Gaussian smoothing kernel with a sigma of 3mm was then applied to the modulated GM images.

All 'region of interest' GM masks, except the dorsolateral prefrontal cortex (DLPFC), were obtained from the Harvard-Oxford cortical and subcortical atlases and included the following bilateral structures: anterior cingulate cortex, amygdala, caudate, hippocampus, insula, pre-central gyrus (M1), post-central gyrus (S1), thalamus, and

nucleus accumbens. Masks were created using the FSLVBM generated GM mask and subsequently thresholding the resulting image to include only the overlap with the ROI. The DLPFC mask was generated using Neurosynth (Yarkoni, Poldrack, Nichols, Van Essen, & Wager, 2011) with the search terms "pain" and "DLPFC". The resulting image was anatomically constrained to the frontal pole, middle, and superior frontal gyrii. Finally, as previously described, the resulting mask was overlaid on the GM mask and thresholded at a value of two and binarized. The entire GM mask was used for whole brain analyses. A voxelwise GLM was applied using FSL's, non-parametric, randomise function, with threshold free cluster enhancement to correct for multiple comparisons. Participants' demeaned age and sex were included as covariates of non-interest, and significance was defined at $p \leq 0.05$.

2. GM Diffusion Processing & Analysis

Subcortical GM mean diffusivity (MD) were analyzed using FSL software similarly to Kim and colleagues (H. J. Kim et al., 2013). The following steps were conducted for each subject individually: T_1-weighted images were initially segmented using the FMRIB Integrated Registration and Segmentation Tool (FIRST; (Patenaude, Smith, Kennedy, & Jenkinson, 2011) generating a single brainstem mask and bilateral putamen, caudate, thalamus amygdala, hippocampus, and pallidum masks (Figure 2.4A). Next, the T_1-weighted image was aligned to the b0 image from the DWI acquisition using affine registration (FLIRT). The subcortical masks from the FIRST output were subsequently backtransformed into b0 space by using the inverse T_1 to b0 affine matrix (Figure 2.4B). Cerebrospinal fluid partial voluming effects were mitigated by thresholding the resulting

MD images. Specifically, voxels with an MD > 1.3 x 10^{-3} mm^2/s were removed from all subcortical GM region MD maps (S. E. Rose, Janke, & Chalk, 2008). Finally, mean MD was extracted bilaterally from each subcortical region using the thresholded mask. Extracted GM MD values were statistically compared using SPSS version 24.0 software (IBM Corporation, Armonk, NY, USA). To compare group GM MD means, a univariate general linear model with age and sex nuisance covariates was implemented for each subcortical region without additional correction for multiple comparisons.

White Matter (WM) Analyses

1. WM Fiber Complexity: Mode of Anisotropy (MA) and Ball & Sticks (F1 & F2)

Raw DWI images were first converted to nifti format using MRIcron software (Rorden & Brett, 2000). DWI scans were subsequently analyzed using FSL FMRIB software (Jenkinson, Beckmann, Behrens, Woolrich, & Smith, 2012; S. M. Smith et al., 2004; Woolrich et al., 2009). Utilizing the Diffusion Toolbox, FDT, images underwent eddy current correction, brain extraction, and a T_2 image was extracted from the initial B0 volume. Data were then processed using both a single tensor, diffusion tensor imaging (DTI) model as well as a multi-compartment, Ball-and-Sticks (BAS) model. The resulting DTI model was implemented using dtifit and yielded the following metric maps: Radial diffusivity RD), Axial diffusivity (AD), Mean diffusivity (MD), Fractional Anisotropy (FA), and Mode of anisotropy (MA). MA provides The BAS model was implemented using the Bayesian Estimation of Diffusion Parameters Obtained Using Sampling Techniques (BEDPOSTX) to enable modeling of multiple fiber populations and orientations within each voxel (Behrens, Berg, Jbabdi, Rushworth, & Woolrich, 2007).

Default BEDPOSTX parameters were used: first a multiexponential model was implemented with a burn-in period of 1000 and up to two fiber populations were defined. The BEDPOSTX output generated estimates of each fiber orientation (i.e., x1 or x2) and a corresponding partial volume fraction metric - F1 and F2. Importantly, the model prevents overfitting by shrinking the corresponding F2 metric to 0 in the absence of a secondary fiber orientation or population. Both F1 and F2 correspond to distinct tracts within each voxel where the major or primary fiber population is defined by F1 and minor or secondary fiber population is expressed as F2.

Prior to inclusion, all raw diffusion scans, and metric maps were visually inspected for artifacts, excessive motion, and anatomical abnormalities. The subsequent WM microstructural analyses steps were first carried out on the FA images using the standard FSL tract based spatial statistics pipeline. Downstream statistical comparison was implemented using only the mode of anisotropy (MA) and the partial volume maps (F1 & F2) due to their sensitivity in regions of multiple fiber populations and complex geometry. In brief, FA images were non-linearly registered to the $1mm^3$ isotropic FMRIB58-FA template followed by affine transformation to MNI152 standard space. FA data were then projected onto an alignment-invariant mean FA skeleton image and with the recommended threshold of 0.2. F1 and F2 maps were then aligned to ensure that each fiber orientation corresponded to the same fiber populations across subjects. Next, the warps generated from the non-linear and affine transformations of the FA images were applied to the MA, F1, and F2 data. Statistical inference was carried out using a binary mask of the FA skeletonized image ensuring that only voxels within the center of each tract were analyzed, preventing partial voluming effects.

Region of interest (ROI) and whole brain exploratory analyses were conducted using FSL's randomise method: a non-parametric, permutation approach with threshold free cluster enhancement (tfce) to correct for multiple comparisons. Whole brain voxel-by-voxel analysis was performed for each WM metric (MA, F1, and F2) using the complete thresholded FA skeleton mask and executing a total of ten thousand permutations per voxel t-test. For the ROI analyses, masks for each of the predetermined WM structures were extracted from the Johns Hopkins ICBM-DTI-81 atlas, overlaid on the FA skeleton mask, thresholded to include only the overlap between the FA skeleton and ROI, and binarized. ROIs included the splenium of the corpus callosum and the following bilateral tracts: Anterior and posterior internal capsules, cerebral peduncle, cingulum adjacent to the hippocampus (temporal lobe cingulum), cingulum, external capsule, superior longitudinal fasciculus, and the uncinate fasciculus. Randomise permutation testing with a total of ten thousand permutations per t-test, was then applied to each skeletonized ROI mask. Participant sex and age were used as nuisance covariates, and significance was defined at $p \leq 0.05$.

2. *WM Fiber Density: Fiber Density (FD) & Fiber Cross-Section (FC)*

The following analyses were conducted using Mrtrix3 software (J.-D. Tournier, Calamante, & Connelly, 2012). Diffusion weighted images were first denoised to improve signal-to-noise ratio and reduce scanner artifacts followed by general preprocessing which consisted of eddy current correction and motion correction. Further processing of diffusion weighted images included bias field correction and global intensity normalization across subjects by referencing the median CSF at b=0. A group average response function was

then computed across the entire study population to account for variation due to the low b-value (b=1000) parameter of the study diffusion images. Fixel-based analysis was then implemented as described in-depth by Raffelt and colleagues (Raffelt et al., 2017). In brief, DW images were upsampled by the recommended scaling factor of 2, and a fiber orientation distribution (FOD) function was estimated by performing constrained spherical deconvolution using the group average response function. Next, an unbiased study specific FOD template was created using 40 participants. To do this, a random list generator was used to arbitrarily select 20 patients and 20 controls from the complete subject population to ensure equal contribution to the study template. 'Fixel' direction (fiber populations within a voxel) and fiber density (FD) were calculated for the template. Each subject's FOD images were subsequently registered to the FOD average template, and an intersection template mask for each image was generated. To ensure correspondence between fiber populations across subjects, the intersection mask was used in a two-step thresholding process to create a white matter template mask representing fixels. The resulting fixel mask was cropped at 0.7 to constrain the mask to WM and limit the number of fixels for downstream statistical analysis. FOD images were then transformed into template space, segmented to generate an estimate of FD, reoriented based on the jacobian matrix at each voxel, and assigned spatial correspondence between subject-template fixels. Fiber cross-section (FC) was then obtained using the jacobian matrix warps and the fixel mask followed by a log transformation of the resulting values to ensure a normal distribution centered around zero. Prior to group statistical comparisons, whole brain probabilistic tractography was performed on the FOD template to generate a whole brain structural tractogram (R. E. Smith, Tournier, Calamante, & Connelly, 2013). Group

statistical analyses were conducted on the FD, FC, and FDC metrics independently using connectivity-based fixel enhancement (Raffelt et al., 2015) with 5000 permutations and family wise error correction for multiple comparisons. Sex and demeaned age were provided as a nuisance covariates in the statistical model, and significance was defined at $p \leq 0.05$.

3. Structural Connectivity Analysis

Differences in structural connectivity were calculated using DSI Studio software (http://dsi-studio.labsolver.org). DWI acquisitions were reconstructed using deterministic Q-Space Dieffomorphic Reconstruction (QSDR; (Yeh & Tseng, 2011). QSDR constructs the spin density function in template space and is a generalized form of GQI (Generalized Q-Space Imaging). Following reconstruction, whole brain tractography was initiated similarly to Muraskin and colleagues (Muraskin et al., 2016). In brief, a random number generator was created to toggle several arbitrary variables including quantitative anisotropy (QA), turning angle threshold, and smoothing. Tractography was performed 1,000 times iteratively using random whole brain seeding with the following fixed parameters: step size (1mm) and fiber length (Minimum = 10mm; Maximum = 400mm), and randomly toggled parameters: QA threshold (0.01-0.10), turning angle threshold (40°-80°), and smoothing (50%-80%). 250,000 streamlines were generated for each of the following tractography iterations.

Whole brain connectivity matrices were generated using the 116 parcellation Automated Anatomical Labeling (AAL) atlas (Tzourio-Mazoyer et al., 2002). To quantify the structural connection strength between regions, subsequent 116x116 connectivity

matrices were created by counting the number of streamlines passing through and/or terminating within the respective atlas GM regions (Figure 2.5). Next, a single connectivity matrix was generated for each subject by averaging the 1,000 matrices using MATLAB 2015b Software (The MathWorks Inc., Natick, MA, 2000). Prior to statistical comparison, cerebellar connections were eliminated from connectivity analyses because of varying coverage of the structure across subjects during data acquisition. Between-group differences in connectivity were statistically analyzed using the Network Based Statistics (NBS) Toolbox (Zalesky, Fornito, & Bullmore, 2010). NBS is a validated statistical toolbox that is designed to attenuate issues of multiple comparison in mass univariate testing and facilitate large scale network comparisons. The method uses nonparametric statistical methods to control for family wise error rate. NBS is the relative equivalent of cluster-based statistical approaches except that NBS clusters in topological space instead of physical space. Each subject's average connectivity matrix was input into the NBS toolbox to test between-group connectivity with age and sex as nuisance regressors. A range of recommended t-value thresholds (2.5-3.1) was compared. A total of 5000 permutations were computed with family wise error correction for multiple comparisons. Significance threshold was defined at $p \leq 0.05$.

Results

Demographics

In this study, 74 chronic pain patients (60 females, 14 males) with a primary diagnosis of musculoskeletal pain were compared to 31 healthy controls (18 females, 13 males). Chi square goodness-of-fit testing revealed significant sex differences between the

chronic pain and control cohorts, X^2 (1, N=105) = 6.06, p=0.015. There were proportionally more females in the pain cohort. There were no significant differences in age between the chronic pain (mean ± standard deviation, 45.7 ± 13.03) and healthy control (mean ± SD = 44.13 ± 13.15) groups t(103) = 0.563, p=0.575. Chronic pain patients had an average pain duration of 11 ± 9.15 years with an average pain level of a 5.27 ± 1.96 on a 10-point Likert scale (Table 2.1).

Volumetric and diffusion changes in subcortical and cortical gray matter

Whole-brain voxel based morphometry analysis revealed several significant differences between groups. Chronic pain patients exhibited a decrease in GM volume within the right cerebellum, right occipital fusiform gyrus, and right occipital pole as compared to healthy controls (corrected p<0.05). In contrast, several subcortical regions exhibited increased GM volume in chronic pain patients compared to healthy controls including the right amygdala, hippocampus, and the caudate (corrected, p<0.05) (Figure 2.6). Consistent with these whole-brain findings, *a priori* ROI analyses revealed significant bilateral increases in subcortical GM volume in the nucleus accumbens, amygdala, and caudate in chronic pain patients. Hippocampal volume was increased in pain patients unilaterally within the right hemisphere. Cortical ROI analyses revealed a significant reduction in cortical GM volume in the left precentral (M1) and postcentral (S1) gyrus and the left dorsolateral prefrontal cortex (DLPFC), compared to healthy controls. No significant GM morphometric alterations were observed in the anterior cingulate cortex (ACC) or insular cortices (Table 2.2). The mean diffusivity analysis performed to better characterize volumetric changes did not reveal significant between-group differences in

subcortical ROIs (this analysis was performed on the available subsample of 73 patients and 28 controls). (Table 2.3)

Fiber Complexity Analyses

Between-group WM ROI analyses of one midline and eight bilateral structures, defined *a priori*, revealed significant results in both the mode of anisotropy (MO) and multi-compartment ball & sticks (F1 & F2) measures (Figure 2.7; Table 2.4). Specifically, chronic musculoskeletal pain patients showed a significant reduction in F1 in the right external capsule, right superior longitudinal fasciculus, and the right uncinate fasciculus. F2 ROI analyses yielded significant differences in the left cingulum and splenium of the corpus callosum, with pain patients showing a reduction (in F2) compared to controls. Several tracts were identified that exhibited significantly lower MO in musculoskeletal pain patients compared to healthy controls, including the left cerebral peduncle, the splenium of the corpus callosum, and bilateral external capsule. No significant differences were observed across metrics for the following structures: anterior and posterior internal capsules or the temporal lobe portion of the cingulum abbreviated (Cing. adj. Hipp).

Exploratory whole-brain ball & sticks analyses of the primary fiber population, F1, did not yield statistically significant WM tract differences between chronic musculoskeletal pain patients and healthy controls. However, there were a number of regions that were statistically significant between groups in the secondary fiber population measure, F2, with pain patients showing a global reduction in F2 compared to controls (Figure 2.8A). These included the bilateral anterior, posterior, and superior corona radiata, the bilateral cingulum, bilateral superior longitudinal fasciculus, the left anterior limb of the internal capsule, the left retrolenticular limb of the internal capsule, the left external

capsule, and the genu, splenium, and body of the corpus callosum. To ensure that significant results were not obtained due to the inability of the algorithm to model two fiber populations, we extracted the F2 values of all regions across every subject. We then generated a WM skeleton map to show the tracts where only single fiber populations were found, however, few in number, these do not overlap with the significant results (Figure 2.8B). Analysis of the single tensor metric, MO, yielded a significant between group difference with chronic pain patients exhibiting a lower MO compared to healthy controls. Regions included primarily unilateral differences in the right external capsule, sagittal stratum, retrolenticular part of the internal capsule, the posterior thalamic radiation, and splenium of the corpus callosum.

Fiber Density (FD) & Fiber Cross-Section (FC)

Whole-brain analyses yielded significant between-group differences in FD in the right temporal section of the inferior fronto-occipital fasciculus and the splenium of the corpus callosum at a significance threshold of ($p<0.05$), controlling for age and sex (Figure 2.9). Specifically, chronic musculoskeletal pain patients exhibited a reduction in fiber density within the splenium of the corpus callosum and the right temporal lobe white matter region of the inferior fronto-occipital fasciculus, as compared to healthy controls. No group differences were identified between the cohorts in FC.

WM Connectometry

Whole brain connectivity was assessed using a permutation analysis in the network based statistics toolbox with several test statistic thresholds (2.5, 2.7, 2.9, 3.1) and a

between-group significance threshold of ($p<0.05$), controlling for age and sex. Chronic pain patients exhibited a significant increase in connectivity compared to healthy controls with test statistic thresholds of 2.9 ($p=0.0476$) and 3.1 ($p=0.03$) (Figure 2.10). Specifically, connectivity increases in chronic pain patents were identified between the hippocampus, parietal cortex, thalamus, precuneus, and several visual cortex structures, including the calcarine and cuneus GM. See figure 2.10 for complete table of results and significance values. Conversely, no between group differences in connectivity were observed with statistical t-value thresholds of 2.5 ($p=0.088$) or 2.7 ($p=0.068$).

Discussion

In this study, we aimed to better characterize WM and GM structural alterations in chronic pain. Specifically, we combined standard volumetric GM analyses with metrics of GM diffusivity in order to better understand GM microstructure. We also combined several novel measures of WM complexity, density, and connectivity to better characterize the nature of WM changes in chronic pain, that is, to discriminate between microstructural alterations of neuronal and non-neuronal origin. We found that chronic musculoskeletal pain patients had: 1) increased subcortical and predominantly decreased cortical GM volume, with no significant microstructural changes in GM mean diffusivity; 2) alterations in white matter complexity (MO, F1, & F2) in several major fibers pathways of the pain matrix; 3) reduced WM fiber tract density in the inferior fronto-occipital fasciculus (IFOF) and splenium of the corpus callosum; 4) increased WM connectivity between prominent structures of the pain matrix, including the thalamus, hippocampus, and superior parietal gyrus.

Significance of Pain Related Structural Alterations on Brain Networks

We discuss these findings in the context of the pain matrix. Functional and structural studies implicate the following networks in pain chronification: dorsal attention, sensorimotor, and salience networks. Although many GM regions and WM tracts may belong to more than one discrete network, this framework helps bring multiple imaging modalities together. We argue that alterations in the dorsal attention network are consistent with non-neuronal origins and involvement of reactive glia, alterations of the sensorimotor and the salience networks are consistent with neuronal etiology.

The Dorsal Attention Network

The *dorsal attention network* relies on superior parietal lobule, frontal eye fields, inferior precentral sulcus, superior occipital gyrus, and the dorsolateral prefrontal cortex in order to guide attention and orienting (Corbetta & Shulman, 2002; Fox et al., 2005; Iannetti & Mouraux, 2010; Uddin, 2015). Activity within the dorsal attention network is related to increased threat value of pain (Legrain, Iannetti, Plaghki, & Mouraux, 2011). Functional MRI studies have reported aberrations in the dorsal attention network in chronic pain cohorts (Napadow et al., 2010), including chronic low back pain (Wasan et al., 2011). Compared to controls, we observed decreased left DLPFC volume, a region involved in cognitive, affective, and sensory processing of pain, and implicated in top-down pain modulation (Ayache et al., 2016; Brighina et al., 2011; Tracey & Mantyh, 2007). The left DLPFC is more commonly involved in pain modulation than the right DLPFC (Seminowicz & Moayedi, 2017), which is consistent with our findings. Factors such as loss of descending pain inhibition or dysfunctional cognitive coping strategies, may potentiate DLPFC structural changes in pain populations. Specifically, associations between GM

volume in the DLPFC and catastrophizing have been documented in pain cohorts (C. S. Hubbard et al., 2014; Seminowicz et al., 2013). In addition to morphometric changes, we also demonstrated microstructural WM alterations in tracts projecting to the DLPFC and other dorsal attention network regions. Compared to healthy controls, chronic pain patients exhibited a reduced WM fiber density in the inferior fronto-occipital fasciculus (IFOF). The IFOF is a long association pathway that contains fibers, which connect frontal (including DLPFC), superior parietal, and occipital lobes via the insula (Martino, Brogna, Robles, Vergani, & Duffau, 2010; Sarubbo, De Benedictis, Maldonado, Basso, & Duffau, 2013; Y. Wu, Sun, Wang, & Wang, 2016). Given the range of anatomical structures that the IFOF connects, it may integrate information across different nodes of the pain matrix, not just the dorsal attention network. Nonetheless, increasing evidence argues for the importance of the IFOF in attention, as well as pain processing, emotional regulation, and reward (Camara, Rodriguez-Fornells, & Munte, 2010; Catani & Thiebaut de Schotten, 2008; Rayhan et al., 2013; Tian et al., 2016).

We further identified WM tract alterations in the splenium of the corpus callosum, which connects to the parietal, including the superior parietal lobule, and temporal lobes (Knyazeva, 2013). We observed changes in white matter complexity (F2 and MO) and density (FD). F2 was reduced in the chronic pain cohort, indicating fewer secondary fiber populations and, therefore, a less complex circuit. Similarly, MO was elevated in pain patients, which suggests decreased complexity. Given the known geometry of the corpus callosum, it is possible that voxels within the splenium included more than two fiber populations and, thus, were more accurately characterized by the less constrained MO

modeling. At the same time, fiber density was decreased in chronic pain, indicating possible involvement of reactive glia.

Connectivity analyses revealed alterations in the dorsal attention network WM pathways. Compared to healthy control participants, increased connectivity was detected between the superior parietal lobule and the hippocampus. This is consistent with the finding of decreased pain-related functional connectivity between DLPFC and the hippocampus in fibromyalgia patients (Napadow et al., 2010).

The Sensorimotor Network

The *sensorimotor network* is involved in sensory and motor integration (Butler, 2017) and is connected to higher-order pain processing regions (Makin et al., 2015; Markov et al., 2013). Structural and functional alterations of the sensorimotor network have been observed in chronic pain subtypes, possibly indicating changes in movement patterns and sensory activity-dependent signaling (Desouza et al., 2013; Maeda et al., 2017; Vrana et al., 2015). Compensatory nocifensive behaviors, e.g. adaptations in movement patterns (Caeyenberghs, Pijnenburg, Goossens, Janssens, & Brumagne, 2017) and motor control (Haavik & Murphy, 2012), are well documented in chronic low back pain cohorts, and are manifested in functional connectivity differences, when chronic pain patients are asked to imagine physical activity (Vrana et al., 2015). Pain chronification and threat or fear of injury can lead to physiological alterations in the musculoskeletal system (Hodges & Tucker, 2011; Lund, Donga, Widmer, & Stohler, 1991; Roland, 1986). At the same time, peripheral and central sensitization contributes to aberrant neuronal signaling in the brain (Ji et al., 2014). All of these factors perpetuate the cycle pain chronification.

The ROI analysis, but not the whole-brain analysis, revealed volumetric decreases in chronic pain within the precentral gyrus (primary motor) and postcentral gyrus (S1). Morphometric findings in these regions are inconsistent across studies. While most studies report increased postcentral (S1) volume in pain syndromes, our results are similar to the investigation of chronic back pain by Mao and colleagues (Mao et al., 2013). We also identified WM complexity differences in sensorimotor tracts, including increased complexity (reduced F1) in the right superior longitudinal fasciculus (SLF) in chronic pain patients, a tract that relays somatosensory information and motor behavior (X. Wang et al., 2016). We identified between-group differences in the left cerebral peduncle, which contains both ascending sensory and descending motor fibers, including the corticospinal tract. Chronic pain patients exhibited increased complexity (reduced MO) in the left cerebral peduncle, compared to healthy control participants. The cerebral peduncles carry both sensory and motor fibers, but are infrequently reported in white matter microstructural investigations of chronic pain. Increased complexity in both the SLF and the cerebral peduncles supports our previously reported increases in RD within these regions in a subsample of this pain cohort (Lieberman et al., 2014).

The basal ganglia, key structures of the sensorimotor network, have profound implications for motor and behavioral responses to pain via thalamo-cortico-basal-ganglia loops and are important for modulation of cognitive, affective, and sensory information (Borsook, Upadhyay, Chudler, & Becerra, 2010; Cohen, Schoene-Bake, Elger, & Weber, 2009). Our findings of increased caudate volume in the chronic pain cohort support the involvement of the basal ganglia network in musculoskeletal pain. While a reduction of subcortical volume is more commonly reported across the pain literature, our subcortical

volumetric increases are consistent with findings of increased GM volume in back pain patients (Mao et al., 2013), as well as in paroxysmal pain disorders, such as trigeminal neuralgia (Desouza et al., 2013). Together, our findings of structural alterations (GM volume and WM complexity) within regions of the sensorimotor network suggest altered sensory, motor, and cognitive activity, which likely contribute to chronic pain pathology. Further studies are warranted to determine the direction of this cause-effect relationship.

The Salience Network

The *salience network* is important for merging internal and external events with particular significance for delineating the value of behaviorally relevant stimuli that are deserving of the individual's attention. In chronic pain states this could include adaptations in response to sensory experiences in seek of relief from pain and discomfort. GM structures classically thought to comprise the salience network include the cingulate cortex, medial prefrontal cortex, anterior insular cortex, the cerebellum, and the pulvinar (Borsook, Edwards, Elman, Becerra, & Levine, 2013). Moreover, amygdalo-hippocampal and amygdalo-frontal circuits have also been implicated in salience processing and are potentially key contributors to network dysfunction and alterations in behavior. The salience network receives inputs from the hypothalamic-pituitary-adrenal axis (HPA axis), which is involved in stress response and endocrine functions, including anxiety (Becerra, Breiter, Wise, Gonzalez, & Borsook, 2001; Maleki et al., 2013).

Whole brain GM morphometry analyses exhibited increased amygdala volume in the chronic pain cohort, which extended to the hippocampal region. Classically, the hippocampus is known for its role in learning and memory, although it also has pivotal functions in the modulation of nociception and integration of nociceptive and emotional

aspects of pain and modulation of sensorimotor processes (Bast & Feldon, 2003; Covey, Ignatowski, Knight, & Spengler, 2000; Fasick, Spengler, Samankan, Nader, & Ignatowski, 2015; S. L. Jones & Gebhart, 1986; Vasic & Schmidt, 2017). Volumetric findings in the hippocampus are inconsistent, and warrant further investigation. Specifically, diminished hippocampal volume has been documented in chronic low back pain, osteoarthritis (Baliki, Schnitzer, et al., 2011), and fibromyalgia (McCrae C. et al., J Pain Res. 2015), whereas others found no osteoarthritis-related changes in the hippocampus (Mutso et al., 2012), and increased volume has been reported in migraineurs (C. S. Hubbard et al., 2014).

In addition to these changes in subcortical GM, WM ROI analyses identified significant tract differences within the salience network, including the right uncinate fasciculus. The uncinate fasciculus is an important white matter pathway connecting limbic structures in the temporal lobe, such as the amygdala and hippocampus, to the frontal cortices and abnormalities in this WM tract have been linked to dysregulation in emotional processing and anxiety (Tromp et al., 2012). Specifically, pain patients exhibited increased complexity (decrease in the F1 metric, the dominant fiber population). Similar diffusivity changes in this tract have also been reported in chronic migraineurs and were associated with cognitive reserve (Gomez-Beldarrain et al., 2016). We speculate that this may suggest weaker uncinate connections in pain patients, indicative of dysfunctional top-down regulation.

Other WM tract alterations that project to GM structures involved in salience processing showed reduced complexity (F2 reduction) in the cingulum bundle. The cingulum is a limbic association pathway with projections spanning the entire cingulate to the limbic regions, thus communicating between GM structures involved in evaluative and

affective components of pain. Neuromodulation of the cingulum via deep brain stimulation has been shown to effectively alleviate pain following spinal cord injury, further highlighting the critical role of this structure in chronic pain syndromes (Spooner, Yu, Kao, Sillay, & Konrad, 2007).

Another important node of the salience network is the insula. Lesion studies suggest that it may serve a key function in 'cortical tuning' of afferent signaling (Starr et al., 2009) and may be integral for pain chronification (Lu et al., 2016). We found increased complexity (reduced F1) in the right external capsule in pain patients, compared to controls. We also found bilateral increases in complexity as measured with a more general metric of tract complexity (reductions in MO). Taken together, our results suggest substantial GM and WM alterations within salience network structures, which may contribute to dysfunction in the emotional aspects of pain processing. Changes in the complexity of neural circuits in chronic pain patients argue for alterations of the neural tracts themselves and not the reactive glia.

Biological Significance of Pain Related Structural Brain Alterations

In this chapter, we identified alterations in GM volume as well as differences in WM fiber complexity, density, and connectivity. Although the mechanisms underlying GM and WM alterations in chronic pain remain unresolved, previous studies have demonstrated plasticity within the affected structures following successful relinquishment of pain symptoms suggesting that changes are not likely due to neuronal degeneration (Maeda et al., 2017; Rodriguez-Raecke et al., 2013). Instead, GM volume could be decreased through neuronal plasticity in the form of dendritic arborization and synaptic pruning, and increased due to variations in receptor density. Conversely, non-neuronal

influences such as cellular crowding via increased glial cell number, reactivity and morphology in pain populations could also contribute to increased GM density (Jutzeler et al., 2016; Loggia et al., 2015; Pomares et al., 2017; Zatorre et al., 2012). To explore cell density changes in the GM, we implemented a GM mean diffusivity analysis which was unsuccessful at delineating subcortical differences in microstructure between participants with pain and healthy controls. One limitation of our investigation is that we generated an average diffusivity value across each GM region and it is possible that specific subnuclei within these structures are differentially affected, diluting the sensitivity of the measurement. Future work using study specific GM ROIs may be more appropriate to substantiate these hypotheses.

Similarly, glial cells are also prevalent within the WM and our findings of decreased fiber density in the IFOF and splenium of the corpus callosum may represent non-neuronal changes that mediate the packing density of the WM tracts. While neuronal factors such as dynamic changes in myelination and degeneration could also feasibly alter GM density, the lack of overlap in our density and complexity findings further support non-neuronal influences. Although we do not interpret the structural findings in this chapter to derive from neuronal degeneration, it is likely that WM alterations in chronic pain are influenced by other glial or neuronal origins. The alterations in WM complexity and connectivity that were identified may be explained by activity-dependent myelin remodeling within pain related fiber tracts or even axonal sprouting (Ganguly & Poo, 2013; Jutzeler et al., 2016; Loggia et al., 2015; Zatorre et al., 2012). Conversely, underlying WM tract differences may not necessarily develop from chronic pain, but could instead predispose individuals to developing a chronic pain condition (Mansour et al., 2013).

Summary & Conclusions

Combined, the results presented in this manuscript provide evidence of structural alterations in the chronic pain brain in comparison to healthy controls. In contrast to previous reports, we found increases in subcortical GM volume, primarily the amygdala and the caudate. We did not observe any significant between-group differences in GM diffusivity (measured as MD) in subcortical GM, thus, the mechanisms leading to GM alterations in pain patients remain unclear. We provide the first evidence of fiber density and complexity alterations in the chronic pain brain within the sensorimotor, salience, and dorsal attention networks. We propose that WM complexity differences may be of neuronal origin and reflective of activity-dependent changes in myelination properties. In contrast, we believe that observed alterations in WM fiber density may be reflective of non-neuronal changes such as increased glial reactivity which has been documented in chronic pain cohorts. Finally, increased connectivity between several regions of the pain matrix supports the notion that structural changes are distributed throughout the pain matrix in chronic pain.

Acknowledgments

Funding for this work was provided by the National Institute of Arthritis and Musculoskeletal and Skin Diseases (NIAMS) grants R21-AR055716 and R01-AR059674. The authors would like to thank the UVM MRI Center for Biomedical Imaging for their assistance with data acquisition.

References for Chapter 2

Alexander, A. L., Lee, J. E., Lazar, M., & Field, A. S. (2007). Diffusion tensor imaging of the brain. *Neurotherapeutics, 4*(3), 316-329. doi:10.1016/j.nurt.2007.05.011

Aojula, A., Botfield, H., McAllister, J. P., 2nd, Gonzalez, A. M., Abdullah, O., Logan, A., & Sinclair, A. (2016). Diffusion tensor imaging with direct cytopathological validation: characterisation of decorin treatment in experimental juvenile communicating hydrocephalus. *Fluids Barriers CNS, 13*(1), 9. doi:10.1186/s12987-016-0033-2

Apkarian, A. V., Sosa, Y., Sonty, S., Levy, R. M., Harden, R. N., Parrish, T. B., & Gitelman, D. R. (2004). Chronic back pain is associated with decreased prefrontal and thalamic gray matter density. *J Neurosci, 24*(46), 10410-10415. doi:10.1523/JNEUROSCI.2541-04.2004

Ayache, S. S., Palm, U., Chalah, M. A., Al-Ani, T., Brignol, A., Abdellaoui, M., . . . Lefaucheur, J. P. (2016). Prefrontal tDCS Decreases Pain in Patients with Multiple Sclerosis. *Front Neurosci, 10*, 147. doi:10.3389/fnins.2016.00147

Bagarinao, E., Johnson, K. A., Martucci, K. T., Ichesco, E., Farmer, M. A., Labus, J., . . . Mackey, S. (2014). Preliminary structural MRI based brain classification of chronic pelvic pain: A MAPP network study. *Pain, 155*(12), 2502-2509. doi:10.1016/j.pain.2014.09.002

Baliki, M. N., Schnitzer, T. J., Bauer, W. R., & Apkarian, A. V. (2011). Brain morphological signatures for chronic pain. *PLoS One, 6*(10), e26010. doi:10.1371/journal.pone.0026010

Bast, T., & Feldon, J. (2003). Hippocampal modulation of sensorimotor processes. *Prog Neurobiol, 70*(4), 319-345.

Becerra, L., Breiter, H. C., Wise, R., Gonzalez, R. G., & Borsook, D. (2001). Reward circuitry activation by noxious thermal stimuli. *Neuron, 32*(5), 927-946.

Behrens, T. E., Berg, H. J., Jbabdi, S., Rushworth, M. F., & Woolrich, M. W. (2007). Probabilistic diffusion tractography with multiple fibre orientations: What can we gain? *Neuroimage, 34*(1), 144-155. doi:10.1016/j.neuroimage.2006.09.018

Bishop, J. H., Fox, J. R., Maple, R., Loretan, C., Badger, G. J., Henry, S. M., . . . Langevin, H. M. (2016). Ultrasound Evaluation of the Combined Effects of Thoracolumbar Fascia Injury and Movement Restriction in a Porcine Model. *PLoS One, 11*(1), e0147393. doi:10.1371/journal.pone.0147393

Borsook, D., Edwards, R., Elman, I., Becerra, L., & Levine, J. (2013). Pain and analgesia: the value of salience circuits. *Prog Neurobiol, 104*, 93-105. doi:10.1016/j.pneurobio.2013.02.003

Borsook, D., Upadhyay, J., Chudler, E. H., & Becerra, L. (2010). A key role of the basal ganglia in pain and analgesia--insights gained through human functional imaging. *Mol Pain, 6*, 27. doi:10.1186/1744-8069-6-27

Brighina, F., De Tommaso, M., Giglia, F., Scalia, S., Cosentino, G., Puma, A., . . . Fierro, B. (2011). Modulation of pain perception by transcranial magnetic stimulation of left prefrontal cortex. *J Headache Pain, 12*(2), 185-191. doi:10.1007/s10194-011-0322-8

Buckalew, N., Haut, M. W., Morrow, L., & Weiner, D. (2008). Chronic pain is associated with brain volume loss in older adults: preliminary evidence. *Pain Med, 9*(2), 240-248. doi:10.1111/j.1526-4637.2008.00412.x

Budde, M. D., Janes, L., Gold, E., Turtzo, L. C., & Frank, J. A. (2011). The contribution of gliosis to diffusion tensor anisotropy and tractography following traumatic brain injury: validation in the rat using Fourier analysis of stained tissue sections. *Brain, 134*(Pt 8), 2248-2260. doi:10.1093/brain/awr161

Burgmer, M., Gaubitz, M., Konrad, C., Wrenger, M., Hilgart, S., Heuft, G., & Pfleiderer, B. (2009). Decreased gray matter volumes in the cingulo-frontal cortex and the amygdala in patients with fibromyalgia. *Psychosom Med, 71*(5), 566-573. doi:10.1097/PSY.0b013e3181a32da0

Butler, S. (2017). Important new insight in pain and pain treatment induced changes in functional connectivity between the Pain Matrix and the Salience, Central Executive, and Sensorimotor networks. *Scandinavian Journal of Pain, 16*, 64-65.

Caeyenberghs, K., Pijnenburg, M., Goossens, N., Janssens, L., & Brumagne, S. (2017). Associations between Measures of Structural Morphometry and Sensorimotor Performance in Individuals with Nonspecific Low Back Pain. *AJNR Am J Neuroradiol, 38*(1), 183-191. doi:10.3174/ajnr.A5020

Camara, E., Rodriguez-Fornells, A., & Munte, T. F. (2010). Microstructural brain differences predict functional hemodynamic responses in a reward processing task. *J Neurosci, 30*(34), 11398-11402. doi:10.1523/JNEUROSCI.0111-10.2010

Catani, M., & Thiebaut de Schotten, M. (2008). A diffusion tensor imaging tractography atlas for virtual in vivo dissections. *Cortex, 44*(8), 1105-1132. doi:10.1016/j.cortex.2008.05.004

Chiapponi, C., Piras, F., Piras, F., Fagioli, S., Caltagirone, C., & Spalletta, G. (2013). Cortical grey matter and subcortical white matter brain microstructural changes in schizophrenia are localised and age independent: a case-control diffusion tensor imaging study. *PLoS One, 8*(10), e75115. doi:10.1371/journal.pone.0075115

Cohen, M. X., Schoene-Bake, J. C., Elger, C. E., & Weber, B. (2009). Connectivity-based segregation of the human striatum predicts personality characteristics. *Nat Neurosci, 12*(1), 32-34. doi:10.1038/nn.2228

Corbetta, M., & Shulman, G. L. (2002). Control of goal-directed and stimulus-driven attention in the brain. *Nat Rev Neurosci, 3*(3), 201-215. doi:10.1038/nrn755

Covey, W. C., Ignatowski, T. A., Knight, P. R., & Spengler, R. N. (2000). Brain-derived TNFalpha: involvement in neuroplastic changes implicated in the conscious perception of persistent pain. *Brain Res, 859*(1), 113-122.

Demaerel, P., Heiner, L., Robberecht, W., Sciot, R., & Wilms, G. (1999). Diffusion-weighted MRI in sporadic Creutzfeldt-Jakob disease. *Neurology, 52*(1), 205-208.

Deppe, M., Muller, D., Kugel, H., Ruck, T., Wiendl, H., & Meuth, S. G. (2013). DTI detects water diffusion abnormalities in the thalamus that correlate with an extremity pain episode in a patient with multiple sclerosis. *Neuroimage Clin, 2*, 258-262. doi:10.1016/j.nicl.2013.01.008

Desouza, D. D., Moayedi, M., Chen, D. Q., Davis, K. D., & Hodaie, M. (2013). Sensorimotor and Pain Modulation Brain Abnormalities in Trigeminal Neuralgia: A Paroxysmal, Sensory-Triggered Neuropathic Pain. *PLoS One, 8*(6), e66340. doi:10.1371/journal.pone.0066340

Dieppe, P. (2013). Chronic musculoskeletal pain. *BMJ, 346*, f3146. doi:10.1136/bmj.f3146

Douaud, G., Smith, S., Jenkinson, M., Behrens, T., Johansen-Berg, H., Vickers, J., . . . James, A. (2007). Anatomically related grey and white matter abnormalities in adolescent-onset schizophrenia. *Brain, 130*(Pt 9), 2375-2386. doi:10.1093/brain/awm184

Ellingson, B. M., Mayer, E., Harris, R. J., Ashe-McNally, C., Naliboff, B. D., Labus, J. S., & Tillisch, K. (2013). Diffusion tensor imaging detects microstructural reorganization in the brain associated with chronic irritable bowel syndrome. *Pain, 154*(9), 1528-1541. doi:10.1016/j.pain.2013.04.010

Farmer, M. A., Huang, L., Martucci, K., Yang, C. C., Maravilla, K. R., Harris, R. E., . . . Network, M. R. (2015). Brain White Matter Abnormalities in Female Interstitial Cystitis/Bladder Pain Syndrome: A MAPP Network Neuroimaging Study. *J Urol, 194*(1), 118-126. doi:10.1016/j.juro.2015.02.082

Fasick, V., Spengler, R. N., Samankan, S., Nader, N. D., & Ignatowski, T. A. (2015). The hippocampus and TNF: Common links between chronic pain and depression. *Neurosci Biobehav Rev, 53*, 139-159. doi:10.1016/j.neubiorev.2015.03.014

Fox, M. D., Snyder, A. Z., Vincent, J. L., Corbetta, M., Van Essen, D. C., & Raichle, M. E. (2005). The human brain is intrinsically organized into dynamic, anticorrelated functional networks. *Proc Natl Acad Sci U S A, 102*(27), 9673-9678. doi:10.1073/pnas.0504136102

Ganguly, K., & Poo, M. M. (2013). Activity-dependent neural plasticity from bench to bedside. *Neuron, 80*(3), 729-741. doi:10.1016/j.neuron.2013.10.028

Gomez-Beldarrain, M., Oroz, I., Zapirain, B. G., Ruanova, B. F., Garcia-Chimeno, Y., Cabrera, A., . . . Garcia-Monco, J. C. (2016). Erratum to: Right fronto-insular white matter tracts link cognitive reserve and pain in migraine patients. *J Headache Pain, 17*, 22. doi:10.1186/s10194-016-0617-x

Good, C. D., Johnsrude, I. S., Ashburner, J., Henson, R. N., Friston, K. J., & Frackowiak, R. S. (2001). A voxel-based morphometric study of ageing in 465 normal adult human brains. *Neuroimage, 14*(1 Pt 1), 21-36. doi:10.1006/nimg.2001.0786

Gwilym, S. E., Filippini, N., Douaud, G., Carr, A. J., & Tracey, I. (2010). Thalamic atrophy associated with painful osteoarthritis of the hip is reversible after arthroplasty: a longitudinal voxel-based morphometric study. *Arthritis Rheum, 62*(10), 2930-2940. doi:10.1002/art.27585

Haavik, H., & Murphy, B. (2012). The role of spinal manipulation in addressing disordered sensorimotor integration and altered motor control. *J Electromyogr Kinesiol, 22*(5), 768-776. doi:10.1016/j.jelekin.2012.02.012

Hodges, P. W., & Tucker, K. (2011). Moving differently in pain: a new theory to explain the adaptation to pain. *Pain, 152*(3 Suppl), S90-98. doi:10.1016/j.pain.2010.10.020

Hotta, J., Zhou, G., Harno, H., Forss, N., & Hari, R. (2017). Complex regional pain syndrome: The matter of white matter? *Brain Behav, 7*(5), e00647. doi:10.1002/brb3.647

Hoza, D., Vlasak, A., Horinek, D., Sames, M., & Alfieri, A. (2015). DTI-MRI biomarkers in the search for normal pressure hydrocephalus aetiology: a review. *Neurosurg Rev, 38*(2), 239-244; discussion 244. doi:10.1007/s10143-014-0584-0

Hubbard, C. S., Khan, S. A., Keaser, M. L., Mathur, V. A., Goyal, M., & Seminowicz, D. A. (2014). Altered Brain Structure and Function Correlate with Disease Severity and Pain Catastrophizing in Migraine Patients. *eNeuro, 1*(1), e20 14. doi:10.1523/ENEURO.0006-14.2014

Iannetti, G. D., & Mouraux, A. (2010). From the neuromatrix to the pain matrix (and back). *Exp Brain Res, 205*(1), 1-12. doi:10.1007/s00221-010-2340-1

Jenkinson, M., Beckmann, C. F., Behrens, T. E., Woolrich, M. W., & Smith, S. M. (2012). Fsl. *Neuroimage, 62*(2), 782-790. doi:10.1016/j.neuroimage.2011.09.015

Ji, R. R., Xu, Z. Z., & Gao, Y. J. (2014). Emerging targets in neuroinflammation-driven chronic pain. *Nat Rev Drug Discov, 13*(7), 533-548. doi:10.1038/nrd4334

Jones, S. L., & Gebhart, G. F. (1986). Quantitative characterization of ceruleospinal inhibition of nociceptive transmission in the rat. *J Neurophysiol, 56*(5), 1397-1410.

Jutzeler, C. R., Huber, E., Callaghan, M. F., Luechinger, R., Curt, A., Kramer, J. L., & Freund, P. (2016). Association of pain and CNS structural changes after spinal cord injury. *Sci Rep, 6*, 18534. doi:10.1038/srep18534

Kairys, A. E., Schmidt-Wilcke, T., Puiu, T., Ichesco, E., Labus, J. S., Martucci, K., . . . Harris, R. E. (2015). Increased brain gray matter in the primary somatosensory cortex is associated with increased pain and mood disturbance in patients with interstitial cystitis/painful bladder syndrome. *J Urol, 193*(1), 131-137. doi:10.1016/j.juro.2014.08.042

Kim, D. J., Lim, M., Kim, J. S., Son, K. M., Kim, H. A., & Chung, C. K. (2014). Altered white matter integrity in the corpus callosum in fibromyalgia patients identified by tract-based spatial statistical analysis. *Arthritis Rheumatol, 66*(11), 3190-3199. doi:10.1002/art.38771

Kim, H. J., Kim, S. J., Kim, H. S., Choi, C. G., Kim, N., Han, S., . . . Lee, C. S. (2013). Alterations of mean diffusivity in brain white matter and deep gray matter in Parkinson's disease. *Neurosci Lett, 550*, 64-68. doi:10.1016/j.neulet.2013.06.050

Knyazeva, M. G. (2013). Splenium of corpus callosum: patterns of interhemispheric interaction in children and adults. *Neural Plast, 2013*, 639430. doi:10.1155/2013/639430

Kong, J., Spaeth, R. B., Wey, H. Y., Cheetham, A., Cook, A. H., Jensen, K., . . . Gollub, R. L. (2013). S1 is associated with chronic low back pain: a functional and structural MRI study. *Mol Pain, 9*, 43. doi:10.1186/1744-8069-9-43

Kregel, J., Meeus, M., Malfliet, A., Dolphens, M., Danneels, L., Nijs, J., & Cagnie, B. (2015). Structural and functional brain abnormalities in chronic low back pain: A systematic review. *Semin Arthritis Rheum, 45*(2), 229-237. doi:10.1016/j.semarthrit.2015.05.002

Kuchinad, A., Schweinhardt, P., Seminowicz, D. A., Wood, P. B., Chizh, B. A., & Bushnell, M. C. (2007). Accelerated brain gray matter loss in fibromyalgia patients: premature aging of the brain? *J Neurosci, 27*(15), 4004-4007. doi:10.1523/JNEUROSCI.0098-07.2007

Langevin, H. M., Fox, J. R., Koptiuch, C., Badger, G. J., Greenan-Naumann, A. C., Bouffard, N. A., . . . Henry, S. M. (2011). Reduced thoracolumbar fascia shear strain in human chronic low back pain. *BMC Musculoskelet Disord, 12*, 203. doi:10.1186/1471-2474-12-203

Legrain, V., Iannetti, G. D., Plaghki, L., & Mouraux, A. (2011). The pain matrix reloaded: a salience detection system for the body. *Prog Neurobiol, 93*(1), 111-124. doi:10.1016/j.pneurobio.2010.10.005

Lieberman, G., Shpaner, M., Watts, R., Andrews, T., Filippi, C. G., Davis, M., & Naylor, M. R. (2014). White matter involvement in chronic musculoskeletal pain. *J Pain*. doi:10.1016/j.jpain.2014.08.002

Loggia, M. L., Chonde, D. B., Akeju, O., Arabasz, G., Catana, C., Edwards, R. R., . . . Hooker, J. M. (2015). Evidence for brain glial activation in chronic pain patients. *Brain, 138*(Pt 3), 604-615. doi:10.1093/brain/awu377

Lu, C., Yang, T., Zhao, H., Zhang, M., Meng, F., Fu, H., . . . Xu, H. (2016). Insular Cortex is Critical for the Perception, Modulation, and Chronification of Pain. *Neurosci Bull, 32*(2), 191-201. doi:10.1007/s12264-016-0016-y

Lund, J. P., Donga, R., Widmer, C. G., & Stohler, C. S. (1991). The pain-adaptation model: a discussion of the relationship between chronic musculoskeletal pain and motor activity. *Can J Physiol Pharmacol, 69*(5), 683-694.

Lutz, J., Jager, L., de Quervain, D., Krauseneck, T., Padberg, F., Wichnalek, M., . . . Schelling, G. (2008). White and gray matter abnormalities in the brain of patients with fibromyalgia: a diffusion-tensor and volumetric imaging study. *Arthritis Rheum, 58*(12), 3960-3969. doi:10.1002/art.24070

Maeda, Y., Kim, H., Kettner, N., Kim, J., Cina, S., Malatesta, C., . . . Napadow, V. (2017). Rewiring the primary somatosensory cortex in carpal tunnel syndrome with acupuncture. *Brain, 140*(4), 914-927. doi:10.1093/brain/awx015

Makin, T. R., Filippini, N., Duff, E. P., Henderson Slater, D., Tracey, I., & Johansen-Berg, H. (2015). Network-level reorganisation of functional connectivity following arm amputation. *Neuroimage, 114*, 217-225. doi:10.1016/j.neuroimage.2015.02.067

Maleki, N., Becerra, L., Brawn, J., McEwen, B., Burstein, R., & Borsook, D. (2013). Common hippocampal structural and functional changes in migraine. *Brain Struct Funct, 218*(4), 903-912. doi:10.1007/s00429-012-0437-y

Mansour, A. R., Baliki, M. N., Huang, L., Torbey, S., Herrmann, K. M., Schnitzer, T. J., & Apkarian, A. V. (2013). Brain white matter structural properties predict transition to chronic pain. *Pain, 154*(10), 2160-2168. doi:10.1016/j.pain.2013.06.044

Mao, C., Wei, L., Zhang, Q., Liao, X., Yang, X., & Zhang, M. (2013). Differences in brain structure in patients with distinct sites of chronic pain: A voxel-based morphometric analysis. *Neural Regen Res, 8*(32), 2981-2990. doi:10.3969/j.issn.1673-5374.2013.32.001

Markov, N. T., Ercsey-Ravasz, M., Van Essen, D. C., Knoblauch, K., Toroczkai, Z., & Kennedy, H. (2013). Cortical high-density counterstream architectures. *Science, 342*(6158), 1238406. doi:10.1126/science.1238406

Martino, J., Brogna, C., Robles, S. G., Vergani, F., & Duffau, H. (2010). Anatomic dissection of the inferior fronto-occipital fasciculus revisited in the lights of brain stimulation data. *Cortex, 46*(5), 691-699. doi:10.1016/j.cortex.2009.07.015

Martucci, K. T., & Mackey, S. C. (2016). Imaging Pain. *Anesthesiol Clin, 34*(2), 255-269. doi:10.1016/j.anclin.2016.01.001

Moayedi, M., Weissman-Fogel, I., Salomons, T. V., Crawley, A. P., Goldberg, M. B., Freeman, B. V., . . . Davis, K. D. (2012a). Abnormal gray matter aging in chronic pain patients. *Brain Res, 1456*, 82-93. doi:10.1016/j.brainres.2012.03.040

Moayedi, M., Weissman-Fogel, I., Salomons, T. V., Crawley, A. P., Goldberg, M. B., Freeman, B. V., . . . Davis, K. D. (2012b). White matter brain and trigeminal nerve abnormalities in temporomandibular disorder. *Pain, 153*(7), 1467-1477. doi:10.1016/j.pain.2012.04.003

Muraskin, J., Dodhia, S., Lieberman, G., Garcia, J. O., Verstynen, T., Vettel, J. M., . . . Sajda, P. (2016). Brain dynamics of post-task resting state are influenced by expertise: Insights from baseball players. *Hum Brain Mapp, 37*(12), 4454-4471. doi:10.1002/hbm.23321

Mutso, A. A., Radzicki, D., Baliki, M. N., Huang, L., Banisadr, G., Centeno, M. V., . . . Apkarian, A. V. (2012). Abnormalities in hippocampal functioning with persistent pain. *J Neurosci, 32*(17), 5747-5756. doi:10.1523/JNEUROSCI.0587-12.2012

Napadow, V., LaCount, L., Park, K., As-Sanie, S., Clauw, D. J., & Harris, R. E. (2010). Intrinsic brain connectivity in fibromyalgia is associated with chronic pain intensity. *Arthritis Rheum, 62*(8), 2545-2555. doi:10.1002/art.27497

Patenaude, B., Smith, S. M., Kennedy, D. N., & Jenkinson, M. (2011). A Bayesian model of shape and appearance for subcortical brain segmentation. *Neuroimage, 56*(3), 907-922. doi:10.1016/j.neuroimage.2011.02.046

Pomares, F. B., Funck, T., Feier, N. A., Roy, S., Daigle-Martel, A., Ceko, M., . . . Schweinhardt, P. (2017). Histological Underpinnings of Grey Matter Changes in Fibromyalgia Investigated Using Multimodal Brain Imaging. *J Neurosci, 37*(5), 1090-1101. doi:10.1523/JNEUROSCI.2619-16.2016

Raffelt, D. A., Smith, R. E., Ridgway, G. R., Tournier, J. D., Vaughan, D. N., Rose, S., . . . Connelly, A. (2015). Connectivity-based fixel enhancement: Whole-brain statistical analysis of diffusion MRI measures in the presence of crossing fibres. *Neuroimage, 117*, 40-55. doi:10.1016/j.neuroimage.2015.05.039

Raffelt, D. A., Tournier, J. D., Smith, R. E., Vaughan, D. N., Jackson, G., Ridgway, G. R., & Connelly, A. (2017). Investigating white matter fibre density and morphology using fixel-based analysis. *Neuroimage, 144*(Pt A), 58-73. doi:10.1016/j.neuroimage.2016.09.029

Rayhan, R. U., Stevens, B. W., Timbol, C. R., Adewuyi, O., Walitt, B., VanMeter, J. W., & Baraniuk, J. N. (2013). Increased brain white matter axial diffusivity associated with fatigue, pain and hyperalgesia in Gulf War illness. *PLoS One, 8*(3), e58493. doi:10.1371/journal.pone.0058493

Rodriguez-Raecke, R., Niemeier, A., Ihle, K., Ruether, W., & May, A. (2009). Brain gray matter decrease in chronic pain is the consequence and not the cause of pain. *J Neurosci, 29*(44), 13746-13750. doi:10.1523/JNEUROSCI.3687-09.2009

Rodriguez-Raecke, R., Niemeier, A., Ihle, K., Ruether, W., & May, A. (2013). Structural brain changes in chronic pain reflect probably neither damage nor atrophy. *PLoS One, 8*(2), e54475. doi:10.1371/journal.pone.0054475

Roland, M. O. (1986). A critical review of the evidence for a pain-spasm-pain cycle in spinal disorders. *Clin Biomech (Bristol, Avon), 1*(2), 102-109. doi:10.1016/0268-0033(86)90085-9

Rorden, C., & Brett, M. (2000). Stereotaxic display of brain lesions. *Behav Neurol, 12*(4), 191-200.

Rose, S. E., Janke, A. L., & Chalk, J. B. (2008). Gray and white matter changes in Alzheimer's disease: a diffusion tensor imaging study. *J Magn Reson Imaging, 27*(1), 20-26. doi:10.1002/jmri.21231

Salminen, L. E., Schofield, P. R., Pierce, K. D., Zhao, Y., Luo, X., Wang, Y., . . . Paul, R. H. (2016). Neuromarkers of the common angiotensinogen polymorphism in healthy older adults: A comprehensive assessment of white matter integrity and cognition. *Behav Brain Res, 296*, 85-93. doi:10.1016/j.bbr.2015.08.028

Sarubbo, S., De Benedictis, A., Maldonado, I. L., Basso, G., & Duffau, H. (2013). Frontal terminations for the inferior fronto-occipital fascicle: anatomical dissection, DTI study and functional considerations on a multi-component bundle. *Brain Struct Funct, 218*(1), 21-37. doi:10.1007/s00429-011-0372-3

Schmidt-Wilcke, T., Leinisch, E., Ganssbauer, S., Draganski, B., Bogdahn, U., Altmeppen, J., & May, A. (2006). Affective components and intensity of pain correlate with structural differences in gray matter in chronic back pain patients. *Pain, 125*(1-2), 89-97. doi:10.1016/j.pain.2006.05.004

Schmidt-Wilcke, T., Leinisch, E., Straube, A., Kampfe, N., Draganski, B., Diener, H. C., . . . May, A. (2005). Gray matter decrease in patients with chronic tension type headache. *Neurology, 65*(9), 1483-1486. doi:10.1212/01.wnl.0000183067.94400.80

Schmidt-Wilcke, T., Luerding, R., Weigand, T., Jurgens, T., Schuierer, G., Leinisch, E., & Bogdahn, U. (2007). Striatal grey matter increase in patients suffering from fibromyalgia--a voxel-based morphometry study. *Pain, 132 Suppl 1*, S109-116. doi:10.1016/j.pain.2007.05.010

Seminowicz, D. A., & Moayedi, M. (2017). The Dorsolateral Prefrontal Cortex in Acute and Chronic Pain. *J Pain*. doi:10.1016/j.jpain.2017.03.008

Seminowicz, D. A., Shpaner, M., Keaser, M. L., Krauthamer, G. M., Mantegna, J., Dumas, J. A., . . . Naylor, M. R. (2013). Cognitive-behavioral therapy increases prefrontal cortex gray matter in patients with chronic pain. *J Pain, 14*(12), 1573-1584. doi:10.1016/j.jpain.2013.07.020

Seminowicz, D. A., Wideman, T. H., Naso, L., Hatami-Khoroushahi, Z., Fallatah, S., Ware, M. A., . . . Stone, L. S. (2011). Effective treatment of chronic low back pain in humans reverses abnormal brain anatomy and function. *J Neurosci, 31*(20), 7540-7550. doi:10.1523/JNEUROSCI.5280-10.2011

Smith, R. E., Tournier, J. D., Calamante, F., & Connelly, A. (2013). SIFT: Spherical-deconvolution informed filtering of tractograms. *Neuroimage, 67*, 298-312. doi:10.1016/j.neuroimage.2012.11.049

Smith, S. M., Jenkinson, M., Woolrich, M. W., Beckmann, C. F., Behrens, T. E., Johansen-Berg, H., . . . Matthews, P. M. (2004). Advances in functional and structural MR image analysis and implementation as FSL. *Neuroimage, 23 Suppl 1*, S208-219. doi:10.1016/j.neuroimage.2004.07.051

Sofroniew, M. V., & Vinters, H. V. (2010). Astrocytes: biology and pathology. *Acta Neuropathol, 119*(1), 7-35. doi:10.1007/s00401-009-0619-8

Spooner, J., Yu, H., Kao, C., Sillay, K., & Konrad, P. (2007). Neuromodulation of the cingulum for neuropathic pain after spinal cord injury. Case report. *J Neurosurg, 107*(1), 169-172. doi:10.3171/JNS-07/07/0169

Starr, C. J., Sawaki, L., Wittenberg, G. F., Burdette, J. H., Oshiro, Y., Quevedo, A. S., & Coghill, R. C. (2009). Roles of the insular cortex in the modulation of pain: insights from brain lesions. *J Neurosci, 29*(9), 2684-2694. doi:10.1523/JNEUROSCI.5173-08.2009

Szabo, N., Kincses, Z. T., Pardutz, A., Tajti, J., Szok, D., Tuka, B., . . . Vecsei, L. (2012). White matter microstructural alterations in migraine: a diffusion-weighted MRI study. *Pain, 153*(3), 651-656. doi:10.1016/j.pain.2011.11.029

Tian, T., Guo, L., Xu, J., Zhang, S., Shi, J., Liu, C., . . . Zhu, W. (2016). Brain white matter plasticity and functional reorganization underlying the central pathogenesis of trigeminal neuralgia. *Sci Rep, 6*, 36030. doi:10.1038/srep36030

Torres-Platas, S. G., Comeau, S., Rachalski, A., Bo, G. D., Cruceanu, C., Turecki, G., . . . Mechawar, N. (2014). Morphometric characterization of microglial phenotypes in human cerebral cortex. *J Neuroinflammation, 11*, 12. doi:10.1186/1742-2094-11-12

Tournier, J.-D., Calamante, F., & Connelly, A. (2012). MRtrix: Diffusion tractography in crossing fiber regions. *International Journal of Imaging Systems and Technology*.

Tracey, I., & Mantyh, P. W. (2007). The cerebral signature for pain perception and its modulation. *Neuron, 55*(3), 377-391. doi:10.1016/j.neuron.2007.07.012

Tromp, D. P., Grupe, D. W., Oathes, D. J., McFarlin, D. R., Hernandez, P. J., Kral, T. R., . . . Nitschke, J. B. (2012). Reduced structural connectivity of a major frontolimbic pathway in generalized anxiety disorder. *Arch Gen Psychiatry, 69*(9), 925-934. doi:10.1001/archgenpsychiatry.2011.2178

Tzourio-Mazoyer, N., Landeau, B., Papathanassiou, D., Crivello, F., Etard, O., Delcroix, N., . . . Joliot, M. (2002). Automated anatomical labeling of activations in SPM using a macroscopic anatomical parcellation of the MNI MRI single-subject brain. *Neuroimage, 15*(1), 273-289. doi:10.1006/nimg.2001.0978

Uddin, L. Q. (2015). Salience processing and insular cortical function and dysfunction. *Nat Rev Neurosci, 16*(1), 55-61. doi:10.1038/nrn3857

Vasic, V., & Schmidt, M. H. (2017). Resilience and Vulnerability to Pain and Inflammation in the Hippocampus. *Int J Mol Sci, 18*(4). doi:10.3390/ijms18040739

Vrana, A., Hotz-Boendermaker, S., Stampfli, P., Hanggi, J., Seifritz, E., Humphreys, B. K., & Meier, M. L. (2015). Differential Neural Processing during Motor Imagery of Daily Activities in Chronic Low Back Pain Patients. *PLoS One, 10*(11), e0142391. doi:10.1371/journal.pone.0142391

Wang, X., Pathak, S., Stefaneanu, L., Yeh, F. C., Li, S., & Fernandez-Miranda, J. C. (2016). Subcomponents and connectivity of the superior longitudinal fasciculus in the human brain. *Brain Struct Funct, 221*(4), 2075-2092. doi:10.1007/s00429-015-1028-5

Wasan, A. D., Loggia, M. L., Chen, L. Q., Napadow, V., Kong, J., & Gollub, R. L. (2011). Neural correlates of chronic low back pain measured by arterial spin labeling. *Anesthesiology, 115*(2), 364-374. doi:10.1097/ALN.0b013e318220e880

Weston, P. S., Simpson, I. J., Ryan, N. S., Ourselin, S., & Fox, N. C. (2015). Diffusion imaging changes in grey matter in Alzheimer's disease: a potential marker of early neurodegeneration. *Alzheimers Res Ther, 7*(1), 47. doi:10.1186/s13195-015-0132-3

Woolrich, M. W., Jbabdi, S., Patenaude, B., Chappell, M., Makni, S., Behrens, T., . . . Smith, S. M. (2009). Bayesian analysis of neuroimaging data in FSL. *Neuroimage, 45*(1 Suppl), S173-186. doi:10.1016/j.neuroimage.2008.10.055

Wu, Y., Sun, D., Wang, Y., & Wang, Y. (2016). Subcomponents and Connectivity of the Inferior Fronto-Occipital Fasciculus Revealed by Diffusion Spectrum Imaging Fiber Tracking. *Front Neuroanat, 10*, 88. doi:10.3389/fnana.2016.00088

Yarkoni, T., Poldrack, R. A., Nichols, T. E., Van Essen, D. C., & Wager, T. D. (2011). Large-scale automated synthesis of human functional neuroimaging data. *Nat Methods, 8*(8), 665-670. doi:10.1038/nmeth.1635

Yeh, F. C., & Tseng, W. Y. (2011). NTU-90: a high angular resolution brain atlas constructed by q-space diffeomorphic reconstruction. *Neuroimage, 58*(1), 91-99. doi:10.1016/j.neuroimage.2011.06.021

Yuan, K., Qin, W., Wang, G., Zeng, F., Zhao, L., Yang, X., . . . Tian, J. (2011). Microstructure abnormalities in adolescents with internet addiction disorder. *PLoS One, 6*(6), e20708. doi:10.1371/journal.pone.0020708

Zalesky, A., Fornito, A., & Bullmore, E. T. (2010). Network-based statistic: identifying differences in brain networks. *Neuroimage, 53*(4), 1197-1207. doi:10.1016/j.neuroimage.2010.06.041

Zatorre, R. J., Fields, R. D., & Johansen-Berg, H. (2012). Plasticity in gray and white: neuroimaging changes in brain structure during learning. *Nat Neurosci, 15*(4), 528-536. doi:10.1038/nn.3045

Zerr, I., Kallenberg, K., Summers, D. M., Romero, C., Taratuto, A., Heinemann, U., . . . Sanchez-Juan, P. (2009). Updated clinical diagnostic criteria for sporadic Creutzfeldt-Jakob disease. *Brain, 132*(Pt 10), 2659-2668. doi:10.1093/brain/awp191

Figure Captions

Figure 2.1. A complete study flow chart illustrating recruitment, data collection, and study timeline. Healthy, pain-free controls, and participants with chronic musculoskeletal pain were recruited and scanned at a single, baseline, time point (TP1), as outlined in red. Chronic pain patients continued in the study and underwent two additional MRI evaluations including a post-intervention and long-term follow-up acquisition (analyzed in the subsequent chapter – chapter 3). The focus of chapter 2 was to investigate baseline WM and GM structural brain differences between patients with chronic pain and healthy controls.

Figure 2.2. A) Mode of anisotropy ranges from 1 to -1: with positive numbers indicating fewer fiber directions or linear diffusion, while negative number are indicative of complex, crossing fiber structure. Three example white matter voxels are shown to highlight differences in fiber complexity from left (least complex) to right (more complex). B) Ball & sticks multi-compartment method models more than one fiber populations within each voxel by accounting for isotropic (ball) and anisotropic (sticks) diffusion. For illustrative purposes two example voxels are shown. Voxel A has a greater major fiber population (F1) than voxel B and fewer secondary or minor fibers (F2). Direction change for standard single tensor diffusion metrics (AD, RD, and FA) and partial volume fraction metrics (F1 and F2) is indicated for each example voxel. This illustrates that in the case of crossing fibers, standard tensor metrics may be mistakenly interpreted as indicative of reduced fiber integrity, whereas partial volume fraction metrics will accurately separate crossing fiber populations.

Figure 2.3. A) Fiber density decreases from left to right with no change in the fiber cross-sectional area. Fiber density is robust to regions of complex fiber geometry. We suggest that changes in fiber density in musculoskeletal pain populations mostly likely indicate non-neuronal origins because there is no existing evidence to support neuronal degeneration in chronic pain. B) Fiber cross-section area is reduced from left to right with no apparent change in the fiber density. A change in fiber cross-section may be reflective of neuronal degeneration, although this is unanticipated in chronic pain.

Figure 2.4. A) Example of individual subcortical segmentation of a single subject's T1-weighted image used for downstream extraction of MD values. B) Back-transformed T1-weighted subcortical segmentations were overlaid on the diffusion weighted image and MD values were extracted from the ROIs for subsequent between-group statistical comparison.

Figure 2.5. A) Whole brain tractography was implemented using DSI studio software and repeated 1,000x for each subject. Connectivity matrices were generated by adding streamlines that passed through or terminated within the 116 GM regions of the AAL atlas. A single connectivity matrix was then generated for each subject by averaging the 1,000 tractography iterations and was used for subsequent statistical comparison. B) Group-wise comparisons using the single subject average connectivity matrices was conducted in network based statistics software using age and sex as nuisance regressors.

Figure 2.6. Whole brain GM volume analysis. A) Subcortical GM volume was significantly increased in participants with chronic pain compared to healthy controls in the right amygdala and caudate, as well as the right hippocampus and accumbens (not shown). B) Cluster statistics for significant between-group differences in GM volume, reflecting number of voxels, peak p-value, and cluster coordinates reported in MNI $2x2x2mm^3$ standard space. Patients with chronic pain exhibited an increase in GM volume compared to healthy controls in four distinct clusters, listed in order of size. Cluster 4 (Cluster index 4) was midline and outside of the GM (see coronal plane on panel A) and, therefore, not interpreted. Compared to healthy controls, participants with chronic pain demonstrated an increase in GM volume within the right occipital fusiform gyrus.

Figure 2.7. A) Anatomical location of the WM ROI tracts. B) Mean WM fiber complexity values extracted from each participant for tracts that yielded significant between-group differences for mode of anisotropy (MO) and the ball & sticks (F1 & F2) metrics. Overall, participants with chronic pain exhibited a reduction in both MO and F1 and F2 indicative of alterations in complexity. Pain patients exhibited regional changes in WM fiber complexity. Specifically, reduced MO and F1 was observed and interpreted as an increase in WM fiber complexity whereas a reduction in F2 is suggestive of decreased fiber complexity. Values reported as mean ± standard deviation, Pain n=74, Healthy n=31.

Figure 2.8. A) Tracts highlighted in red indicate regions where participants with chronic pain have significantly reduced complexity (F2) as compared to healthy controls. Significance was evaluated at threshold $p \leq 0.05$, Pain n=74, Healthy n=31. B) To rule out

the possibility that F2 was reduced because it was not modeled across all subjects, we obtained a group measure of F2 overlap between subjects. The regions in green indicate that a F1 and F2 fiber population was found for every participant in the study. Conversely, the regions in blue (circled) indicate a failure to obtain a secondary fiber population for at least one subject. Overall, the majority of voxels are observed to have both major and minor fiber populations. We do not report any significant differences between patients and controls in regions where F2 fiber populations was missing.

Figure 2.9. A) Chronic pain participants had reduced fiber density within the right inferior fronto-occipital fasciculus (IFOF) and the splenium of the corpus callosum (not pictured) compared to healthy controls, significance threshold $p \leq 0.05$. B) Probabilistic tractography illustrating the anatomical location of the IFOF in similar planes from the JHU white matter tractography atlas. C) Deterministic tractography highlighting the IFOF projections from occipital, temporal and frontal cortices (Yeh et al., 2017, used with permission).

Figure 2.10. A) Significant increases in connectivity are shown on a standard brain for threshold value of 2.9. The thickness of the line connecting the GM nodes indicates the test statistic threshold and is not representative of connection strength, but instead, reflects test statistic value. B) Connectivity was assessed for statistical thresholds between 2.7-3.1 in increments of 0.2. No significant connectivity differences were observed for threshold values of 2.7 (not shown), however, both 2.9 and 3.1 threshold values yielded significant connectivity increases in participants with chronic pain. (Pain n=74, Healthy n=31).

Table Captions

Table 2.1. The groups were balanced for age, however, there was a significant between-group difference in sex, driven by an increased ratio of male participants in the healthy control group.

Table 2.2. ROI analysis yielded a robust increase in subcortical GM volume in the chronic pain population. Cortically, patients with chronic pain exhibited both increased and decreased GM volume compared to healthy controls in regions involved in executive functioning (DLPFC) and sensorimotor processing (M1 and S1). Significance was evaluated at threshold $p \leq 0.05$, Pain n=74, Healthy n=31.

Table 2.3. Average GM mean diffusivity (MD) was extracted from subcortical structures and analyzed to identify microstructural alterations associated with GM volume change. No significant alterations in GM MD were detected between patients with chronic pain and healthy controls. (Pain n=73, Healthy n=28).

Table 2.4. ROI analysis of WM fiber complexity measures demonstrated increased complexity within the splenium of the corpus callosum, left cerebral peduncle, and bilateral external capsule as well as a decreased fiber complexity within the right external capsule, superior longitudinal fasciculus, and uncinate fasciculus. Significance was evaluated at threshold $p \leq 0.05$, Pain n=74, Healthy n=31.

Figure 2.1 Study design.

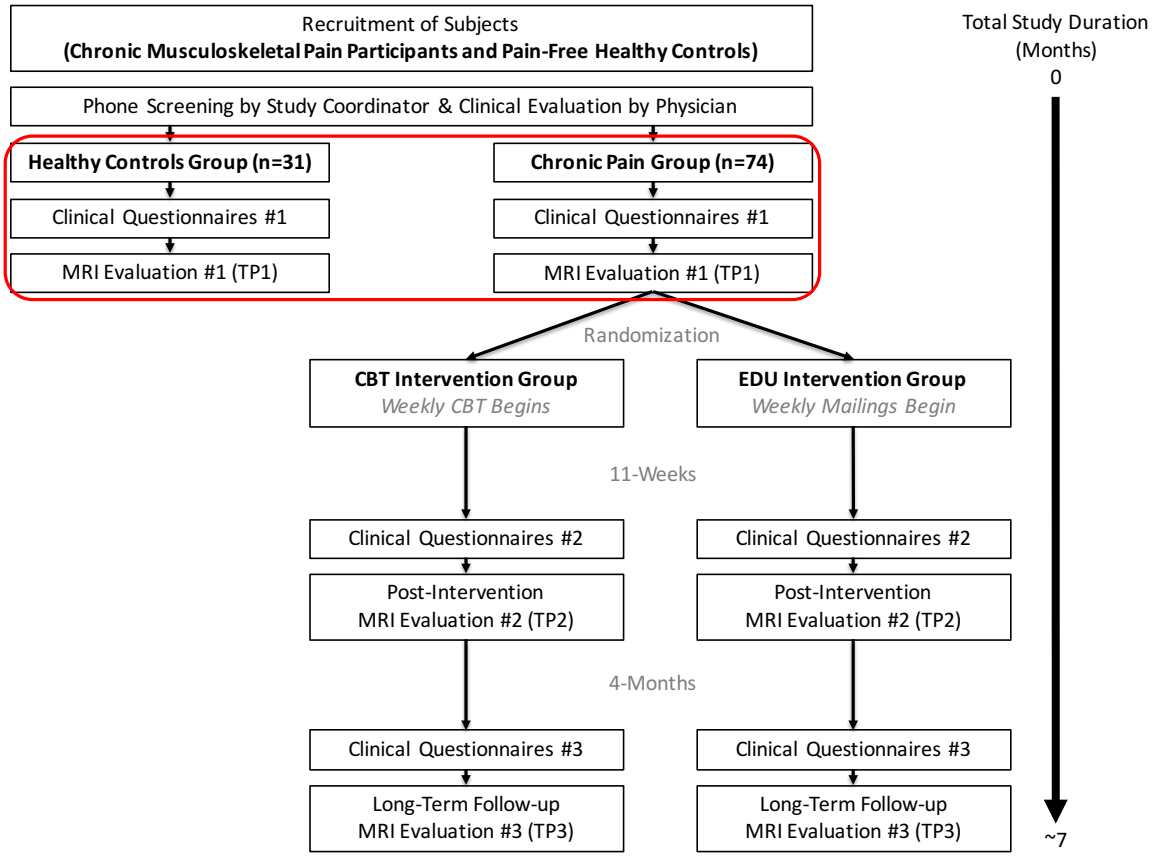

Figure 2.2 Schematic of white matter complexity metrics.

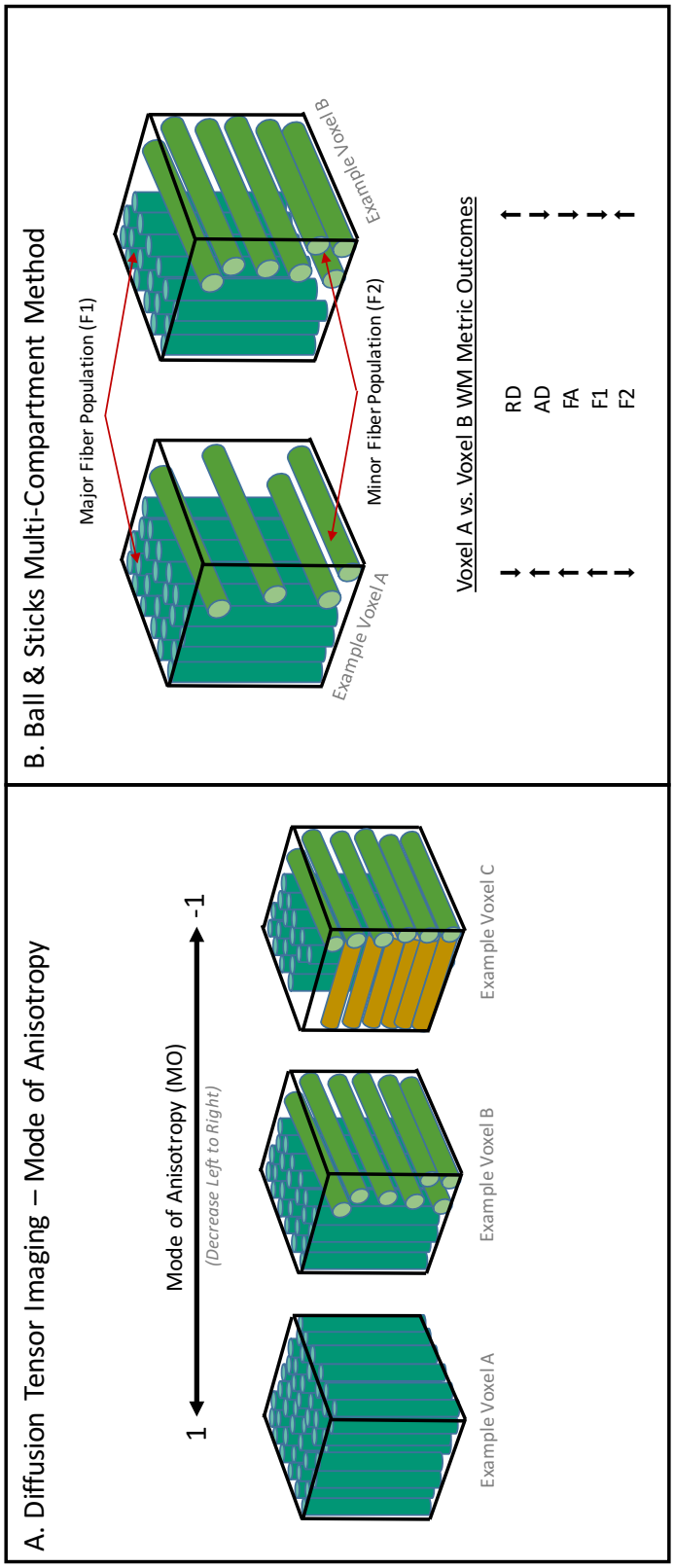

Figure 2.3. Schematic of white matter fiber density & cross-section metrics.

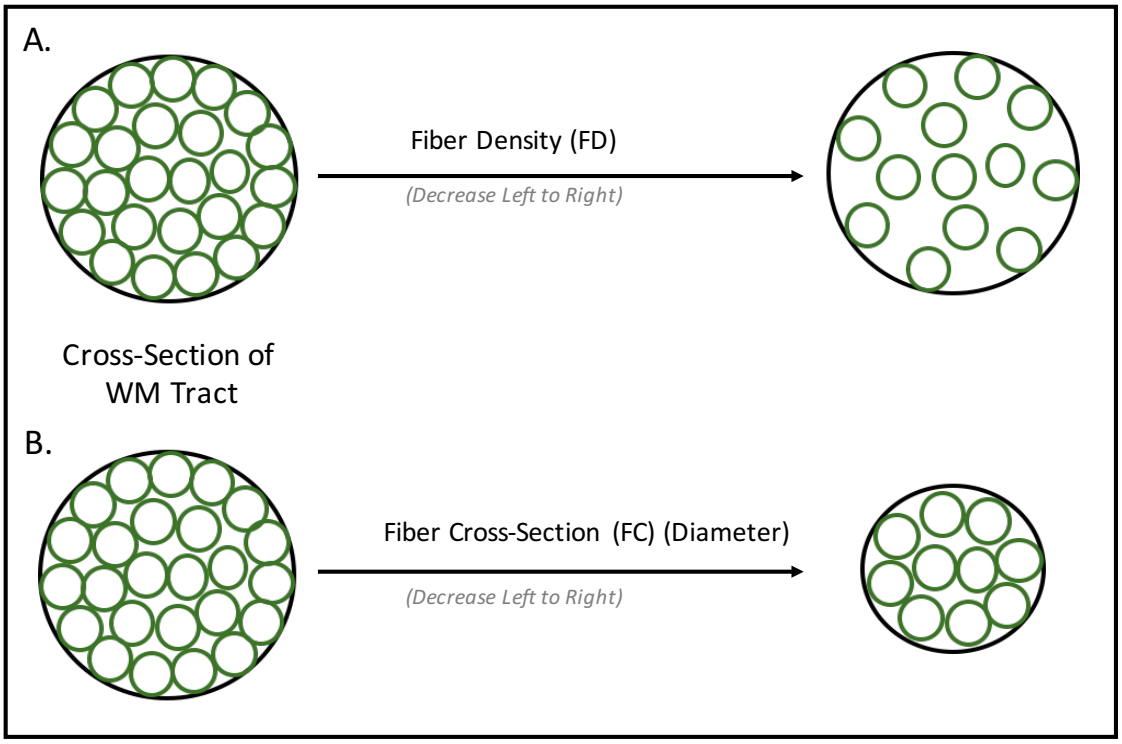

Figure 2.4. GM mean diffusivity analysis.

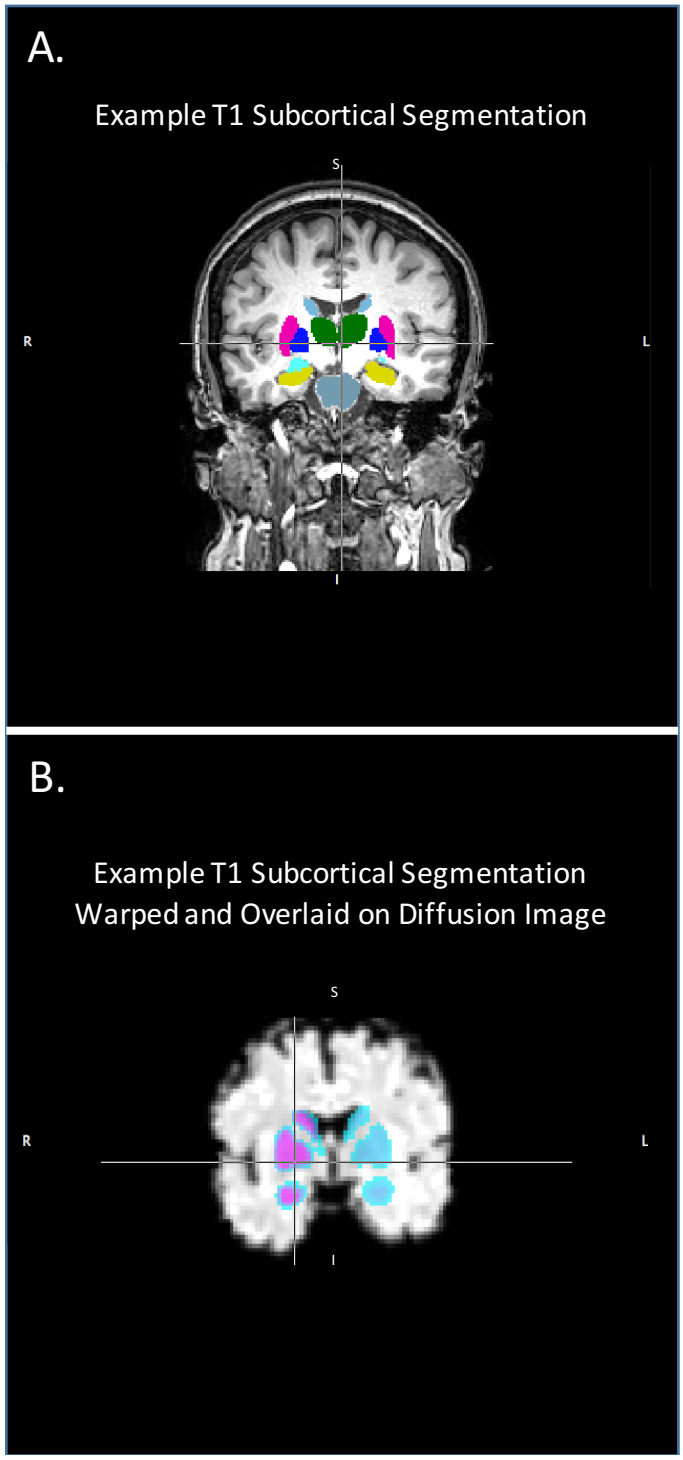

Figure 2.5. White matter connectivity pipeline.

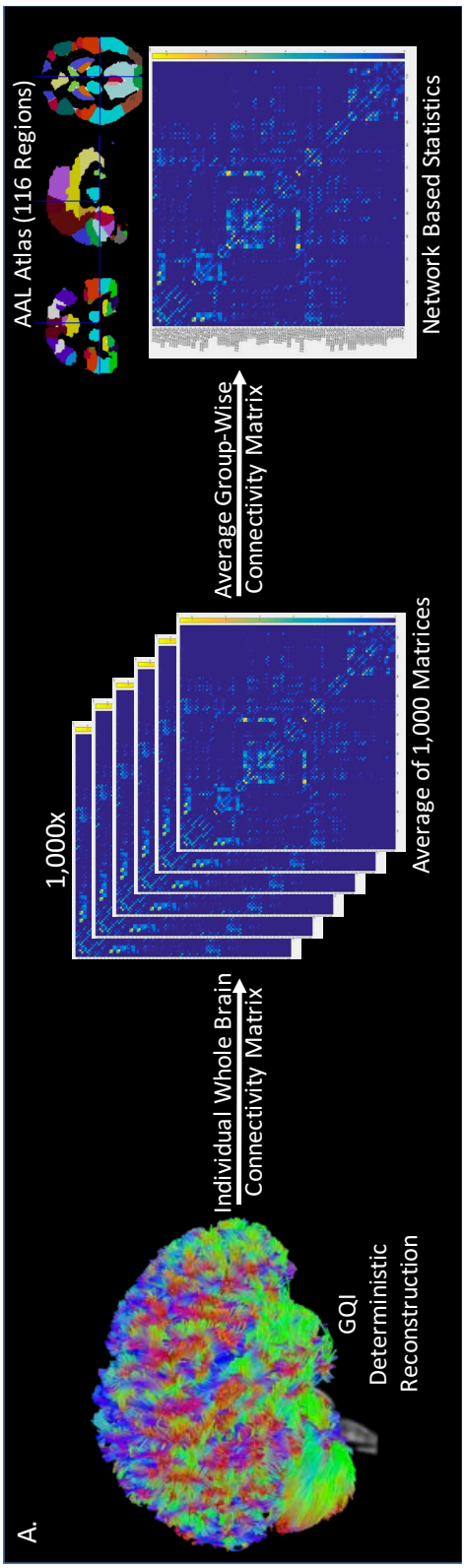

Figure 2.6. Whole brain GM volume results.

A.

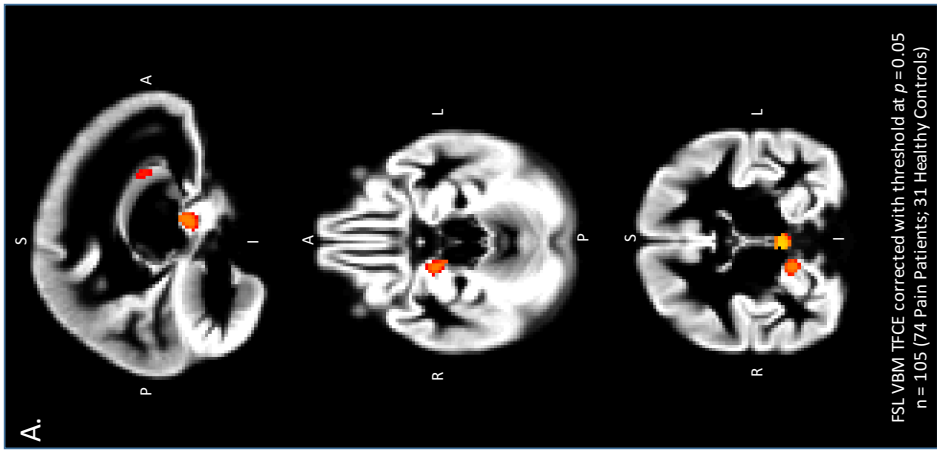

B.

Pain > Controls

Cluster Index	Voxels	p-Value	Max X	Max Y	Max Z	Structure
4	213	0.007	44	59	30	Outside of Grey Matter
3	90	0.024	37	59	27	Right Amygdala / Hippocampus
2	68	0.043	38	73	42	Right Caudate
1	3	0.049	42	66	33	Right Accumbens

Pain < Controls

Cluster Index	Voxels	p-Value	Max X	Max Y	Max Z	Structure
1	1302	0.014	32	19	30	Right Occipital Fusiform Gyrus

Figure 2.7. WM regions of interest and complexity results.

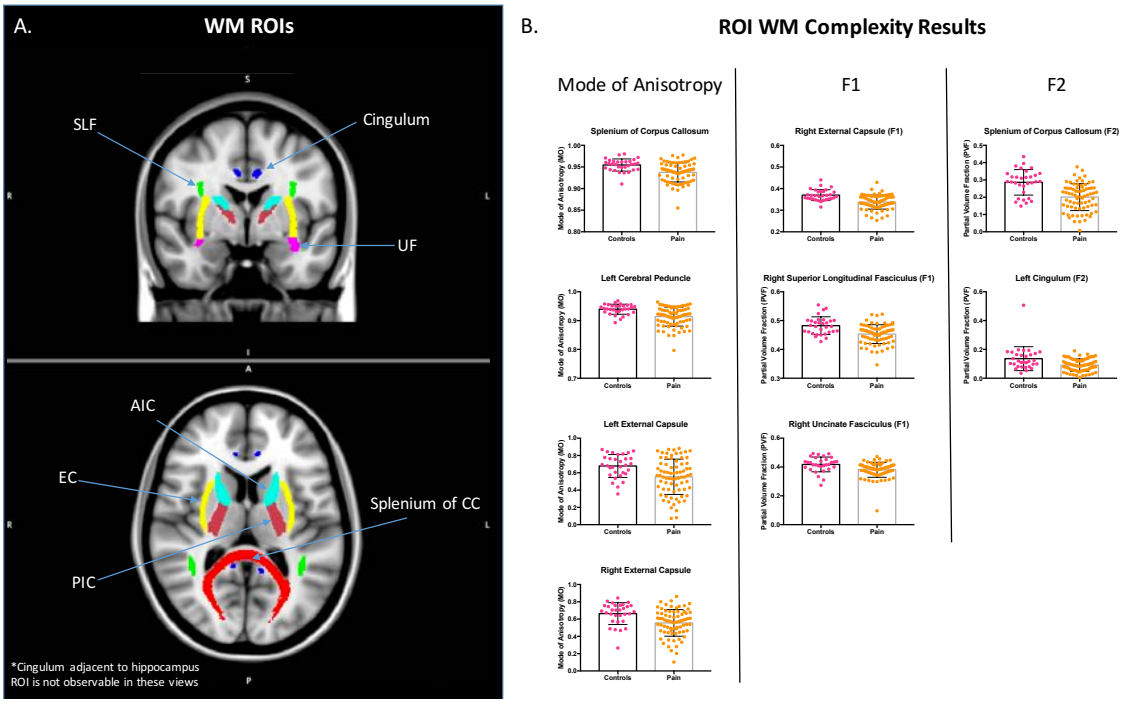

Figure 2.8. Whole brain F2 complexity results and fiber modeling confirmation.

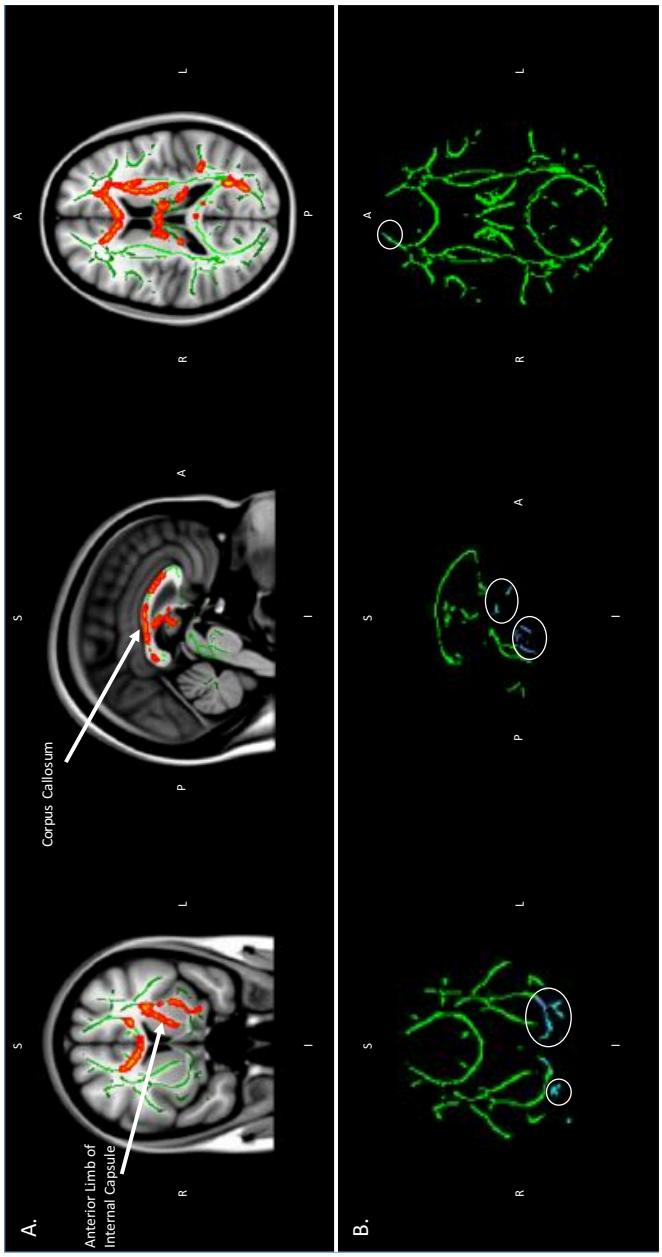

Figure 2.9. WM fiber density results and inferior fronto-occipital fasciculus tractography.

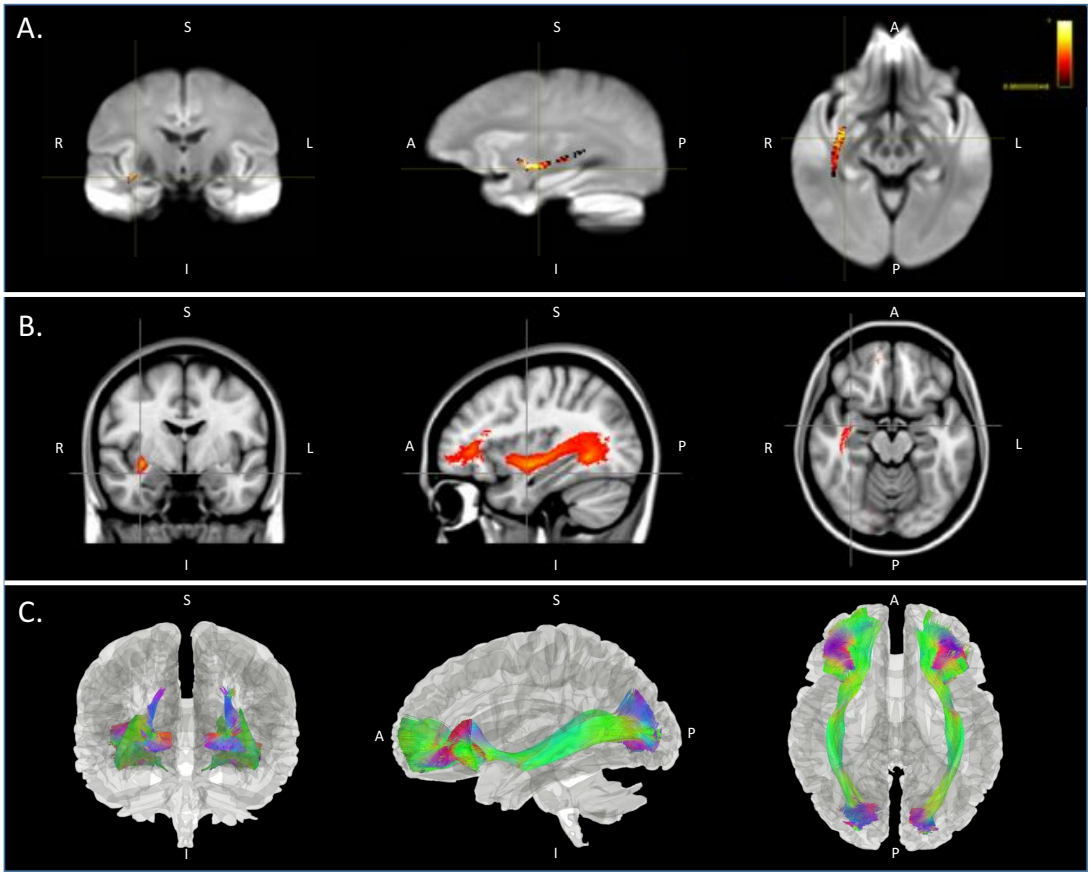

Figure 2.10. WM connectivity results.

A.

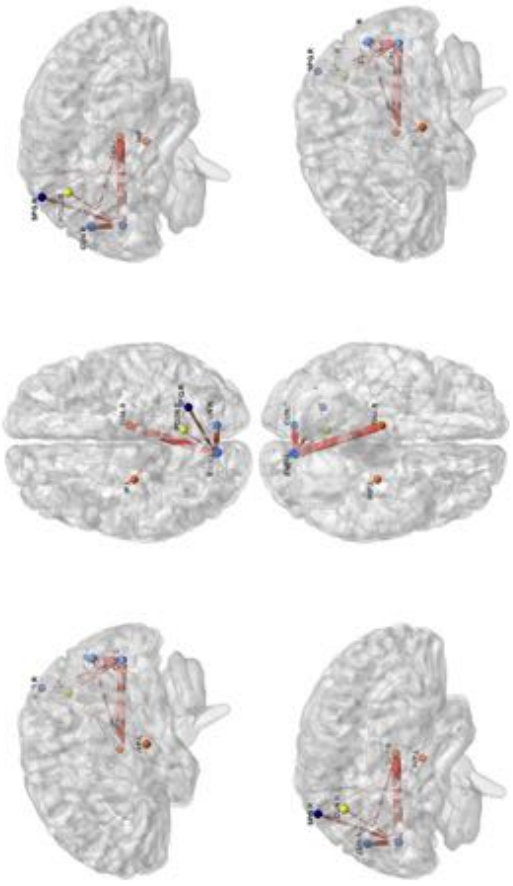

B.

Connection	Test Statistic	t-value Thresh.	Significance (p-value)
Calcarine L. to Cuneus R.	3.57	2.9	0.0476
Hippocampus L. to Parietal Sup. R.	3.07	2.9	0.0476
Calcarine L. to Parietal Sup. R.	3.37	2.9	0.0476
Calcarine L. to Precuneus R.	3.15	2.9	0.0476
Calcarine L. to Thalamus R.	3.84	2.9	0.0476
Cuneus L. to Thalamus R.	3.25	2.9	0.0476

Connection	Test Statistic	t-value Thresh.	Significance (p-value)
Calcarine L. to Cuneus R.	3.57	3.1	0.0308
Calcarine L. to Parietal Sup. R.	3.37	3.1	0.0308
Calcarine L. to Precuneus R.	3.15	3.1	0.0308
Calcarine L. to Thalamus R.	3.84	3.1	0.0308
Cuneus L. to Thalamus R.	3.25	3.1	0.0308

Table 2.1. Study demographics and pain assessment.

	Chronic Pain Participants	Healthy Controls
Number of Subjects	74	31
Sex	Female: 60 (81.1%) Male: 14 (18.9%)	Female: 18 (58.1%) Male: 13 (41.9%)
Age	45.7 ± 13.03 years	44.12 ± 13.15 years
Years of Education	15 ± 1.62 years	Mean= 16.5 ± 0.78 years (missing two data points)
Pain Duration	11 ± 9.15 years	N/A
Pain Now	5.27 ± 1.96	0.32 ± 0.67 (missing three data points)

Mean ± Standard Deviation

Table 2.2. Region of interest GM volume results.

ROI	Hemisphere	Volume
ACC	Right	ns
	Left	ns
Amygdala	Right	↑
	Left	↑
Caudate	Right	↑
	Left	↑
DLPFC	Right	ns
	Left	↓
Hippocampus	Right	↑
	Left	ns
Insula	Right	ns
	Left	ns
M1	Right	ns
	Left	↓
S1	Right	ns
	Left	↓
Thalamus	Right	ns
	Left	↑
Nucleus Accumbens	Right	↑
	Left	↑

Table Legend:
↑ = Increased volume in pain patients
↓ = Decreased volume in pain patients
ns = Not significant between groups

Analysis:
FSL VBM TFCE corrected with threshold at $p = 0.05$
n=105 (74 Pain Patients; 31 Healthy Controls)

Table 2.3. GM subcortical mean diffusivity results.

			Mean	SD	F-Value	P-Value
Amygdala	Right	Pain Patients	7.77	2.43	0.10	0.75
		Controls	7.79	1.81		
	Left	Pain Patients	7.80	2.47	0.08	0.78
		Controls	7.83	2.38		
Nucleus Accumbens	Right	Pain Patients	7.58	2.64	0.00	1.00
		Controls	7.57	2.31		
	Left	Pain Patients	7.60	2.28	2.31	0.13
		Controls	7.53	1.82		
Caudate	Right	Pain Patients	6.83	2.97	1.80	0.18
		Controls	6.77	2.84		
	Left	Pain Patients	6.79	3.04	2.25	0.14
		Controls	6.70	2.39		
Hippocampus	Right	Pain Patients	7.61	3.29	0.04	0.85
		Controls	7.59	4.27		
	Left	Pain Patients	7.71	3.60	0.27	0.60
		Controls	7.75	3.88		
Pallidum	Right	Pain Patients	7.12	4.44	0.30	0.86
		Controls	7.21	2.70		
	Left	Pain Patients	7.12	2.67	1.50	0.22
		Controls	7.18	1.89		
Thalamus	Right	Pain Patients	6.93	2.10	1.08	0.30
		Controls	6.91	1.76		
	Left	Pain Patients	7.01	2.21	0.39	0.53
		Controls	7.00	1.73		
Brainstem	Bilateral	Pain Patients	5.83	3.44	1.50	0.22
		Controls	5.75	2.61		

Mean values reported as $x10^{-4}$
SD values reported as $x10^{-5}$

n=101 (73 Pain Patients; 28 Healthy Controls)

Table 2.4. Summary of WM ROI complexity results.

White Matter Region of Interest	White Matter Microstructural Metric: MO	F1	F2
Corpus Callosum (Splenium)	↓		↓
Left Cerebral Peduncle	↓		
Left Cingulum			↓
Left External Capsule	↓		
Right External Capsule	↓	↓	
Right Superior Longitudinal Fasciculus		↓	
Right Uncinate Fasciculus		↓	

↓ = Decreased in pain participants compared to healthy controls

CHAPTER 3: STRUCTURAL PLASTICITY FOLLOWING CBT FOR THE TREATMENT OF CHRONIC MUSCULOSKELETAL PAIN

Abstract

Grey matter (GM) volume and density as well as white matter (WM) microstructure and connectivity are altered across chronic pain populations; however, the structural neuroplasticity following successful psychological intervention remains unknown. In the current study, we characterized alterations in GM morphometry and WM complexity and connectivity before and after cognitive behavioral therapy (CBT) for the treatment of chronic musculoskeletal pain. Patients were randomized into two groups: a once-weekly CBT for 11-weeks (CBT Group) or an active patient control group that received educational materials by mail (EDU Group). All subjects were assessed at baseline (TP1), 11-weeks following either CBT or EDU (TP2), and at a four-month follow-up (TP3). CBT resulted in significant clinical improvements assessed by behavioral self reports, compared to EDU controls. No GM volumetric differences were observed following CBT at either of the follow-up visits. Region of interest (ROI) WM analysis exhibited several fiber tracts that had significantly increased WM complexity following CBT intervention including the bilateral posterior internal capsule and, the left cingulum within the temporal lobe. Conversely, several tracts exhibited a decrease in WM complexity including the right external capsule, the left posterior internal capsule, and the right cingulum within the temporal lobe. No between-group differences were observed in connectivity. We propose that changes in complexity reflect activity-dependent WM remodeling due to changes in pain processing following successful CBT intervention. This is the first study to

demonstrate WM neuroplasticity following a psychotherapeutic intervention, suggesting that changes in behavioral and cognitive coping strategies can influence brain structure.

Introduction

Descriptions of the pain experience date back to early philosophers including Aristotle and Galen, yet effective treatment options remain elusive to this day (Perl, 2007). Presently, common treatment options for chronic pain include surgery, pharmacotherapy, and integrative health interventions, such as acupuncture and psychotherapy. Surgery is indicated only for select pain subtypes, carries inherent risks, is not always effective and may sometimes exacerbate the problem. Alternatively, pharmacological agents may effectively mask pain symptoms, but do not resolve the cause of chronic pain itself. Long-term pharmaceutical use for chronic conditions is associated with poor treatment outcomes that carry the risk of addiction. For these reasons, behavioral and psychotherapeutic strategies are gaining traction as safe and effective options to treat a spectrum of chronic pain disorders, including musculoskeletal pain.

Non-pharmacological alternatives to managing chronic pain include cognitive behavioral therapy (CBT), yoga, meditation, and hypnosis. These treatments are typically aimed at increasing physical functioning, while decreasing maladaptive cognitive and behavioral phenotypes. The most recent Cochrane review confirmed short-term effectiveness of CBT for pain management, but noted long-term relapse, likely due to decreased adherence to skill practice (Williams, Eccleston, & Morley, 2012). CBT addresses aberrant psychopathologies, such as depression, anxiety, and catastrophizing that are associated with increased pain experience and psychosocial dysfunction in chronic pain

populations (Ehde et al., 2014). Fear avoidance behavior is also common amongst chronic pain populations, inhibiting social and professional interactions, causing motor dysfunction (Hodges & Tucker, 2011; Lund et al., 1991; Roland, 1986), and often leading to a profound loss of physical activity. Together, this triad of behavioral, psychological and physical disturbances act as a positive feedback loop to potentiate disability over time. CBT targets these maladaptive traits by modifying emotional, behavioral, and cognitive imbalances through goal-oriented, "problem focused" intervention.

Treatment efficacy of CBT has traditionally been demonstrated through patient self-reports, but therapeutic success has not been quantified with more objective measures of brain plasticity. More recent investigations have begun to unravel the functional network changes following CBT in pain subtypes, such as low back pain (Shpaner et al., 2014) and fibromyalgia (Lazaridou et al., 2017), as well CBT's influence on network connectivity related to repeated sensory exposure (Kucyi, Salomons, & Davis, 2016). Structural neuroplasticity following CBT intervention is less known and may help delineate the underlying neurocircuitry involved in therapeutic efficacy. In a seminal investigation of structural CNS changes related to CBT intervention in a mixed etiology chronic pain cohort, Seminowicz and colleagues demonstrated that 11-week group CBT reduced maladaptive behavioral traits such as catastrophizing that were associated with GM volume in the dorsolateral prefrontal cortex (DLPFC) (Seminowicz et al., 2013). Given the established function of the DLPFC for cognitive control, and its involvement in descending pain modulation, interventions that modify incoming nociceptive signaling may impact GM, as already reported, but may also influence WM microstructure and connectivity.

Although the current literature suggests a role for GM structural and functional plasticity following CBT intervention, the field would benefit from large-scale randomized controlled studies of homogenous pain subtypes. Thus, the objective of the current study was to assess structural GM and WM plasticity following 11-week CBT for musculoskeletal pain. Increasing evidence suggests that changes in neural activity can induce WM plasticity in an activity-dependent manner (Baraban, Mensch, & Lyons, 2016); we will assess WM plasticity by measuring microstructure and connectivity. We hypothesized that CBT would facilitate CNS plasticity by altering GM and WM structure in regions important for cognitive, affective, and emotional pain regulation. Based on existing literature, we predicted that CBT would lead to normalization of reported structural aberrations, that is, to volumetric increase in regions responsible for pain modulation, such as the prefrontal (DLPFC, VMPFC), anterior cingulate (ACC), and insular cortices, and to volumetric decrease in the primary somatosensory cortex. We also conducted exploratory whole-brain and ROI analysis of WM complexity and connectivity. Changes in WM complexity may reflect activity dependent WM remodeling, a dynamic process that affects fiber myelination (Chang et al., 2016; Fields, 2008b; Ganguly & Poo, 2013). Together, these measures provide novel insight into the CNS neuroplasticity surrounding the efficacy of CBT intervention for the treatment of chronic musculoskeletal pain.

Materials and Methods

Participant Recruitment and Evaluation

The study was approved by the University of Vermont Institutional Review Board (IRB). All procedures were in compliance with the Declaration of Helsinki. Healthy pain-

free control participants (analyzed and compared in chapter 2) and patients with chronic musculoskeletal pain were recruited for the initial study. In this chapter, we longitudinally evaluated chronic pain patients following behavioral intervention to compare structural brain plasticity after treatment (Figure 3.1 & 3.2). Prior to imaging, participants were first clinically evaluated, in-person, by a study physician and provided informed consent. Initial evaluation of pain participants included an extensive medical history work-up where data including demographics, medical history, mental health, medication history and management, as well as current and typical pain levels were collected. All patients had a primary diagnosis of musculoskeletal pain with mixed diagnoses consisting of chronic low back pain, osteoarthritis, post-trauma or post-surgical pain, temporomandibular disorder, or mixed sources of musculoskeletal pain. Inclusionary criteria for chronic pain participants were: symptoms of pain for at least one year in duration as indicated by self-reports, and a minimum of 4 out of 10 score on a pain likert scale. Exclusionary criteria for pain participants included standard MRI contraindications, current opioid regimens, a history of traumatic brain injury, unmanaged hypertension or diabetes, and psychiatric disorders including major depression, schizophrenia, and bipolar disorder. Refer to consort diagram for study recruitment details (Figure 3.1).

Pain participants were randomized by a study statistician into either the CBT intervention group or into an educational active control group (EDU). Patients were randomized to control for sex, age, and pain level. The participants in the CBT cohort underwent ninety-minute group CBT sessions once a week for 11-weeks (11, 90-minute sessions total). CBT intervention was designed to incorporate the following pain management strategies: alter cognitions and reduce maladaptive coping strategies such as

catastrophizing, promote attention-based diversion approaches, and monitor and regulate activity patterns. A thorough description of the program is outlined in the following manuscripts by Naylor and colleagues (Naylor, Helzer, Naud, & Keefe, 2002; Naylor, Keefe, Brigidi, Naud, & Helzer, 2008).

Alternatively, pain participants randomized to the EDU cohort received weekly at-home mailings pertaining broadly to pain physiology and management. These included pain chronification, physiology, positive effects of physical activity, the importance of diet and sleep patterns, and stress, anxiety, and depression management. Importantly, these topics were also discussed in the CBT sessions, with the critical distinction that EDU participants did not receive any information on cognitive or behavioral coping strategies nor was feedback given by study personnel.

Participants enrolled in the study underwent three separate behavioral assessments and MRI study sessions: 1) baseline, prior to treatment randomization (TP1); 2) after 11-week CBT or EDU control intervention (TP2); and 3) at a four-month follow-up after intervention (TP3) (Figure 3.2). At each imaging session, participants underwent an MRI evaluation consisting of structural (T_1-weighted and diffusion-weighted imaging) and functional (resting state, task-based, and evoked) acquisitions. For this chapter, structural images were analyzed and interpreted.

Clinical Assessment

Clinical assessments were analyzed similarly to (Shpaner et al., 2014) and were obtained by participant self-reports after each study session: Baseline (TP1), following 11-week intervention (TP2), and lastly, after a final follow-up study session (TP3). All

participants were instructed to think about their chronic musculoskeletal pain when answering the questionnaires. Broadly, we evaluated measures of depression, pain experience, self-efficacy, and catastrophizing.

Depression was measured using the Beck Depression Inventory (BDI; (Beck, Ward, Mendelson, Mock, & Erbaugh, 1961) with the following clinical parameters: < 13 = minimal depression, 14-19 = minor depression, 20-28 = moderate depression, and > 29 = major depression.

Pain and disability measures were evaluated using the following Total Outcomes and Pain Survey (TOPS; (Rogers, Wittink, Ashburn, Cynn, & Carr, 2000)), which consisted of the following subscales: Pain Symptoms, Total Pain Experience, Perceived Family Disability, Passive Coping, as well as SF-36 Mental and Physical Health Composites. Each subscale ranged from a 0 to 100.

Pain efficacy, or perceived ability to cope with chronic pain disability, was evaluated using an adapted Chronic Pain Self-Efficacy Scale (Anderson, Dowds, Pelletz, Edwards, & Peeters-Asdourian, 1995) with the following three subscales: Self-Efficacy for Pain Management, Self-Efficacy for Physical Function, and Self-Efficacy for Coping with Symptoms. These attributes are measured on a 0-10 scale with 0 indicating "very uncertain" and 10 indicating "very certain."

Pain catastrophizing is well documented in chronic pain conditions (Quartana, Campbell, & Edwards, 2009) and was evaluated using the Pain Catastrophizing Scale (M. Sullivan, Bishop, & Pivak, 1995). Scores closer to 0 reflect less catastrophizing, and the maximum score of 52 is indicative of the greatest level of pain catastrophizing.

Clinical assessments for TP2 and TP3 were analyzed using SPSS Statistical software version 24.0 (IBM Corporation, Armonk, NY, USA). Analyses were conducted separately for TP1 vs. TP2 and TP1 vs TP3. A repeated measures ANOVA with one within- and one between-subject factors was implemented to investigate the interaction of time (pre vs. post) and group (CBT vs. EDU).

Magnetic Resonance Imaging Acquisition

All data were collected using a Philips 3T Achieva MRI scanner (Philips Healthcare, Best, Netherlands). The scanner underwent an upgrade in the course of the study and an 8-channel sensitivity encoding (SENSE) head coil was replaced with a 15-channel SENSE digital head coil. All scan visits were completed either before or after the upgrade. The same pulse sequences were used before and after the upgrade: T_1-weighted structural imaging data were acquired using a spoiled gradient volumetric sequence oriented perpendicular to the anterior commissure-posterior commissure with 9.9ms TR, 4.6ms TE, 8º flip angle, 256mm FOV, 1.0 NSA, 256 X 256 matrix, and 1.0mm slice thickness with no gap for 140 contiguous slices as well as an axial T2-weighted gradient spin echo sequence using 28 contiguous 5mm slices, 2466ms TR, 80ms TE, 3.0 NSA, and 230mm FOV. Diffusion weighted imaging data were acquired using an axial 2-dimensional spin echo echo planar imaging (EPI) sequence with 46 diffusion directions and the following specifications: 59 slices, 2mm slice thickness, 10,000ms TR, 68ms TE, 2x2mm in-plane resolution, 1000 s/mm^2 B-value, and 63 EPI factor.

Grey Matter (GM) Analysis

Chronic pain patients (n=33) receiving CBT intervention were compared to EDU controls (n=15) across all time points (TP1, TP2, and TP3), cumulatively representing 144 scans. Voxel-based morphometry (VBM) analysis was implemented using SPM12 (Statistical Parametric Mapping, Institute of Neurology, London, UK) and the computational anatomy toolbox (CAT12; C. Gaser, Structural Brain Mapping Group, Jena University Hospital, Jena, Germany). Default settings were used. In brief, T1-weighted images were first biased corrected for magnetic field inhomogeneity. In the CAT12 toolbox, bias corrected images were longitudinally segmented using the diffeomorphic anatomical registration using exponentiated lie algebra (DARTEL) algorithm (Ashburner, 2007) and resulting in cerebrospinal fluid (CSF), grey matter (GM), and white matter (WM) compartments. The images then underwent spatial normalization to 1.5x1.5x1.5mm3 MNI space. Finally, all images were smoothed with an 8mm (FWHM) smoothing kernel. No modulation was applied. Segmentations for each participant were visually inspected and sample homogeneity was assessed for outliers.

Statistical analysis was implemented using the Multivariate Repeated Measures (MRM) toolbox designed for flexible repeated measures investigation of longitudinal neuroimaging data (http://www.click2go.umip.com/i/software/mrm.html; (McFarquhar et al., 2016). A non-parametric, 3 (time) x 2 (groups) repeated measures MANOVA with 5000 permutations was implemented with age, sex, and upgrade as nuisance regressors and family wise error correction for multiple comparisons. Significance was assessed with a cluster threshold of $p \leq 0.05$.

White Matter (WM) Analysis

1. *WM Complexity: Mode of Anisotropy (MO) and Ball & Sticks (F1 & F2)*

Given the lack of longitudinal or repeated measures pipelines in FSL two separate analyses were carried out: 1) TP1 vs. TP2, and 2) TP1 vs TP3. In the first comparison, forty-two chronic pain patients receiving CBT intervention were compared to twenty-one active pain controls (TP1 vs. TP2). In the second comparison, 38 chronic pain patients receiving CBT intervention were compared to 15 EDU controls to compare between baseline vs. four-month follow-up analysis; TP1 vs. TP3.

Raw DWI images were first converted to nifti format using MRIcron software (Rorden & Brett, 2000). DWI scans were subsequently analyzed using FSL FMRIB software (Jenkinson et al., 2012; S. M. Smith et al., 2004; Woolrich et al., 2009). Utilizing the Diffusion Toolbox, FDT, images underwent eddy current correction, brain extraction, and a T_2-weighted image was extracted from the initial B0 volume. Data were then processed using both a single tensor, diffusion tensor imaging (DTI) model as well as a multi-compartment, Ball-and-Sticks (BAS) model. The resulting DTI model was implemented using dtifit and yielded the following metric maps: Radial diffusivity RD), Axial diffusivity (AD), Mean diffusivity (MD), Fractional Anisotropy (FA), and Mode of anisotropy (MO). The BAS model was implemented using the Bayesian Estimation of Diffusion Parameters Obtained Using Sampling Techniques (BEDPOSTX) to enable modeling of multiple fiber populations and orientations within each voxel (Behrens et al., 2007). Default BEDPOSTX parameters were used: first a multiexponential model was implemented with a burn-in period of 1000 and up to two fiber populations were defined. The BEDPOSTX output generated estimates of each fiber orientation (i.e., x1 or x2) and a

corresponding partial volume fraction metric - F1 and F2. Importantly, the model prevents overfitting by shrinking the corresponding F2 metric to 0 in the absence of a secondary fiber orientation or population. Both F1 and F2 correspond to distinct tracts within each voxel where the major or primary fiber population is defined by F1 and minor or secondary fiber population is expressed as F2.

Prior to inclusion, all raw diffusion scans, and metric maps were visually inspected for artifacts, excessive motion, and anatomical abnormalities. The subsequent WM microstructural analyses steps were first carried out on the FA images using the standard FSL tract based spatial statistics pipeline. Downstream statistical comparison was implemented using only the mode of anisotropy (MO) and the partial volume maps (F1 & F2) due to their sensitivity in regions of multiple fiber populations and complex geometry. In brief, FA images were non-linearly registered to the $1mm^3$ isotropic FMRIB58 FA template followed by affine transformation to MNI152 standard space. FA data were then projected onto an alignment-invariant mean FA skeleton image with the recommended threshold of 0.2. F1 and F2 maps were then aligned to ensure that each fiber orientation corresponded to the same fiber populations across subjects. The previous step was not required for MO because the ball and sticks method defines specific fiber populations whereas MO does not. Next, the warps generated from the non-linear and affine transformations of the FA images were applied to the MO, F1, and F2 data. Skeletonized images for MO, F1, and F2 were then split, and either TP2 (analysis #1) or TP3 (analysis #2) was subtracted from the TP1 baseline scan, generating a single 4D file with one difference image per subject. Statistical inference was carried out using a binary mask of

the FA skeletonized image ensuring that only voxels within the center of each tract were analyzed, preventing partial voluming effects.

Region of interest (ROI) and whole brain exploratory analyses were conducted using FSL's randomise method: a non-parametric, permutation approach with threshold free cluster enhancement (tfce) to correct for multiple comparisons. Whole brain voxel-by-voxel analysis was performed for each WM metric (MO, F1, and F2) using the complete thresholded FA skeleton mask and executing a total of ten thousand permutations per voxel t-test. For the ROI analyses, masks for each of the predetermined WM structures were extracted from the Johns Hopkins ICBM-DTI-81 atlas, combined with FA skeleton mask, thresholded by a value of two to obtain the overlap between the skeleton and the mask, and binarized. Randomise permutation testing with a total of ten thousand permutations per t-test, was then applied to each skeletonized ROI mask. Participant ages were input into the general linear model as nuisance covariates and significance was defined by $p \leq 0.05$.

2. *Structural Connectivity Analysis*

In the first comparison of baseline (TP1) to post-intervention (TP2), forty-two chronic pain patients receiving CBT intervention (CBT Group) were compared to eighteen active pain controls (EDU Group). In the second comparison of baseline (TP1) to follow-up (TP3), thirty-eight chronic pain patients receiving CBT intervention were compared to fifteen active pain controls. Structural connectivity was calculated using DSI Studio software (http://dsi-studio.labsolver.org). DWI acquisitions were reconstructed using deterministic Q-Space Dieffomorphic Reconstruction (QSDR; (Yeh & Tseng, 2011). QSDR constructs the spin density function in template space and is a generalized form of GQI (Generalized

Q-Sampling Imaging). Following reconstruction, whole brain tractography was initiated similarly to Muraskin and colleagues (Muraskin et al., 2016). In brief, a Random number generator was created to toggle several arbitrary variables including quantitative anisotropy (QA), turning angle threshold, and smoothing. Tractography was performed 1,000 times iteratively using random whole brain seeding with the following fixed parameters: step size (1mm) and fiber length (Minimum = 10mm; Maximum = 400mm), and randomly toggled parameters: QA threshold (0.01-0.10), turning angle threshold (40°-80°), and smoothing (50%-80%). 250,000 streamlines were generated for each of the following tractography iterations.

Whole brain connectivity matrices were generated using the 116 parcellation Automated Anatomical Labeling (AAL) atlas (Tzourio-Mazoyer et al., 2002). To quantify the structural connection strength between regions, subsequent 116x116 connectivity matrices were created by counting the number of streamlines passing through and/or terminating within the respective atlas GM regions. Next, a single connectivity matrix was generated for each subject by averaging the 1,000 matrices using MATLAB 2015b Software (The MathWorks Inc., Natick, MA, 2000). Between-group differences in connectivity were statistically analyzed using the Network Based Statistics (NBS) Toolbox (Zalesky et al., 2010). NBS is a validated statistical toolbox that is designed to attenuate issues of multiple comparison in mass univariate testing and facilitate large scale network comparisons. The method uses nonparametric statistical methods to control for family wise error rate. NBS is the relative equivalent of cluster-based statistical approaches except that NBS clusters in topological space instead of physical space. Each subject's average connectivity matrix was input into the NBS toolbox to test between-group connectivity. A

total of 5000 permutations were computed with family wise error correction for multiple comparisons. An ANCOVA with 5000 permutations was computed utilizing the NBS test statistic and fully corrected for multiple comparisons via False Discovery Rate (FDR). NBS requires that a test statistic threshold is given which can be arbitrary and thus a range of suggested values between 2.7-3.1 were investigated in .2 increments. Significance threshold was defined at $p \leq 0.05$.

Results

Demographics and Clinical Response to Intervention

The CBT and EDU groups were matched for age and sex. Comparison of demographics between the group demonstrated an imbalance in depression composite scores at TP2 and in pain duration at TP3 (Table 3.1). The CBT group showed significant clinical improvements over time compared to the EDU cohort on 9 out of 10 composite measures following 11-week intervention (TP2) (Table 3.2) and 5 out of 10 composite measures after 4-month follow-up (Table 3.3).

GM Whole Brain Morphometry Analyses (Longitudinal – TP1, TP2, & TP3)

A longitudinal analysis assessing baseline (TP1), post 11-week intervention (TP2), and follow-up (TP3) visits was implemented using the Multivariate and Repeated Measures for Neuroimaging (MRM) toolbox. To investigate the possible main effects of group and group by time interactions, permutation testing was conducted with age, sex, and upgrade as nuisance regressors, family-wise error correction for multiple comparisons,

and a cluster threshold of $p \leq 0.05$. No significant main effects or interactions were observed at the predetermined statistical threshold of $p \leq 0.05$.

WM Whole Brain Complexity Analyses Baseline (Tp1) vs. Post-Intervention Follow-up (Tp2) and Baseline (Tp1) vs. Final Follow-up (Tp3)

Whole brain permutation analyses of the tensor derived metric of complexity (MO) yielded a significant between-group result in an unlabeled track adjacent to the thalamus ($p=.05$) with the CBT cohort exhibiting a reduction in complexity compared to EDU controls at TP2. No significant between-group differences in complexity metrics were observed at TP3.

WM Region of Interest Complexity Analyses: (Baseline (TP1) vs. Post-Intervention (TP2))

A subtraction (TP2 – TP1) analysis assessing baseline and post 11-week intervention visits was implemented to compare EDU controls to patients receiving CBT with age, sex, and scanner upgrade as nuisance covariates. The ball & sticks multi-compartment metric, F1, yielded several significant between-group differences at a threshold of $p<0.05$. Specifically, the CBT cohort exhibited an increase in fiber complexity (a reduction in the major fiber population F1), compared to EDU controls within the left posterior internal capsule and the right external capsule. In addition, the CBT group exhibited greater fiber complexity (increased F2), compared to EDU controls, within the left cingulum adjacent to the hippocampus, the bilateral posterior internal capsule. The left posterior internal capsule, therefore, exhibited increased CBT-related complexity as

assessed with both the major and the minor fiber population metrics. ROI permutation analyses of the tensor derived metric of complexity (MO) yielded several significant between-group differences. The CBT cohort demonstrated a reduction in complexity (MO) within the right cingulum adjacent to the hippocampus, as compared to EDU controls. EDU controls exhibited increased complexity compared to patients that received CBT within the right posterior internal capsule (Table 3.4).

WM Region of Interest Complexity Analyses: Baseline (TP1) vs. Final Follow-up (TP3)

CBT group exhibited increased fiber complexity (increased F2) when we compared CBT vs. EDU from baseline to final follow-up. Significant increases in F2 were observed within left posterior internal capsule and the right anterior internal capsule. Increased complexity in the left posterior internal capsule was, therefore, consistent across the entire study. In the tensor derived metric of complexity, CBT participants demonstrated reduced complexity (increased MO) compared to EDU controls in the right cerebral peduncle (Table 3.5).

WM Whole Brain Complexity Analyses: Baseline (TP1) vs. Post-Follow-up (TP2)

A subtraction (TP3 - TP1) analysis assessing baseline and post 11-week intervention visits was implemented to compare EDU controls to patients receiving CBT with age, sex, and scanner upgrade as nuisance covariates. Whole brain permutation analyses of the ball & sticks multi-compartment metric, F1, did not yield any significant between-group results at a threshold of $p<0.05$. The ball & sticks multi-compartment metric, F2, also did not yield any significant between-group results at a threshold of $p<0.05$,

however several notable clusters were observed by slight relaxation of the statistical threshold. Although not significant, patients receiving CBT exhibited increased F2 or the minor fiber population metric in the left anterior corona radiata ($p=0.08$) and the left genu of the corpus callosum ($p=0.1$). Whole brain permutation analyses of the tensor derived metric of complexity (MO) yielded a significant between-group result in an unlabeled track adjacent to the thalamus ($p=0.05$) with the CBT cohort exhibiting a reduction in complexity compared to EDU controls.

WM Whole Brain Complexity Analyses: Pre- (Tp1) vs. Follow-up (Tp3)

An analysis assessing baseline and four-month post-intervention follow-up visits was implemented to compare EDU controls to patients receiving CBT with age, sex, and scanner upgrade as nuisance covariates. Whole brain permutation analyses of both ball & sticks multi-compartment metrics, F1 and F2, did not yield any significant between-group results at a threshold of $p<0.05$. Whole brain permutation analyses of the tensor derived metric of complexity (MO) also did not yield any significant between-group results at a threshold of $p<0.05$.

WM Connectivity

A longitudinal comparison of connectivity did not yield any significant whole brain differences between patients receiving CBT compared to EDU controls (Table 3.6A). A significant effect of time was observed, with both groups demonstrating less connectivity at TP3 compared to TP1 evaluation at t-value thresholds of 2.9 ($p<0.036$) and 3.1 ($p<0.041$) (Table 3.6B)

Discussion

In this investigation, we longitudinally evaluated GM morphometry, WM complexity, and WM connectivity, in chronic musculoskeletal pain patients randomized to either CBT intervention or an active educational control group (EDU). Although we did not reproduce CBT-related GM changes previously demonstrated by our lab (Seminowicz et al., 2013), this is the first study reporting CBT-related WM neuroplasticity. Specifically, we demonstrated significant between-group alterations in WM fiber complexity following both TP2 and TP3. We propose that these structural alterations reflect observed clinical improvements, suggesting either compensation or normalization. Although CBT does not treat the underlying peripheral pathology that provokes disease chronification, it may mitigate abnormal signaling within the brain, promoting CNS activity-dependent neuroplasticity (Ganguly & Poo, 2013). WM neuroplasticity has been demonstrated in the somatosensory cortex following clinical improvements in median nerve latency (Maeda et al., 2017). This suggests that learning to cope with chronic pain may facilitate dynamic changes in WM microstructure and activity-dependent WM remodeling.

Sensorimotor Pathways

Sensorimotor tracts, including the posterior internal capsule and cerebral peduncles, comprise the pathways through which sensations and motor signals are relayed between the brain and spinal cord, and are central in developing chronic pain. The posterior internal capsule contains ascending fibers that project to the somatosensory cortex, however, this pathway also includes descending motor fiber projections. Following intervention, CBT patients exhibited a bilateral increase in posterior internal capsule

complexity, however, only the left remained significant after the final follow-up. Post-intervention (TP2) analysis also identified decreased complexity (increased MO) in the CBT group that was not present at final follow-up (TP3). This may reflect the fact that the internal capsule contains both somatosensory and motor pathways that are differentially influenced following CBT. For patients receiving CBT, a decrease in the major fiber population (F1) that carries sensory information may suggest a reduction in pain signaling, similar to previous reports (Maeda et al., 2017), while in increase in the minor fiber population (F2) may reflect alterations in physical functioning and motor patterns. Strengthening of motor pathways was revealed at TP3, where a decrease in complexity (MO) was observed in the right cerebral peduncle in CBT participants compared to EDU controls. The cerebral peduncle contains motor pathways, such as the descending corticospinal tract, possibly reflective of increased patterns of physical activity at TP2 compared to TP3, although this interpretation necessitates further investigation. Maladaptive fear avoidance behavior in chronic pain populations may contribute to pain chronification by limiting a patient's physical functioning and further potentiating aberrations in peripheral structure and pain signaling (Langevin & Sherman, 2007). Interventions that address psychological aspects of pain, therefore, may stimulate dynamic changes across both somatosensory and motor networks.

Emotion Processing Pathways

Affective dysregulation is central to the development of chronic pain, and thus remediation of these maladaptive traits is a major goal of CBT. Accomplishing better affective regulation may be reflected in plasticity of the neural tracts that integrate affective information. The external capsule exhibited significant between-group differences

immediately post-therapy, but this change was not maintained at TP3. The external capsule contains projections to the amygdala and the insular cortex, important nodes of the affective-motivational aspects of pain. Pain patients receiving CBT showed a reduction in the primary fiber population metric, F1, compared to EDU pain controls in this region. In a previous investigation where we compared pain patients to healthy controls (Chapter 2), we report reductions in F1 in the posterior external capsule. A further reduction in the metric following CBT would be indicative of a compensatory mechanism. There is inconsistency in single tensor diffusion metrics literature within the external capsule. Consistent with the results reported in Chapter 2, FA was elevated in irritable bowel pain patients (J. Y. Chen et al., 2011), as well as in dysmenorrhea patients (P. Liu et al., 2016). Increased external capsule RD in chronic pain has also been reported previously by our lab (Lieberman et al., 2014) and others (Mansour et al., 2013; Moayedi et al., 2012b). The present study is the first to report changes in external capsule following treatment. Further investigations are is required to better characterize the potential relationship between changes in external capsule and affective-motivational aspects of chronic pain.

The cingulum bundle in the temporal lobe adjacent to the hippocampus demonstrated increased WM fiber complexity following CBT intervention (TP2), which was absent at follow-up (TP3). Compared to EDU, CBT participants demonstrated an increase in F2 (minor fiber population) with the left hemisphere and a decrease in MO within the right. The cingulum provides connections between an array of brain regions in the temporal, parietal, and frontal lobes (Y. Wu et al., 2016). The temporal lobe subcomponent of the cingulum may be particularly relevant to pain processing and memory encoding given projections to the hippocampus, the entorhinal cortex, and the cingulate

cortex, another node in the affective-motivational pain network. Interestingly, cingulotomy has been performed as a treatment for numerous intractable chronic pain states, including low back pain and has been shown to diminish the affective response to noxious stimuli (See Review: (Fuchs, Peng, Boyette-Davis, & Uhelski, 2014)). Thus, alterations in WM complexity within this structure may reflect changes in the affective appraisal of chronic pain following CBT.

Cognitive Pathways

We also found increased CBT-related complexity in the anterior limb of the internal capsule at TP3. This structure may be important for cognitive processing of pain because it connects the thalamus to the prefrontal cortex, including the DLPFC (Giguere & Goldman-Rakic, 1988). Alterations in this thalamo-cortical pathway at TP3 in CBT patients may be indicative of long-term changes in cognitive processing of pain.

Conclusions

Following 11-week CBT intervention (TP2), WM complexity differences were observed bilaterally within the temporal lobe region of the cingulum and the posterior internal capsule as well as unilaterally in the right external capsule (Table 3.4). At the final follow-up visit (TP3), WM complexity changes were similarly observed in the left posterior internal capsule, as well the right anterior internal capsule, and right cerebral peduncle (Table 3.5). Interestingly, the left posterior internal capsule was the only region to exhibit alterations in the same direction across both timepoints, which could be reflective of long-term changes associated with learned cognitive coping strategies. The inconsistencies of WM changes across assessments may reflect psychological, biological

or methodological limitations. Further assessment of patient adherence to CBT practices over time would help to clarify the significance of these changes. Although we demonstrated several WM complexity alterations in pain matrix WM circuitry, we did not observe a difference in whole brain connectivity. The diffusion acquisition with a b-value of 1000 is standard for microstructural investigation but may not be ideal for tractography applications. Alternatively, the effects of CBT may be subtle during the initial training period, and long-term adherence may facilitate more robust differences in connectivity.

In conclusion, we demonstrate for the first time, WM neuroplasticity associated with CBT for the treatment of musculoskeletal pain. We suggest that WM plasticity reflects alterations in aberrant pain signaling through effective remediation of maladaptive behavioral traits that are reminiscent of the chronic pain condition.

Acknowledgments

Funding for this work was provided by the National Institute of Arthritis and Musculoskeletal and Skin Diseases (NIAMS) grant R01-AR059674. The authors would like to thank the UVM MRI Center for Biomedical Imaging for their assistance with data acquisition.

References for Chapter 3

Anderson, K. O., Dowds, B. N., Pelletz, R. E., Edwards, W. T., & Peeters-Asdourian, C. (1995). Development and initial validation of a scale to measure self-efficacy beliefs in patients with chronic pain. *Pain, 63*(1), 77-84.

Ashburner, J. (2007). A fast diffeomorphic image registration algorithm. *Neuroimage, 38*(1), 95-113. doi:10.1016/j.neuroimage.2007.07.007

Baraban, M., Mensch, S., & Lyons, D. A. (2016). Adaptive myelination from fish to man. *Brain Res, 1641*(Pt A), 149-161. doi:10.1016/j.brainres.2015.10.026

Beck, A. T., Ward, C. H., Mendelson, M., Mock, J., & Erbaugh, J. (1961). An inventory for measuring depression. *Arch Gen Psychiatry, 4*, 561-571.

Behrens, T. E., Berg, H. J., Jbabdi, S., Rushworth, M. F., & Woolrich, M. W. (2007). Probabilistic diffusion tractography with multiple fibre orientations: What can we gain? *Neuroimage, 34*(1), 144-155. doi:10.1016/j.neuroimage.2006.09.018

Chang, K. J., Redmond, S. A., & Chan, J. R. (2016). Remodeling myelination: implications for mechanisms of neural plasticity. *Nat Neurosci, 19*(2), 190-197. doi:10.1038/nn.4200

Chen, J. Y., Blankstein, U., Diamant, N. E., & Davis, K. D. (2011). White matter abnormalities in irritable bowel syndrome and relation to individual factors. *Brain Res, 1392*, 121-131. doi:10.1016/j.brainres.2011.03.069

Ehde, D. M., Dillworth, T. M., & Turner, J. A. (2014). Cognitive-behavioral therapy for individuals with chronic pain: efficacy, innovations, and directions for research. *Am Psychol, 69*(2), 153-166. doi:10.1037/a0035747

Fields, R. D. (2008b). White matter in learning, cognition and psychiatric disorders. *Trends Neurosci, 31*(7), 361-370. doi:10.1016/j.tins.2008.04.001

Fuchs, P. N., Peng, Y. B., Boyette-Davis, J. A., & Uhelski, M. L. (2014). The anterior cingulate cortex and pain processing. *Front Integr Neurosci, 8*, 35. doi:10.3389/fnint.2014.00035

Ganguly, K., & Poo, M. M. (2013). Activity-dependent neural plasticity from bench to bedside. *Neuron, 80*(3), 729-741. doi:10.1016/j.neuron.2013.10.028

Giguere, M., & Goldman-Rakic, P. S. (1988). Mediodorsal nucleus: areal, laminar, and tangential distribution of afferents and efferents in the frontal lobe of rhesus monkeys. *J Comp Neurol, 277*(2), 195-213. doi:10.1002/cne.902770204

Hodges, P. W., & Tucker, K. (2011). Moving differently in pain: a new theory to explain the adaptation to pain. *Pain, 152*(3 Suppl), S90-98. doi:10.1016/j.pain.2010.10.020

Jenkinson, M., Beckmann, C. F., Behrens, T. E., Woolrich, M. W., & Smith, S. M. (2012). Fsl. *Neuroimage, 62*(2), 782-790. doi:10.1016/j.neuroimage.2011.09.015

Kucyi, A., Salomons, T. V., & Davis, K. D. (2016). Cognitive behavioral training reverses the effect of pain exposure on brain network activity. *Pain, 157*(9), 1895-1904. doi:10.1097/j.pain.0000000000000592

Langevin, H. M., & Sherman, K. J. (2007). Pathophysiological model for chronic low back pain integrating connective tissue and nervous system mechanisms. *Med Hypotheses, 68*(1), 74-80. doi:10.1016/j.mehy.2006.06.033

Lazaridou, A., Kim, J., Cahalan, C. M., Loggia, M. L., Franceschelli, O., Berna, C., . . . Edwards, R. R. (2017). Effects of Cognitive-Behavioral Therapy (CBT) on Brain

Connectivity Supporting Catastrophizing in Fibromyalgia. *Clin J Pain, 33*(3), 215-221. doi:10.1097/AJP.0000000000000422

Lieberman, G., Shpaner, M., Watts, R., Andrews, T., Filippi, C. G., Davis, M., & Naylor, M. R. (2014). White matter involvement in chronic musculoskeletal pain. *J Pain*. doi:10.1016/j.jpain.2014.08.002

Liu, P., Wang, G., Liu, Y., Yu, Q., Yang, F., Jin, L., . . . Calhoun, V. D. (2016). White matter microstructure alterations in primary dysmenorrhea assessed by diffusion tensor imaging. *Sci Rep, 6*, 25836. doi:10.1038/srep25836

Lund, J. P., Donga, R., Widmer, C. G., & Stohler, C. S. (1991). The pain-adaptation model: a discussion of the relationship between chronic musculoskeletal pain and motor activity. *Can J Physiol Pharmacol, 69*(5), 683-694.

Maeda, Y., Kim, H., Kettner, N., Kim, J., Cina, S., Malatesta, C., . . . Napadow, V. (2017). Rewiring the primary somatosensory cortex in carpal tunnel syndrome with acupuncture. *Brain, 140*(4), 914-927. doi:10.1093/brain/awx015

Mansour, A. R., Baliki, M. N., Huang, L., Torbey, S., Herrmann, K. M., Schnitzer, T. J., & Apkarian, A. V. (2013). Brain white matter structural properties predict transition to chronic pain. *Pain, 154*(10), 2160-2168. doi:10.1016/j.pain.2013.06.044

McFarquhar, M., McKie, S., Emsley, R., Suckling, J., Elliott, R., & Williams, S. (2016). Multivariate and repeated measures (MRM): A new toolbox for dependent and multimodal group-level neuroimaging data. *Neuroimage, 132*, 373-389. doi:10.1016/j.neuroimage.2016.02.053

Moayedi, M., Weissman-Fogel, I., Salomons, T. V., Crawley, A. P., Goldberg, M. B., Freeman, B. V., . . . Davis, K. D. (2012b). White matter brain and trigeminal nerve abnormalities in temporomandibular disorder. *Pain, 153*(7), 1467-1477. doi:10.1016/j.pain.2012.04.003

Muraskin, J., Dodhia, S., Lieberman, G., Garcia, J. O., Verstynen, T., Vettel, J. M., . . . Sajda, P. (2016). Brain dynamics of post-task resting state are influenced by expertise: Insights from baseball players. *Hum Brain Mapp, 37*(12), 4454-4471. doi:10.1002/hbm.23321

Naylor, M. R., Helzer, J. E., Naud, S., & Keefe, F. J. (2002). Automated telephone as an adjunct for the treatment of chronic pain: a pilot study. *J Pain, 3*(6), 429-438.

Naylor, M. R., Keefe, F. J., Brigidi, B., Naud, S., & Helzer, J. E. (2008). Therapeutic Interactive Voice Response for chronic pain reduction and relapse prevention. *Pain, 134*(3), 335-345. doi:10.1016/j.pain.2007.11.001

Perl, E. R. (2007). Ideas about pain, a historical view. *Nat Rev Neurosci, 8*(1), 71-80. doi:10.1038/nrn2042

Quartana, P. J., Campbell, C. M., & Edwards, R. R. (2009). Pain catastrophizing: a critical review. *Expert Rev Neurother, 9*(5), 745-758. doi:10.1586/ern.09.34

Rogers, W. H., Wittink, H. M., Ashburn, M. A., Cynn, D., & Carr, D. B. (2000). Using the "TOPS," an outcomes instrument for multidisciplinary outpatient pain treatment. *Pain Med, 1*(1), 55-67. doi:10.1046/j.1526-4637.2000.99101.x

Roland, M. O. (1986). A critical review of the evidence for a pain-spasm-pain cycle in spinal disorders. *Clin Biomech (Bristol, Avon), 1*(2), 102-109. doi:10.1016/0268-0033(86)90085-9

Rorden, C., & Brett, M. (2000). Stereotaxic display of brain lesions. *Behav Neurol, 12*(4), 191-200.

Seminowicz, D. A., Shpaner, M., Keaser, M. L., Krauthamer, G. M., Mantegna, J., Dumas, J. A., . . . Naylor, M. R. (2013). Cognitive-behavioral therapy increases prefrontal cortex gray matter in patients with chronic pain. *J Pain, 14*(12), 1573-1584. doi:10.1016/j.jpain.2013.07.020

Shpaner, M., Kelly, C., Lieberman, G., Perelman, H., Davis, M., Keefe, F. J., & Naylor, M. R. (2014). Unlearning chronic pain: A randomized controlled trial to investigate changes in intrinsic brain connectivity following Cognitive Behavioral Therapy. *Neuroimage Clin, 5*, 365-376. doi:10.1016/j.nicl.2014.07.008

Smith, S. M., Jenkinson, M., Woolrich, M. W., Beckmann, C. F., Behrens, T. E., Johansen-Berg, H., . . . Matthews, P. M. (2004). Advances in functional and structural MR image analysis and implementation as FSL. *Neuroimage, 23 Suppl 1*, S208-219. doi:10.1016/j.neuroimage.2004.07.051

Sullivan, M., Bishop, S., & Pivak, J. (1995). The pain catastrophizing scale: development and validation. *Psychological Assessment, 7* 524-532.

Tzourio-Mazoyer, N., Landeau, B., Papathanassiou, D., Crivello, F., Etard, O., Delcroix, N., . . . Joliot, M. (2002). Automated anatomical labeling of activations in SPM using a macroscopic anatomical parcellation of the MNI MRI single-subject brain. *Neuroimage, 15*(1), 273-289. doi:10.1006/nimg.2001.0978

Williams, A. C., Eccleston, C., & Morley, S. (2012). Psychological therapies for the management of chronic pain (excluding headache) in adults. *Cochrane Database Syst Rev, 11*, Cd007407. doi:10.1002/14651858.CD007407.pub3

Woolrich, M. W., Jbabdi, S., Patenaude, B., Chappell, M., Makni, S., Behrens, T., . . . Smith, S. M. (2009). Bayesian analysis of neuroimaging data in FSL. *Neuroimage, 45*(1 Suppl), S173-186. doi:10.1016/j.neuroimage.2008.10.055

Wu, Y., Sun, D., Wang, Y., & Wang, Y. (2016). Subcomponents and Connectivity of the Inferior Fronto-Occipital Fasciculus Revealed by Diffusion Spectrum Imaging Fiber Tracking. *Front Neuroanat, 10*, 88. doi:10.3389/fnana.2016.00088

Yeh, F. C., & Tseng, W. Y. (2011). NTU-90: a high angular resolution brain atlas constructed by q-space diffeomorphic reconstruction. *Neuroimage, 58*(1), 91-99. doi:10.1016/j.neuroimage.2011.06.021

Zalesky, A., Fornito, A., & Bullmore, E. T. (2010). Network-based statistic: identifying differences in brain networks. *Neuroimage, 53*(4), 1197-1207. doi:10.1016/j.neuroimage.2010.06.041

Figure Captions

Figure 3.1. Consort diagram for the randomized clinical trial highlighting participant recruitment, allocation, follow-up, and analysis.

Figure 3.2. A complete study flow chart illustrating recruitment, data collection, and study timeline. Healthy controls were recruited and scanned at a single, baseline, time point (TP1) as part of the broader study (not analyzed or compared in this chapter). In this chapter, we longitudinally investigated participants with chronic pain, as outlined in red. In brief, all chronic pain patients underwent a baseline (TP1) MRI session and were subsequently randomized to either CBT intervention or an active educational materials control group (EDU). Both CBT and EDU interventions were 11-weeks in duration after which all participants with chronic pain underwent a second, identical MRI session (TP2). Patients were then brought back for a third MRI session four months after completion of either CBT or EDU intervention (TP3). Total study duration from time of initial visit to completion of the final MRI was approximately seven months for each participant.

Table Captions

Table 3.1. Top) TP2 demographics indicating that the groups were balanced for age, sex, and pain duration, however, there was a significant between-group difference in depression index, with the CBT cohort exhibiting elevated depression compared to EDU controls. Bottom) TP3 demographics indicating that the groups were balanced for age, sex, and depression, however, there was a significant between-group difference in pain duration with CBT participants having a longer pain duration than EDU controls.

Table 3.2. At TP2, CBT participants demonstrated significant clinical improvements compared to EDU controls in all clinical assessments except for self-efficacy for physical functioning (FSE), however, the combined mean score which encompasses FSE was significant. Values reported as mean ± standard deviation, CBT n=42, Healthy n=21.

Table 3.3. At TP3, CBT participants demonstrated significant clinical improvements compared to EDU controls in the following clinical assessments: mental composite, passive coping, catastrophizing, and self-efficacy for coping with symptoms. Values reported as mean ± standard deviation, CBT n=38, Healthy n=15.

Table 3.4. At TP2, CBT participants exhibited an increase in complexity compared to EDU bilaterally in the cingulum adjacent to the hippocampus, right external capsule, and left posterior internal capsule. CBT participants demonstrated a decrease in complexity compared to EDU controls within the right posterior internal capsule. Significance was evaluated at threshold $p \leq 0.05$, CBT n=42, EDU n=21.

Table 3.5. At TP3, CBT participants exhibited an increase in complexity compared to EDU in the right anterior internal capsule and the posterior internal capsule. CBT participants demonstrated a decrease in complexity compared to EDU controls within the right cerebral peduncle. Significance was evaluated at threshold $p \leq 0.05$, CBT n=38, EDU n=15.

Table 3.6. A) Longitudinal analysis of connectivity demonstrated a main effect of time at threshold values 2.9 and 3.1, with both CBT and EDU participants exhibiting reduced connectivity at TP3 compared to TP1. This finding was not significant at a threshold of 2.7. No significant group by time effects in connectivity were observed following TP2 or TP3 study visits. Significance was evaluated at threshold $p \leq 0.05$, CBT n=38, EDU n=12. B) Increased connectivity was observed between cortical and subcortical regions several t-value thresholds.

Figure 3.1. Study consort diagram.

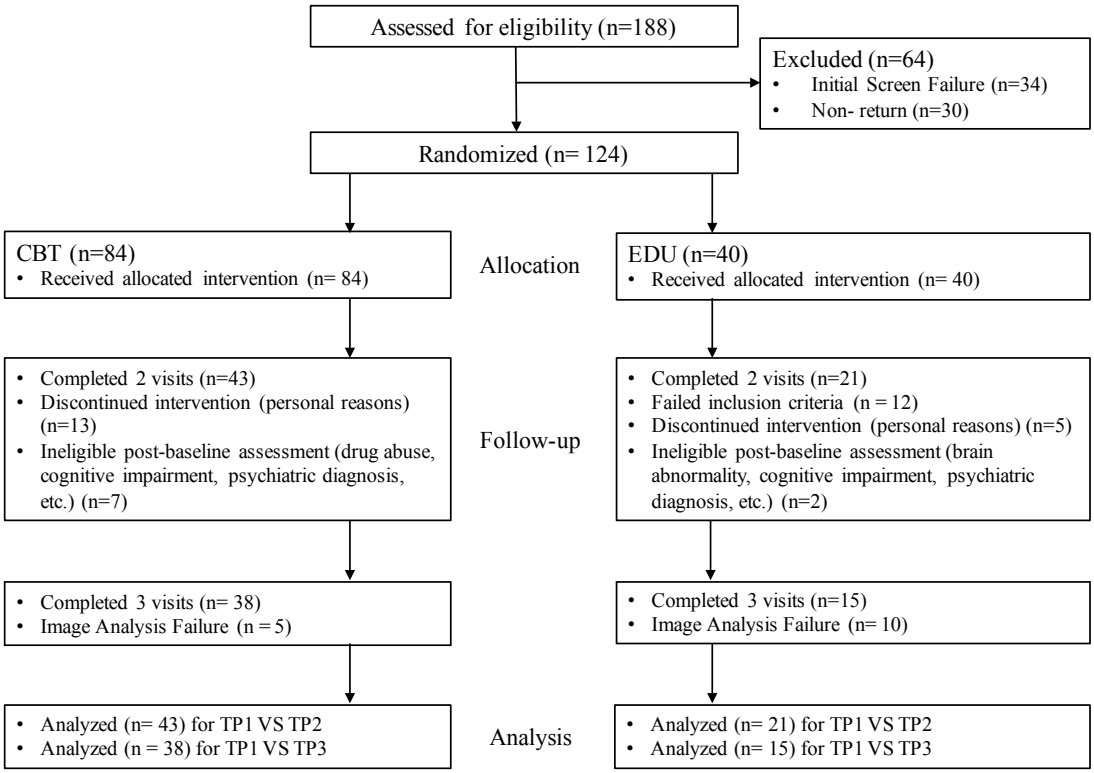

Figure 3.2. Study design.

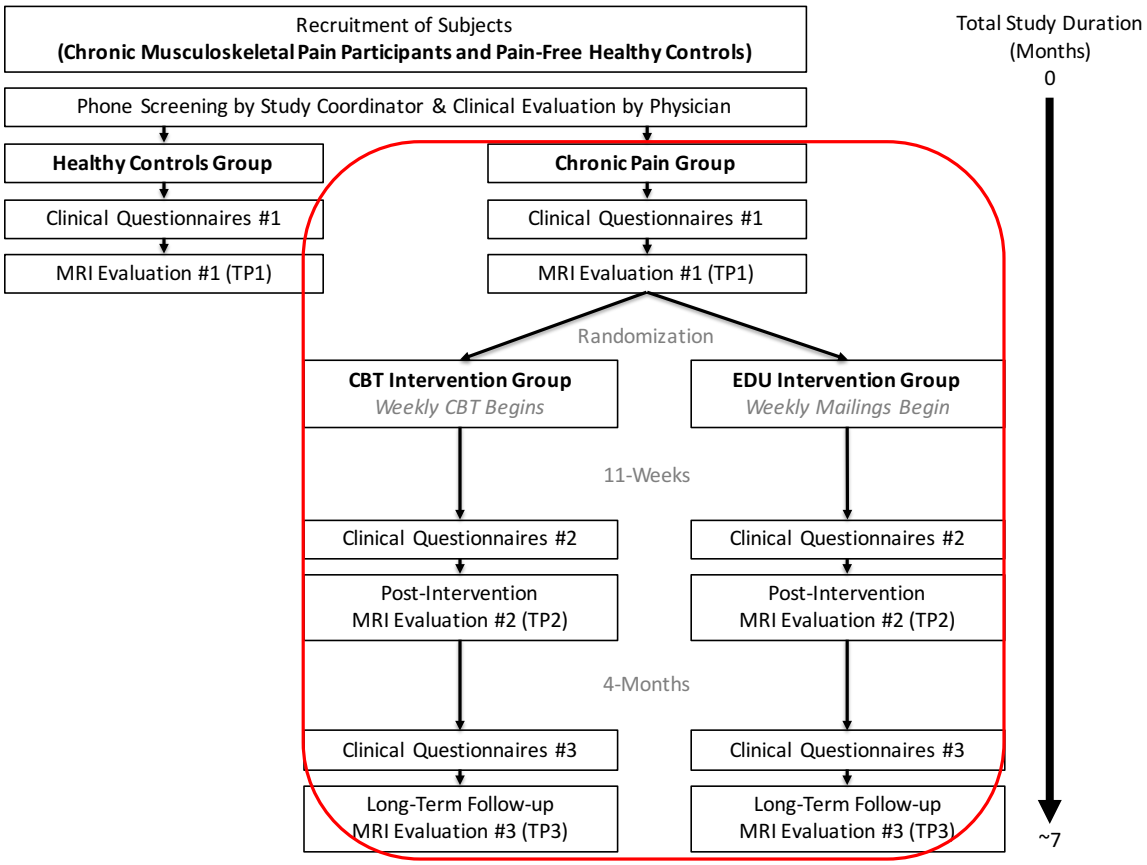

Table 3.1. Study demographics.

Post Intervention – TP2 (n (CBT) = 42, n (EDU) = 21)

Mean (SD)	CBT	EDU	P value
Age	46 (12.4)	43 (12.5)	1.0
Females/Males	34/8	16/5	0.54
Depression from BDI	16.4(8.1)	14.2(9.5)	0.001
Pain duration	11.7(7.9)	8.7(8.77)	1.0

Long-term Follow-up – TP3 (n (CBT) = 38, n (EDU) = 15)

Mean (SD)	CBT	EDU	P value
Age	46 (11.9)	43 (12.8)	0.44
Females/Males	31/7	13/2	0.32
Depression from BDI	16.68 (8.38)	13.7(10.42)	0.84
Pain duration	11.61(7.6)	5.9(4.6)	0.001

Table 3.2. Clinical improvements after 11-week intervention (TP2).

Post Intervention – TP2 (n (CBT) = 42, n (EDU) = 21)

Clinical Measure (SD)	CBT TP1	CBT TP2	EDU TP1	EDU TP2	TP2-TP1 CBT	TP2-TP1 EDU	Time X Group F	Time X Group P
Total Pain Experience (TOPS)	52.8 (14.5)	39.2 (14.1)	52.8 (13.3)	47.2 (16.3)	13.6 (9.6)	-5.6 (3.9)	8.7	0.004
Pain Symptoms (TOPS)	31.9 (17.4)	49.8 (19.9)	30.5 (13.3)	39.0 (17.5)	17.9 (12.6)	8.5 (6.01)	4.5	0.036
Physical Composite Score (SF-36)	31.7 (9.7)	37.9 (9.6)	32.4 (8.6)	35.5 (9.4)	6.2 (4.3)	3.1 (2.1)	4.2	0.044
Mental Composite Score (SF-36)	42.2 (12.2)	49.5 (10.7)	42.3 (12.8)	43.3 (12.8)	7.3 (5.1)	1.0 (0.71)	5.7	0.020
Perceived Family Disability (TOPS)	47.8 (20.9)	33.3 (21.3)	48.5 (20.1)	42.1 (20.8)	-14.5 (10.2)	-6.4 (4.5)	4.1	0.046
Passive Coping (TOPS)	41.9 (19.7)	30.6 (19.2)	40.7 (26.0)	41.1 (18.4)	-11.3 (7.9)	0.4 (0.28)	7.3	0.009
Catastrophizing	19.8 (10.4)	9.4 (6.5)	21.4 (11.8)	17.8 (12.0)	-10.4 (7.3)	-3.6 (2.5)	9.2	0.003
Self-Efficacy for Pain Management (PSE)	49.7 (19.7)	70.3 (17.5)	41.0 (19.3)	48.8 (22.3)	20.6 (14.5)	7.8 (14.5)	7.3	0.009
Self-Efficacy for Physical Function (FSE)	71.3 (18.0)	81.9 (15.9)	67.4 (28.8)	75.1 (22.4)	10.6 (7.5)	7.7 (7.5)	0.7	0.385
Self-Efficacy for Coping with Symptoms (CSE)	49.8 (16.4)	72.5 (12.5)	47.6 (18.4)	52.0 (21.4)	22.7 (16)	4.4 (16.0)	28.9	0.000
Mean PSE, FSE, CSE	57.0 (16.0)	74.9 (12.5)	52.0 (18.1)	58.6 (19.8)	17.9 (12.6)	6.6 (4.6)	12.5	0.001

Table 3.3. Clinical improvements after intervention follow-up (TP3).

Long-term Follow-up – TP3 (n (CBT) = 38, n (EDU) = 15)

Clinical Measure (SD)	CBT TP1	CBT TP3	EDU TP1	EDU TP3	TP3-TP1 CBT	TP3-TP1 EDU	Time X Group F	Time X Group P
Total Pain Experience (TOPS)	52.8 (15.2)	35.5 (14.5)	51.3 (14.2)	42.4 (18.8)	-17.3 (12.3)	-8.9 (6.2)	3.6	0.060
Pain Symptoms (TOPS)	32.4 (17.8)	52.7 (19.4)	31.5 (14.7)	41.2 (18.0)	20.3 (14.3)	9.7 (6.8)	2.8	0.100
Physical Composite Score (SF-36)	32.2 (9.8)	39.0 (10.2)	32.8 (9.4)	38.6 (10.9)	6.8 (4.8)	5.8 (4.1)	0.09	0.764
Mental Composite Score (SF-36)	41.7 (12.3)	48.2 (11.9)	43.6 (14.7)	43.9 (11.6)	6.5 (4.6)	0.3 (0.21)	5.4	0.024
Perceived Family Disability (TOPS)	48.0 (21.5)	26.2 (19.2)	44.7 (21.0)	38.8 (21.6)	-21.4 (10.3)	-5.9 (4.1)	3.5	0.066
Passive Coping (TOPS)	41.2 (20.3)	26.7 (18.9)	37.2 (25.8)	38.5 (20.7)	-14.5 (10.2)	1.3 (0.92)	7.2	0.010
Catastrophizing	19.7 (10.4)	8.5 (7.9)	21.5 (11.9)	17.7 (12.0)	-11.2 (7.9)	-3.8 (2.6)	4.4	0.041
Self-Efficacy for Pain Management (PSE)	51.3 (20.0)	70.2 (18.3)	45.6 (19.3)	59.0 (23.8)	18.9 (13.3)	13.4 (9.4)	0.70	0.406
Self-Efficacy for Physical Function (FSE)	72.8 (18.1)	81.9 (16.7)	72.2 (29.5)	76.9 (23.2)	9.1 (6.4)	4.7 (2.9)	0.55	0.460
Self-Efficacy for Coping with Symptoms (CSE)	50.7 (16.7)	70.2 (15.3)	51.1 (19.0)	59.2 (18.8)	19.5 (13.7)	8.1 (5.4)	5.2	0.026
Mean PSE, FSE, CSE	58.3 (16.2)	74.2 (14.4)	56.3 (18.4)	65.0 (20.4)	15.9 (11.2)	8.7 (6.1)	2.7	0.105

Table 3.4. ROI complexity results after 11-week intervention (TP2).

TP2 vs TP1 - CBT vs EDU - Age, Sex, Upgrade Covariates n63
(n (CBT) = 42, n (EDU) = 21)

WM ROI	Hemisphere	F1		F2		MO	
		CBT > EDU	*CBT < EDU*	*CBT > EDU*	*CBT < EDU*	*CBT > EDU*	*CBT < EDU*
Anterior Internal Capsule	Left						
	Right						
Cerebral Peduncle	Left						
	Right						
Cingulum	Left						
	Right						
Cingulum Adjacent to Hippocampus	Left			↑			
	Right						↑
External Capsule	Left						
	Right		↑				
Posterior Internal Capsule	Left		↑	↑			
	Right			↑		↓	
Uncinate Fasciculus	Left						
	Right						

↑ = CBT participants demonstrated increased complexity compared to EDU controls
↓ = CBT participants demonstrated decreased complexity compared to EDU controls

Table 3.5. ROI complexity results after intervention follow-up (TP3).

TP3 vs TP1 - CBT vs EDU - Age, Sex, Upgrade Covariates n53
(n (CBT) = 38, n (EDU) = 15)

WM ROI	Hemisphere	F1		F2		MO	
		CBT > EDU	*CBT < EDU*	*CBT > EDU*	*CBT < EDU*	*CBT > EDU*	*CBT < EDU*
Anterior Internal Capsule	Left						
	Right			↑			
Cerebral Peduncle	Left						
	Right					↓	
Cingulum	Left						
	Right						
Cingulum Adjacent to Hippocampus	Left						
	Right						
External Capsule	Left						
	Right						
Posterior Internal Capsule	Left		↑	↑			
	Right						
Uncinate Fasciculus	Left						
	Right						

↑ = CBT participants demonstrated increased complexity compared to EDU controls
↓ = CBT participants demonstrated decreased complexity compared to EDU controls

Table 3.6. Whole brain WM connectivity over time.

A.

Longitudinal (TP1, TP2, TP3) - CBT= 38; EDU=12

Contrast	t-value Threshold	Permutations	Lowest p-value
TP1>TP2	3.1	5000	0.94
TP1>TP3	3.1	5000	0.04
TP1<TP2	3.1	5000	0.66
TP1<TP3	3.1	5000	0.66
CBT>EDU (TP1>TP2)	3.1	5000	0.44
CBT>EDU (TP1>TP3)	3.1	5000	0.12
EDU>CBT (TP1>TP2)	3.1	5000	0.94
EDU>CBT (TP1>TP3)	3.1	5000	0.94
TP1>TP2	2.9	5000	0.87
TP1>TP3	2.9	5000	0.03
TP1<TP2	2.9	5000	0.70
TP1<TP3	2.9	5000	0.87
CBT>EDU (TP1>TP2)	2.9	5000	0.69
CBT>EDU (TP1>TP3)	2.9	5000	0.20
EDU>CBT (TP1>TP2)	2.9	5000	0.99
EDU>CBT (TP1>TP3)	2.9	5000	0.68
TP1>TP2	2.7	5000	0.31
TP1>TP3	2.7	5000	0.07
TP1<TP2	2.7	5000	0.91
TP1<TP3	2.7	5000	0.81
CBT>EDU (TP1>TP2)	2.7	5000	0.55
CBT>EDU (TP1>TP3)	2.7	5000	0.31
EDU>CBT (TP1>TP2)	2.7	5000	0.89
EDU>CBT (TP1>TP3)	2.7	5000	0.51

*No Covariates

B.

TP1>TP3			
Connection	Test Statistic	t-value Thresh.	Significance (p-value)
Hippocampus R. to Lingual L.	3.60	3.1	0.041
Cingulum Post. R. to Lingual L.	3.44	3.1	0.041
Amygdala R. to Lingual L.	3.13	3.1	0.041

TP1>TP3			
Connection	Test Statistic	t-value Thresh.	Significance (p-value)
Hippocampus R. to Lingual L.	3.60	2.9	0.036
Cingulum Post. R. to Lingual L.	3.44	2.9	0.036
Amygdala R. to Lingual L.	3.13	2.9	0.036
Frontal Med. Orb. R. to Temporal Sup. R.	3.05	2.9	0.036
Frontal Med. Orb. R. to Heschl R.	2.94	2.9	0.036
Frontal Med. Orb. R. to Supramarginal R.	2.91	2.9	0.036

CHAPTER 4: POST-MORTEM *IN SITU* NEUROIMAGING OF THE DOMESTIC PORCINE BRAIN FOR MECHANISTIC MRI-HISTOLOGICAL VALIDATION OF STRUCTURAL PLASTICITY

Abstract

Neuroimaging evidence suggests that chronic pain profoundly influences brain structure including both grey matter (GM) and white matter (WM) tissue types. We previously extended this claim to suggest that chronic pain manifests in alterations of WM complexity and connectivity that can potentially be mediated through successful intervention. A methodological proof of concept is presented here to promote subsequent interpretation of structural imaging findings in clinical chronic pain populations. We first delineated a post-mortem *in situ* imaging paradigm in a validated porcine model of low back pain-like pathophysiology. Next, we highlight a novel tissue preservation technique that enables both perfusion fixation by cannulation of the internal carotid arteries followed by immersion fixation. This protocol provides a step-by-step methodology for analogous translational imaging followed by intact brain removal and fixation for subsequent MRI-histological comparison. We speculate that implementing this protocol in our porcine model of low back pain would result in structural (GM & WM) brain abnormalities, and further, propose that these are largely attributed to changes in glia reactivity. Although we describe a detailed protocol, we do not have sufficient power to make statistical assessments, and a full investigation is warranted to test the validity of these theories. Lastly, although we outline many methods to support feasibility, additional work is required to ensure that the MRI analysis pipelines described are fully functional in the porcine brain. In summary, neuroimaging modalities often do little to provide mechanistic inference of cellular mechanisms. The protocol described here capitalizes on a novel

musculoskeletal pain model relevant for translational comparison of neuroimaging findings strengthened by histological tissue assessment.

Introduction

In the preceding chapters, we defined substantial evidence to support brain neuroplasticity in clinical chronic pain populations. First, we broadly reviewed the literature to define cellular and activity-dependent mechanisms that may potentiate brain changes during chronic pain genesis such as peripheral and central sensitization (Woolf, 2011), neurogenic neuroinflammation (Xanthos & Sandkuhler, 2014) and gliopathy (Ji et al., 2013). Additionally, previous work from our lab (Lieberman et al., 2014; Seminowicz et al., 2013) and the experimental data from this dissertation provide further evidence of pain-related CNS changes in grey matter (GM) morphometry as well as novel findings of altered white matter (WM) neurocircuitry. We also report one of the first longitudinal studies with an adequate active control group to investigate the potential of CBT to elicit brain plasticity in chronic musculoskeletal pain patients. While these studies elucidate the structural manifestations of chronic pain and treatment, neuroimaging methodology is limited to macrostructural assessment.

Magnetic resonance imaging is a useful tool to investigate brain pathology and plasticity, especially for *in vivo* clinical populations given the diverse amount of data obtained in a single imaging session. These include, but are not limited to, blood flow and volume measures, WM and GM structure via T1 relaxometry and diffusion weighted imaging, neurochemical composition, and metabolic processing, among others. Clever multi-modal techniques have been developed and implemented to probe diverse research

hypotheses, although MRI often lacks the resolution to enable mechanistic study. This is further exacerbated in complex and heterogeneous clinical populations such as chronic pain where the mechanistic onset is still largely unresolved. Additionally, few laboratories follow-up clinical investigations with fundamental basic science to strengthen the interpretability of macroscopic brain and behavioral findings. In this capacity, we initially developed a novel animal model of musculoskeletal pathophysiology mimicking the hallmarks of pain genesis that are relevant to chronicity such as movement alterations and soft tissue injury. The specific attributes and validation of our described porcine model have been previously published (Bishop et al., 2016) and are presented within this document as supplemental chapter 6. In an attempt to promote translational research and facilitate mechanistic investigation of brain plasticity associated with chronic pain, we outline a post-mortem imaging and histological approach in our pig model. Although we were unable to obtain adequate sample sizes to generate valid statistical comparisons, we do, however, summarize a complete methodological proof of principle.

Specifically, we provide a post-mortem imaging paradigm complete with a novel whole-brain fixation protocol for subsequent cellular investigation. Animal studies often lack translatability due to anatomical differences between species and disparate methodological approaches. To combat these limitations, we selected the domestic pig as our model of choice given the anatomical and physiological similarities to humans (Crick, Sheppard, Ho, Gebstein, & Anderson, 1998; Meyer, Neurand, & Radke, 1981; M. M. Swindle, A. Makin, A. J. Herron, F. J. Clubb, Jr., & K. S. Frazier, 2012) as well as congruencies in immune function (Meurens, Summerfield, Nauwynck, Saif, & Gerdts, 2012; Summerfield, Meurens, & Ricklin, 2015) and wound repair (T. P. Sullivan, W. H.

Eaglstein, S. C. Davis, & P. Mertz, 2001). Furthermore, domestic swine as models for neurological applications are gaining prevalence because of their correspondences in brain structure and neurochemistry (Lind et al., 2007b).

To ensure that findings in our animal model translated to experimental outcomes in clinical pain populations, our goal was to obtain imaging acquisitions *in situ*, in unfixed and intact brain tissue that were analogous to our clinical investigation. The MRI session paralleled that of our clinical population and included high-resolution T1- and T2-weighted structural imaging, multi-shell diffusion weighted imaging, and ^{1}H magnetic resonance spectroscopy thermometry to assess and control for post-mortem changes in brain temperature. Procuring equivalent MR images permits the use of comparable image processing and statistical pipelines, further promoting translatability between clinical and pre-clinical investigations.

Another limitation of clinical investigations is variance in human populations, including genetic and environmental influences. To reiterate, chronic pain is a multifaceted pathology with diverse etiology and subjectivity between patients. This results in augmented challenges for clinical investigations because patients often present with disparate sites of pain, complex medical and medication histories, and accompanying pathological comorbidities such depression and anxiety disorders. Fortunately, pre-clinical pain models allow investigators to regulate many of these heterogeneous confounds by controlling for the site of injury, pain duration, diet, exercise, and medications such as analgesics, many of which are known to influence brain structure.

Furthermore, when evaluating treatment efficacy in clinical populations, it is challenging to assess compliance and adherence to intervention regimens across patients

which can dilute the effect of interest. Once again, pre-clinical approaches allow investigators to precisely monitor the duration of intervention and intensity across animals. Although not described in this document, we have already carried out seminal work in our validated pig model (Supplementary Chapter 6; (Bishop et al., 2016)) to investigate the efficacy and mechanisms of static stretch intervention to treat low back pain pathophysiology (Langevin et al., 2017, In Press). Our use of a porcine model, as opposed to standard murine models, strengthens our investigation and ultimately increases translatability and applicability to the human condition. Thus, it is imperative to first build a solid conceptual porcine imaging framework prior to application in a large cohort.

The work described in this chapter is strictly a methodological proof of concept and prerequisite to delineate the feasibility of the approach on a large-scale pain experiment. Animal imaging protocols pose additional challenges to their clinical counterparts. Often times they are confounded by motion artifacts, necessitate anesthetics, and require specialized instrumentation such as high-field, small-bore magnets. Data analysis can also be more problematic in less frequently studied species such as the domestic pig. Automated analysis pipelines and image processing tools designed for human acquisitions typically breakdown in animal data. Aside from the methodological challenges of imaging, alignment of potential findings with histology is quite difficult. This is further exacerbated in large species such as the pig where cardiac perfusion techniques are impractical, and thus jeopardize the comparison of brain imaging results to histology because of the potential for tissue degradation.

In summary, substantial methodological consideration is warranted prior to conducting large scale pre-clinical experiments. In this capacity, our objective was to

define a feasible approach for future investigations. Here we present a novel post-mortem *in situ* neuroimaging framework that has not previously been described, and an innovative perfusion fixation method coupled with immersion fixation to enable valid MRI-histology comparisons. Lastly, we perform the outlined neuroimaging using a clinical 3T MRI that is more common across institutions than specialized animal magnets, ultimately broadening the applicability of our proposed method. This is the first step in achieving our overarching goal to promote translatability and increase interpretability of structural imaging findings across chronic pain conditions.

Materials and Methods

Specimen Acquisition:

All specimens for the subsequent experiments were obtained from euthanized animals in ordinance with the University of Vermont's tissue sharing policy. Animals were part of an ongoing study and appropriate experimental protocols were approved by the University of Vermont Institutional Animal Care and Use Committee (IACUC). Refer to supplemental chapter 6 for experimental details prior to euthanasia. In brief, male domestic pigs, between 4-6 weeks old, were acquired from E.M. Parson's Hadley, MA. Each pig was randomized to one of four experimental groups for the 8-week duration of experimentation: 1) controls that underwent no physiological manipulation, 2) surgical soft tissue injury, 3) movement restriction via leg hobble device, and 4) combination of soft tissue injury and hobble. Following an 8-week experimental duration, pigs were euthanized to assess dorsal tissue mechanics, after which the internal carotid arteries were dissected for cannulation, and decapitated for post-mortem, *in situ*, brain imaging.

Specimen (Head) Preparation

Following euthanasia, animals were placed in a supine position and a ventral midline incision was made parallel to the cervical spine. Next, we used blunt dissection to isolate the internal carotid arteries bilaterally. Using a scalpel, a small incision was made to expose the lumen of each artery. On one side, a size 7 catheter connected to a perfusion pump was inserted rostrally into the artery, using a surgical suture to create a seal and hold the cannula in place. This was followed by perfusion of physiological (38.8°C) Krebs solution at a flow rate of 50 mL/kg/min (Sasaki et al., 2010). The jugular vein was then cut and outflow assessed to ensure that the cerebral vascular system was adequately flushed of blood. Finally, bilateral sutures were fixed inferior to the site of cannulation and the carotids were severed completely. These sutures enabled quick identification of the arteries post-MRI for re-cannulation. The head was then removed at approximately the C2-C3 vertebral level and transported to the MRI facility for *in situ* brain imaging (MRI). A similar approach has been described to fix whole brain post-mortem human specimens via cannulation of the intact neurovasculature (H. J. Waldvogel, Curtis, Baer, Rees, & Faull, 2006).

Magnetic Resonance Imaging Acquisition

Post-Mortem Neuroimaging: Immediately following euthanasia and internal carotid artery cannulation, individual pig heads were transported to the UVM MRI research facility for *in situ* imaging. The specimen, still contained within insulating plastic was placed in the MRI coil. We then began acquisition consisting of baseline MR thermometry,

WM and GM structural scans (diffusion weighted imaging and T1-weighted anatomical images), and lastly a follow-up MR thermometry scan. Based on our pilot study, the time between euthanasia and MRI acquisition was approximately 85 minutes (Figure 4.1D).

DWI data were acquired using a Phillips Achieva 3T magnet (Phillips Healthcare, Best, Netherlands) and a 32-channel head coil with the following acquisition specifications:

Anatomical (Grey Matter) Acquisition: T1-weighted spoiled gradient volumetric sequence oriented perpendicular to the anterior commissure-posterior commissure with 11.5ms TR, 5.6ms TE, 8º flip angle, 256mm FOV, 1.0 NSA, 256 X 256 matrix, and 0.6mm slice thickness with no gap for 290 contiguous slices.

Diffusion Weighted Imaging (DWI) Acquisition: An axial 2-dimensional spin echo echo planar imaging (EPI) sequence with 56 diffusion directions and the following specifications was implemented: 59 slices, 1.5mm slice thickness, 6828 TR, 120.9ms TE, 1.45x1.45mm in-plane resolution, Multi-Shell 1000, 2000, and 3000 s/mm^2 B-values, and 71 EPI factor.

^{1}H MR Spectroscopy: A single voxel point-resolved spectroscopy (PRESS) sequence was used to obtain relative brain temperature with the following parameters: 10x10x10mm^3 voxel of interest (VOI) aligned in the white matter, TR=2s, TE=144ms, 140Hz water suppression, frequency stabilization, automated shimming equipped on the scanner, spectral correction with number of signal averages (NSA)=4, spectral bandwidth=2000Hz, and 1024 points per spectrum. Total scan duration was one minute and sixteen seconds.

Image Processing

GM image processing was conducted using FSL 5.0 software (FMRIB Software Library, Oxford Centre for Functional Magnetic Resonance of the Brain) (Jenkinson et al., 2012). Study personnel manually generated a mask of the of T1-weighted images which was subsequently used to conduct brain extraction. To assess the possibility of pig brain segmentation, FSL's FAST tool was used. Although not conducted, GM volume statistics can be obtained through this process and further analyzed in either alternative statistical software or within FSL. (Figure 4.2A-C)

WM diffusion weighted image processing was also conducted using FSL 5.0 software on a single animal (FMRIB Software Library, Oxford Centre for Functional Magnetic Resonance of the Brain) (Jenkinson et al., 2012). Diffusion weighted images were corrected for eddy current and susceptibility induced echo planar imaging distortion. The diffusion tensor model was fitted to the images using dtifit, part of FSL 5.0. An individual animal was processed to assess feasibility of generating a white matter skeleton for subsequent statistical comparison (Figure 4.2D). In addition to WM skeletonization, the advanced diffusion sequence with multiple b-values is optimal for tractography and connectivity applications. Images were first reconstructed using generalized Q-sampling imaging (GQI) and deterministic tractography streamlines were generated using DSI studio.

Thermometry was performed using ^{1}H MRI spectroscopy in four animals, by implementing the proton resonance frequency method with N-Acetylaspartic Acid (NAA) as a reference metabolite (Figure 4.1A). We used a point resolved spectroscopy (PRESS) sequence to obtain single voxel localization. MRI spectroscopy thermometry data were

obtained at the beginning of the imaging session (baseline) and then subsequently following our anatomical T1, T2, and diffusion acquisitions, and once more, prior to removal from the imager. The following equation was used to determine the relative temperature in °C:

$$Temperature\ in\ °C = 296.068\ - 97.134\ *(\delta_{H_2O} - \delta_{NAA})$$

Where the initial values are scanner calibrated constants and δ_{H2O} / δ_{NAA} are the measured chemical shifts of water and NAA respectively (Figure 4.1B-C).

Specimen (Head) Fixation

Following MRI acquisition, the specimens were brought back to the surgical suite for fixation and brain extraction. First, the bilateral internal carotid arteries were identified using the sutures that were left in place. Within a fume hood, a cannula was reintroduced into the vessels, angled toward the brain, and 4% paraformaldehyde (PFA) was perfused at a flow rate of 50 mL/kg/min (Sasaki et al., 2010) for a total of 30 minutes. Next, the cannula was removed and brain extraction was initiated. In brief, a bone saw, was used to perform a craniotomy, exposing the cortex dorsally and the cerebellum and brainstem posteriorly. Using blunt dissection, we carefully separated the meningeal tissue from the skull surface using a scalpel to sever cranial nerves and the caudal brain stem. The brain was then lifted in an anterior to posterior direction to remove it from the skull. Once extracted, the brain was immersion fixed in 4% PFA at 4˚C for 60 hours (Henry J. Waldvogel, Curtis, Baer, Rees, & Faull, 2007). After an initial 60-hour fixation process,

the brain was cryo-protected over three days by step-wise submersion in 10%, 20% and 30% sucrose diluted in 0.1M phosphate buffered saline (PBS) and stored with 0.1% sodium azide to protect against bacterial or fungal growth. After cryoprotection, the brains were stored in 30% sucrose, 0.1M PBS and 0.1% sodium azide at 4˚C indefinitely.

Feasibility

GM Segmentation

In situ post-mortem T1-weighted imaging maintained analogous relaxation parameters to that of healthy, living tissue (Figure 4.3). This enabled sufficient contrast for tissue segmentation via standard imaging pipelines such as FSL. Cortical and subcortical structures were clearly delineated without manual user input (Figure 4.2B). Obtaining a large-scale dataset would allow for subsequent GM morphometric comparisons between the porcine groups, enabling delineation associated with different contributions of chronic pain pathology – such as movement restriction and soft tissue injury.

WM Skeleton and Tractography

Here we demonstrated the feasibility of obtaining WM microstructural information from our post-mortem diffusion weighted images. Using a single animal's T1 image as a reference, we were able to skeletonize the WM image using FSL's diffusion toolbox and overlay it on a high-resolution image (Figure 4.2D). We were also able to perform global tractography using GQI reconstruction (Figure 4.2E), which will enable the comparison of WM connectivity differences between groups. Additionally, we will be able to perform standard diffusion tensor imaging metrics such as fractional anisotropy, and mean, radial,

and axial diffusivity, in addition to advanced diffusion complexity metrics such as ball and sticks multi-compartment method.

MR Thermometry

The use of ^{1}H MRI spectroscopy provided a robust measure of relative brain temperature in the post-mortem pig. As expected, an evident trend emerged indicating brain cooling over time. Longer post-mortem times preceding MRI acquisition were accompanied by lower initial brain temperature at scanning onset. We were also able to observe temperature changes over the course of the imaging procedure confirming the sensitivity of the technique (Figure 4.1C). Unfortunately, for piloting purposes and lack of personnel we did not track specific time intervals between MR thermometry acquisitions, partially due to sequence testing which varied in duration. During full scale implementation, specific timing would be more accurately monitored and recorded.

Discussion

Here, we demonstrate the conceptual framework to conduct analogous pain imaging experiments in a porcine musculoskeletal pain model. Our outlined protocol provides a unique methodological approach to identify macro- and microstructural CNS alterations associated with chronic pain to promote mechanistic investigations. The important differences between our method and standard post-mortem studies coupled with histological evaluation, is that we perform MRI scanning soon after euthanasia in fresh, unfixed tissue. This preserves the tissue properties required for analogous imaging acquisitions whereas the fixation process produces crosslinking which ultimately

influences T1/T2 relaxation times (Dawe, Bennett, Schneider, Vasireddi, & Arfanakis, 2009; Schmierer et al., 2010) and diffusion properties (Shepherd, Thelwall, Stanisz, & Blackband, 2009; Sun et al., 2005; Sun, Neil, & Song, 2003). Other factors such as tissue storage and temperature have also been demonstrated to influence MRI parameters (Moseley, Nishimura, Pitts, Bartkowski, & James, 1984) . Interestingly, Schmierer and colleagues showed that MRI relaxation times of post-mortem, unfixed human brain slices, were similar to those acquired *in vivo*, even at room temperature (Schmierer et al., 2010). This further confirms that our T1-weighted imaging paradigm should remain reliable in the short period of time leading up to evaluation.

Alternatively, the length of time and method by which tissue is processed post-mortem may considerably influence diffusion properties. For example, fixation has been shown to alter diffusion parameters such as the b-value, and echo times require fine tuning for post-mortem application (Miller, 2012). In a study assessing the use of DWI for forensic applications, investigators imaged recently deceased individuals (group average of 40-hours post-mortem) and found that fractional anisotropy values remained similar to healthy living volunteers. Conversely, a significant alteration in apparent diffusion coefficient was noted but only within GM tissue and not WM (Scheurer et al., 2011). In a more controlled study assessing diffusivity changes resulting from post-mortem neural degeneration, unfixed pig brains were serially imaged (14 times) over a sixteen-hour window. The authors concluded that diffusivity contrasts were preserved within a timeframe of approximately 6-10 hours (Landman, Huang, Prince, & Ying, 2007). This is well within the timeframe outlined in our method and upon finalization of the protocol, we anticipate that specimens could undergo imaging within one hour post-euthanasia. Together, these

reports strengthen our suggested post-mortem diffusion approach and allude to the maintenance of imaging properties while alleviating artefactual drawbacks of *in vivo* alternatives.

One additional consideration that was not addressed in the above literature is the influence of temperature change on diffusion measurements. Diffusion weighted imaging relies on the principles of Brownian motion which is inherently dependent on the laws of thermodynamics. Temperature fluctuations therefore will ensue changes in the diffusion constant which should be adequately addressed. Fortunately, adjustments of the diffusion constant measurement have been proposed by using a correction factor of 2% per degree Celsius (Quesson, de Zwart, & Moonen, 2000). This technique has been implemented successfully in unfixed cadaveric diffusion studies (Scheurer et al., 2011) while others using fixation methods allow the tissue to equilibrate to room temperature prior to acquisition (Schmierer et al., 2010). The latter method is a less viable option in unfixed tissue due to the concerns of tissue degradation. Nonetheless we have demonstrated a method to obtain relative brain temperature fluctuation in the specimens by bookending and interleaving a short ^{1}H spectroscopy scan between T1 and diffusion acquisitions. This temperature readout is derived by comparing the chemical shift of a temperature stable metabolite (NAA) to temperature-dependent H_20 (Cady, 1995), and has previously been validated with an accuracy of 0.2°C (De Poorter et al., 1995). This will facilitate necessary corrections due to temperature dependencies and discrepancies in time-to-scan between specimens.

Aside from imaging, the overall objective of this work is to mechanistically define the cellular influences driving structural alterations in the chronic pain brain. Though

statistical outcomes are not provided in this protocol, we have laid out the groundwork for analytical comparison of the T1 and diffusion scans. In brief, we first anticipate conducting whole brain statistical analyses prior to sectioning the tissue for mechanistic investigation. This will permit localization of structural CNS abnormalities that can then be targeted using previously established MR histopathology protocols such as described by Guy and colleagues (Guy et al., 2016).

Nonetheless, to obtain reliable histology results it is imperative to minimize the duration of post-mortem imaging and fix the brain tissue as quickly as possible. Empirically, perfusion fixation is commonplace among researchers and is used to preserve many tissue types including the brain, however, these techniques are challenging and require substantial materials to be implemented in large specimens. In this capacity, we demonstrated a novel fixation protocol that capitalizes on the intact neurovasculature based loosely of Waldvogel and colleagues' protocol (H. J. Waldvogel et al., 2006) that facilitates constrained perfusion fixation to the pig cranium. This approach enables us to circulate fixative to the inner brain prior to immersion fixation ensuring uniformity in the process and reducing the fixation time. Immersion fixation alone has been shown to take more than 20 days to penetrate whole human brain specimens (Dawe et al., 2009; Moseley et al., 1984) diminishing the reliability of histology in deep brain regions. To address this concern, we assessed our tissue perfusion protocol with MR relaxometry (T2), *ex vivo*, in a single specimen and demonstrated that cortical and subcortical GM relaxation properties were uniform. Though underlying cellular changes may be inevitable, coupling perfusion and submersion techniques is a promising alternative.

Although we describe an innovative imaging and fixation methodology, it is critical to point out the strengths and novelty of the described translational pig model for pain investigations. Pre-clinical pain studies are predominated by murine models (Mogil, 2009) which, unfortunately, have substantial variation from human anatomy - both peripherally and centrally. Peripherally, murine species have an additional dorsal back muscle called the pannicular muscle that is neither part of human nor pig anatomy. Thus, to objectively create an accurate animal model of low back pain, it is essential that the site of pathology is representative of the clinical condition. Centrally, rat and mouse brains are lissencephalic, whereas the human brain has significant gyral folding. Pigs also have gyrencephalic brains and their brain growth and development parallels that of humans (Conrad, Dilger, & Johnson, 2012). Further, they have analogous histological features and neuroanatomy including an equivalent GM-to-WM ratio (Dobbing & Sands, 1979). This includes similar primary and secondary somatosensory cortex representations which have previously been mapped out in the domestic pig brain (Andrews, Knight, & Kirby, 1990; Craner & Ray, 1991a, 1991b; Woolsey & Fairman, 1946). One disadvantage of the domestic porcine as a preclinical model is the rapid growth of the animals. To combat this, investigators have proposed the use of minipig models. Unfortunately, there are important limitations to address even within pig species. For example, the Göttingen minipig has been shown to undergo neocortical neurogenesis in the postnatal period which is dissimilar to both humans and domestic swine (Jelsing et al., 2006). This is an important limitation and potential consideration for longitudinal investigation of brain structure associated with disease pathogenesis.

Although some would view post-mortem imaging as a potential drawback, we have provided substantial literature to support its robustness and also provide a framework to overcome many of the associated pitfalls. The methods outlined in this chapter support the feasibility of translational imaging in a pig model of musculoskeletal pain and highlight novel methodological approaches needed to promote valid comparisons. Although primarily a proof of concept study, we define several of the current limitations to our anticipated approach and also provide plausible alternatives. Nonetheless, successful implementation could aid in mechanistic evaluations of neuroplasticity across a variety of conditions including chronic pain.

Acknowledgments

The authors would like to thank the Jay Gonyea, Scott Hipko, and Dr. Richard Watts of the UVM MRI Center for Biomedical Imaging for their assistance with data acquisition and scan optimization. The authors would also like to thank Steve Bell, James Fox, Rhonda Maple, and Caitlin Loretan for their assistance with the animals.

References for Chapter 4

Andrews, R. J., Knight, R. T., & Kirby, R. P. (1990). Evoked potential mapping of auditory and somatosensory cortices in the miniature swine. *Neurosci Lett, 114*(1), 27-31.

Bishop, J. H., Fox, J. R., Maple, R., Loretan, C., Badger, G. J., Henry, S. M., . . . Langevin, H. M. (2016). Ultrasound Evaluation of the Combined Effects of Thoracolumbar Fascia Injury and Movement Restriction in a Porcine Model. *PLoS One, 11*(1), e0147393. doi:10.1371/journal.pone.0147393

Cady, E. B. (1995). Quantitative combined phosphorus and proton PRESS of the brains of newborn human infants. *Magn Reson Med, 33*(4), 557-563.

Conrad, M. S., Dilger, R. N., & Johnson, R. W. (2012). Brain growth of the domestic pig (Sus scrofa) from 2 to 24 weeks of age: a longitudinal MRI study. *Dev Neurosci, 34*(4), 291-298. doi:10.1159/000339311

Craner, S. L., & Ray, R. H. (1991a). Somatosensory cortex of the neonatal pig: I. Topographic organization of the primary somatosensory cortex (SI). *J Comp Neurol, 306*(1), 24-38. doi:10.1002/cne.903060103

Craner, S. L., & Ray, R. H. (1991b). Somatosensory cortex of the neonatal pig: II. Topographic organization of the secondary somatosensory cortex (SII). *J Comp Neurol, 306*(1), 39-48. doi:10.1002/cne.903060104

Crick, S. J., Sheppard, M. N., Ho, S. Y., Gebstein, L., & Anderson, R. H. (1998). Anatomy of the pig heart: comparisons with normal human cardiac structure. *J Anat, 193 (Pt 1)*, 105-119.

Dawe, R. J., Bennett, D. A., Schneider, J. A., Vasireddi, S. K., & Arfanakis, K. (2009). Postmortem MRI of human brain hemispheres: T2 relaxation times during formaldehyde fixation. *Magn Reson Med, 61*(4), 810-818. doi:10.1002/mrm.21909

De Poorter, J., De Wagter, C., De Deene, Y., Thomsen, C., Stahlberg, F., & Achten, E. (1995). Noninvasive MRI thermometry with the proton resonance frequency (PRF) method: in vivo results in human muscle. *Magn Reson Med, 33*(1), 74-81.

Dobbing, J., & Sands, J. (1979). Comparative aspects of the brain growth spurt. *Early Hum Dev, 3*(1), 79-83.

Guy, J. R., Sati, P., Leibovitch, E., Jacobson, S., Silva, A. C., & Reich, D. S. (2016). Custom fit 3D-printed brain holders for comparison of histology with MRI in marmosets. *J Neurosci Methods, 257*, 55-63. doi:10.1016/j.jneumeth.2015.09.002

Jelsing, J., Nielsen, R., Olsen, A. K., Grand, N., Hemmingsen, R., & Pakkenberg, B. (2006). The postnatal development of neocortical neurons and glial cells in the Gottingen minipig and the domestic pig brain. *J Exp Biol, 209*(Pt 8), 1454-1462. doi:10.1242/jeb.02141

Jenkinson, M., Beckmann, C. F., Behrens, T. E., Woolrich, M. W., & Smith, S. M. (2012). Fsl. *Neuroimage, 62*(2), 782-790. doi:10.1016/j.neuroimage.2011.09.015

Ji, R. R., Berta, T., & Nedergaard, M. (2013). Glia and pain: is chronic pain a gliopathy? *Pain, 154 Suppl 1*, S10-28. doi:10.1016/j.pain.2013.06.022

Landman, B. A., Huang, H., Prince, J. L., & Ying, S. H. (2007). *A Window for High-Resolution Post-Mortem DTI: Mapping Contrast Changes in Neural Degeneration.* Paper presented at the ISMRM Berlin, Germany.

Lieberman, G., Shpaner, M., Watts, R., Andrews, T., Filippi, C. G., Davis, M., & Naylor, M. R. (2014). White matter involvement in chronic musculoskeletal pain. *J Pain*. doi:10.1016/j.jpain.2014.08.002

Lind, N. M., Moustgaard, A., Jelsing, J., Vajta, G., Cumming, P., & Hansen, A. K. (2007b). The use of pigs in neuroscience: modeling brain disorders. *Neurosci Biobehav Rev, 31*(5), 728-751. doi:10.1016/j.neubiorev.2007.02.003

Meurens, F., Summerfield, A., Nauwynck, H., Saif, L., & Gerdts, V. (2012). The pig: a model for human infectious diseases. *Trends Microbiol, 20*(1), 50-57. doi:10.1016/j.tim.2011.11.002

Meyer, W., Neurand, K., & Radke, B. (1981). Elastic fibre arrangement in the skin of the pig. *Arch Dermatol Res, 270*(4), 391-401.

Miller, K. L. (2012). FMRI using balanced steady-state free precession (SSFP). *Neuroimage, 62*(2), 713-719. doi:10.1016/j.neuroimage.2011.10.040

Mogil, J. S. (2009). Animal models of pain: progress and challenges. *Nat Rev Neurosci, 10*(4), 283-294. doi:10.1038/nrn2606

Moseley, M. E., Nishimura, M. C., Pitts, L. H., Bartkowski, H. M., & James, T. L. (1984). Proton nuclear magnetic resonance spectroscopy of normal and edematous brain tissue in vitro: changes in relaxation during tissue storage. *Magn Reson Imaging, 2*(3), 205-209.

Quesson, B., de Zwart, J. A., & Moonen, C. T. (2000). Magnetic resonance temperature imaging for guidance of thermotherapy. *J Magn Reson Imaging, 12*(4), 525-533.

Sasaki, T., Tsuda, S., Riemer, R. K., Ramamoorthy, C., Reddy, V. M., & Hanley, F. L. (2010). Optimal flow rate for antegrade cerebral perfusion. *The Journal of Thoracic and Cardiovascular Surgery, 139*(3), 530-535. doi:http://dx.doi.org/10.1016/j.jtcvs.2009.12.005

Scheurer, E., Lovblad, K. O., Kreis, R., Maier, S. E., Boesch, C., Dirnhofer, R., & Yen, K. (2011). Forensic application of postmortem diffusion-weighted and diffusion tensor MR imaging of the human brain in situ. *AJNR Am J Neuroradiol, 32*(8), 1518-1524. doi:10.3174/ajnr.A2508

Schmierer, K., Thavarajah, J. R., An, S. F., Brandner, S., Miller, D. H., & Tozer, D. J. (2010). Effects of formalin fixation on magnetic resonance indices in multiple sclerosis cortical gray matter. *J Magn Reson Imaging, 32*(5), 1054-1060. doi:10.1002/jmri.22381

Seminowicz, D. A., Shpaner, M., Keaser, M. L., Krauthamer, G. M., Mantegna, J., Dumas, J. A., . . . Naylor, M. R. (2013). Cognitive-behavioral therapy increases prefrontal cortex gray matter in patients with chronic pain. *J Pain, 14*(12), 1573-1584. doi:10.1016/j.jpain.2013.07.020

Shepherd, T. M., Thelwall, P. E., Stanisz, G. J., & Blackband, S. J. (2009). Aldehyde fixative solutions alter the water relaxation and diffusion properties of nervous tissue. *Magn Reson Med, 62*(1), 26-34. doi:10.1002/mrm.21977

Sullivan, T. P., Eaglstein, W. H., Davis, S. C., & Mertz, P. (2001). The pig as a model for human wound healing. *Wound Repair Regen, 9*(2), 66-76.

Summerfield, A., Meurens, F., & Ricklin, M. E. (2015). The immunology of the porcine skin and its value as a model for human skin. *Mol Immunol, 66*(1), 14-21. doi:10.1016/j.molimm.2014.10.023

Sun, S. W., Neil, J. J., Liang, H. F., He, Y. Y., Schmidt, R. E., Hsu, C. Y., & Song, S. K. (2005). Formalin fixation alters water diffusion coefficient magnitude but not anisotropy in infarcted brain. *Magn Reson Med, 53*(6), 1447-1451. doi:10.1002/mrm.20488

Sun, S. W., Neil, J. J., & Song, S. K. (2003). Relative indices of water diffusion anisotropy are equivalent in live and formalin-fixed mouse brains. *Magn Reson Med, 50*(4), 743-748. doi:10.1002/mrm.10605

Swindle, M. M., Makin, A., Herron, A. J., Clubb, F. J., Jr., & Frazier, K. S. (2012). Swine as models in biomedical research and toxicology testing. *Vet Pathol, 49*(2), 344-356. doi:10.1177/0300985811402846

Waldvogel, H. J., Curtis, M. A., Baer, K., Rees, M. I., & Faull, R. L. (2006). Immunohistochemical staining of post-mortem adult human brain sections. *Nat Protoc, 1*(6), 2719-2732. doi:10.1038/nprot.2006.354

Waldvogel, H. J., Curtis, M. A., Baer, K., Rees, M. I., & Faull, R. L. M. (2007). Immunohistochemical staining of post-mortem adult human brain sections. *Nat. Protocols, 1*(6), 2719-2732.

Woolf, C. J. (2011). Central sensitization: implications for the diagnosis and treatment of pain. *Pain, 152*(3 Suppl), S2-15. doi:10.1016/j.pain.2010.09.030

Woolsey, C. N., & Fairman, D. (1946). Contralateral, ipsilateral, and bilateral representation of cutaneous receptors in somatic areas I and II of the cerebral cortex of pig, sheep, and other mammals. *Surgery, 19*, 684-702.

Xanthos, D. N., & Sandkuhler, J. (2014). Neurogenic neuroinflammation: inflammatory CNS reactions in response to neuronal activity. *Nat Rev Neurosci, 15*(1), 43-53. doi:10.1038/nrn3617

Figure Captions

Figure 4.1. A) Single voxel ^{1}H MRI spectroscopy thermometry. A) Post-mortem brain temperature is derived by measuring the chemical shift of a temperature independent metabolite, N-Acetylaspartic Acid (NAA), and temperature dependent H_2O. B) Temperature is derived using calibrated scanner constants which are multiplied by δ which represents the chemical shifts of H_2O and NAA. C) Temperature plots over the duration of scanning for each animal and the length of time MRI acquisition where each point reflects a ^{1}H MRI thermometry acquisition. D) Time from euthanasia to MRI for each specimen.

Figure 4.2. Coronal views of domestic pig brain and structural analysis of single specimen A) T1-weighted anatomical MRI. B) GM segmentation of T1 image using FSL software. C) WM segmentation of T1 image using FSL software. D) Illustrative example of a dilated white matter skeleton (green) from a single pig overlaid on the domestic pig standard brain atlas. Analysis of a cohort of animals will yield a more robust skeleton to serve as a template for WM microstructural analysis (RD, AD, FA, MD, F1, F2, MO). E) Diffusion weighted image of pig brain reconstructed using generalized q-sampling imaging to demonstrate the feasibility of performing connectivity comparisons.

Figure 4.3. From left to right: Sagittal, axial, and coronal T1 MRI of a domestic pig brain as a representative example of the proposed *in situ* imaging paradigm. *In situ* imaging preserves both the GM and WM relaxation times providing comparable contrast and relaxation times to *in vivo* tissue. This also provides a more direct comparison between clinically acquired data since *ex vivo* MRI studies on fixed brains have been shown to alter

diffusion properties and brain volume. Additionally, loss of data to motion or physiological artifacts can be substantial in long scan acquisitions such as diffusion weighted imaging which will be mediated by our *in situ* imaging paradigm.

Figure 4.4. *Ex vivo* T2-weighted MRI relaxometry of single pig brain approximately one year after initial *in situ* MRI. Cannulation of the internal carotid arteries enabled deep brain perfusion of formalin prior to immersion fixation. Panels A, B, and C illustrate T2-relaxation times in the WM, cortical GM, and deep GM respectively. The uniformity of the MR relaxation throughout the deep and cortical GM tissues is a positive indication that the fixation process we propose is consistent throughout the brain and reliably penetrating the tissue.

Figure 4.1. Porcine post-mortem, *in situ*, T1-weighted acquisition.

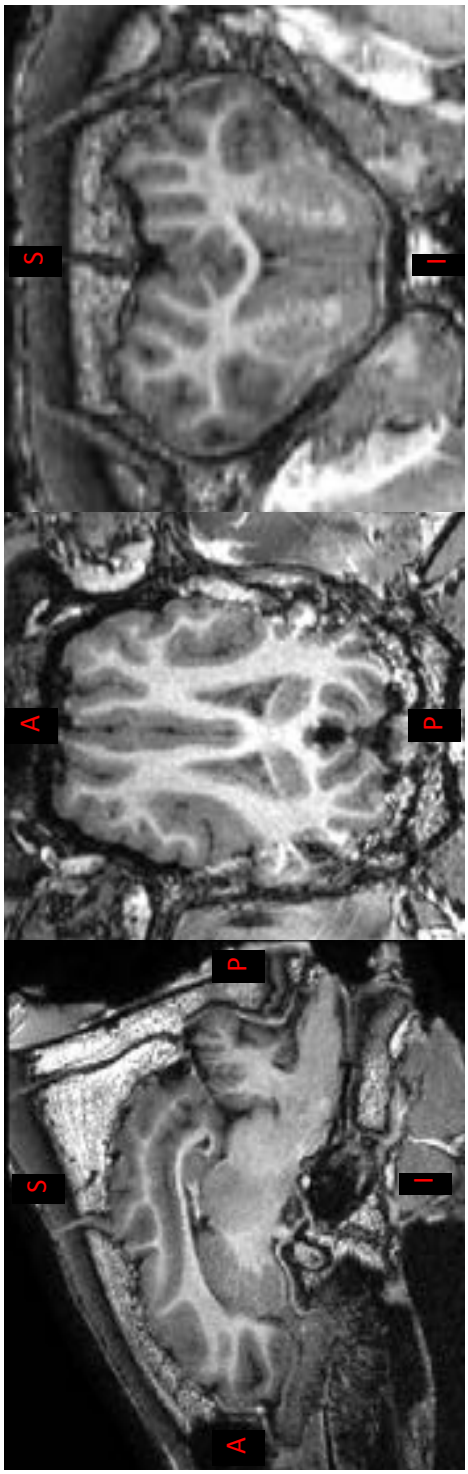

Figure 4.2. ^{1}H MR spectroscopy thermometry.

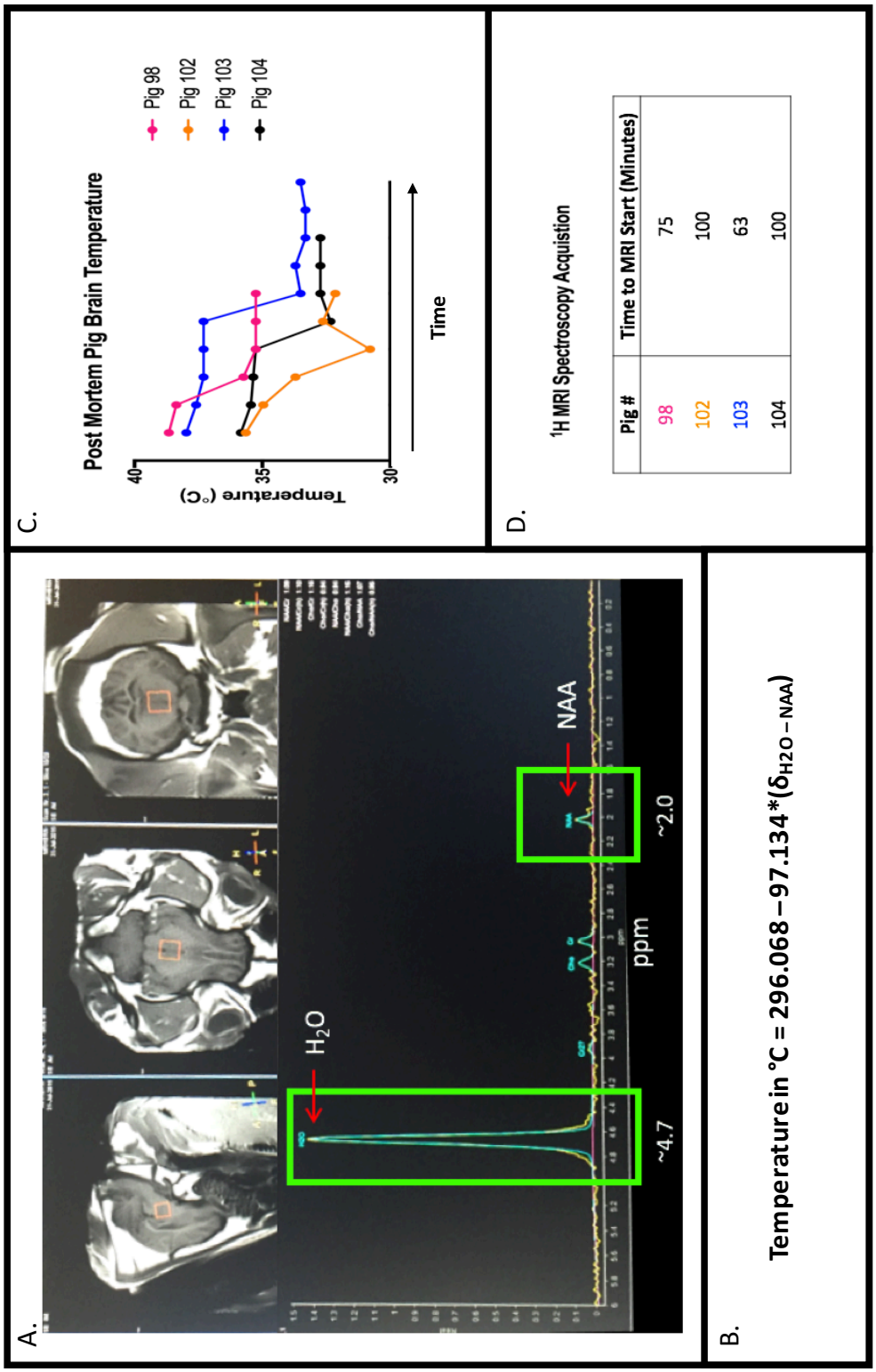

Figure 4.3. ***Ex vivo*** **T2-weighted MRI relaxometry of formalin fixed pig brain approximately one-year after initial MRI acquisition.**

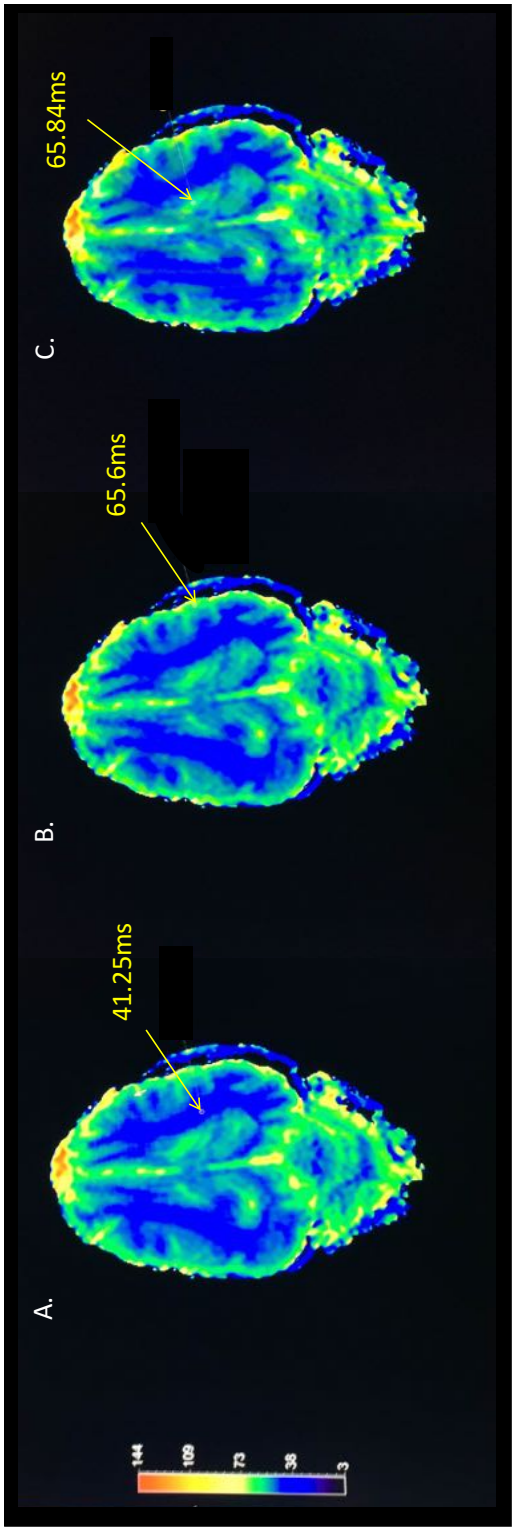

Figure 4.4. Porcine structural imaging, segmentation, and analysis.

CHAPTER 5: COMPREHENSIVE DISCUSSION

Vicious Cycle of Chronic Pain

The research described in this thesis is grounded within the framework of the vicious cycle of chronic musculoskeletal pain. To recap, this cycle begins in the periphery: injury to various tissue types can unleash a cascade of cellular and molecular events that potentiate peripheral sensitization. In this process, inflammation and neuronal excitability promote aberrant peripheral signaling and also facilitate changes in structure and function of the central nervous system (CNS). Influences on the CNS include heightened glial reactivity, neuroinflammation, increased neuronal excitability, and a broadening of the nociceptive field, together termed central sensitization. The significance and extent of brain plasticity associated with chronic pain is still unknown, however, motor abnormalities (such a loss of mobility) and maladaptive psychological coping (such as catastrophizing and anxiety) may further propagate pain chronification. Without intervention or natural resolution of pain, maladaptive coping patterns can induce physiological changes to the musculoskeletal system, such as connective tissue fibrosis. The progression of all of these factors contributes to the 'vicious cycle of chronic pain.' We proposed that remediation of maladaptive behavioral, emotional, cognitive, and motor patterns will improve the suffering of patients with chronic pain, and will be manifested in the CNS grey matter (GM) and white matter (WM) structural plasticity.

To investigate this question, we first established baseline WM and GM differences between chronic pain patients and healthy controls in a large clinical chronic musculoskeletal pain sample (Chapter 2). Then, we assessed neuroplasticity over time to

uncover dynamic changes in brain structure that parallel improvement of clinical outcomes (Chapter 3). We utilized standard pipelines to assess GM morphometry and novel WM analyses of complexity, density and connectivity. In addition, prior to conducting the WM connectivity analysis, we examined several deterministic diffusion algorithms in a phantom and in human neural data in order to select the appropriate algorithm for the diffusion sequence used in this study (Supplementary Chapter 7) (Lichenstein et al., 2016)[1]. Chronic musculoskeletal pain research lacks realistic animal models, impeding progress in the field. To address this gap, we validated a novel porcine model of low-back pain (Supplementary Chapter 6) (Bishop et al., 2016). In order to better characterize the nature of CNS WM alterations in chronic pain patients, we developed a protocol for evaluating CNS abnormalities in the porcine model (Chapter 4). This protocol can be used to understand how morphological alterations affect neuroimaging metrics, a topic of much speculation in the field.

Overview of Neuroimaging Findings

In the preceding chapters, we investigated the structural brain alterations underlying CNS dysfunction in chronic musculoskeletal pain patients and neuroplasticity associated with psychotherapeutic CBT intervention. In chapter 2, we presented compelling evidence of pain-related alterations in WM metrics of complexity, density, and connectivity, as well as macrostructural differences in GM volume compared to healthy, pain-free, volunteers. In chapter 3, chronic pain patients were randomized into two groups, either CBT intervention or educational materials active control group (EDU), and were longitudinally assessed at three time points to investigate brain plasticity associated with

[1] Note co-first authorship of the manuscript with Bishop and Lichenstein

treatment. At both TP2 and TP3, we discovered WM alterations in complexity associated with CBT. Our structural findings yielded little overlap with our baseline results between pain patients and healthy controls at TP1. We suggest that, instead of a reversal of underlying abnormal pain neurocircuitry, these findings may reflect compensatory mechanisms following acquisition of cognitive coping strategies and changes in behavioral patterns. CBT-related changes in sensorimotor and affective circuitry predominated at TP2, and additional alterations in cognitive pathways were observed at TP3. Future work in larger samples could uncover more consistent CBT-related changes.

Biological Significance of Pain Related Structural Alterations

We identified an array of structural alterations across GM and WM tissue types in the chronic pain brain. Some debate still remains whether alterations in brain structure in chronic pain reflect a predisposition to chronic pain, however, evidence suggests that GM alterations are a consequence of disease chronification (Rodriguez-Raecke et al., 2009). We suggest that altered GM morphometry may be a consequence of a host of factors on the cellular level, including cellular crowding, glial reactivity and morphology, dendritic arborization, remodeling, and neurodegeneration (Zatorre et al., 2012). Previous longitudinal evaluations in surgical and behavioral pain interventions demonstrated an increase in GM following successful treatment, challenging the neurodegeneration hypothesis of chronic pain etiology (Rodriguez-Raecke et al., 2013; Seminowicz et al., 2013; Seminowicz et al., 2011). Multi-modal PET and T1-weighted imaging evidence in fibromyalgia patients suggests that decreases in GM may be reflective of variable individual T1-relaxation times, a surrogate of water content within the brain region

(Pomares et al., 2016). These parameters are rarely optimized on an individual level, and, thus, findings of GM decreases in the chronic pain literature may not be indicative of any neuropathology. In contrast to volumetric decreases, local GM increases in fibromyalgia patients were associated with increased $GABA_A$ receptor concentration, suggesting that volumetric increases could, in fact, be clinically significant (Pomares et al., 2016). We attempted to uncover microstructural changes on the cellular level by conducting a mean diffusivity analysis within the GM. GM mean diffusivity changes may be indicative of molecular hindrance of the free water, which could also explain the volumetric differences observed in the GM. Between-group comparisons did not yield significant findings, which may be a function of the relatively low resolution of the diffusion-weighed imaging. Future experiments with high field MRI scanners (>3T) would enable greater spatial resolution, enabling investigation of GM on a sub-nucleus level. Several laboratories have already published investigations of mean diffusivity in specific GM nuclei within subcortical structures, such as the thalamus, hippocampus, amygdala, and brainstem (Eapen, Zald, Gatenby, Ding, & Gore, 2011; Faull, Jenkinson, Clare, & Pattinson, 2015; Forstmann et al., 2014; Goubran et al., 2014; Satpute et al., 2013; Torrisi et al., 2015). Overall, more inquiries are necessitated to resolve the nature of GM morphometric and microstructural alterations in chronic pain and can be greatly informed by translational work in animal models on a cellular level, as suggested in Chapter 4.

The vast majority of WM investigations implement diffusion tensor imaging (DTI) to examine microstructure, which is inherently flawed in regions of complex fiber tract geometry, such as crossing or kissing fibers (J. D. Tournier, Calamante, King, Gadian, & Connelly, 2002; Wheeler-Kingshott & Cercignani, 2009). At the same time, over 90% of

WM voxels contain multiple fiber orientations (Jeurissen et al., 2013). This puts under question the common interpretation of conventional DTI measures, as a proxy of 'tract integrity.' To remedy this methodological concern, we utilized methods that accurately characterize the underlying WM properties, such as complexity and density. We also complemented the ball and sticks fiber complexity analysis, which models up to two fiber populations in a given voxel, with the less constrained mode of anisotropy (MO) analysis. Aside from neuronal influences on WM metrics, non-neuronal contributions warrant careful consideration, particularly in chronic pain populations.

Glia have been postulated to comprise a large percentage of volume (~48%) within a standard imaging voxel (Walhovd et al., 2014) and have been shown to influence single tensor metrics in animal models (Budde et al., 2011). Increases in glial reactivity have been documented in low back pain populations (Loggia et al., 2015), defining a mechanism by which cellular changes could influence diffusion properties such as WM density in the chronic pain brain. Although neurodegeneration commonly underlies diffusion metrics in other disease states, there is no evidence of such pathology in chronic musculoskeletal pain conditions. Therefore, we complemented our WM investigations with a fiber density analysis to explore the non-neuronal influence on WM microstructure. We demonstrated a reduced tract density in the chronic pain population compared to healthy controls within the inferior fronto-occipital fasciculus and the splenium of the corpus callosum. While we speculate that these density changes are non-neuronal in nature given the lack of overlap with alterations in WM complexity, we cannot rule out neuronal influences such as degeneration. Thus confirmatory studies should be carried out to test this non-neuronal

hypothesis using glial specific radioligands, such as TSPO, and positron emission tomography.

We also identified increased connectivity in the chronic pain cohort at baseline. We propose that changes in the neurocircuitry may be representative of network alterations, such as amplified sensory and general allostatic load on the networks from aberrant pain signaling that influence WM in an activity-dependent manner (Peters, McEwen, & Friston, 2017). Alternatively, WM connectivity differences may predispose individuals to developing a chronic pain condition. One report demonstrated that abnormal WM microstructural metrics were predictive of the transition from acute to chronic low back pain, and that connectivity between superior longitudinal fasciculus and lateral prefrontal cortex changed over time in patients who experienced resolution of chronic pain (Mansour et al., 2013). Several studies have shown that functional connectivity is predictive of pain chronification (Baliki et al., 2012) or pain symptom change (Kutch et al., 2017), however, more work is needed to confirm the value of structural connectivity as a biomarker for chronic pain.

In summary, we have identified significant GM and WM brain alterations associated with the clinical pain state and have determined that behavioral interventions, such as CBT, may induce neuroplasticity. To mechanistically evaluate the underpinnings of structural brain changes in chronic pain subtypes, the state of the field requires translational imaging approaches to be conducted in animal models with parallel investigation of cellular and molecular markers. Such experiments will inform both the interpretation of imaging findings in clinical populations and the development of treatment alternatives.

A Porcine Pre-Clinical Model of Pain

Animal models of pain that adequately represent the clinical pathology are essential to our basic understanding of the chronic pain condition and aid in the development of potential therapies (Henze & Urban, 2010). Most existing models have been developed in murine species. Unfortunately, translation of findings to clinical pain populations from murine models are often complicated by poor correspondence between human and murine anatomy, physiology, and immune function. Thus, animals that have analogous structure and function to humans are better proxies for the clinical comparison.

In supplementary chapter 6, we describe for the first time, a novel porcine model of low back pain pathophysiology (Bishop et al., 2016). The model originates from findings of reduced fascia mobility in non-specific low back pain patients (Langevin et al., 2011; Langevin et al., 2009). Briefly, we reproduced thoracolumbar fascia dysfunction by emulating two hallmarks of chronic musculoskeletal pain - soft tissue injury and movement restriction. Fascia thickness and shear strain dynamics were assessed via ultrasound imaging in the same manner as in the original clinical studies in low back pain patients. We determined that injury and movement restriction were independently sufficient to reduce fascia shear strain, and that, in combination, the manipulations were additive, reducing shear plane mobility by more than 50%. Injury significantly increased fascia thickness on the contralateral side with contributions from several fascial planes, including the deep subcutaneous tissue and perimuscular fascia. Significant alterations in gait were also revealed in the movement restricted animals, even upon removal of an immobilizing device. The immunoreactivity of spinal cord neuropeptides, including substance P and CGRP, were not significantly different between groups. This finding suggests that animals

were not truly experiencing chronic pain, restricting our interpretation of this model to movement and connective tissue implications of chronic musculoskeletal pain.

While the described porcine model mimics the human low back pain condition in terms of fascia dysfunction, one drawback to the model is the absence of pain sensitization indicators, such as elevated neuropeptides. It is possible that our methods used to induce fascia dysfunction did not produce sufficient levels of pain to initiate peripheral and central sensitization. The opposite is frequently observed in clinical populations, where diagnostic imaging is a poor indicator of chronic low back pain (Boden et al., 1990; Brinjikji et al., 2015) and patients often have subclinical imaging findings and still report pain (Maher, Underwood, & Buchbinder, 2017).

According to the vicious cycle of pain chronification, altered neuronal excitability is critical to initiate structural and functional brain changes. Future work is required to fine-tune the animal model to reflect additional hallmarks of chronic pain, including peripheral and central sensitization. A possible solution is to add an inflammatory component to the model, in order to induce central sensitization and activity-dependent structural brain changes (Fehrenbacher, Vasko, & Duarte, 2012; Hedo, Laird, & Lopez-Garcia, 1999; Iannitti, Graham, & Dolan, 2012). In addition, behavioral assessments of pain (e.g., Hargreaves' test or Von Frey) were not collected and will have to be included in future investigations (Castel, Sabbag, Brenner, & Meilin, 2016; Castel, Willentz, Doron, Brenner, & Meilin, 2014).

Imaging Pain in the Post-Mortem Pig Brain

Using our described pig model, we developed a novel post-mortem, *in situ*, imaging protocol to augment translational animal imaging (MRI) with histological assessment (Chapter 4). Utilizing fresh, unfixed brain specimens, preserves imaging parameters and facilitates the use of imaging acquisition schemes that are comparable to *in vivo* scans, thus bolstering the potential for translational applicability. In addition to our imaging protocol, we also described a novel method for perfusion fixation via the internal carotid arteries followed by immersion fixation to mitigate post-mortem degradation effects. This animal model and imaging method will promote future investigation into pain related brain plasticity. An unexpected, but potential strength of the model is that it does not induce pain. Coupling the described model with a validated inflammatory pain agent will facilitate discrete investigations of movement- and pain-related central dysfunctions and their interaction in order to better characterize pain-related etiology in the CNS. This approach will clarify GM morphometry and WM complexity and density observations in chronic pain. The model can also be used to investigate treatment-related mechanisms. We have already conducted a study examining the use of static stretch to reverse thoracolumbar fascia dysfunction (Langevin et al., 2017, In Press). Lastly, an overall strength of the proposed method is that it can be implemented using standard clinical imaging systems, expanding the applicability to a wide number of imaging facilities.

It is also important to point out several potential drawbacks of our method, which include the effects of temperature change on scanning parameters and post-mortem tissue degradation (see Chapter 4 for additional details). Using proton magnetic resonance spectroscopy allowed us to obtain a global measure of brain temperature, which could be

used to control for the effect of temperature in the analysis sequence. Alternatively, one could maintain the temperature of the brain by enveloping the specimen in a temperature-controlled surgical heating pad.

To mitigate post-mortem cellular degradation following euthanasia, we adapted a unique fixation protocol, allowing us to rapidly perfuse the brain with fixative prior to the slow immersion fixation (~20 days) (Dawe et al., 2009). Although we identified several critical limitations, we have also documented alternative methods to overcome them. Tissue integrity was confirmed using MR relaxation, however, histological evaluation of brain specimens should be carried out to rule out tissue degradation.

Significance

The vicious cycle of pain chronification changes human behavior and brain structure. Documenting structural neuroplasticity of non-pharmacological treatments for chronic pain, such as CBT, will facilitate a wider utilization in clinical populations, ultimately reducing the reliance and consumption of opioid medications, and alleviating the burden of chronic pain on individuals and society. Proper characterization of neuroplasticity rests on the accuracy of human neuroimaging methods, necessitating rigorous investigation in preclinical models that closely resemble features of human chronic pain. In this body of research, we characterize WM alterations in chronic pain and treatment and, additionally, develop an animal model for future investigations of CNS contributions to pain chronification and pain recovery.

References for Chapter 5

Baliki, M. N., Petre, B., Torbey, S., Herrmann, K. M., Huang, L., Schnitzer, T. J., . . . Apkarian, A. V. (2012). Corticostriatal functional connectivity predicts transition to chronic back pain. *Nat Neurosci, 15*(8), 1117-1119. doi:10.1038/nn.3153

Bishop, J. H., Fox, J. R., Maple, R., Loretan, C., Badger, G. J., Henry, S. M., . . . Langevin, H. M. (2016). Ultrasound Evaluation of the Combined Effects of Thoracolumbar Fascia Injury and Movement Restriction in a Porcine Model. *PLoS One, 11*(1), e0147393. doi:10.1371/journal.pone.0147393

Boden, S. D., McCowin, P. R., Davis, D. O., Dina, T. S., Mark, A. S., & Wiesel, S. (1990). Abnormal magnetic-resonance scans of the cervical spine in asymptomatic subjects. A prospective investigation. *J Bone Joint Surg Am, 72*(8), 1178-1184.

Brinjikji, W., Luetmer, P. H., Comstock, B., Bresnahan, B. W., Chen, L. E., Deyo, R. A., . . . Jarvik, J. G. (2015). Systematic literature review of imaging features of spinal degeneration in asymptomatic populations. *AJNR Am J Neuroradiol, 36*(4), 811-816. doi:10.3174/ajnr.A4173

Budde, M. D., Janes, L., Gold, E., Turtzo, L. C., & Frank, J. A. (2011). The contribution of gliosis to diffusion tensor anisotropy and tractography following traumatic brain injury: validation in the rat using Fourier analysis of stained tissue sections. *Brain, 134*(Pt 8), 2248-2260. doi:10.1093/brain/awr161

Castel, D., Sabbag, I., Brenner, O., & Meilin, S. (2016). Peripheral Neuritis Trauma in Pigs: A Neuropathic Pain Model. *J Pain, 17*(1), 36-49. doi:10.1016/j.jpain.2015.09.011

Castel, D., Willentz, E., Doron, O., Brenner, O., & Meilin, S. (2014). Characterization of a porcine model of post-operative pain. *Eur J Pain, 18*(4), 496-505. doi:10.1002/j.1532-2149.2013.00399.x

Dawe, R. J., Bennett, D. A., Schneider, J. A., Vasireddi, S. K., & Arfanakis, K. (2009). Postmortem MRI of human brain hemispheres: T2 relaxation times during formaldehyde fixation. *Magn Reson Med, 61*(4), 810-818. doi:10.1002/mrm.21909

Eapen, M., Zald, D. H., Gatenby, J. C., Ding, Z., & Gore, J. C. (2011). Using high-resolution MR imaging at 7T to evaluate the anatomy of the midbrain dopaminergic system. *AJNR Am J Neuroradiol, 32*(4), 688-694. doi:10.3174/ajnr.A2355

Faull, O. K., Jenkinson, M., Clare, S., & Pattinson, K. T. (2015). Functional subdivision of the human periaqueductal grey in respiratory control using 7 tesla fMRI. *Neuroimage, 113*, 356-364. doi:10.1016/j.neuroimage.2015.02.026

Fehrenbacher, J. C., Vasko, M. R., & Duarte, D. B. (2012). Models of inflammation: Carrageenan- or complete Freund's Adjuvant (CFA)-induced edema and hypersensitivity in the rat. *Curr Protoc Pharmacol, Chapter 5*, Unit5 4. doi:10.1002/0471141755.ph0504s56

Forstmann, B. U., Keuken, M. C., Schafer, A., Bazin, P. L., Alkemade, A., & Turner, R. (2014). Multi-modal ultra-high resolution structural 7-Tesla MRI data repository. *Sci Data, 1*, 140050. doi:10.1038/sdata.2014.50

Goubran, M., Rudko, D. A., Santyr, B., Gati, J., Szekeres, T., Peters, T. M., & Khan, A. R. (2014). In vivo normative atlas of the hippocampal subfields using multi-echo susceptibility imaging at 7 Tesla. *Hum Brain Mapp, 35*(8), 3588-3601. doi:10.1002/hbm.22423

Hedo, G., Laird, J. M., & Lopez-Garcia, J. A. (1999). Time-course of spinal sensitization following carrageenan-induced inflammation in the young rat: a comparative electrophysiological and behavioural study in vitro and in vivo. *Neuroscience, 92*(1), 309-318.

Henze, D. A., & Urban, M. O. (2010). *Translational Pain Research: From Mouse to Man.* (K. L. & L. A.R. Eds.): CRC Press/Taylor & Francis.

Iannitti, T., Graham, A., & Dolan, S. (2012). Increased central and peripheral inflammation and inflammatory hyperalgesia in Zucker rat model of leptin receptor deficiency and genetic obesity. *Exp Physiol, 97*(11), 1236-1245. doi:10.1113/expphysiol.2011.064220

Jeurissen, B., Leemans, A., Tournier, J. D., Jones, D. K., & Sijbers, J. (2013). Investigating the prevalence of complex fiber configurations in white matter tissue with diffusion magnetic resonance imaging. *Hum Brain Mapp, 34*(11), 2747-2766. doi:10.1002/hbm.22099

Kutch, J. J., Labus, J. S., Harris, R. E., Martucci, K. T., Farmer, M. A., Fenske, S., . . . Network, M. R. (2017). Resting-state functional connectivity predicts longitudinal pain symptom change in urologic chronic pelvic pain syndrome: a MAPP network study. *Pain, 158*(6), 1069-1082. doi:10.1097/j.pain.0000000000000886

Langevin, H. M., Fox, J. R., Koptiuch, C., Badger, G. J., Greenan-Naumann, A. C., Bouffard, N. A., . . . Henry, S. M. (2011). Reduced thoracolumbar fascia shear strain in human chronic low back pain. *BMC Musculoskelet Disord, 12*, 203. doi:10.1186/1471-2474-12-203

Langevin, H. M., Stevens-Tuttle, D., Fox, J. R., Badger, G. J., Bouffard, N. A., Krag, M. H., . . . Henry, S. M. (2009). Ultrasound evidence of altered lumbar connective tissue structure in human subjects with chronic low back pain. *BMC Musculoskelet Disord, 10*, 151. doi:10.1186/1471-2474-10-151

Lichenstein, S. D., Bishop, J. H., Verstynen, T. D., & Yeh, F. C. (2016). Diffusion Capillary Phantom vs. Human Data: Outcomes for Reconstruction Methods Depend on Evaluation Medium. *Front Neurosci, 10*, 407. doi:10.3389/fnins.2016.00407

Loggia, M. L., Chonde, D. B., Akeju, O., Arabasz, G., Catana, C., Edwards, R. R., . . . Hooker, J. M. (2015). Evidence for brain glial activation in chronic pain patients. *Brain, 138*(Pt 3), 604-615. doi:10.1093/brain/awu377

Maher, C., Underwood, M., & Buchbinder, R. (2017). Non-specific low back pain. *Lancet, 389*(10070), 736-747. doi:10.1016/S0140-6736(16)30970-9

Mansour, A. R., Baliki, M. N., Huang, L., Torbey, S., Herrmann, K. M., Schnitzer, T. J., & Apkarian, A. V. (2013). Brain white matter structural properties predict transition to chronic pain. *Pain, 154*(10), 2160-2168. doi:10.1016/j.pain.2013.06.044

Peters, A., McEwen, B. S., & Friston, K. (2017). Uncertainty and stress: Why it causes diseases and how it is mastered by the brain. *Prog Neurobiol*. doi:10.1016/j.pneurobio.2017.05.004

Pomares, F. B., Funck, T., Feier, N. A., Roy, S., Daigle-Martel, A., Ceko, M., . . . Schweinhardt, P. (2016). Histological Underpinnings of Grey Matter Changes in Fibromyalgia Investigated Using Multimodal Brain Imaging. *J Neurosci, 37*(5), 1090-1101. doi:10.1523/JNEUROSCI.2619-16.2016

Rodriguez-Raecke, R., Niemeier, A., Ihle, K., Ruether, W., & May, A. (2009). Brain gray matter decrease in chronic pain is the consequence and not the cause of pain. *J Neurosci, 29*(44), 13746-13750. doi:10.1523/JNEUROSCI.3687-09.2009

Rodriguez-Raecke, R., Niemeier, A., Ihle, K., Ruether, W., & May, A. (2013). Structural brain changes in chronic pain reflect probably neither damage nor atrophy. *PLoS One, 8*(2), e54475. doi:10.1371/journal.pone.0054475

Satpute, A. B., Wager, T. D., Cohen-Adad, J., Bianciardi, M., Choi, J. K., Buhle, J. T., . . . Barrett, L. F. (2013). Identification of discrete functional subregions of the human periaqueductal gray. *Proc Natl Acad Sci U S A, 110*(42), 17101-17106. doi:10.1073/pnas.1306095110

Seminowicz, D. A., Shpaner, M., Keaser, M. L., Krauthamer, G. M., Mantegna, J., Dumas, J. A., . . . Naylor, M. R. (2013). Cognitive-behavioral therapy increases prefrontal cortex gray matter in patients with chronic pain. *J Pain, 14*(12), 1573-1584. doi:10.1016/j.jpain.2013.07.020

Seminowicz, D. A., Wideman, T. H., Naso, L., Hatami-Khoroushahi, Z., Fallatah, S., Ware, M. A., . . . Stone, L. S. (2011). Effective treatment of chronic low back pain in humans reverses abnormal brain anatomy and function. *J Neurosci, 31*(20), 7540-7550. doi:10.1523/JNEUROSCI.5280-10.2011

Torrisi, S., O'Connell, K., Davis, A., Reynolds, R., Balderston, N., Fudge, J. L., . . . Ernst, M. (2015). Resting state connectivity of the bed nucleus of the stria terminalis at ultra-high field. *Hum Brain Mapp, 36*(10), 4076-4088. doi:10.1002/hbm.22899

Tournier, J. D., Calamante, F., King, M. D., Gadian, D. G., & Connelly, A. (2002). Limitations and requirements of diffusion tensor fiber tracking: an assessment using simulations. *Magn Reson Med, 47*(4), 701-708.

Walhovd, K. B., Johansen-Berg, H., & Karadottir, R. T. (2014). Unraveling the secrets of white matter--bridging the gap between cellular, animal and human imaging studies. *Neuroscience, 276*, 2-13. doi:10.1016/j.neuroscience.2014.06.058

Wheeler-Kingshott, C. A., & Cercignani, M. (2009). About "axial" and "radial" diffusivities. *Magn Reson Med, 61*(5), 1255-1260. doi:10.1002/mrm.21965

Zatorre, R. J., Fields, R. D., & Johansen-Berg, H. (2012). Plasticity in gray and white: neuroimaging changes in brain structure during learning. *Nat Neurosci, 15*(4), 528-536. doi:10.1038/nn.3045

CHAPTER 6: ULTRASOUND EVALUATION OF THE COMBINED EFFECTS OF THORACOLUMBAR FASCIA INJURY AND MOVEMENT RESTRICTION IN A PORCINE MODEL

James H. Bishop[1], James R. Fox[1], Rhonda L. Maple[1], Caitlin G. Loretan[1], Gary J. Badger[2], Sharon M. Henry [3], Margaret A. Vizzard[1] and Helene M. Langevin[1,4]
[1]Department of Neurological Sciences, University of Vermont, Burlington, VT
[2]Department of Medical Biostatistics, University of Vermont, Burlington, VT
[3]Department of Rehabilitation and Movement Science, University of Vermont, Burlington, VT
[4]Division of Preventive Medicine, Brigham and Women's Hospital, Harvard Medical School, Boston. MA

Corresponding author:
Helene M. Langevin, M.D.
Division of Preventive Medicine, Brigham and Women's Hospital, Harvard Medical School
Email: hlangevin@partners.org
Phone: 617-525-8734
Fax: 617-731-3843

Running title: Porcine model of fascia injury and movement restriction

Abstract

The persistence of back pain following acute back 'sprains' is a serious public health problem with poorly understood pathophysiology. The recent finding that human subjects with chronic low back pain (LBP) have increased thickness and decreased mobility of the thoracolumbar fascia measured with ultrasound suggest that the fasciae of the back may be involved in LBP pathophysiology. This study used a porcine model to test the hypothesis that similar ultrasound findings can be produced experimentally in a porcine model by combining a local injury of fascia with movement restriction using a 'hobble' device linking one foot to a chest harness for 8 weeks. Ultrasound measurements of thoracolumbar fascia thickness and shear plane mobility (shear strain) during passive hip flexion were made at the 8 week time point on the non-intervention side (injury and/or hobble). Injury alone caused both an increase in fascia thickness ($p=0.007$) and a decrease in fascia shear strain on the non-injured side ($p=0.027$). Movement restriction alone did not change fascia thickness but did decrease shear strain on the non-hobble side ($p=0.024$). The combination of injury plus movement restriction had additive effects on reducing fascia mobility with a 52% reduction in shear strain compared with controls and a 28% reduction compared to movement restriction alone. These results suggest that a back injury involving fascia, even when healed, can affect the relative mobility of fascia layers away from the injured area, especially when movement is also restricted.

Introduction

The thoracolumbar fascia is a prominent anatomical structure in the dorsal trunk region whose role in chronic low back pain is increasingly recognized (Corey, Vizzard,

Badger, & Langevin, 2011; Langevin et al., 2011; Langevin et al., 2009; Malanga & Cruz Colon; Taguchi, Hoheisel, & Mense, 2008; Willard, Vleeming, Schuenke, Danneels, & Schleip, 2012; Yahia, Rhalmi, Newman, & Isler, 1992). This thick, multilayered structure is composed of dense aponeuroses that can bear significant loads (Willard et al., 2012), as well as loose connective tissue layers separating the aponeuroses and allowing shear plane mobility that contributes to the range of motion of the trunk (Benetazzo et al., 2011). Recent studies also have demonstrated that the thoracolumbar fascia has a substantial sensory innervation including small caliber nociceptors that can be activated by mechanical stimulation (Corey et al., 2011; Tesarz, Hoheisel, Wiedenhofer, & Mense, 2011; Yahia et al., 1992)

In a previous human cross-sectional study, we found that subjects with chronic 'non-specific' LBP for more than 12 months had both an increase in thickness and a decrease in mobility of the thoracolumbar fascia measured with ultrasound, compared with subjects without LBP (Langevin et al., 2011; Langevin et al., 2009). We hypothesized that these structural and functional abnormalities of fascia in subjects with LBP could represent a fibrotic process resulting from an initial soft tissue injury involving fascia, followed by movement restriction that could be worsened by pain or fear of pain. Loss of shear plane mobility between adjacent layers within the thoracolumbar fascia could been one of several interrelated factors in the development of low back pain since the lack of mobility may alter the biomechanics trunk as well as the sensory input (nociceptive and/or non-nociceptive) originating from the fascia. Subjects with low back pain have abnormal motor control strategies that may be in part due to altered proprioceptive input (Johanson et al., 2011), and although the role of fascia in motor control feedback loops is poorly understood,

there is evidence that pathological processes involving connective tissue can affect the behavior of overlying muscles (Solomonow, 2012).

The goal of this study was to test whether an animal model of fascia injury combined with experimentally-induced movement restriction for two months could produce thoracolumbar fascia pathology similar to that observed in human subjects with LBP. Fascia thickness and mobility were measured using ultrasound and ultrasound elastography, respectively, as in our previous human studies (Langevin et al., 2011; Langevin et al., 2009). We also tested whether injury and/or movement restriction would produce nervous system neuroplasticity consistent with increased pain sensitivity by measuring spinal cord dorsal horn substance P and calcitonin gene-related peptide (CGRP) expression.

We chose the domestic pig for this study because of its comparable size to humans and substantial similarities in physiology, immune function and wound healing (Crick, Sheppard, Ho, Gepstein, & Anderson, 1998; Lind et al., 2007a; Meurens et al., 2012; Tory P Sullivan, William H Eaglstein, Stephen C Davis, & Patricia Mertz, 2001; Summerfield et al., 2015; M. M. Swindle, A. Makin, A. J. Herron, F. J. Clubb, & K. S. Frazier, 2012), as well as skin and subcutaneous tissue structure (Meyer et al., 1981). In particular, pigs and humans are among the few mammals that, unlike mice, rats, rabbits, dogs, and cats, do not have a subcutaneous (pannicular) muscle in the dorsal trunk region, and therefore have a similar relationship between the skin, subcutaneous tissue and perimuscular fascia in the back (Douglas, 1972; Kerrigan, Zelt, Thomson, & Diano, 1986; Marcarian & Calhoun, 1966; Meyer, Schwarz, & Neurand, 1978; E. H. Rose, Vistnes, & Ksander, 1978; Tory P Sullivan et al., 2001; Vardaxis, Brans, Boon, Kreis, & Marres, 1997). Movement

restriction was induced using a 'hobble' device which restricts full hip extension and reduces pelvic lateral flexion in both pigs and humans when walking in the quadruped position.

Materials and Methods

Experimental Design

The experimental protocols in this manuscript were approved by the University of Vermont (UVM) Institutional Animal Care and Use Committee (IACUC). Castrated male domestic swine (n=20) between 4-6 weeks old, weighing approximately 4-7 kg were acquired from E.M. Parson's Hadley, MA. Pigs were group-housed in the UVM animal facility on a 12 hour light-dark cycle and food intake was adjusted to gain approximately 1 lb/day. Animals were trained to stand on scales without restraint to monitor weight weekly. All pigs were exercised daily in a 20'x10' space for the same amount of time. The remainder of the time, the pigs were allowed to move ad lib in 4'X8' enclosures. A stabilization period of seven days was allowed before subsequent randomization (week 0) into one of four cohorts: Hobble (n = 5), Injury (n = 5), Injury + Hobble (n = 5) or Control (n = 5) for the duration of eight weeks.

Gait Analysis

Prior to surgery and/or hobble placement, all pigs including control animals were familiarized with the gait measurement set-up in a controlled environment, weekly over a span of 5 weeks. The apparatus consisted of a PVC tube totaling 3.048 meter (10 feet) in length with evenly spaced floor markers demarcated every .3048 meters (1 foot). Gait

measurements were acquired in trials; with one trial representing a distance of 1.626 meters (6 feet) out of the entire PVC tube length. Pigs were trained to walk on a rubber mat alongside the PVC tubing with hobbles removed (if present) during training and also during data collection. At week 7, a maximum of 7 trials (1 trial = 1 lap by 6 markers) per pig were videotaped. Videos were downloaded and analyzed using VideoPad Video Editor Version 2.41. Gait speed was calculated by dividing the distance (6 feet) by the time duration between the pig's first foot entering past the first marker and the last foot passing the final marker. Stride length (feet) was determined by observing the distance from where the pig set down its front foot in relation to the distance on the bar to when it set the same front foot down again. Counting for number of steps (defining 'step' as the moment that either right or left front foot touches the ground) began when the first front foot was placed near/on the first marker, and ending when one of the front feet passed the end marker.

Movement Restriction (Hobble)

Custom nylon hobbles were created in-house. At week 0, a conventional dog harness was fitted and a nylon cuff was placed on one hind limb (side randomized) which was connected to the chest harness by interchangeable links that allow for a custom fit (Fig 6.1A). With proper adjustment, the hobble device restricted hind limb positioning so that the standing distance between fore and hind limb was approximately two-thirds the distance of an unrestrained animal. Additional adjustments to the hobbles were made accordingly as the animals increased in size to maintain the restricted hind-limb positioning. Hobbles were and kept in place for 8 weeks. Pigs underwent daily inspection

for any sign of chafing and hobbles were adjusted accordingly. When in place, the hobble prevents full hip extension and pelvic lateral flexion in the transverse plane during gait.

Fascia Injury

At week 0, pigs in the injury groups underwent a unilateral fascia injury in the dorsal trunk (side randomized) at the L3-4 vertebral level 2 cm from the midline (Fig 6.1B). Anesthesia was induced by intramuscular injection of ketamine (20 mg/kg) and atropine (0.05 mg/kg) followed by maintenance with 4% isoflurane inhalation with 100% oxygen. Pigs were shaved and surgically prepared with betadine scrub and isopropyl alcohol. A 4 cm longitudinal skin incision was made 2.0 cm lateral to midline. Target depth of incision was the deep subcutaneous tissue layer between the subcutaneous membranous layer and the thoracolumbar fascia and great care was taken during the skin incision and closure to not penetrate the superficial layers of the thoracolumbar fascia (Fig 6.1C). Blunt and microsurgical dissection tools were used to detach the perimuscular fascia from the adjacent deep subcutaneous tissue, producing a 4 cm x 4 cm injury centered 2 cm lateral to midline. The incision was closed with five interrupted nylon skin sutures and the animals were monitored daily. There were no wound infections among any of the groups. After 8 weeks of growth, the location of the surgical incision was ~2 cm from the lateral edge of the vertebral body, which was used as a landmark during ultrasound imaging (Fig 6.2A).

Fascia Injury and Movement Restriction

At week 0, pigs randomized to injury plus hobble underwent the perimuscular microsurgical technique described above. On the day following the surgical procedure, a hobble device was fitted on the same side as the injury.

Non-Intervention (Control)

Animals in the control group were fitted with a harness but not an ankle cuff and did not receive any surgical intervention or movement restriction.

B-Scan ultrasound data acquisition

All ultrasound imaging was performed immediately after euthanasia by intravenous lethal injection of Fatal Plus (100 mg/kg) to prevent respiration artifact during imaging. Pigs were placed in the prone position on a surgical table. Ultrasound imaging was performed with a Terason 3000 (Terason, Burlington, MA. USA) scanner with a 4.0 mm, 10 MHz linear array transducer. Ultrasound images were acquired bilaterally at L2-3, L3-4 and L4-5 levels with the ultrasound probe oriented transversely, and the edge of the probe aligned with the lateral border of the vertebral body (Fig 6.2A). To measure tissue displacement within the connective tissue layers of the thoracolumbar fascia, ultrasound cine-recordings were acquired during passive flexion of the trunk (Fig 6.2B). After the ultrasound image acquisition described above, the pigs were repositioned so that the L4 level was at the edge of the table. The transducer was placed longitudinally on side of the dorsal trunk contralateral to the intervention (injury and/or hobble, with side randomized in control animals) at the level of the L3/L4 interspace, 2 cm from midline. A cine-loop (25 Hz frame rate) was captured over a 10 second period while the hips of the pig were manually flexed 90 degrees and returned to neutral position for 5 cycles at 0.5 Hz.

Ultrasound image measurement of subcutaneous and perimuscular fascia tissue thickness

Ultrasound images on the injury side were reviewed to ensure consistency of intervention. All ultrasound measurements were performed on the side contralateral to the intervention (hobble and/or injury). This allowed examination of connective tissue remodeling away from the injury itself, with and without movement restriction. In control animals, the measured side was randomized. Ultrasound images were imported in Matlab and measured using a custom software program. In all images, the thickness of tissue layers was measured 2 cm from the lateral border of the vertebral body by identifying the following locations as shown in Fig 6.3: 1) superficial aspect of the dermis, 2) superficial edge of the subcutaneous membranous layer, 3) superficial edge of the thoracolumbar fascia, 4) superficial edge of the erector spinae muscle. The thickness of four discrete zones was calculated based on these measurements as illustrated in Fig 6.3.

Measurement of thoracolumbar fascia shear strain

Ultrasound radio frequency (RF) data was captured and analyzed on the non-intervention side during the third flexion/extension cycle as previously described (Langevin et al., 2011). Subsequent analysis was conducted using an in-house program written in MATLAB (2010a, The MathWorks, Natick, MA USA). A 10x15 mm region of interest (ROI) encompassing the dermis, subcutaneous fat, fasciae layers, and muscle was identified. Shear strain was calculated in ten half-millimeter increments using a moving window starting 1 mm deep to the muscle boundary. The average shear strain was calculated among all the window positions and the average value was used for subsequent statistical analysis.

Measurement of spinal cord substance P and CGRP

Spinal cord with attached dorsal root ganglia from levels L1-L5 were dissected immediately after death of the pig. The location of interest (L3) was marked with placement of suture, and immersion fixed in 4% PFA for 48 hours at 4˚ C. Samples were dissected while immersed in 0.1 M SPBS (sodium phosphate buffered saline, pH 7.4) into sections 1, 2, 3, and 4, with 1 being the most caudal. Samples were placed in 30% sucrose in 0.1 M SPBS for cryoprotection and stored at -20˚ C, then -80˚ C after taking samples for immunostaining. Spinal cord segment L3 was sectioned at a thickness of 40 μm on a freezing microtome. Substance P and CGRP immunostaining was performed using a 50-well plate. Antigen retrieval was done using 1% normal goat serum, 0.3% Triton X diluted in SPBS. Primary antibodies for substance P and CGRP (Phoenix Pharmaceuticals, Inc., Burlingame, CA) were diluted at 1:1000. Samples remained in primary antibody overnight on a shaker. Secondary antibody (Cy3 goat anti-rabbit, Jackson Immunoresearch, Inc., West Grove, PA) was diluted at 1:500. Samples were dried onto slides and rehydrated with SPBS before being covered. Samples were imaged with fluorescence microscopy (Olympus BX50 research microscope). Images were analyzed using Metamorph image analysis. A common threshold was used for each batch of images. Six square-shaped regions of dimension 50 microns x 50 microns were placed evenly along the areas of interest and values were logged, then averaged for the dorsal horn and lateral horn.

Salivary cortisol measurements

Morning (8 am) and afternoon (4 pm) saliva samples were collected on a weekly basis using salivettes (Sarstedt, Numbrecht, Germany). Briefly, a cotton roll was placed in forceps and the pigs chewed on it, moistening it with saliva. The rolls were placed in the collection tubes and centrifuged for 2 minutes at 1000 x g. The saliva samples were frozen at -20C and batch analyzed using ENZO Cortisol EIA kits (cat. ADI-900-071) according to assay instructions.

Statistical Analysis

Two-way analyses of variance were performed to examine the effects of movement restriction and injury on gait, ultrasound outcomes, substance P, CGRP, and cortisol measures. The model included terms representing the main effects of the two factors and their interaction. Repeated measures analysis of variance was used to compare weight among experimental conditions and across time. The model included three factors represented movement restriction, injury and time (0, 5 and 8 weeks), with the latter a within-subject factor. All analyses were done using SAS statistical software version 9.3 (SAS Institute, Cary, NC). Statistical significance was evaluated using $\alpha=0.05$.

Results

Pig weights were consistent among the four cohorts over the course of the study (Fig 6.4). There was a significant increase in weight over time (Repeated measured ANOVA, $F(2, 32) = 983.65$, $p=<0.001$) across the 8 week period in all groups, consistent

with a normal growth pattern. There were no significant weight differences among experimental groups at any of the time points (0, 5, and 8 weeks).

Gait analysis

Motor function was assessed by gait speed, number of steps and stride length with hobble (if present) taken off. There was a significant main effect of movement restriction on gait speed (ANOVA, $F(1, 15) = 5.51$, $p=0.03$), but no significant effect of injury ($F(1,15)=1.41$, $p=2.56$) (Fig 6.5).

Ultrasound measurement of subcutaneous and perimuscular fascia tissue thickness

There was no significant difference in the thickness of dermis and superficial connective tissue (Zone 1) between groups (ANOVA, $F(1,16)=0.29$, $p=0.60$) (Fig 6.6). In contrast, the thickness of deep subcutaneous tissue and perimuscular fascia (Zone 2) at the L3-4 vertebral level was significantly greater in the injured pigs compared with the non-injured groups (ANOVA, main effect of injury $F(1, 16) = 9.57$, $p=0.007$) (Fig 6.6). Additional analyses showed that both the deep subcutaneous tissue (Zone 3: $F(1, 16) = 6.04$, $p=0.026$) and the perimuscular fascia (Zone 4: $F(1, 16) = 4.80$, $p=0.04$) individually contributed to the increased Zone 2 tissue thickness in the injured animals (Fig 6.6). A similar pattern was observed at the L-2-3 and L4-5 vertebral levels, but differences between groups were not statistically significant.

Ultrasound measurement of thoracolumbar fascia mobility (shear strain)

Both injury and movement restriction (hobble) led to a significant reduction in thoracolumbar fascia shear strain (ANOVA main effects of injury $F(1, 16) = 5.86$, p=0.027, and hobble $F(1, 16) = 6.52$, p=0.021) (Fig 6.7). There was no significant interaction between injury and hobble with the combined injury plus hobble group showing additive effects of the two factors on fascia mobility. There additive effects resulted in a 52% reduction in shear strain compared to controls (compared with a 28% reduction for movement restriction alone).

Spinal cord dorsal horn Substance P and CGRP expression

In both the medial and lateral dorsal horn, there were no significant differences in either Substance P or CGRP immunoreactivity between groups (ANOVA, Substance P in dorsal horn F(3,13)=0.49, p=0.70, lateral horn F(3,13)=0.36, p=0.78, CGRP in dorsal horn F(3,14)=0.23, p=0.87, lateral horn F(3,14)=0.66, p=0.59).

Salivary cortisol measurements

No significant differences in AM or PM cortisol levels were found between groups (ANOVA for AM cortisol F(3,17) =0.48, p=0.70, PM cortisol F(3,17)=0.39, p=0.76).

Discussion

In pigs, a combination of fascia injury and movement restriction produced increased fascia thickness and decreased mobility in connective tissue layers similar to those observed in a study of humans with chronic LBP (Langevin et al., 2011; Langevin et

al., 2009). We found no significant differences in spinal cord dorsal horn Substance P or CGRP among groups, suggesting that none of the experimental conditions induced severe chronic pain. It is possible that the injury or hobble could have caused discomfort or pain not severe enough to cause spinal cord neuroplastic changes detectable using our methods, or that the expression of these neuropeptide could have been altered at earlier or later time points. Importantly, however, because the reductions in fascia mobility found in this study were not accompanied by spinal cord neuroplastic changes suggesting chronic pain, our results do not support the notion that loss of shear plane mobility directly alters nociceptive input from the fascia. This is also consistent with our previous results in humans showing a lack of significant correlation between thoracolumbar shear strain and pain symptoms (Langevin et al., 2011). On the other hand, restricted fascia mobility may cause altered proprioception and movement patterns, and thus could be involved in low back pain pathophysiology without being the direct source of nociceptive input.

Injury alone caused both a significant increase in fascia thickness and decrease in fascia mobility on the non-injured side, demonstrating the presence of a pathological process involving the thoracolumbar fascia extending beyond the injured area. Movement restriction alone, on the other hand, did not change fascia thickness but did decrease fascia shear plane mobility, consistent with the formation of connective tissue adhesions due to chronically reduced movement (Weinstein Stuart M, 2005). The combination of injury plus movement restriction had additive effects on fascia mobility. This suggests that adding movement restriction to a soft tissue injury can worsen an already increased tendency of fasciae to adhere together and lose shear plane mobility.

It is well known clinically that restricting movement of joints causes adhesions in periarticular connective tissue, especially after an injury or surgery (Eakin, 2001; Tillman & Cummings, 1992). Our previous studies in humans, and the results of our porcine model, indicate that a similar pathology can occur in the fasciae of the dorsal trunk in response to a mild fascia injury, especially in the presence of movement restriction. Although back 'sprains' are a common occurrence, we currently have no diagnostic method to measure their extent or impact. Our results suggest that a back injury involving fascia, even when healed, can affect the relative mobility of fascia layers in tissues on the other side of the back that were not immediately involved in the initial injury, especially when movement is restricted. Our measurements at the L2-3 and L4-5 levels showed similar trends to those observed at the L3-4 level (increased thickness and decreased mobility), however these did not reach statistical significance at the L2-3 and L4-5 levels. The reason for this may be technical, as the connective tissue planes are at their flattest and most parallel to the skin in the middle of the back (L-3-4 level) and these are the optimal conditions for making our measurements. The presence of slight curves in the connective tissue planes at L2-3 and L4-5 may have introduced some additional variability in the data that obscured any differences that may have been present between groups. We are therefore not able to make a statement at the present time as to whether our findings represent local or generalized connective tissue changes in the back.

The injury in our porcine model was intended to produce a mild tear between the membranous subcutaneous layer and the perimuscular fascia through a small skin incision. It is interesting that the deep tissue layers involved on the side contralateral to the injury are the equivalent layers involved in humans with LBP (deep subcutaneous layer and

perimuscular fascia). In contrast, even though the superficial subcutaneous layer was involved in the injury in the porcine model, we found no evidence that this layer was affected on the non-injured side, and the equivalent layer was similarly unaffected in the human subjects with LBP.

Injury alone did not affect gait speed, compared with controls, which is consistent with an injury that has healed over the 8 week period without causing functional impairment. In contrast, hobbled animals had decreased gait velocity, even with the hobble taken off. This suggests that the effect of the hobble on gait mechanics was more pronounced than the effect of the injury. Nevertheless, movement restriction alone did not increase fascia thickness, as an injury was needed to produce the combined pathology (increased thickness and decreased mobility) seen in humans with LBP.

Our initial study using this porcine model did not intend to investigate specific pathological mechanisms, but rather aimed at using ultrasound as a translational tool to determine whether clinically relevant pathology could be produced experimentally. A notable difference between our human and porcine studies is that our perimuscular fascia shear plane measurements were made 10 minutes post-mortem in pigs, which had the advantage of eliminating brain and spinal cord mediated reflex muscle activity, including breathing, while still allowing us to measure the structural and biomechanical behavior of fascia.

An inevitable limitation of any animal model in relation to human low back pain is the animal's quadruped posture, compared with the biped posture of humans. Consideration of biomechanical differences between humans and animals is especially important in studies of the spine and intervertebral discs due to the different gravitational

loads on the spine in biped vs. quadruped posture (Alini et al., 2008). However, the structural organization and function of the trunk musculature and associated fasciae are essentially conserved with little alteration between quadruped mammals and humans (Schilling, Arnold, Wagner, & Fischer, 2005) (Vleeming A, 1995). This includes the thoracolumbar fascia whose principal biomechanical function is to transfer loads from the upper spine and arms to the pelvis and legs during walking which applies both to biped and quadruped gait

A further limitation of our study is that the study period (2 months) was shorter than the duration of LBP in our previous human study (greater than 12 months). Due to practical considerations, we were not able to study fully-grown animals, since skeletal maturity in domestic pigs is 12-14 months at which point the pigs would have been ~200 kg by the end of the experiment which would not have been manageable, and thus the pigs were growing while the experiment was taking place, which is different from the adult population that was studied in our LBP study. Nevertheless, we did see pathology relevant to that observed in humans and thus extending this model further in time may be useful in future studies.

In conclusion, a porcine model combining thoracolumbar fascia injury and movement restriction for 8 weeks resulted in increased thickness and decreased mobility of the thoracolumbar fascia similar to that observed in human subjects with chronic LBP. However, the application of these findings to people with chronic low back pain must be carefully considered, especially given our lack of evidence of differences in spinal cord nociceptive neuropeptides between experimental groups. Our results do, on the other hand, suggest that a back injury involving fascia, even when healed, can affect the relative

mobility of fascia layers in tissues on the other side of the back that were not immediately involved in the initial injury, especially when movement is also restricted. Future studies will be needed to examine the mechanisms responsible for these abnormalities, and their potential reversibility in response to treatment.

Acknowledgements

The authors thank Dr. Ruth Blauwiekel, Mr. Stephen Bell and the University of Vermont animal care staff for invaluable assistance with the care of the animals. This project was supported by Research Grants RO1 AT004400 from the National Center for Complementary and Integrative Health. The contents of this article are solely the responsibility of the authors and do not necessarily represent the official views of the National Center for Complementary and Integrative Health, National Institutes of Health.

References for Chapter 6

Alini, M., Eisenstein, S. M., Ito, K., Little, C., Kettler, A. A., Masuda, K., . . . Wilke, H. J. (2008). Are animal models useful for studying human disc disorders/degeneration? *Eur Spine J, 17*(1), 2-19. doi:10.1007/s00586-007-0414-y

Benetazzo, L., Bizzego, A., De Caro, R., Frigo, G., Guidolin, D., & Stecco, C. (2011). 3D reconstruction of the crural and thoracolumbar fasciae. *Surg Radiol Anat, 33*(10), 855-862. doi:10.1007/s00276-010-0757-7

Corey, S. M., Vizzard, M. A., Badger, G. J., & Langevin, H. M. (2011). Sensory Innervation of the Nonspecialized Connective Tissues in the Low Back of the Rat. *Cells Tissues Organs*. doi:000323875 [pii]
10.1159/000323875

Crick, S. J., Sheppard, M. N., Ho, S. Y., Gepstein, L., & Anderson, R. H. (1998). Anatomy of the pig heart: comparisons with normal human cardiac structure. *Journal of Anatomy, 193*, 105-119. doi:Doi 10.1046/J.1469-7580.1998.19310105.X

Douglas, W. R. (1972). Of pigs and men and research: a review of applications and analogies of the pig, sus scrofa, in human medical research. *Space Life Sci, 3*(3), 226-234.

Eakin, C. L. (2001). Knee arthrofibrosis: prevention and management of a potentially devastating condition. *Phys Sportsmed, 29*(3), 31-42. doi:10.3810/psm.2001.03.668

Johanson, E., Brumagne, S., Janssens, L., Pijnenburg, M., Claeys, K., & Paasuke, M. (2011). The effect of acute back muscle fatigue on postural control strategy in people with and without recurrent low back pain. *Eur Spine J, 20*(12), 2152-2159. doi:10.1007/s00586-011-1825-3

Kerrigan, C. L., Zelt, R. G., Thomson, J. G., & Diano, E. (1986). The pig as an experimental animal in plastic surgery research for the study of skin flaps, myocutaneous flaps and fasciocutaneous flaps. *Lab Anim Sci, 36*(4), 408-412.

Langevin, H. M., Fox, J. R., Koptiuch, C., Badger, G. J., Greenan-Naumann, A. C., Bouffard, N. A., . . . Henry, S. M. (2011). Reduced thoracolumbar fascia shear strain in human chronic low back pain. *BMC Musculoskelet Disord, 12*, 203. doi:10.1186/1471-2474-12-203

Langevin, H. M., Stevens-Tuttle, D., Fox, J. R., Badger, G. J., Bouffard, N. A., Krag, M. H., . . . Henry, S. M. (2009). Ultrasound evidence of altered lumbar connective tissue structure in human subjects with chronic low back pain. *BMC Musculoskelet Disord, 10*, 151. doi:10.1186/1471-2474-10-151

Lind, N. M., Moustgaard, A., Jelsing, J., Vajta, G., Cumming, P., & Hansen, A. K. (2007a). The use of pigs in neuroscience: Modeling brain disorders. *Neuroscience and Biobehavioral Reviews, 31*(5), 728-751. doi:Doi 10.1016/J.Neubiorev.2007.02.003

Malanga, G. A., & Cruz Colon, E. J. Myofascial low back pain: a review. *Phys Med Rehabil Clin N Am, 21*(4), 711-724. doi:S1047-9651(10)00039-2 [pii]
10.1016/j.pmr.2010.07.003

Marcarian, H. Q., & Calhoun, M. L. (1966). Microscopic anatomy of the integument of adult swine. *Am J Vet Res, 27*(118), 765-772.

Meurens, F., Summerfield, A., Nauwynck, H., Saif, L., & Gerdts, V. (2012). The pig: a model for human infectious diseases. *Trends Microbiol, 20*(1), 50-57. doi:10.1016/j.tim.2011.11.002

Meyer, W., Neurand, K., & Radke, B. (1981). Elastic fibre arrangement in the skin of the pig. *Arch Dermatol Res, 270*(4), 391-401.

Meyer, W., Schwarz, R., & Neurand, K. (1978). The skin of domestic mammals as a model for the human skin, with special reference to the domestic pig. *Current problems in dermatology, 7*, 39-52.

Rose, E. H., Vistnes, L. M., & Ksander, G. A. (1978). A microarchitectural model of regional variations in hypodermal mobility in porcine and human skin. *Ann Plast Surg, 1*(3), 252-266.

Schilling, N., Arnold, D., Wagner, H., & Fischer, M. S. (2005). Evolutionary aspects and muscular properties of the trunk--implications for human low back pain. *Pathophysiology, 12*(4), 233-242. doi:10.1016/j.pathophys.2005.09.005

Solomonow, M. (2012). Neuromuscular manifestations of viscoelastic tissue degradation following high and low risk repetitive lumbar flexion. *J Electromyogr Kinesiol, 22*(2), 155-175. doi:10.1016/j.jelekin.2011.11.008

Sullivan, T. P., Eaglstein, W. H., Davis, S. C., & Mertz, P. (2001). The pig as a model for human wound healing. *Wound Repair and Regeneration, 9*(2), 66-76.

Summerfield, A., Meurens, F., & Ricklin, M. E. (2015). The immunology of the porcine skin and its value as a model for human skin. *Mol Immunol, 66*(1), 14-21. doi:10.1016/j.molimm.2014.10.023

Swindle, M. M., Makin, A., Herron, A. J., Clubb, F. J., & Frazier, K. S. (2012). Swine as Models in Biomedical Research and Toxicology Testing. *Veterinary Pathology, 49*(2), 344-356. doi:Doi 10.1177/0300985811402846

Taguchi, T., Hoheisel, U., & Mense, S. (2008). Dorsal horn neurons having input from low back structures in rats. *Pain, 138*(1), 119-129.

Tesarz, J., Hoheisel, U., Wiedenhofer, B., & Mense, S. (2011). Sensory innervation of the thoracolumbar fascia in rats and humans. *Neuroscience, 194*, 302-308. doi:10.1016/j.neuroscience.2011.07.066

Tillman, L. J., & Cummings, G. S. (1992). Biologic mechanisms of connective tissue mutability. In D. P. Currier & R. M. Nelson (Eds.), *Dynamics of human biologic tissues*

Contemporary perspectives in rehabilitation. Philadelphia: F.A. Davis.

Vardaxis, N. J., Brans, T. A., Boon, M. E., Kreis, R. W., & Marres, L. M. (1997). Confocal laser scanning microscopy of porcine skin: implications for human wound healing studies. *Journal of Anatomy, 190*(4), 601-611.

Vleeming A, P.-G. A., Stoeckart R, van Wingerden JP, Snijders CJ. (1995). The posterior layer of the thoracolumbar fascia. Its function in load transfer from spine to legs. *Spine, 20*(7), 753-758.

Weinstein Stuart M, H. S., and Standaert CJ Low back pain (2005). In D. Lisa (Ed.), *Physical Medicine and Rehabilitaiton 4th ed.* New York: Lipincott Williams and Wilkins.

Willard, F. H., Vleeming, A., Schuenke, M. D., Danneels, L., & Schleip, R. (2012). The thoracolumbar fascia: anatomy, function and clinical considerations. *Journal of Anatomy, 221*(6), 507-536. doi:Doi 10.1111/J.1469-7580.2012.01511.X

Yahia, L., Rhalmi, S., Newman, N., & Isler, M. (1992). Sensory innervation of human thoracolumbar fascia. An immunohistochemical study. *Acta Orthop Scand, 63*(2), 195-197.

Figure Captions

Fig 6.1. (A) Hobble device used to induce movement restriction. (B) Location of fascia injury. (C) Location of fascia injury plane.

Fig 6.2. (A) Location of ultrasound images used for determination of fascia thickness. (B) Method used for acquisition of ultrasound cine-recording during passive trunk flexion.

Fig 6.3. Location of tissue zones used for measurement of tissue thickness in ultrasound images D: dermis, SST: superficial subcutaneous tissue, DST: deep subcutaneous tissue, TF: thoracolumbar fascia.

Fig 6.4. There were no significant weight differences among groups at 0, 5, and 8 weeks.

Fig 6.5. Gait speed (m/sec) was measured at week 8. There was a significant main effect of movement restriction on gait speed *(*ANOVA p=0.03), but no significant effect of injury (ANOVA p=2.56*)*.

Fig 6.6. The tissue thickness in four Zones (See Fig 3 for Zone locations) was measured at the L3-4 vertebral level on the non-intervention side. There was no significant difference in the combined thickness of dermis and superficial connective tissue (Zone 1) among groups (p=0.60*)*. The thickness of Zone 2 (deep subcutaneous tissue and perimuscular fascia), Zone 3 (deep subcutaneous tissue) and Zone 4 (perimuscular fascia) all were

significantly greater in the injured pigs compared with the other groups (ANOVA, main effect of injury for p=0.007 (Zone 2), p=0.026 (Zone 3) p=.04 (Zone 4)).

Fig 6.7. Both injury and movement restriction (hobble) led to a significant reduction in thoracolumbar fascia shear strain (ANOVA main effects of injury p=0.027, and hobble p=0.021). There was no significant interaction between the effects of injury and hobble.

Figure 6.1. Movement restriction and fascia injury methods.

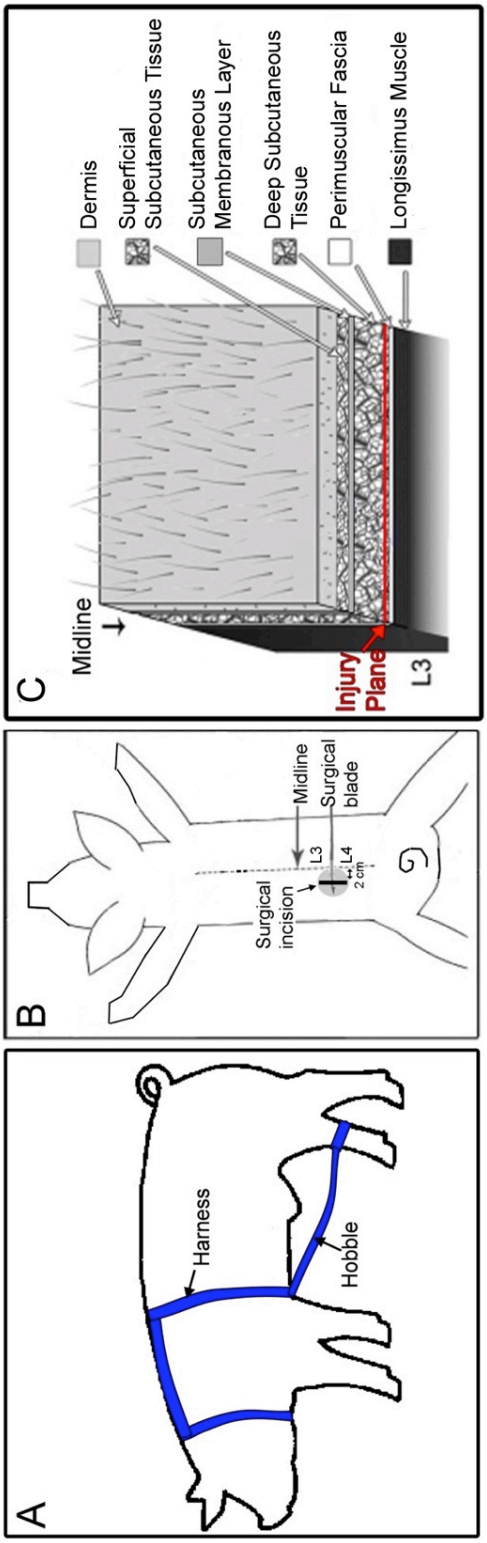

Figure 6.2. Ultrasound data acquisition methods.

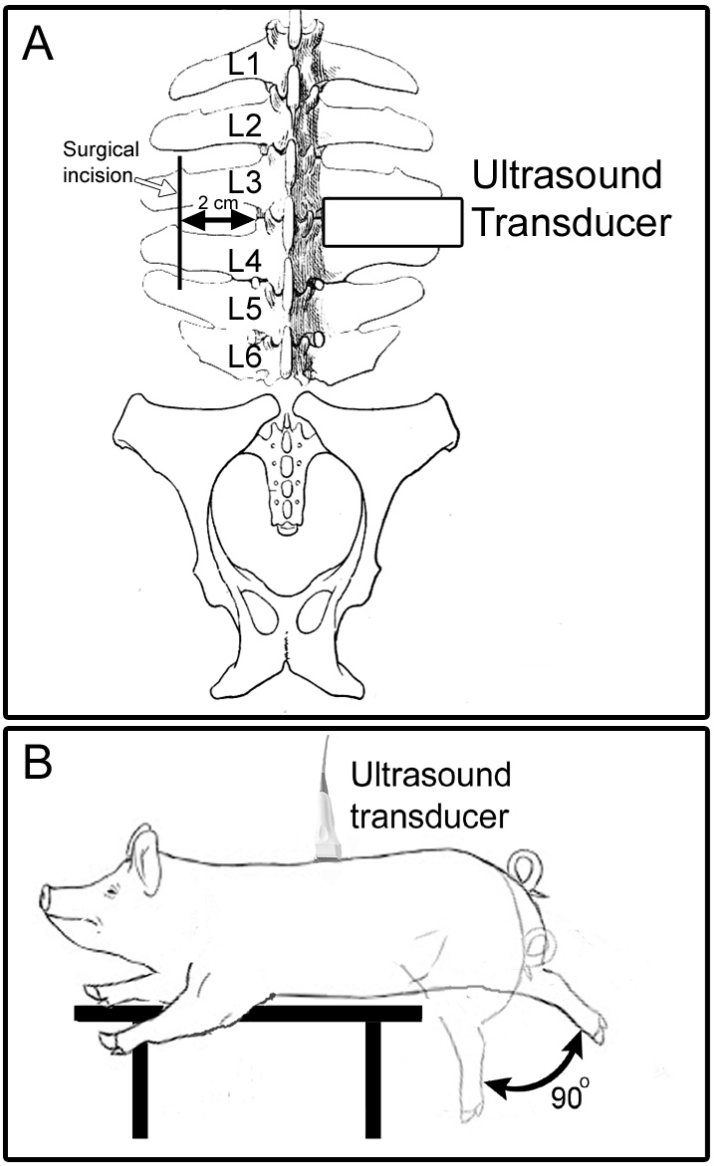

Figure 6.3. Location of tissue zones used for measurement of tissue thickness in ultrasound images.

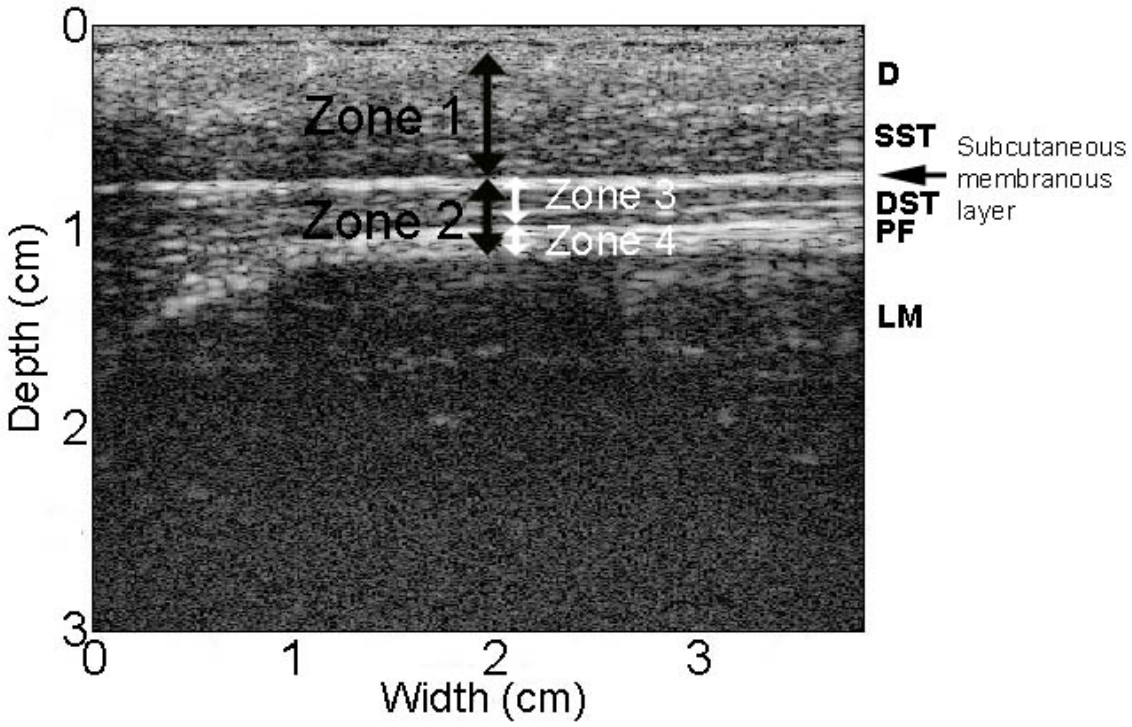

Figure 6.4. Pig growth over the course of the experiment.

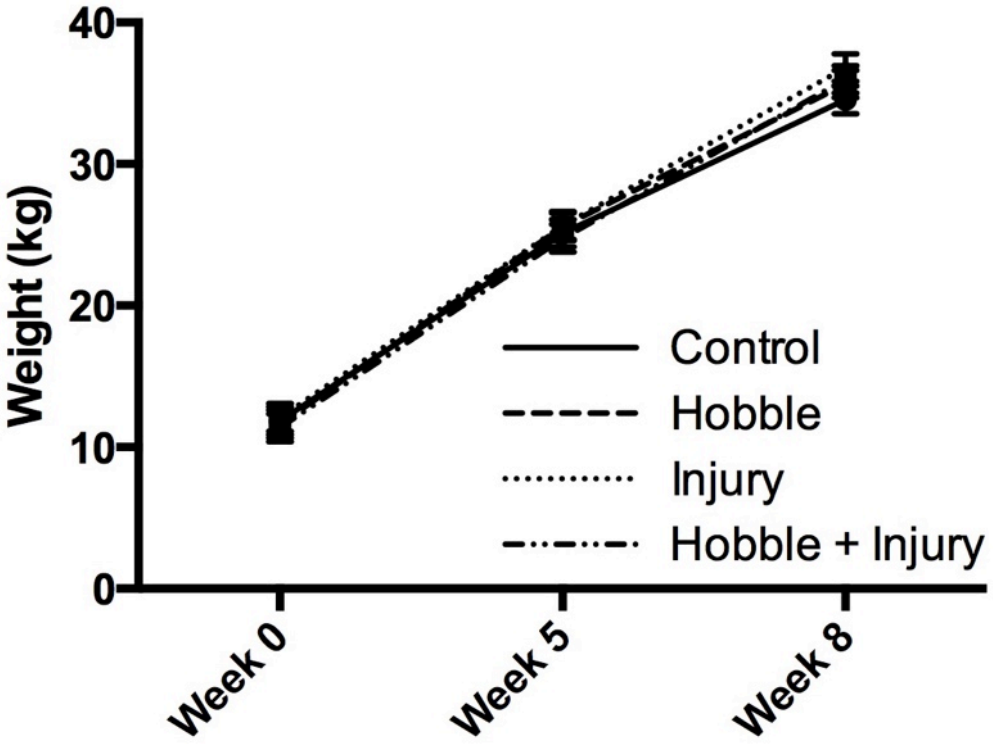

Figure 6.5. Gait analysis.

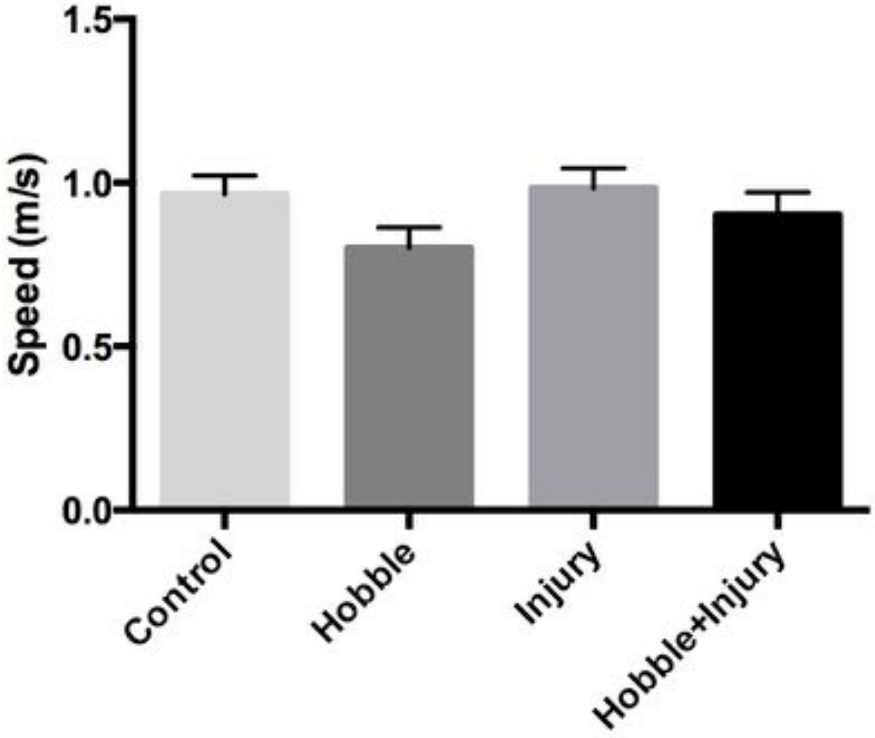

Figure 6.6. Ultrasound measurements of tissue thickness.

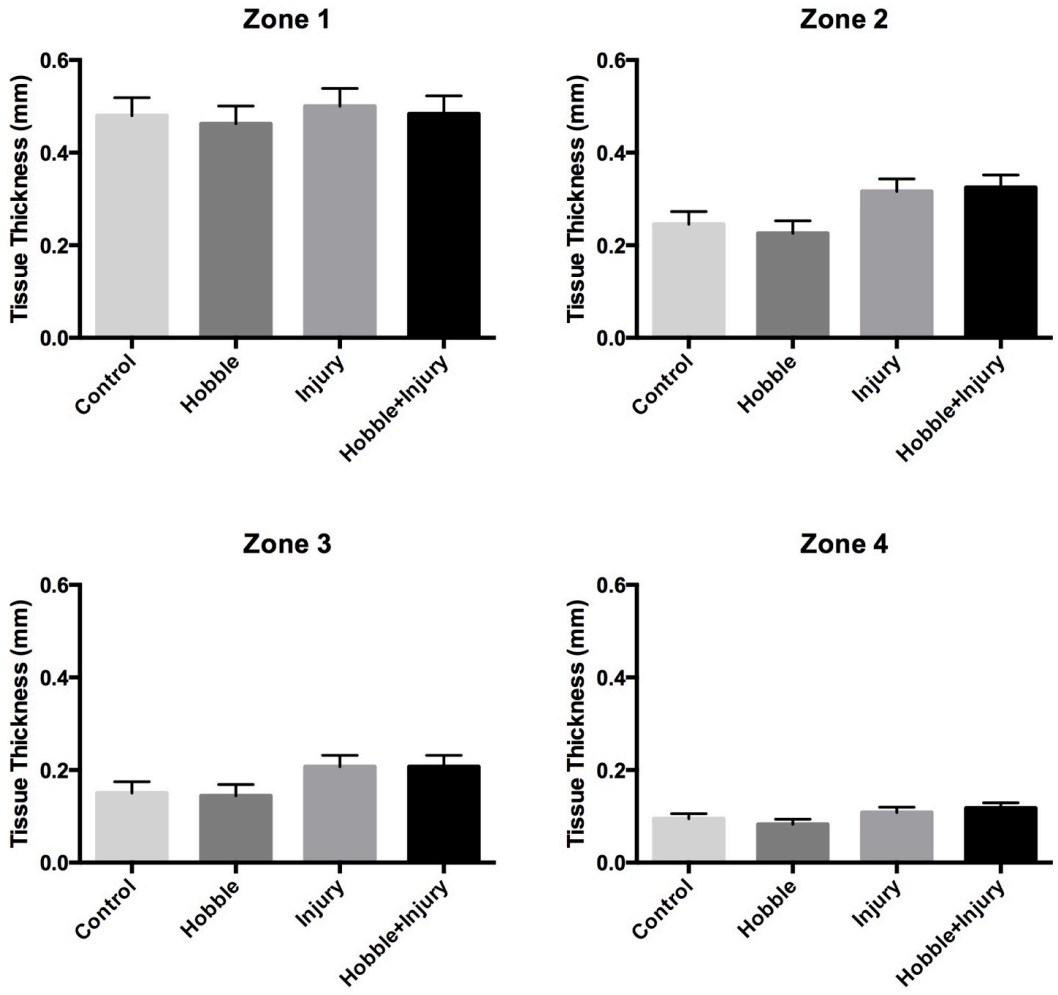

Figure 6.7. Perimuscular fascia shear strain measurements.

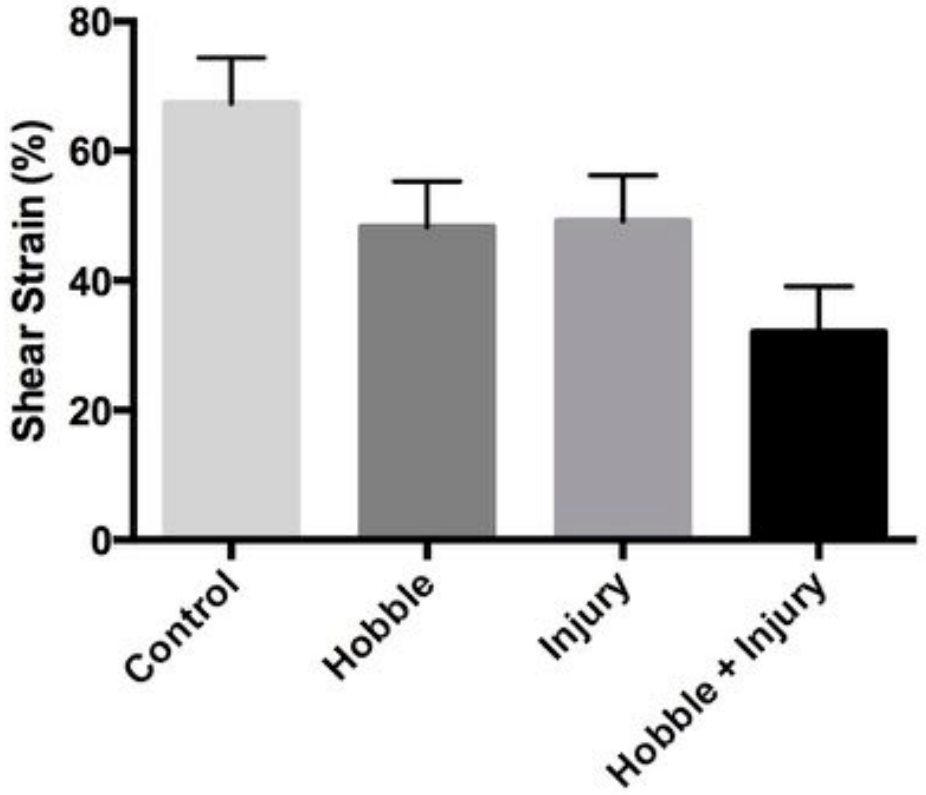

CHAPTER 7: DIFFUSION CAPILLARY PHANTOM VS. HUMAN DATA: OUTCOMES FOR RECONSTRUCTION METHODS DEPEND ON EVALUATION MEDIUM

Sarah D. Lichenstein, M.S.[1*], James H. Bishop, B.S.[2*], Timothy D. Verstynen, Ph.D.[3], and Fang-Cheng Yeh, M.D., Ph.D.[4†]

[1]Department of Psychology, Center for the Neural Basis of Cognition, University of Pittsburgh, Pittsburgh, PA USA
[2]Department of Neurological Sciences, University of Vermont, Burlington, VT USA
[3]Department of Psychology, Center for the Neural Basis of Cognition, Carnegie Mellon University, Pittsburgh, PA USA
[4]Deparment of Neurological Surgery, University of Pittsburgh, Pittsburgh, PA USA
*Both authors contributed equally to this manuscript

Correspondence:
[†]Fang-Cheng Yeh, M.D. Ph.D.
Assistant Professor of Neurological Surgery
University of Pittsburgh
3550 Terrace Street, Scaife A507
Pittsburgh, PA 15261
Email: frank.yeh@pitt.edu

Abstract

Purpose: Diffusion MRI provides a non-invasive way of estimating structural connectivity in the brain. Many studies have used diffusion phantoms as benchmarks to assess the performance of different tractography reconstruction algorithms and assumed that the results can be applied to *in vivo* studies. Here we examined whether quality metrics derived from a common, publically available, diffusion phantom can reliably predict tractography performance in human white matter tissue. Material and Methods: We compared estimates of fiber length and fiber crossing among a simple tensor model (diffusion tensor imaging), a more complicated model (ball-and-sticks) and model-free (diffusion spectrum imaging, generalized q-sampling imaging) reconstruction methods using a capillary phantom and *in vivo* human data (N=14). Results: Our analysis showed that evaluation outcomes differ depending on whether they were obtained from phantom or human data. Specifically, the diffusion phantom favored a more complicated model over a simple tensor model or model-free methods for resolving crossing fibers. On the other hand, the human studies showed the opposite pattern of results, with the model-free methods being more advantageous than model-based methods or simple tensor models. This performance difference was consistent across several metrics, including estimating fiber length and resolving fiber crossings in established white matter pathways. Conclusions: These findings indicate that the construction of current capillary diffusion phantoms tends to favor complicated reconstruction models over a simple tensor model or model-free methods, whereas the *in vivo* data tends to produce opposite results. This brings into question the previous phantom-based evaluation approaches and suggests that a more

realistic phantom or simulation is necessary to accurately predict the relative performance of different tractography reconstruction methods.

Keywords: diffusion MRI, reconstruction, phantom, human brain, tractography

Acronyms: BSM: ball-and-sticks model; dODF diffusion orientation distribution function; DSI: diffusion spectrum imaging; DTI: diffusion tensor imaging; GQI: generalized q-sampling imaging; ODF: orientation distribution function.

Introduction

Diffusion MRI is an increasingly popular imaging approach for visualizing *in vivo* white matter architecture. It detects the movement of water, which is less constrained along the axons in the brain tissue than in the perpendicular direction. The diffusion signals can reveal such an anisotropy that can be used as a proxy for the general orientation of the fiber, making it possible to draw inferences about the microstructural properties of white matter pathways (Hagmann et al., 2006; D. K. Jones, Knosche, & Turner, 2013). This information has been applied to study normal white matter connectivity as well as to elucidate the neural basis of various forms of clinical pathology (D. K. Jones et al., 2013; Seizeur et al., 2012), including multiple sclerosis (Filippi & Rocca, 2011), stroke (Sotak, 2002), Alzheimer's disease (Amlien & Fjell, 2014), and a variety of neuropsychiatric conditions such as schizophrenia, mood and anxiety disorders (White, Nelson, & Lim, 2008).

While diffusion MRI holds great promise for characterizing structural connectivity of the brain, there is substantial methodological heterogeneity that can pose challenges for interpreting findings across studies. In particular, different reconstruction methods vary in the degree to which they can capture complex patterns of water diffusion within voxels.

Therefore, it is important to delineate the relative strengths and weaknesses of different diffusion imaging analysis techniques in order to help researchers select the most appropriate methods when designing studies of white matter architecture.

Model-based reconstruction approaches parameterize the diffusion signal using either a tensor model, i.e. diffusion tensor imaging (DTI) (Basser, Mattiello, & LeBihan, 1994), ball-and-sticks model (BSM; (Behrens et al., 2003), kurtosis model (Jensen, Helpern, Ramani, Lu, & Kaczynski, 2005), or a response function (J. D. Tournier et al., 2008) to calculate the fiber directions and assume that specific diffusion geometries arise from axonal structures within a voxel. On the other hand, model-free reconstruction methods, such as diffusion spectrum imaging (DSI) (Wedeen et al., 2005), q-ball imaging (Tuch, 2004), and generalized q-sampling imaging (GQI) (Yeh et al., 2010), use nonparametric approaches to estimate the orientation distribution function (ODF) of diffusion, also known as the diffusion ODF (dODF). These methods do not assume a specific model, and the local maxima in the dODFs are used to guide fiber tracking (Wedeen et al., 2012; Yeh, Verstynen, Wang, Fernandez-Miranda, & Tseng, 2013).

To evaluate the performance of different methods, diffusion algorithm development and imaging parameter optimization is an active field of study with several seminal studies exhaustively comparing diffusion reconstructions in phantom data sets. Fillard and colleagues, the creators of the Fibercup phantom utilized in this investigation, developed the phantom for a tractography competition comparing the results of 10 novel tractography algorithms (Fillard et al., 2011). In another report, Daducci and colleagues investigated 20 reconstruction approaches across several classes of diffusion algorithms in two distinct phantom data sets, including many classically implemented options available in freely

available software (Daducci et al., 2014). Additionally, Côte et al. recently developed an online evaluation method and compared 57, 096 different diffusion imaging analysis pipelines using the Fibercup dataset (Cote et al., 2013). These studies have highlighted how model-based reconstruction approaches, particularly more complicated models such as constrained spherical deconvolution (J. D. Tournier et al., 2008) and the ball-and-sticks model (BSM; (Behrens et al., 2007), have higher angular resolution in the reconstructed fiber orientations than model-free methods (Fillard et al., 2011; J. D. Tournier et al., 2008) (Daducci et al., 2014) and emphasized that methods with higher angular resolution should lead to more accurate mapping of brain connections *in vivo*. However, a recent tractography competition revealed a dramatically different result (http://www.tractometer.org/ismrm_2015_challenge/), showing that a simple tensor model and model-free approaches, such as GQI, provided more accurate mapping, whereas methods with a much higher angular resolution did not necessarily yield more valid connections. This leads to a critical question on whether current diffusion phantoms built by capillary tubes are representative of diffusion characteristics observed in *in vivo* white matter fascicles.

Here we use publicly available phantom data and *in vivo* human data to evaluate the relative performance of a simple tensor model, a more complicated ball-and-sticks model, and model-free reconstruction methods. In particular, we hypothesize that the capillary diffusion phantom can discriminate the performance between reconstruction approaches in the same way as is observed in established human pathways. To consider the influence of the diffusion sampling schemes, we selected methods that can be equally applied to both single b-value and multiple b-value acquisitions. This includes model-based

methods such as DTI and ball-and-sticks as well as model-free methods such as GQI, and DSI. We focused on phantom pathways that are representative of the complex fiber geometry of the human centrum semiovale in order to provide a comparable benchmark test between phantom and human data. Additional consideration for sampling scheme selection was made based on implementation in commonly available freeware image processing packages.

Material and Methods

2.1. Phantom Study

2.1.1. Phantom Design

The Fibercup diffusion MR phantom (Fillard et al., 2011; Poupon et al., 2008) is the only currently publicly available phantom data with complex fiber geometry. It consists of seven distinct bundles of hydrophobic acrylic fibers contained within a MRI-compatible cylindrical container. The phantom was designed to simulate a coronal section of the human brain and includes a number of different anatomically relevant crossing and kissing fiber configurations with different curvatures. In particular, the upper portion of the Fibercup phantom contains several crossing pathways that are intended to approximate the complex fiber-crossing geometry of the human centrum semiovale. Additionally, the straight arm of the phantom with minimal fiber crossings is anatomically indicative of the human corticospinal pathway. Together, these geometries provide an ideal analogue to compare the performance of different diffusion analysis methods for resolving crossing fibers between the Fibercup phantom and *in vivo* human data. Phantom fibers are 20μm in

diameter, distributed evenly, and compressed, resulting in approximately 1900 fibers/mm^2 throughout the device, including points of intersection.

2.1.2. Phantom Image Acquisition and Reconstruction

Diffusion-weighted images were acquired on a Siemens 3T Tim Trio MRI scanner at the NeuroSpin centre using a 12-channel head coil, and a single-shot diffusion-weighted twice refocused spin echo planar pulse sequence. Acquisition parameters included spatial resolution=3mm isotropic, FOV=19.2cm, matrix 64x64, slice thickness TH=3mm, read bandwidth=1775 Hz/pixel, partial Fourier factor 6/8, parallel reduction factor GRAPPA=2, repetition time TR=5s, 2 repetitions. A total of 64 diffusion directions were obtained with multiple b-values = 650/1500/2000 s/mm², corresponding to the echo times TE=77/94/102 ms respectively. 3 slices were acquired. The image data are publicly available at http://www.lnao.fr/.

Diffusion tensors were calculated using DSI Studio (http://dsi-studio.labsolver.org), and fractional anisotropy (FA) was used to guide the deterministic fiber tracking (Yeh, Verstynen, et al., 2013). In addition to diffusion tensor, the ball-and-sticks model was calculated using *bedpost* in the FSL Diffusion Toolkit (Behrens et al., 2007) (http://fsl.fmrib.ox.ac.uk/fsl/). GQI (Yeh et al., 2010) was calculated in DSI Studio (http://dsi-studio.labsolver.org) with a diffusion sampling length ratio of 1.5 and a maximum of 3 fibers resolved. Additionally, a second iteration of the GQI reconstruction was performed that applied a deconvolution algorithm to sharpen the ODFs, which has been shown to improve the angular resolution of non-tensor based reconstruction

techniques (Yeh, Wedeen, & Tseng, 2011). In the current analysis, a regularization parameter of 7 was applied as suggested by the original study.

Deterministic fiber tracking was performed with DSI Studio (http://dsi-studio.labsolver.org). A generalized deterministic tracking algorithm (Yeh, Verstynen, et al., 2013) was used and two million seeds were randomly generated at subvoxel positions and random orientations. Tracking progression continued with a step size of 0.5mm, and each step was weighted by 40% of the previous direction to smooth the tracks. Otsu's method (Otsu, 1979) was used to set the anisotropy thresholds for the DTI (FA) and GQI (QA) reconstructions. In the ball-and-sticks model, the fiber ratio was used as the stopping criteria. Because the ball-and-sticks analysis has been traditionally applied with probabilistic tractography (Behrens et al., 2007), there is no established method for setting a fiber ratio threshold for deterministic tractography with this approach. Therefore, in order to avoid biasing our evaluation of the ball-and-sticks reconstruction by selecting a single fiber ratio threshold, we selected two different thresholds based on a comparison of phantom fiber tracking results with a range of different thresholds from .01-.05. The .01 threshold yielded the greatest number of streamlines, whereas thresholds above 0.03 failed to produce any streamlines. Therefore, the .01 and .03 fiber ratio thresholds were selected for the ball-and-sticks analysis. Tracking was terminated if the anisotropy/fiber ratio of the next step fell below the assigned threshold, or exceeded an angular threshold of 65°. Streamline lengths were constrained to 1-150mm. Ten randomized iterations of the fiber tracking were performed in order to evaluate the variability of streamlines in addition to comparing their accuracy to absolute fiber measurements. Mean values were calculated across iterations of each reconstruction method for across method comparisons.

2.1.3. Phantom Fiber Length Analysis

The arm of the Fibercup phantom with the least fiber crossings was selected to examine the accuracy of streamline length estimates obtained with different reconstruction methods. A seed region was placed at the center of the pathway, and fiber tracking was initiated from this point. In order to attenuate the confounding effect of crossing fibers on our measure of streamline length, ROIs were drawn beyond each intersecting fiber to isolate those streamlines that successfully navigated these crossings (Figure 7.1). The distributions of streamline length estimates derived from different reconstruction methods were directly compared. Each streamline length was multiplied by its probability to approximate the area under the curve to quantify the modal streamline length estimate for each reconstruction approach. Univariate analysis of variance (ANOVA) was used to compare streamline length measurements across reconstruction methods, and Bonferroni post-hoc tests were utilized to determine which pairwise differences were significant.

2.1.4. Phantom Fiber Crossing Analysis

In order to compare the performance of different reconstruction methods for resolving crossing fibers, a seed region was defined at the intersection between two crossing tracts in the upper portion of the phantom with geometry similar to the human centrum semiovale (Figure 7.2). Fiber tracking in these two known pathways was conducted, and regions of interest were drawn manually at each end of both pathways. Accuracy was assessed by quantifying the number of streamlines that passed through the seed region and both endpoints of the respective pathways.

2.2. Human Study

2.2.1. Human Participants

14 healthy adults (5 men, 9 women, mean age = 27.2 ± 3.8, age range 21-33) participated in the study. Subjects were screened for any contraindications to MRI scanning, and provided informed consent prior to participation. All procedures were approved by the Institutional Review Board at Carnegie Mellon University.

2.2.2. Human Imaging Acquisition and Reconstruction

Diffusion spectrum imaging data were acquired on a Siemens 3T Verio scanner, in the Scientific Imaging for Brain Research Center on the Carnegie Mellon University campus, using a 32-channel coil and a twice-refocused spin-echo echo planar imaging (EPI) diffusion sequence. Acquisition parameters included spatial resolution=2.4mm isotropic, TR=9916ms, TE=157ms, in-plane resolution=2.4mm. A total of 512 diffusion directions were obtained using a half-sphere scheme with a maximum b-value of 5,000 s/mm^2.

Diffusion tensor, ball-and-sticks model, and GQI were conducted using the same parameters as the phantom study. DSI reconstruction was also performed with ODFs with 642 sampling directions, a diffusion sampling length ratio of 1.5, a hanning filter of 16, and 3 fibers resolved. A second iteration of the DSI reconstruction was performed using a deconvolution algorithm with a regularization parameter of 7.

2.2.3. Human Fiber Length Analysis

The same streamline (Euler) deterministic tracking algorithm was used as in the phantom study and 100,000 tracts were generated using random whole brain seeding at subvoxel positions and in random orientations. Tracking progression continued with a step size of 0.5mm, and each step was weighted by 40% of the previous direction to smooth the tracks. Otsu's method was used to set the anisotropy thresholds for the DTI (FA), DSI (QA), and GQI (QA) reconstructions, and two different fiber ratio thresholds were selected for the ball-and-sticks analysis, 0.01 and 0.03, as described above. Tracking was terminated if the anisotropy of the next step fell below the assigned threshold, or exceeded an angular threshold of 65°. Streamline lengths were constrained to 1-160mm. In the ball-and-sticks model, the fiber ratio was used instead of anisotropy as the stopping criteria.

For each reconstruction method, the distribution of streamline length estimates for each subject was generated and means and standard deviations were calculated. Modal streamline length measurements were estimated by multiplying each streamline length by its probability. ANOVA analyses were used to compare modal streamline length estimates derived with different reconstruction methods and Bonferroni post-hoc tests were conducted to determine which pairwise comparisons were significant.

2.2.4. Human Fiber Crossing Analysis

In order to examine the accuracy of different methods for navigating complex fiber crossings, we compared the performance of each reconstruction method for recovering streamlines passing through the centrum semiovale, a region where several prominent white matter tracts intersect (D. K. Jones, 2008; Schmahmann & Pandya, 2006;

Sotiropoulos et al., 2013; Tuch et al., 2005). Previous research has demonstrated that poor reconstructions of fiber crossings results in biases that tend to resolve only a single pathway or section of a pathway (Farquharson et al., 2013). Although corpus callosum fibers are known to terminate throughout the frontal cortex, poor resolution of crossing fibers in the centrum semiovale creates a bias towards the medial callosal U-shaped fibers due to an inability to capture more lateral streamlines that traverse the centrum semiovale crossing. Here, we evaluated whether different reconstruction methods differ in their ability to capture the lateral spread of corpus callosum pathways by comparing the relative number of streamlines that terminate in different sections of the frontal cortex.

Tractography for the fiber crossing analysis was conducted with a streamline (Euler) deterministic tracking algorithm. One million seeds were placed at random subvoxel positions throughout the brain. Tracking was initiated in random orientations, and was propagated with a step size of 1.2 mm and smoothing of 0.4. Anisotropy thresholds were determined using Otsu's method for reconstructions other than the ball-and-sticks, for which two thresholds were set at 0.01 and 0.03. Streamlines were terminated when the anisotropy at the subsequent step fell below the assigned threshold or the turning angle exceeded 60°.

Connectivity matrices for each participant were constructed using frontal cortex ROIs from the automated anatomic labeling (AAL) atlas (Tzourio-Mazoyer et al., 2002), including the left and right superior frontal gyrus (SFG), middle frontal gyrus (MFG), inferior frontal gyrus (IFG) operculum, IFG triangularis, and the IFG orbitalis. The number of streamlines that connect each hemisphere of the superior, middle, and inferior frontal gyrus ROIs were extracted from each connectivity matrix, and values from the three

regions of the inferior frontal gyrus were summed (see Figure 7.3). Ratios of the number of SFG, MFG and IFG streamlines relative to the total number of streamlines were calculated so although an exact streamline count is unknown, higher ratios of MFG and IFG streamlines would be indicative of better lateral coverage. Therefore, more accurate reconstruction methods should estimate greater proportions of streamlines in the medial and inferior regions of the frontal cortex, whereas less successful reconstructions will show a greater bias towards the superior, u-shaped fibers.

In order to quantitatively compare between reconstruction methods, a 7 x 3 ANOVA was conducted to assess the effects of reconstruction method and ROI on the ratio of streamlines resolved. In order to evaluate whether the application of a deconvolution algorithm improves lateral coverage, an additional analysis was conducted within the DSI and GQI data using a 2 x 2 ANOVA to test the effect of reconstruction method and deconvolution algorithm on the ratio of streamlines recovered for each ROI individually. Where significant group differences were found, follow-up analyses were conducted to determine which pairwise comparisons were significant.

Results

3.1. Phantom Study Results

3.1.1. Phantom Fiber Length Results

Fiber tracking with the DTI reconstruction was unable to detect any streamlines passing through the long leg of the phantom that navigated both crossings. Means and standard deviations for number of streamlines detected with each of the other reconstruction methods are: ball-and-sticks (0.01 fiber ratio threshold) 43320.2 ± 224.96;

ball-and-sticks (0.03 fiber ratio threshold) 10988.5 ± 141.84; GQI 213 ± 15.76; GQI with deconvolution 22942.8 ± 166.33. Analysis of variance for the four reconstruction methods that were able to detect streamlines within this arm of the phantom demonstrated that there is a significant group difference in the number of streamlines resolved with different reconstruction methods ($F(3,36)$=138362.57, $p<0.001$). Post-hoc pairwise comparisons show that each reconstruction method yields a significantly different number of tracts relative to each of the other reconstruction methods (all $p<0.001$).

The distribution of streamline length estimates demonstrates that the ball-and-sticks model (0.01 fiber ratio threshold) yields the greatest number of streamlines within this pathway, but the length measurements were less accurate and more variable relative to the estimates generated with the GQI approaches (Figure 7.4). The GQI and GQI with deconvolution reconstructions produce fewer streamlines, but their length measurements are longer and had less variability. Analysis of variance demonstrates a significant group difference in modal streamline length estimates generated using the different reconstruction methods ($F(3,36)$=7568.65, $p<0.001$). Post-hoc pairwise comparisons show that each reconstruction method yields significantly different length estimates relative to each of the other reconstruction methods (all $p<0.01$).

3.1.2. Phantom Fiber Crossing Results

For pathway 1, the DTI reconstruction produces the greatest number of streamlines, detecting a mean of 4399.7 ± 46.76 streamlines, relative to the 2956.9 ± 42.53, 366.5 ± 14.80, 2212.1 ± 45.26, and 3243.1 ± 76.64 streamlines for ball-and-sticks (0.01 fiber ratio threshold), ball-and-sticks (0.03 fiber ratio threshold), GQI, and GQI with deconvolution, respectively (Figure 7.5). Analysis of variance indicates that there is a significant group

difference in the number of tracts detected within pathway 1 ($F(4,45) = 9179.71$, $p<0.001$). Post-hoc pairwise comparisons show that each method yields a significantly different number of tracts relative to each other reconstruction (all $p<0.001$).

In pathway 2, no streamlines were detected with the DTI or GQI reconstructions, whereas 537.6 ± 18.18 streamlines were identified with the ball-and-sticks model at a fiber ratio threshold of 0.01, 15.3 ± 3.09 streamlines were detected with the ball-and-sticks model at a 0.03 fiber ratio threshold, and 148.1 ± 15.70 were found using GQI with deconvolution. ANOVA results show a significant group difference in the number of tracts detected within pathway 2 ($F(4,45) = 4538.48$, $p<0.001$). Post-hoc pairwise comparisons show that the two ball-and-sticks reconstructions and GQI with deconvolution yield significantly different streamline measurements (all $p<0.05$). DTI and GQI do not differ significantly because both methods failed to identify any tracts within this pathway.

3.2. Human Study Results

3.2.1. Human Fiber Length Results

For the human data, the distribution of streamline length estimates for each reconstruction method shows that the DTI approach produces the greatest quantity of small, noisy streamlines, whereas the ball-and-sticks model yields the fewest number of short streamlines, i.e., those shorter than 10 mm (Figure 7.6). Means and standard deviations for modal streamline length estimates acquired with each reconstruction method were: DTI 30.94 ± 1.23; ball-and-sticks (0.01 fiber ratio threshold) 38.51 ± 1.96; ball-and-sticks (0.03 fiber ratio threshold) 35.02 ± 1.58; DSI 37.9 ± 0.82; DSI with deconvolution 37.35 ± 1.63; GQI 36.41 ± 1.14; GQI with deconvolution 37.72 ± 3.36. Analysis of variance reveals a

significant group difference in modal streamline length estimates generated using the different reconstruction methods ($F(6,91)$=28.08, $p<0.001$) (Figure 7.7). Post-hoc pairwise comparisons show that the DTI method yields significantly shorter length estimates relative to each other reconstruction (all $p<0.01$). Additionally, there is a significant difference between the ball-and-sticks model at a .01 fiber ratio threshold and the ball-and-sticks model using a .03 fiber ratio threshold ($p<0.001$). The ball-and-sticks reconstruction (.03 QA) also differs significantly from the DSI, DSI with deconvolution and GQI with deconvolution methods (all $p<0.05$). Streamline length estimates derived with the ball-and-sticks model at a 0.01 fiber ratio threshold, DSI or GQI reconstruction methods do not significantly differ from one another, with or without the application of the deconvolution algorithm.

3.2.2. Human Fiber Crossing Results

Means and standard deviations for the total number of streamlines connecting the right and left superior, medial, and inferior frontal gyrus ROIs are presented in Table 1. The total number of streamlines differs significantly by reconstruction method ($F(6, 91)=18.387$, $p<0.001$). Post-hoc analysis revealed that this group difference is driven primarily by a greater number of streamlines detected with the DTI reconstruction and relatively fewer streamlines detected using the ball-and-sticks (0.01) approach; whereas the number of total streamlines does not differ between the ball-and-sticks reconstruction at the .03 fiber ratio threshold, DSI, or GQI, regardless of deconvolution (all $p>0.05$). Looking at the number of streamlines connecting the two hemispheres of the SFG, MFG, and IFG ROIs, a significant effect of reconstruction on the number of MFG streamlines is

observed ($F(6, 91) = 15.216$, $p<0.001$), but no significant effect is found for superior or inferior frontal gyrus streamlines. Post-hoc Bonferroni tests demonstrate that the DSI with deconvolution reconstruction produces significantly more MFG streamlines than all other methods (all $p<0.05$). The DTI, ball-and-sticks (0.01 and 0.03), and GQI reconstructions do not differ significantly in the number of MFG streamlines recovered, nor do the DSI, GQI, and GQI with deconvolution methods, but the mean trends show that the model-free methods all capture more MFG streamlines than the model-based methods (See Table 1). DSI and GQI with deconvolution yield a significantly greater number of MFG streamlines relative to the single- and multi-tensor methods (all $p<0.05$). Means and standard deviations for the ratio of SFG, MFG, and IFG streamlines resolved with each reconstruction methods are listed in Table 2.

A 7 x 3 ANOVA reveals a significant main effect of reconstruction method ($F(6, 273) = 9.313$, $p<0.001$) and ROI ($F(2, 273) = 77.2$, $p<0.001$) on the ratio of streamlines relative to the total number of streamlines, as well as a significant reconstruction by ROI interaction ($F(12, 273) = 5.78$, $p<0.001$). In order to interpret this interaction, additional ANOVA analyses were performed to look at the effect of reconstruction method on the ratio of streamlines resolved for each ROI separately. These analyses reveal that the effect of reconstruction was only significant for the ratio of MFG streamlines relative to the total number of streamlines. No significant difference is observed between the DTI and ball-and-sticks (.01 and .03 fiber ratio thresholds), but both approaches perform significantly worse than the DSI and GQI reconstructions. Similarly, DSI, DSI with deconvolution and GQI with deconvolution do not differ significantly, but the GQI without deconvolution

resolves a significantly smaller proportion of MFG streamlines relative to the DSI with deconvolution reconstruction (Figure 7.8).

In order to assess the impact of applying a deconvolution algorithm, a 2 x 2 ANOVA was conducted to determine the effect of reconstruction (DSI and GQI only) and deconvolution on the ratio of MFG streamlines resolved. No significant effect of reconstruction method is present, but a significant main effect of deconvolution is observed ($F(1,52)=10.358$, $p<0.01$). No significant interaction is present, indicating that for both DSI and GQI methods, the application of a deconvolution algorithm increases the amount of MFG streamlines resolved.

Discussion

The results shown here reject the hypothesis that the current capillary phantom can faithfully provide a performance evaluation consistent with the *in vivo* human study. When benchmarked on regions with similarly complex multiple crossing geometry in both the phantom and human pathways, validation results were highly dependent upon the medium used. Specifically, in the phantom, the model-based ball-and-sticks model outperformed all other approaches for resolving crossing fibers, whereas the model-free methods performed better in the human pathways. The phantom results showed that the ball-and-sticks reconstruction at a .01 fiber ratio threshold produces significantly more correct streamlines along the crossing pathway than GQI. Interestingly, DTI also outperformed GQI in the U-fiber region of the phantom. GQI reconstruction underperforms, particularly, in the quantity of streamlines generated. This is evident from the straight arm crossing fiber configuration where both GQI and DTI fail to produce any correct streamlines. The overall

phantom results reveal a performance order that a complicated model works better than a simple tensor model, and a simple tensor model was better than model-free methods.

The *in vivo* study showed a completely opposite results. The GQI reconstructions showed marked improvements over the model-based methods for resolving crossing fibers *in vivo*. Both the DSI and GQI methods produced better lateral coverage of the frontal cortex than the DTI or ball-and-sticks reconstructions in human subjects. GQI results are consistent with measurements obtained using the DSI reconstruction within the MFG. The advantage of adding the deconvolution algorithm to DSI and GQI reconstructions is also evident in the *in vivo* results, showing greater lateral coverage in both circumstances. DSI with deconvolution produces a greater ratio of MFG streamlines relative to all other reconstruction methods. More importantly, DTI performed better than a more complicated ball-and-sticks model, and thus the overall results revealed that a model-free method was better than a simple tensor model, and a single tensor model was better than a complicated model.

Thus, there is a substantial discrepancy between the phantom and *in vivo* studies in the performance. A possible explanation for this discrepancy is the design of the diffusion phantom. The DTI and ball-and-sticks approaches use the tensor model that implicitly assumes uniformity of the diffusion pattern in the fiber populations. This assumption fits well with the design of the diffusion phantom, in which, the composition of fiber bundles is constant. The uniformity of fiber populations in typical phantom constructions may explain why the model-based methods are better suited to capture crossing fibers in phantom studies. For example, the ball-and-sticks model assumes that the characteristics of diffusion are identical in each direction. While this matches the phantom configuration,

the synthetic fiber bundles in the phantom are not structurally congruent with axons found in the brain due to their homogenous diameters and lengths. The axonal fibers that make up major white matter pathways of the brain are heterogeneous in terms of size and myelination (i.e. Aboitiz, Scheibel, Fisher, & Zaidel, 1992). Besides axonal structure, there are additional complexities such as cellular microstructure that may also contribute to the diffusion signal in neural tissue. Recent literature suggests that as much as 40% of a 2.5 mm isotropic voxel, standard for *in vivo* high angular resolution diffusion imaging sequences, is composed of neuroglia such as astrocytes (Walhovd et al., 2014). Therefore, it is likely the simplicity of a diffusion phantom may overestimate the performance of model-based methods such as DTI and ball-and-sticks model.

This conclusion can also be applied to most simulation studies that have also assumed uniformity in the diffusion pattern and thus used a uniform diffusion model to simulate diffusion signals. Therefore, such numerical simulations may also favor model-based methods over model-free methods. Alternatively, more recent simulation approaches, such as tractometer (Cote, Bore, Girard, Houde, & Descoteaux, 2012) and diffantom (Esteban et al., 2016), use real data to create digital phantoms, and may represent a useful alternative to simple capillary phantoms for evaluating different diffusion imaging analysis methods. Future research is necessary to establish whether the performance of different reconstruction methods in more advanced simulated data would accurately predict the relative performance of these reconstruction methods *in vivo*.

Another important issue highlighted in this study is that the model-free methods were underestimated in the capillary phantom. For *in vivo* studies, model-free methods, such as GQI, may be more appropriate than the model-based reconstructions for studying

biologically relevant fiber geometry as they use a data-driven approach to identify peaks in the diffusion ODF without imposing *a priori* assumptions about the properties of diffusion in the complex axonal structures. Interestingly, this finding is consistent with the recent result of the ISMRM 2015 tractography competition (http://www.tractometer.org/ismrm_2015_challenge/), in which GQI (ID#03) demonstrated the highest percentage of valid connections over all other model-based methods. Even more surprisingly, complicated modeling methods such as constrained spherical harmonics and ball-and-sticks performed worse than a simple DTI-based tractography. This result strongly suggests that the previous phantom and simulation studies may have overestimated the complicated modeling approach over the simple, robust methodology, leading to a serious doubt on the accuracy and reliability of diffusion MRI tractography (Reveley et al., 2015; Thomas et al., 2014).

The use of different acquisition schemes may also have contributed to the discrepant results obtained with the phantom and human datasets. Nonetheless, previous studies have compared reconstruction methods using different acquisition schemes (i.e. Daducci et al. 2013), and the results of reconstruction methods comparisons are often used to guide the selection of reconstruction approach regardless of the acquisition scheme used. Moreover, these acquisition schemes are often specifically tailored to optimize a specific reconstruction method or analysis approach biasing direct comparison. Future studies should confirm whether reconstruction approaches would also perform differently in phantom and human datasets acquired using the same acquisition scheme. Furthermore, the current analysis focused on the use of different reconstruction methods with a deterministic tractography approach. Future research is necessary to compare the relative

performance of model based and model free reconstructions using probabilistic tractography.

The large discrepancy between the phantom and *in vivo* results suggest that more realistic diffusion phantoms are needed to replace the current designs that are composed of a host of synthetically derived materials that often do not exhibit diffusion properties similar to biological tissue. Advances in materials engineering provide promising new methods to generate biomimetic phantoms. For example, Hubbard and colleagues utilized electrospinning methods to develop reproducible diffusion phantoms of tunable fiber diameters (1- 20 μM) and geometries (P. L. Hubbard, Zhou, Eichhorn, & Parker, 2015). Inhomogeneous fiber size, diameter and geometry are consistent with neural architecture and would provide a better testing platform for diffusion reconstruction comparisons.

Overall, our results cast doubt on the assumption that diffusion imaging analysis methods perform comparably in capillary phantom and *in vivo* human data. While the use of diffusion phantoms to test novel reconstruction methods provides valuable quantifiable information, it may not be used as a sole methodology to evaluate the performance of a method.

4.1. Conclusions

The hypothesis that diffusion phantoms built with capillary tubes can faithfully reveal the performance of reconstruction in the in vivo human study is rejected. Diffusion phantoms built with capillary tubes tend to favor more complicated reconstruction models over a simple tensor model or model-free approaches, while in the *in vivo* human brain model-free approaches tended to come out on top. The current findings highlight the need

for more biologically realistic diffusion phantoms or simulation to adequately predict the performance of different methods of analysis in neural tissue and to accurately evaluate the relative strengths and weaknesses of various diffusion imaging methods.

Conflict of Interest Statement

The authors have no conflicts of interest to declare.

Author Contributions

SL and JB conducted the data analysis and made substantial contributions to the interpretation of the findings, in addition to drafting and revising the manuscript and providing final approval of the version to be published. TV and FY each made substantial contributions to the conception and design, acquisition, analysis and interpretation of the data, as well as revising the manuscript critically for important intellectual content and providing final approval of the version to be published. All authors agree to be accountable for all aspects of the work.

Funding

Funding was provided in part by the Army Research Laboratory under Cooperative Agreement Number W911NF-10-2-0022, NSF BIGDATA 1247658, NSF GRFP DGE-1247842 and the Multimodal Neuroimaging Training Program (MNTP) at the University of Pittsburgh, in collaboration with Carnegie Mellon University, and with funding from the National Institutes of Health (NIH) (grants R90DA023420 and T90DA022761). The views and conclusions contained in this document are those of the authors and should not be interpreted as representing the official policies, either expressed or implied, of the Army Research Laboratory or the U.S. Government. The U.S. Government is authorized to

reproduce and distribute reprints for Government purposes notwithstanding any copyright notation herein.

Acknowledgements

We would like to thank Drs. Peter Gianaros and William Eddy for their advice and support. The views and conclusions contained in this document are those of the authors and should not be interpreted as representing the official policies, either expressed or implied, of the Army Research Laboratory or the U.S. Government.

References for Chapter 7

Aboitiz, F., Scheibel, A. B., Fisher, R. S., & Zaidel, E. (1992). Fiber composition of the human corpus callosum. *Brain Res, 598*(1-2), 143-153.

Amlien, I. K., & Fjell, A. M. (2014). Diffusion tensor imaging of white matter degeneration in Alzheimer's disease and mild cognitive impairment. *Neuroscience*. doi:10.1016/j.neuroscience.2014.02.017

Basser, P. J., Mattiello, J., & LeBihan, D. (1994). Estimation of the effective self-diffusion tensor from the NMR spin echo. *J Magn Reson B, 103*(3), 247-254.

Behrens, T. E., Berg, H. J., Jbabdi, S., Rushworth, M. F., & Woolrich, M. W. (2007). Probabilistic diffusion tractography with multiple fibre orientations: What can we gain? *Neuroimage, 34*(1), 144-155. doi:10.1016/j.neuroimage.2006.09.018

Behrens, T. E., Woolrich, M. W., Jenkinson, M., Johansen-Berg, H., Nunes, R. G., Clare, S., . . . Smith, S. M. (2003). Characterization and propagation of uncertainty in diffusion-weighted MR imaging. *Magn Reson Med, 50*(5), 1077-1088. doi:10.1002/mrm.10609

Cote, M. A., Bore, A., Girard, G., Houde, J. C., & Descoteaux, M. (2012). Tractometer: online evaluation system for tractography. *Med Image Comput Comput Assist Interv, 15*(Pt 1), 699-706.

Cote, M. A., Girard, G., Bore, A., Garyfallidis, E., Houde, J. C., & Descoteaux, M. (2013). Tractometer: towards validation of tractography pipelines. *Med Image Anal, 17*(7), 844-857. doi:10.1016/j.media.2013.03.009

Daducci, A., Canales-Rodriguez, E. J., Descoteaux, M., Garyfallidis, E., Gur, Y., Lin, Y. C., . . . Thiran, J. P. (2014). Quantitative comparison of reconstruction methods for intra-voxel fiber recovery from diffusion MRI. *IEEE Trans Med Imaging, 33*(2), 384-399. doi:10.1109/TMI.2013.2285500

Esteban, O., Caruyer, E., Daducci, A., Bach-Cuadra, M., Ledesma-Carbayo, M. J., & Santos, A. (2016). Diffantom: Whole-Brain Diffusion MRI Phantoms Derived from Real Datasets of the Human Connectome Project. *Front Neuroinform, 10*, 4. doi:10.3389/fninf.2016.00004

Farquharson, S., Tournier, J. D., Calamante, F., Fabinyi, G., Schneider-Kolsky, M., Jackson, G. D., & Connelly, A. (2013). White matter fiber tractography: why we need to move beyond DTI. *J Neurosurg, 118*(6), 1367-1377. doi:10.3171/2013.2.JNS121294

Filippi, M., & Rocca, M. A. (2011). MR imaging of multiple sclerosis. *Radiology, 259*(3), 659-681. doi:10.1148/radiol.11101362

Fillard, P., Descoteaux, M., Goh, A., Gouttard, S., Jeurissen, B., Malcolm, J., . . . Poupon, C. (2011). Quantitative evaluation of 10 tractography algorithms on a realistic diffusion MR phantom. *Neuroimage, 56*(1), 220-234. doi:10.1016/j.neuroimage.2011.01.032

Hagmann, P., Jonasson, L., Maeder, P., Thiran, J. P., Wedeen, V. J., & Meuli, R. (2006). Understanding diffusion MR imaging techniques: from scalar diffusion-weighted imaging to diffusion tensor imaging and beyond. *Radiographics, 26 Suppl 1*, S205-223. doi:10.1148/rg.26si065510

Hubbard, P. L., Zhou, F. L., Eichhorn, S. J., & Parker, G. J. (2015). Biomimetic phantom for the validation of diffusion magnetic resonance imaging. *Magn Reson Med, 73*(1), 299-305. doi:10.1002/mrm.25107

Jensen, J. H., Helpern, J. A., Ramani, A., Lu, H., & Kaczynski, K. (2005). Diffusional kurtosis imaging: the quantification of non-gaussian water diffusion by means of magnetic resonance imaging. *Magn Reson Med, 53*(6), 1432-1440. doi:10.1002/mrm.20508

Jones, D. K. (2008). Studying connections in the living human brain with diffusion MRI. *Cortex, 44*(8), 936-952. doi:10.1016/j.cortex.2008.05.002

Jones, D. K., Knosche, T. R., & Turner, R. (2013). White matter integrity, fiber count, and other fallacies: the do's and don'ts of diffusion MRI. *Neuroimage, 73*, 239-254. doi:10.1016/j.neuroimage.2012.06.081

Otsu, N. (1979). A threshold selection method from gray-level histograms. *IEEE Trans Sys Man Cyber, 9*(1), 62-66. doi:10.1109/TSMC.1979.4310076

Poupon, C., Rieul, B., Kezele, I., Perrin, M., Poupon, F., & Mangin, J. F. (2008). New diffusion phantoms dedicated to the study and validation of high-angular-resolution diffusion imaging (HARDI) models. *Magn Reson Med, 60*(6), 1276-1283. doi:10.1002/mrm.21789

Reveley, C., Seth, A. K., Pierpaoli, C., Silva, A. C., Yu, D., Saunders, R. C., . . . Ye, F. Q. (2015). Superficial white matter fiber systems impede detection of long-range cortical connections in diffusion MR tractography. *Proc Natl Acad Sci U S A, 112*(21), E2820-2828. doi:10.1073/pnas.1418198112

Schmahmann, J. D., & Pandya, D. N. (2006). *Fiber Pathways of the Brain*. New York: Oxford University Press.

Seizeur, R., Wiest-Daessle, N., Prima, S., Maumet, C., Ferre, J. C., & Morandi, X. (2012). Corticospinal tractography with morphological, functional and diffusion tensor MRI: a comparative study of four deterministic algorithms used in clinical routine. *Surg Radiol Anat*. doi:10.1007/s00276-012-0951-x

Sotak, C. H. (2002). The role of diffusion tensor imaging in the evaluation of ischemic brain injury - a review. *NMR Biomed, 15*(7-8), 561-569. doi:10.1002/nbm.786

Sotiropoulos, S. N., Jbabdi, S., Andersson, J. L., Woolrich, M. W., Ugurbil, K., & Behrens, T. E. (2013). RubiX: combining spatial resolutions for Bayesian inference of crossing fibers in diffusion MRI. *IEEE Trans Med Imaging, 32*(6), 969-982. doi:10.1109/TMI.2012.2231873

Thomas, C., Ye, F. Q., Irfanoglu, M. O., Modi, P., Saleem, K. S., Leopold, D. A., & Pierpaoli, C. (2014). Anatomical accuracy of brain connections derived from diffusion MRI tractography is inherently limited. *Proc Natl Acad Sci U S A, 111*(46), 16574-16579. doi:10.1073/pnas.1405672111

1405672111 [pii]

Tournier, J. D., Yeh, C. H., Calamante, F., Cho, K. H., Connelly, A., & Lin, C. P. (2008). Resolving crossing fibres using constrained spherical deconvolution: validation using diffusion-weighted imaging phantom data. *Neuroimage, 42*(2), 617-625. doi:10.1016/j.neuroimage.2008.05.002

Tuch, D. S. (2004). Q-ball imaging. *Magn Reson Med, 52*(6), 1358-1372. doi:10.1002/mrm.20279

Tuch, D. S., Wisco, J. J., Khachaturian, M. H., Ekstrom, L. B., Kotter, R., & Vanduffel, W. (2005). Q-ball imaging of macaque white matter architecture. *Philos Trans R Soc Lond B Biol Sci, 360*(1457), 869-879. doi:10.1098/rstb.2005.1651

Tzourio-Mazoyer, N., Landeau, B., Papathanassiou, D., Crivello, F., Etard, O., Delcroix, N., . . . Joliot, M. (2002). Automated anatomical labeling of activations in SPM using a macroscopic anatomical parcellation of the MNI MRI single-subject brain. *Neuroimage, 15*(1), 273-289. doi:10.1006/nimg.2001.0978

Walhovd, K. B., Johansen-Berg, H., & Karadottir, R. T. (2014). Unraveling the secrets of white matter--bridging the gap between cellular, animal and human imaging studies. *Neuroscience, 276*, 2-13. doi:10.1016/j.neuroscience.2014.06.058

Wedeen, V. J., Hagmann, P., Tseng, W. Y., Reese, T. G., & Weisskoff, R. M. (2005). Mapping complex tissue architecture with diffusion spectrum magnetic resonance imaging. *Magn Reson Med, 54*(6), 1377-1386. doi:10.1002/mrm.20642

Wedeen, V. J., Rosene, D. L., Wang, R., Dai, G., Mortazavi, F., Hagmann, P., . . . Tseng, W. Y. (2012). The geometric structure of the brain fiber pathways. *Science, 335*(6076), 1628-1634. doi:335/6076/1628 [pii]

10.1126/science.1215280

White, T., Nelson, M., & Lim, K. O. (2008). Diffusion tensor imaging in psychiatric disorders. *Top Magn Reson Imaging, 19*(2), 97-109. doi:10.1097/RMR.0b013e3181809f1e

Yeh, F. C., Verstynen, T. D., Wang, Y., Fernandez-Miranda, J. C., & Tseng, W. Y. (2013). Deterministic diffusion fiber tracking improved by quantitative anisotropy. *PLoS One, 8*(11), e80713. doi:10.1371/journal.pone.0080713

Yeh, F. C., Wedeen, V. J., & Tseng, W. Y. (2010). Generalized q-sampling imaging. *IEEE Trans Med Imaging, 29*(9), 1626-1635. doi:10.1109/TMI.2010.2045126

Yeh, F. C., Wedeen, V. J., & Tseng, W. Y. (2011). Estimation of fiber orientation and spin density distribution by diffusion deconvolution. *Neuroimage, 55*(3), 1054-1062. doi:10.1016/j.neuroimage.2010.11.087

Figure Captions

Figure 7.1. (A) (Left) Illustrates ground truth fiber orientations within each segment of the Fibercup phantom. Each color represents a distinct fiber pathway. (B) To test the accuracy of each reconstruction scheme for estimating fiber length, we placed a seed in one pathway and defined regions of interest immediately following the fiber crossings (blue and green) to isolate only those streamlines that traverse the crossings. For resulting streamline length estimates refer to Figure 4. ROIs: regions of interest.

Figure 7.2. (A) The dotted red lines define two pathways of interest in the Fibercup phantom, representative of the corpus callosum architecture. The first pathway (Pathway 1) is indicative of cortical 'U' fibers and the second pathway (Pathway 2) represents traversing callosal fibers. (B) Regions of interest were defined at the end of each pathway (shown in yellow, pink, blue, and green) and single seed region (red) was placed at the center of pathways 1 and 2. The accuracy of each reconstruction method was assessed based on the number of streamlines passing through the seed region and both endpoints of the respective pathways (refer to Figure 5). ROIs: regions of interest.

Figure 7.3. (A) Depicted in a coronal plane, the automated anatomic labeling AAL atlas (Tzourio-Mazoyer et al, 2002) was used to define three topographical regions: the left and right superior frontal gyrus (Green), middle frontal gyrus (Blue), and inferior frontal gyrus (IFG) operculum, IFG triangularis, and the IFG orbitalis, which were merged to create one ROI for the inferior frontal gyrus (red). (B) A single subject was used to illustrate the topography of corpus callosum fibers connecting the left and right superior, medial, and

inferior frontal gyri, respectively. Single-subject data were reconstructed using diffusion spectrum imaging and deterministic (Euler) fiber tracking was conducted in native space. 100,000 tracts were generated connecting the right and left hemispheres of the superior, medial, and inferior frontal gyri, respectively, using random whole brain seeding at subvoxel positions and in random orientations. Tracking progression continued with a step size of 0.5mm, and each step was weighted by 40% of the previous direction to smooth the tracks. Otsu's method was used to set the anisotropy (QA) threshold, and tracking was terminated if the anisotropy of the next step fell below the assigned threshold, or exceeded an angular threshold of 65°. Streamline lengths were constrained to 1-160mm. (C) In order to clearly illustrate the topography of each group of corpus callosum fibers, fibers connecting left and right superior, medial, and inferior frontal gyri are visualized separately.

Figure 7.4. (A) Example fiber tracking and the mean number of streamlines are represented for each reconstruction method in the Fibercup phantom. Fiber tracking with the DTI reconstruction was unable to detect any streamlines that navigated both crossings. (B) Distribution of streamline length estimates for each reconstruction method. GQI reconstructions produced longer and less variable streamline estimates compared to the ball-and-sticks model (BSM 0.01, BSM 0.03). (C) To quantitatively evaluate length estimates, the streamline lengths were multiplied by the probability. Each reconstruction method yields significantly different modal streamline length estimates relative to each other reconstruction method. DTI: diffusion tensor imaging, GQI: generalized q-sampling imaging, decon: deconvolution, M: mean, BSM: ball-and-sticks model.

Figure 7.5. (A) The top row illustrates the reconstruction tractography results for pathway 1, characteristic of cortical 'U' fibers. The second row shows the tractography results across reconstruction methods in pathway 2 demonstrating successful traversal of the 'U' fiber geometry. (B) Quantitative analysis based on the number of correct 'U' streamlines demonstrated significant differences between all reconstruction methods with DTI providing the greatest number of correct streamlines. (C) Quantitative analysis based on the number of correct straight streamlines demonstrated that the ball-and-sticks reconstruction (0.01) generated the greatest number of correct streamlines while DTI and GQI were unable to produce any streamlines. DTI: diffusion tensor imaging, GQI: generalized q-sampling imaging, decon: deconvolution, M: mean, BSM: ball-and-sticks model.

Figure 7.6. The DTI reconstruction produced the greatest number of streamlines < 10 mm that is indicative of noise. The model-free (GQI, GQI Deconvolution, DSI, and DSI Deconvolution) and ball-and-sticks (BSM 0.01, BSM 0.03) reconstructions yielded a greater number of streamlines with increased length (>10 mm) suggestive of physiologically relevant dimensions. GQI: generalized q-sampling imaging, DSI: diffusion spectrum imaging, BSM: ball-and-sticks model, DTI: diffusion tensor imaging.

Figure 7.7. To quantitatively evaluate length estimates the streamline lengths were multiplied by the probability. Results shown indicate significant differences between model-free (GQI, GQI Decon., DSI, and DSI Decon.) and ball-and-sticks (BSM 0.01, BSM

0.03) reconstructions. Additionally, single tensor (DTI) reconstruction showed a significantly lower modal streamline length compared to all other reconstruction methods tested. DTI: diffusion tensor imaging, BSM: ball-and-sticks model, DSI: diffusion spectrum imaging, GQI: generalized q-sampling imaging.

Figure 7.8. (A) Tractography results of two human participants demonstrate the variations across reconstruction approach in the corpus callosum. (B). DTI and ball-and-sticks (0.01 and 0.03) reconstruction methods resolved a smaller percentage of MFG streamlines compared to the GQI and DSI approaches. There was no significant difference between DSI or GQI approaches in the MFG. There were no significant differences found between reconstruction methods for the SFG or IFG. DTI: diffusion tensor imaging, DSI: diffusion spectrum imaging, Decon: deconvolution, GQI: generalized q-sampling imaging, BSM: ball-and-sticks model, SFG: superior frontal gyrus, MFG: medial frontal gyrus, IFG: inferior frontal gyrus.

Figure 7.1. Phantom Fiber Length Analysis.

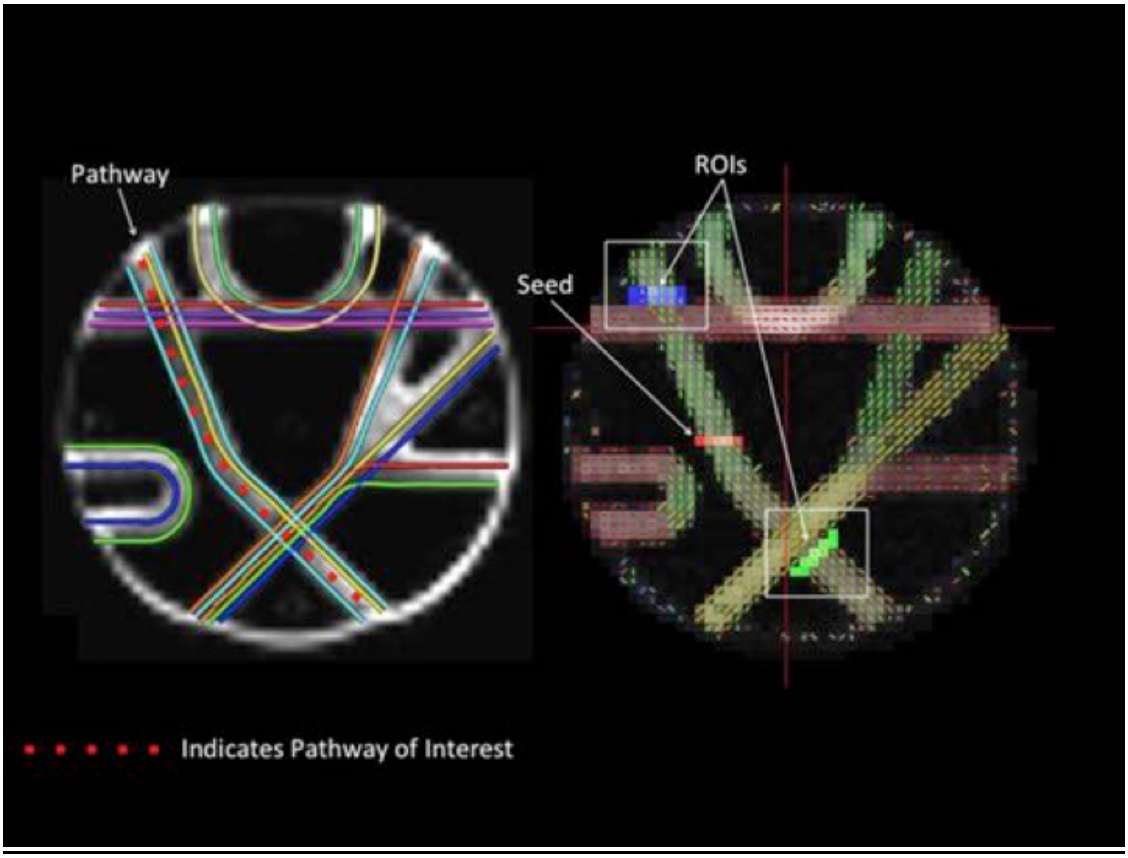

Figure 7.2. Phantom Fiber Crossing Analysis.

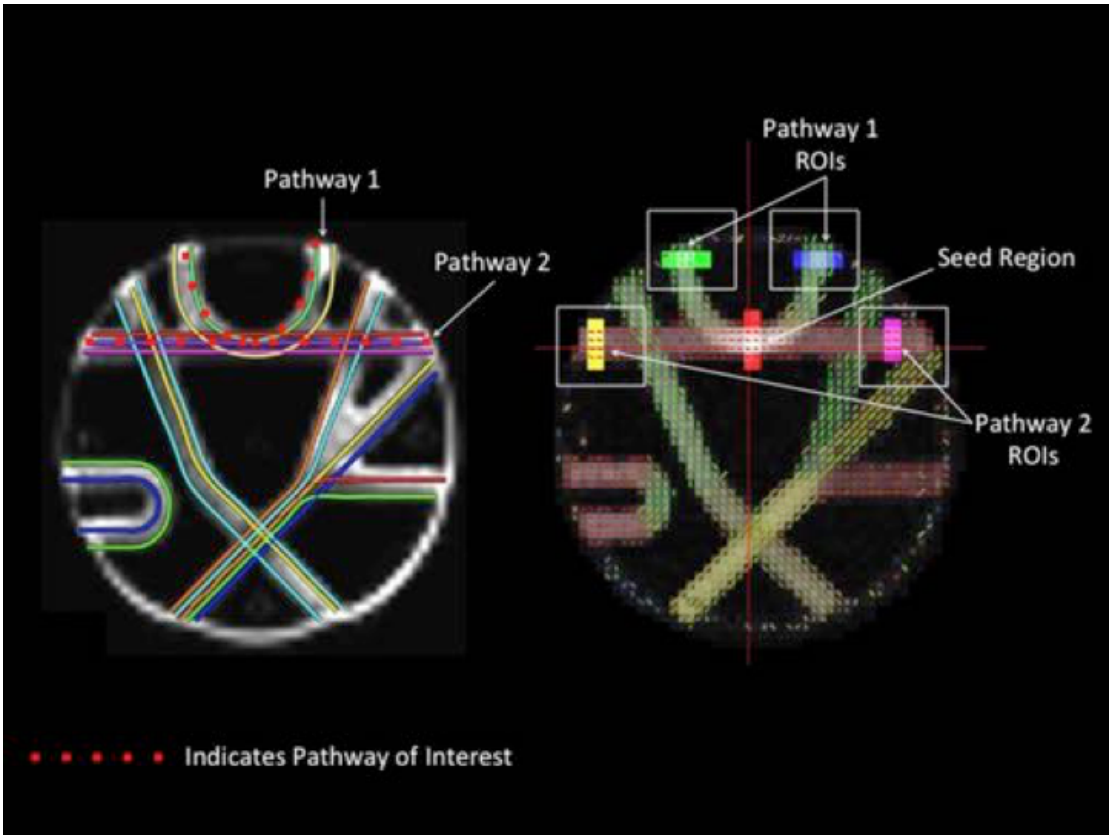

Figure 7.3. Human Fiber Crossing Analysis.

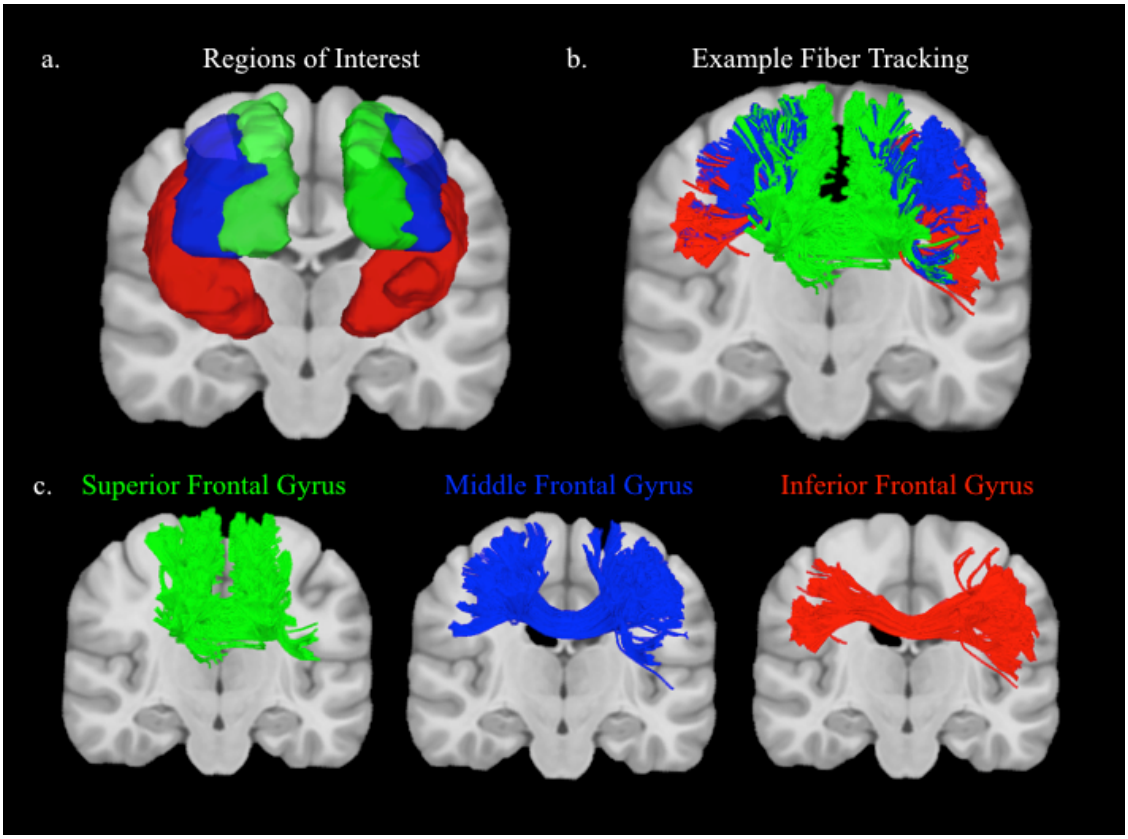

Figure 7.4. Phantom Fiber Length Results.

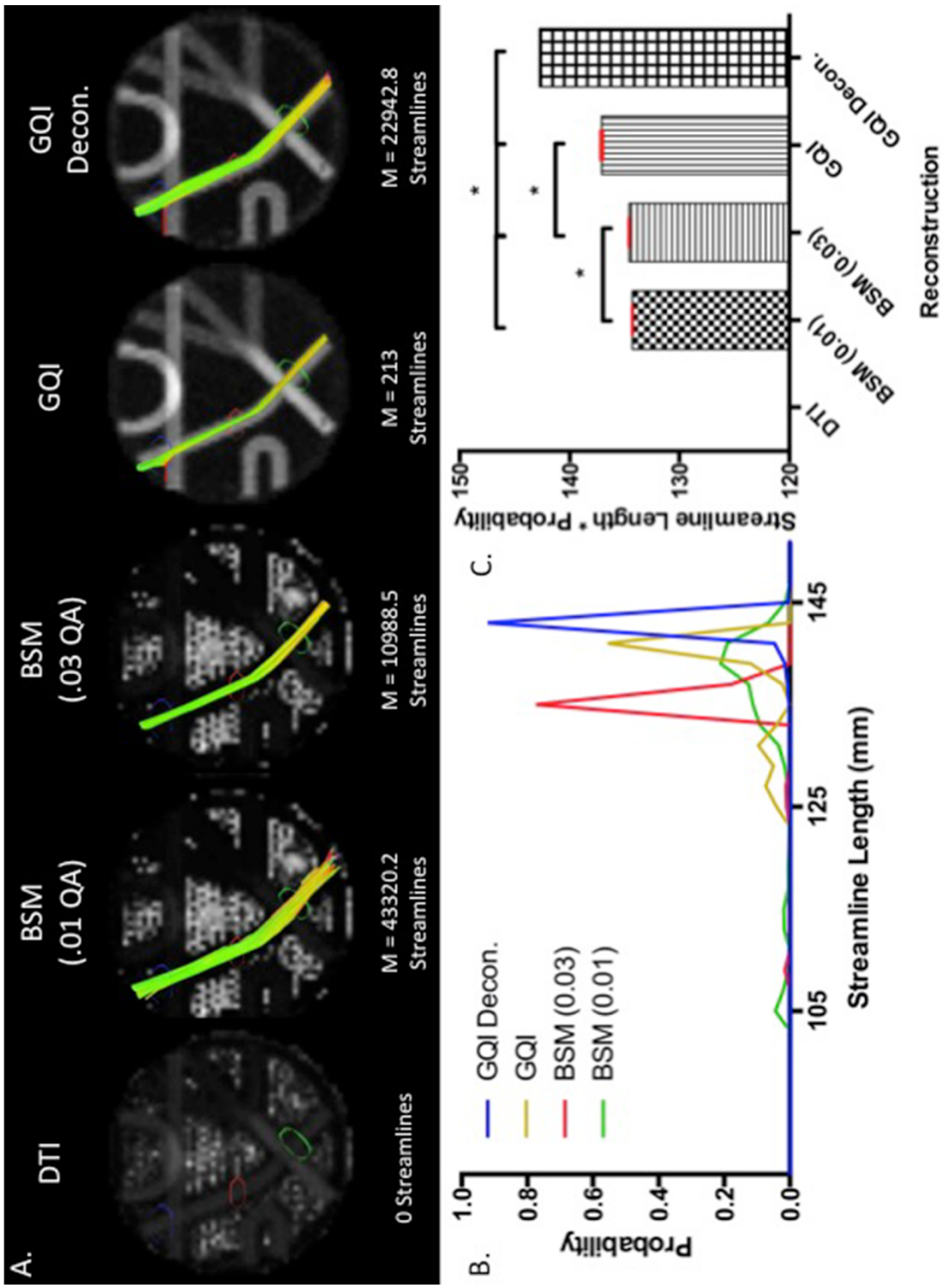

Figure 7.5. Phantom Fiber Crossing Results.

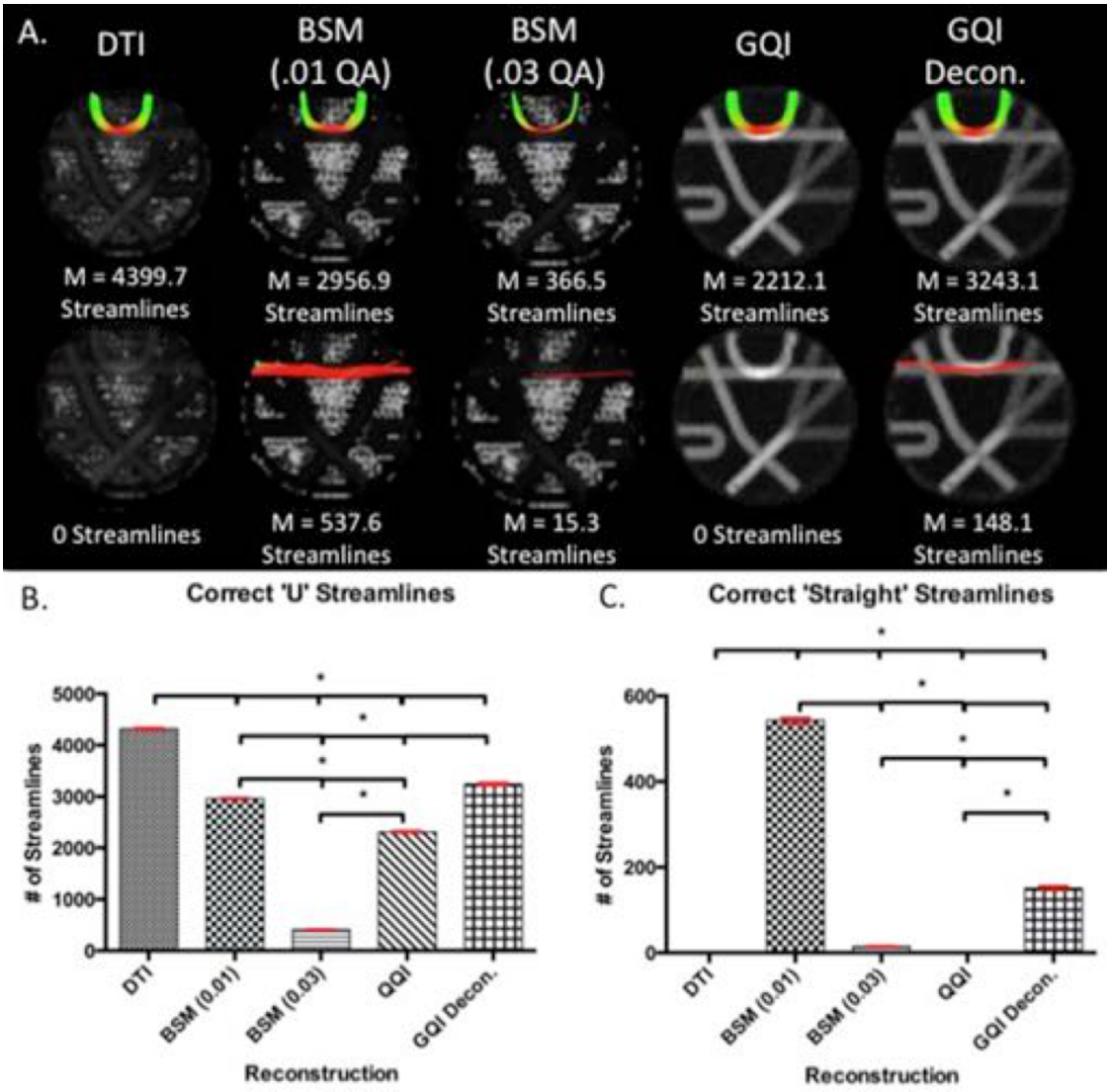

Figure 7.6. Distribution of Human Streamline Length Estimates.

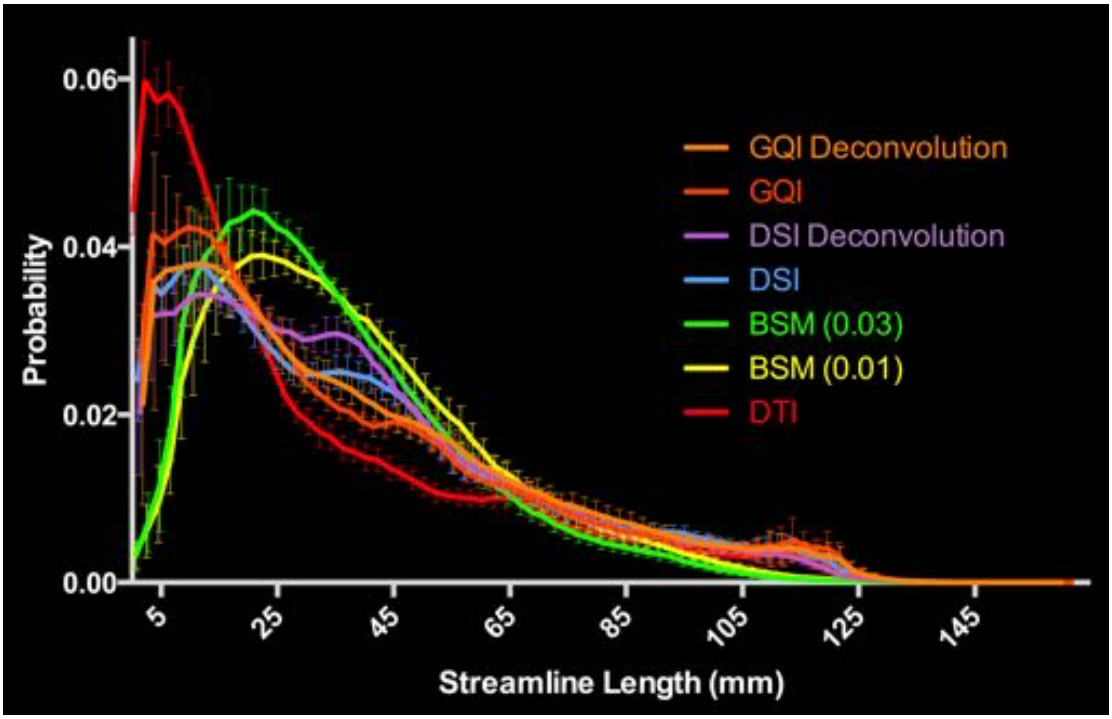

Figure 7.7. Human Fiber Length Results.

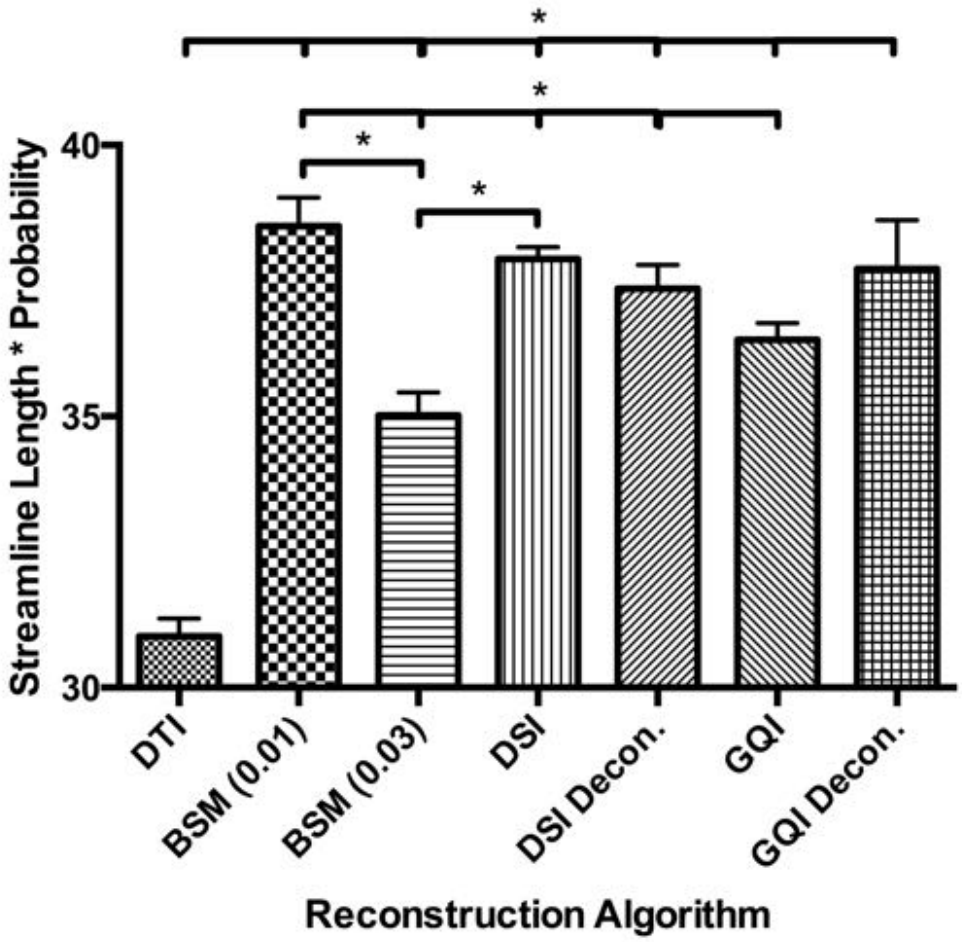

Figure 7.8. Human Fiber Crossing Results.

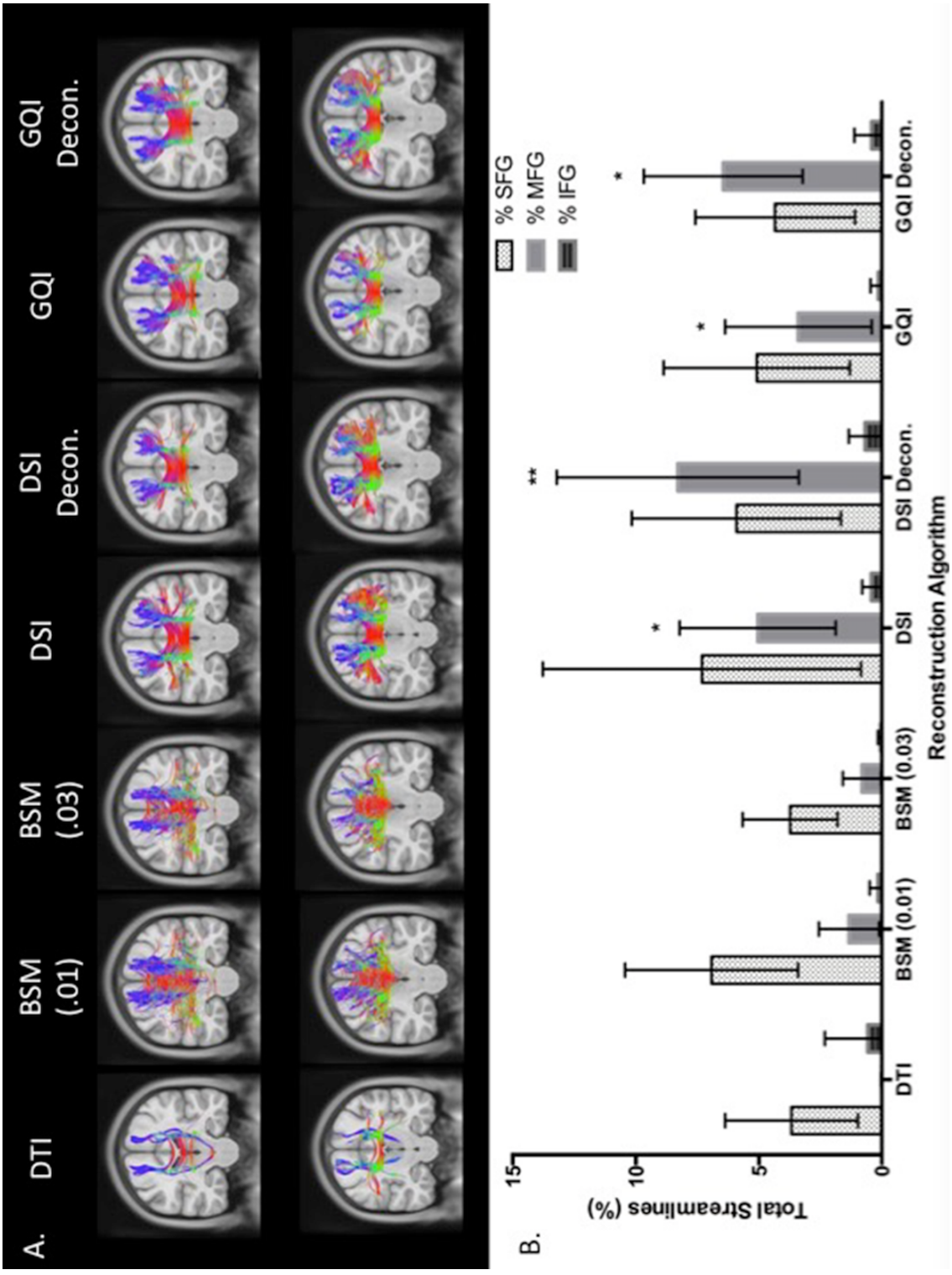

COMPLETE LIST OF REFERENCES

Aboitiz, F., Scheibel, A. B., Fisher, R. S., & Zaidel, E. (1992). Fiber composition of the human corpus callosum. *Brain Res, 598*(1-2), 143-153.

Alexander, A. L., Lee, J. E., Lazar, M., & Field, A. S. (2007). Diffusion tensor imaging of the brain. *Neurotherapeutics, 4*(3), 316-329. doi:10.1016/j.nurt.2007.05.011

Alini, M., Eisenstein, S. M., Ito, K., Little, C., Kettler, A. A., Masuda, K., . . . Wilke, H. J. (2008). Are animal models useful for studying human disc disorders/degeneration? *Eur Spine J, 17*(1), 2-19. doi:10.1007/s00586-007-0414-y

Amlien, I. K., & Fjell, A. M. (2014). Diffusion tensor imaging of white matter degeneration in Alzheimer's disease and mild cognitive impairment. *Neuroscience*. doi:10.1016/j.neuroscience.2014.02.017

Anderson, K. O., Dowds, B. N., Pelletz, R. E., Edwards, W. T., & Peeters-Asdourian, C. (1995). Development and initial validation of a scale to measure self-efficacy beliefs in patients with chronic pain. *Pain, 63*(1), 77-84.

Andre, J. B., & Bammer, R. (2010). Advanced diffusion-weighted magnetic resonance imaging techniques of the human spinal cord. *Top Magn Reson Imaging, 21*(6), 367-378. doi:10.1097/RMR.0b013e31823e65a1

Andrew, D., & Greenspan, J. D. (1999). Mechanical and heat sensitization of cutaneous nociceptors after peripheral inflammation in the rat. *J Neurophysiol, 82*(5), 2649-2656.

Andrews, R. J., Knight, R. T., & Kirby, R. P. (1990). Evoked potential mapping of auditory and somatosensory cortices in the miniature swine. *Neurosci Lett, 114*(1), 27-31.

Aojula, A., Botfield, H., McAllister, J. P., 2nd, Gonzalez, A. M., Abdullah, O., Logan, A., & Sinclair, A. (2016). Diffusion tensor imaging with direct cytopathological validation: characterisation of decorin treatment in experimental juvenile communicating hydrocephalus. *Fluids Barriers CNS, 13*(1), 9. doi:10.1186/s12987-016-0033-2

Apkarian, A. V., Bushnell, M. C., Treede, R. D., & Zubieta, J. K. (2005). Human brain mechanisms of pain perception and regulation in health and disease. *Eur J Pain, 9*(4), 463-484. doi:10.1016/j.ejpain.2004.11.001

Apkarian, A. V., Sosa, Y., Sonty, S., Levy, R. M., Harden, R. N., Parrish, T. B., & Gitelman, D. R. (2004). Chronic back pain is associated with decreased prefrontal and thalamic gray matter density. *J Neurosci, 24*(46), 10410-10415. doi:10.1523/JNEUROSCI.2541-04.2004

Arout, C. A., Edens, E., Petrakis, I. L., & Sofuoglu, M. (2015). Targeting Opioid-Induced Hyperalgesia in Clinical Treatment: Neurobiological Considerations. *CNS Drugs, 29*(6), 465-486. doi:10.1007/s40263-015-0255-x

Ashburner, J. (2007). A fast diffeomorphic image registration algorithm. *Neuroimage, 38*(1), 95-113. doi:10.1016/j.neuroimage.2007.07.007

Ayache, S. S., Palm, U., Chalah, M. A., Al-Ani, T., Brignol, A., Abdellaoui, M., . . . Lefaucheur, J. P. (2016). Prefrontal tDCS Decreases Pain in Patients with Multiple Sclerosis. *Front Neurosci, 10*, 147. doi:10.3389/fnins.2016.00147

Bagarinao, E., Johnson, K. A., Martucci, K. T., Ichesco, E., Farmer, M. A., Labus, J., . . . Mackey, S. (2014). Preliminary structural MRI based brain classification of chronic pelvic pain: A MAPP network study. *Pain, 155*(12), 2502-2509. doi:10.1016/j.pain.2014.09.002

Baliki, M. N., Baria, A. T., & Apkarian, A. V. (2011). The cortical rhythms of chronic back pain. *J Neurosci, 31*(39), 13981-13990. doi:10.1523/JNEUROSCI.1984-11.2011

Baliki, M. N., Geha, P. Y., Jabakhanji, R., Harden, N., Schnitzer, T. J., & Apkarian, A. V. (2008). A preliminary fMRI study of analgesic treatment in chronic back pain and knee osteoarthritis. *Mol Pain, 4*, 47. doi:10.1186/1744-8069-4-47

Baliki, M. N., Petre, B., Torbey, S., Herrmann, K. M., Huang, L., Schnitzer, T. J., . . . Apkarian, A. V. (2012). Corticostriatal functional connectivity predicts transition to chronic back pain. *Nat Neurosci, 15*(8), 1117-1119. doi:10.1038/nn.3153

Baliki, M. N., Schnitzer, T. J., Bauer, W. R., & Apkarian, A. V. (2011). Brain morphological signatures for chronic pain. *PLoS One, 6*(10), e26010. doi:10.1371/journal.pone.0026010

Baraban, M., Mensch, S., & Lyons, D. A. (2016). Adaptive myelination from fish to man. *Brain Res, 1641*(Pt A), 149-161. doi:10.1016/j.brainres.2015.10.026

Basser, P. J., Mattiello, J., & LeBihan, D. (1994). Estimation of the effective self-diffusion tensor from the NMR spin echo. *J Magn Reson B, 103*(3), 247-254.

Bast, T., & Feldon, J. (2003). Hippocampal modulation of sensorimotor processes. *Prog Neurobiol, 70*(4), 319-345.

Becerra, L., Breiter, H. C., Wise, R., Gonzalez, R. G., & Borsook, D. (2001). Reward circuitry activation by noxious thermal stimuli. *Neuron, 32*(5), 927-946.

Beck, A. T., Ward, C. H., Mendelson, M., Mock, J., & Erbaugh, J. (1961). An inventory for measuring depression. *Arch Gen Psychiatry, 4*, 561-571.

Beggs, S., Currie, G., Salter, M. W., Fitzgerald, M., & Walker, S. M. (2012). Priming of adult pain responses by neonatal pain experience: maintenance by central neuroimmune activity. *Brain, 135*(Pt 2), 404-417. doi:10.1093/brain/awr288

Behrens, T. E., Berg, H. J., Jbabdi, S., Rushworth, M. F., & Woolrich, M. W. (2007). Probabilistic diffusion tractography with multiple fibre orientations: What can we gain? *Neuroimage, 34*(1), 144-155. doi:10.1016/j.neuroimage.2006.09.018

Behrens, T. E., Woolrich, M. W., Jenkinson, M., Johansen-Berg, H., Nunes, R. G., Clare, S., . . . Smith, S. M. (2003). Characterization and propagation of uncertainty in diffusion-weighted MR imaging. *Magn Reson Med, 50*(5), 1077-1088. doi:10.1002/mrm.10609

Beitz, A. J., & Buggy, J. (1981). Brain functional activity during PAG stimulation-produced analgesia: a 2-DG study. *Brain Res Bull, 6*(6), 487-494.

Benetazzo, L., Bizzego, A., De Caro, R., Frigo, G., Guidolin, D., & Stecco, C. (2011). 3D reconstruction of the crural and thoracolumbar fasciae. *Surg Radiol Anat, 33*(10), 855-862. doi:10.1007/s00276-010-0757-7

Billeci, L., Calderoni, S., Tosetti, M., Catani, M., & Muratori, F. (2012). White matter connectivity in children with autism spectrum disorders: a tract-based spatial statistics study. *BMC Neurol, 12*, 148. doi:10.1186/1471-2377-12-148

Bishop, J. H., Fox, J. R., Maple, R., Loretan, C., Badger, G. J., Henry, S. M., . . . Langevin, H. M. (2016). Ultrasound Evaluation of the Combined Effects of

Thoracolumbar Fascia Injury and Movement Restriction in a Porcine Model. *PLoS One, 11*(1), e0147393. doi:10.1371/journal.pone.0147393

Boden, S. D., McCowin, P. R., Davis, D. O., Dina, T. S., Mark, A. S., & Wiesel, S. (1990). Abnormal magnetic-resonance scans of the cervical spine in asymptomatic subjects. A prospective investigation. *J Bone Joint Surg Am, 72*(8), 1178-1184.

Booth, J., Moseley, G. L., Schiltenwolf, M., Cashin, A., Davies, M., & Hubscher, M. (2017). Exercise for chronic musculoskeletal pain: A biopsychosocial approach. *Musculoskeletal Care*. doi:10.1002/msc.1191

Borsook, D., Edwards, R., Elman, I., Becerra, L., & Levine, J. (2013). Pain and analgesia: the value of salience circuits. *Prog Neurobiol, 104*, 93-105. doi:10.1016/j.pneurobio.2013.02.003

Borsook, D., Moulton, E. A., Schmidt, K. F., & Becerra, L. R. (2007). Neuroimaging revolutionizes therapeutic approaches to chronic pain. *Mol Pain, 3*, 25. doi:10.1186/1744-8069-3-25

Borsook, D., Upadhyay, J., Chudler, E. H., & Becerra, L. (2010). A key role of the basal ganglia in pain and analgesia--insights gained through human functional imaging. *Mol Pain, 6*, 27. doi:10.1186/1744-8069-6-27

Brighina, F., De Tommaso, M., Giglia, F., Scalia, S., Cosentino, G., Puma, A., . . . Fierro, B. (2011). Modulation of pain perception by transcranial magnetic stimulation of left prefrontal cortex. *J Headache Pain, 12*(2), 185-191. doi:10.1007/s10194-011-0322-8

Brinjikji, W., Luetmer, P. H., Comstock, B., Bresnahan, B. W., Chen, L. E., Deyo, R. A., . . . Jarvik, J. G. (2015). Systematic literature review of imaging features of spinal degeneration in asymptomatic populations. *AJNR Am J Neuroradiol, 36*(4), 811-816. doi:10.3174/ajnr.A4173

Buckalew, N., Haut, M. W., Morrow, L., & Weiner, D. (2008). Chronic pain is associated with brain volume loss in older adults: preliminary evidence. *Pain Med, 9*(2), 240-248. doi:10.1111/j.1526-4637.2008.00412.x

Budde, M. D., Janes, L., Gold, E., Turtzo, L. C., & Frank, J. A. (2011). The contribution of gliosis to diffusion tensor anisotropy and tractography following traumatic brain injury: validation in the rat using Fourier analysis of stained tissue sections. *Brain, 134*(Pt 8), 2248-2260. doi:10.1093/brain/awr161

Burgmer, M., Gaubitz, M., Konrad, C., Wrenger, M., Hilgart, S., Heuft, G., & Pfleiderer, B. (2009). Decreased gray matter volumes in the cingulo-frontal cortex and the amygdala in patients with fibromyalgia. *Psychosom Med, 71*(5), 566-573. doi:10.1097/PSY.0b013e3181a32da0

Bushnell, M. C., Ceko, M., & Low, L. A. (2013). Cognitive and emotional control of pain and its disruption in chronic pain. *Nat Rev Neurosci, 14*(7), 502-511. doi:10.1038/nrn3516

Butler, S. (2017). Important new insight in pain and pain treatment induced changes in functional connectivity between the Pain Matrix and the Salience, Central Executive, and Sensorimotor networks. *Scandinavian Journal of Pain, 16*, 64-65.

Cady, E. B. (1995). Quantitative combined phosphorus and proton PRESS of the brains of newborn human infants. *Magn Reson Med, 33*(4), 557-563.

Caeyenberghs, K., Pijnenburg, M., Goossens, N., Janssens, L., & Brumagne, S. (2017). Associations between Measures of Structural Morphometry and Sensorimotor Performance in Individuals with Nonspecific Low Back Pain. *AJNR Am J Neuroradiol, 38*(1), 183-191. doi:10.3174/ajnr.A5020

Camara, E., Rodriguez-Fornells, A., & Munte, T. F. (2010). Microstructural brain differences predict functional hemodynamic responses in a reward processing task. *J Neurosci, 30*(34), 11398-11402. doi:10.1523/JNEUROSCI.0111-10.2010

Castel, D., Sabbag, I., Brenner, O., & Meilin, S. (2016). Peripheral Neuritis Trauma in Pigs: A Neuropathic Pain Model. *J Pain, 17*(1), 36-49. doi:10.1016/j.jpain.2015.09.011

Castel, D., Willentz, E., Doron, O., Brenner, O., & Meilin, S. (2014). Characterization of a porcine model of post-operative pain. *Eur J Pain, 18*(4), 496-505. doi:10.1002/j.1532-2149.2013.00399.x

Catani, M., & Thiebaut de Schotten, M. (2008). A diffusion tensor imaging tractography atlas for virtual in vivo dissections. *Cortex, 44*(8), 1105-1132. doi:10.1016/j.cortex.2008.05.004

Cauda, F., Palermo, S., Costa, T., Torta, R., Duca, S., Vercelli, U., . . . Torta, D. M. (2014). Gray matter alterations in chronic pain: A network-oriented meta-analytic approach. *Neuroimage Clin, 4*, 676-686. doi:10.1016/j.nicl.2014.04.007

Ceko, M., Shir, Y., Ouellet, J. A., Ware, M. A., Stone, L. S., & Seminowicz, D. A. (2015). Partial recovery of abnormal insula and dorsolateral prefrontal connectivity to cognitive networks in chronic low back pain after treatment. *Hum Brain Mapp, 36*(6), 2075-2092. doi:10.1002/hbm.22757

Chang, K. J., Redmond, S. A., & Chan, J. R. (2016). Remodeling myelination: implications for mechanisms of neural plasticity. *Nat Neurosci, 19*(2), 190-197. doi:10.1038/nn.4200

Charlton, R. A., Barrick, T. R., McIntyre, D. J., Shen, Y., O'Sullivan, M., Howe, F. A., . . . Markus, H. S. (2006). White matter damage on diffusion tensor imaging correlates with age-related cognitive decline. *Neurology, 66*(2), 217-222. doi:10.1212/01.wnl.0000194256.15247.83

Chen, F. L., Dong, Y. L., Zhang, Z. J., Cao, D. L., Xu, J., Hui, J., . . . Gao, Y. J. (2012). Activation of astrocytes in the anterior cingulate cortex contributes to the affective component of pain in an inflammatory pain model. *Brain Res Bull, 87*(1), 60-66. doi:10.1016/j.brainresbull.2011.09.022

Chen, G., Park, C. K., Xie, R. G., Berta, T., Nedergaard, M., & Ji, R. R. (2014). Connexin-43 induces chemokine release from spinal cord astrocytes to maintain late-phase neuropathic pain in mice. *Brain, 137*(Pt 8), 2193-2209. doi:10.1093/brain/awu140

Chen, J. Y., Blankstein, U., Diamant, N. E., & Davis, K. D. (2011). White matter abnormalities in irritable bowel syndrome and relation to individual factors. *Brain Res, 1392*, 121-131. doi:10.1016/j.brainres.2011.03.069

Cherkin, D. C., Sherman, K. J., Balderson, B. H., Cook, A. J., Anderson, M. L., Hawkes, R. J., . . . Turner, J. A. (2016). Effect of Mindfulness-Based Stress Reduction vs Cognitive Behavioral Therapy or Usual Care on Back Pain and Functional Limitations in Adults With Chronic Low Back Pain: A Randomized Clinical Trial. *JAMA, 315*(12), 1240-1249. doi:10.1001/jama.2016.2323

Cherkin, D. C., Sherman, K. J., & Turner, J. A. (2016). Mindfulness-Based Stress Reduction vs Cognitive Behavioral Therapy for Chronic Low Back Pain--Reply. *JAMA, 316*(6), 663-664. doi:10.1001/jama.2016.7951

Chiappelli, J., Hong, L. E., Wijtenburg, S. A., Du, X., Gaston, F., Kochunov, P., & Rowland, L. M. (2015). Alterations in frontal white matter neurochemistry and microstructure in schizophrenia: implications for neuroinflammation. *Transl Psychiatry, 5*, e548. doi:10.1038/tp.2015.43

Chiapponi, C., Piras, F., Piras, F., Fagioli, S., Caltagirone, C., & Spalletta, G. (2013). Cortical grey matter and subcortical white matter brain microstructural changes in schizophrenia are localised and age independent: a case-control diffusion tensor imaging study. *PLoS One, 8*(10), e75115. doi:10.1371/journal.pone.0075115

Chou, R., Turner, J. A., Devine, E. B., Hansen, R. N., Sullivan, S. D., Blazina, I., . . . Deyo, R. A. (2015). The effectiveness and risks of long-term opioid therapy for chronic pain: a systematic review for a National Institutes of Health Pathways to Prevention Workshop. *Ann Intern Med, 162*(4), 276-286. doi:10.7326/M14-2559

Chung, W. S., Welsh, C. A., Barres, B. A., & Stevens, B. (2015). Do glia drive synaptic and cognitive impairment in disease? *Nat Neurosci, 18*(11), 1539-1545. doi:10.1038/nn.4142

Cimmino, M. A., Ferrone, C., & Cutolo, M. (2011). Epidemiology of chronic musculoskeletal pain. *Best Pract Res Clin Rheumatol, 25*(2), 173-183. doi:10.1016/j.berh.2010.01.012

Cohen, M. X., Schoene-Bake, J. C., Elger, C. E., & Weber, B. (2009). Connectivity-based segregation of the human striatum predicts personality characteristics. *Nat Neurosci, 12*(1), 32-34. doi:10.1038/nn.2228

Conrad, M. S., Dilger, R. N., & Johnson, R. W. (2012). Brain growth of the domestic pig (Sus scrofa) from 2 to 24 weeks of age: a longitudinal MRI study. *Dev Neurosci, 34*(4), 291-298. doi:10.1159/000339311

Corbetta, M., & Shulman, G. L. (2002). Control of goal-directed and stimulus-driven attention in the brain. *Nat Rev Neurosci, 3*(3), 201-215. doi:10.1038/nrn755

Corder, G., Tawfik, V. L., Wang, D., Sypek, E. I., Low, S. A., Dickinson, J. R., . . . Scherrer, G. (2017). Loss of mu opioid receptor signaling in nociceptors, but not microglia, abrogates morphine tolerance without disrupting analgesia. *Nat Med, 23*(2), 164-173. doi:10.1038/nm.4262

Corey, S. M., Vizzard, M. A., Badger, G. J., & Langevin, H. M. (2011). Sensory Innervation of the Nonspecialized Connective Tissues in the Low Back of the Rat. *Cells Tissues Organs*. doi:000323875 [pii]

10.1159/000323875

Costigan, M., & Woolf, C. J. (2002). No DREAM, No pain. Closing the spinal gate. *Cell, 108*(3), 297-300.

Cote, M. A., Bore, A., Girard, G., Houde, J. C., & Descoteaux, M. (2012). Tractometer: online evaluation system for tractography. *Med Image Comput Comput Assist Interv, 15*(Pt 1), 699-706.

Cote, M. A., Girard, G., Bore, A., Garyfallidis, E., Houde, J. C., & Descoteaux, M. (2013). Tractometer: towards validation of tractography pipelines. *Med Image Anal, 17*(7), 844-857. doi:10.1016/j.media.2013.03.009

Covey, W. C., Ignatowski, T. A., Knight, P. R., & Spengler, R. N. (2000). Brain-derived TNFalpha: involvement in neuroplastic changes implicated in the conscious perception of persistent pain. *Brain Res, 859*(1), 113-122.

Craner, S. L., & Ray, R. H. (1991a). Somatosensory cortex of the neonatal pig: I. Topographic organization of the primary somatosensory cortex (SI). *J Comp Neurol, 306*(1), 24-38. doi:10.1002/cne.903060103

Craner, S. L., & Ray, R. H. (1991b). Somatosensory cortex of the neonatal pig: II. Topographic organization of the secondary somatosensory cortex (SII). *J Comp Neurol, 306*(1), 39-48. doi:10.1002/cne.903060104

Crick, S. J., Sheppard, M. N., Ho, S. Y., Gebstein, L., & Anderson, R. H. (1998). Anatomy of the pig heart: comparisons with normal human cardiac structure. *J Anat, 193 (Pt 1)*, 105-119.

Crick, S. J., Sheppard, M. N., Ho, S. Y., Gepstein, L., & Anderson, R. H. (1998). Anatomy of the pig heart: comparisons with normal human cardiac structure. *Journal of Anatomy, 193*, 105-119. doi:Doi 10.1046/J.1469-7580.1998.19310105.X

Daducci, A., Canales-Rodriguez, E. J., Descoteaux, M., Garyfallidis, E., Gur, Y., Lin, Y. C., . . . Thiran, J. P. (2014). Quantitative comparison of reconstruction methods for intra-voxel fiber recovery from diffusion MRI. *IEEE Trans Med Imaging, 33*(2), 384-399. doi:10.1109/TMI.2013.2285500

Daducci, A., Dal Palu, A., Lemkaddem, A., & Thiran, J. P. (2015). COMMIT: Convex optimization modeling for microstructure informed tractography. *IEEE Trans Med Imaging, 34*(1), 246-257. doi:10.1109/TMI.2014.2352414

Dawe, R. J., Bennett, D. A., Schneider, J. A., Vasireddi, S. K., & Arfanakis, K. (2009). Postmortem MRI of human brain hemispheres: T2 relaxation times during formaldehyde fixation. *Magn Reson Med, 61*(4), 810-818. doi:10.1002/mrm.21909

De Poorter, J., De Wagter, C., De Deene, Y., Thomsen, C., Stahlberg, F., & Achten, E. (1995). Noninvasive MRI thermometry with the proton resonance frequency (PRF) method: in vivo results in human muscle. *Magn Reson Med, 33*(1), 74-81.

DeLeo, J. A., & Yezierski, R. P. (2001). The role of neuroinflammation and neuroimmune activation in persistent pain. *Pain, 90*(1-2), 1-6.

Demaerel, P., Heiner, L., Robberecht, W., Sciot, R., & Wilms, G. (1999). Diffusion-weighted MRI in sporadic Creutzfeldt-Jakob disease. *Neurology, 52*(1), 205-208.

Deppe, M., Muller, D., Kugel, H., Ruck, T., Wiendl, H., & Meuth, S. G. (2013). DTI detects water diffusion abnormalities in the thalamus that correlate with an extremity pain episode in a patient with multiple sclerosis. *Neuroimage Clin, 2*, 258-262. doi:10.1016/j.nicl.2013.01.008

Desouza, D. D., Moayedi, M., Chen, D. Q., Davis, K. D., & Hodaie, M. (2013). Sensorimotor and Pain Modulation Brain Abnormalities in Trigeminal Neuralgia: A Paroxysmal, Sensory-Triggered Neuropathic Pain. *PLoS One, 8*(6), e66340. doi:10.1371/journal.pone.0066340

Di Biase, M. A., Cropley, V. L., Baune, B. T., Olver, J., Amminger, G. P., Phassouliotis, C., . . . Zalesky, A. (2017). White matter connectivity disruptions in early and chronic schizophrenia. *Psychol Med*, 1-14. doi:10.1017/S0033291717001313

Dieppe, P. (2013). Chronic musculoskeletal pain. *BMJ, 346*, f3146. doi:10.1136/bmj.f3146

Dobbing, J., & Sands, J. (1979). Comparative aspects of the brain growth spurt. *Early Hum Dev, 3*(1), 79-83.

Douaud, G., Smith, S., Jenkinson, M., Behrens, T., Johansen-Berg, H., Vickers, J., . . . James, A. (2007). Anatomically related grey and white matter abnormalities in adolescent-onset schizophrenia. *Brain, 130*(Pt 9), 2375-2386. doi:10.1093/brain/awm184

Douglas, W. R. (1972). Of pigs and men and research: a review of applications and analogies of the pig, sus scrofa, in human medical research. *Space Life Sci, 3*(3), 226-234.

Eakin, C. L. (2001). Knee arthrofibrosis: prevention and management of a potentially devastating condition. *Phys Sportsmed, 29*(3), 31-42. doi:10.3810/psm.2001.03.668

Eapen, M., Zald, D. H., Gatenby, J. C., Ding, Z., & Gore, J. C. (2011). Using high-resolution MR imaging at 7T to evaluate the anatomy of the midbrain dopaminergic system. *AJNR Am J Neuroradiol, 32*(4), 688-694. doi:10.3174/ajnr.A2355

Ehde, D. M., Dillworth, T. M., & Turner, J. A. (2014). Cognitive-behavioral therapy for individuals with chronic pain: efficacy, innovations, and directions for research. *Am Psychol, 69*(2), 153-166. doi:10.1037/a0035747

Ellingson, B. M., Mayer, E., Harris, R. J., Ashe-McNally, C., Naliboff, B. D., Labus, J. S., & Tillisch, K. (2013). Diffusion tensor imaging detects microstructural reorganization in the brain associated with chronic irritable bowel syndrome. *Pain, 154*(9), 1528-1541. doi:10.1016/j.pain.2013.04.010

Ellis, A., & Bennett, D. L. (2013). Neuroinflammation and the generation of neuropathic pain. *Br J Anaesth, 111*(1), 26-37. doi:10.1093/bja/aet128

Eroglu, C., & Barres, B. A. (2010). Regulation of synaptic connectivity by glia. *Nature, 468*(7321), 223-231. doi:10.1038/nature09612

Esteban, O., Caruyer, E., Daducci, A., Bach-Cuadra, M., Ledesma-Carbayo, M. J., & Santos, A. (2016). Diffantom: Whole-Brain Diffusion MRI Phantoms Derived from Real Datasets of the Human Connectome Project. *Front Neuroinform, 10*, 4. doi:10.3389/fninf.2016.00004

Farmer, M. A., Huang, L., Martucci, K., Yang, C. C., Maravilla, K. R., Harris, R. E., . . . Network, M. R. (2015). Brain White Matter Abnormalities in Female Interstitial Cystitis/Bladder Pain Syndrome: A MAPP Network Neuroimaging Study. *J Urol, 194*(1), 118-126. doi:10.1016/j.juro.2015.02.082

Farquharson, S., Tournier, J. D., Calamante, F., Fabinyi, G., Schneider-Kolsky, M., Jackson, G. D., & Connelly, A. (2013). White matter fiber tractography: why we need to move beyond DTI. *J Neurosurg, 118*(6), 1367-1377. doi:10.3171/2013.2.JNS121294

Fasick, V., Spengler, R. N., Samankan, S., Nader, N. D., & Ignatowski, T. A. (2015). The hippocampus and TNF: Common links between chronic pain and depression. *Neurosci Biobehav Rev, 53*, 139-159. doi:10.1016/j.neubiorev.2015.03.014

Faull, O. K., Jenkinson, M., Clare, S., & Pattinson, K. T. (2015). Functional subdivision of the human periaqueductal grey in respiratory control using 7 tesla fMRI. *Neuroimage, 113*, 356-364. doi:10.1016/j.neuroimage.2015.02.026

Fehrenbacher, J. C., Vasko, M. R., & Duarte, D. B. (2012). Models of inflammation: Carrageenan- or complete Freund's Adjuvant (CFA)-induced edema and hypersensitivity in the rat. *Curr Protoc Pharmacol, Chapter 5*, Unit5 4. doi:10.1002/0471141755.ph0504s56

Ferrini, F., Trang, T., Mattioli, T. A., Laffray, S., Del'Guidice, T., Lorenzo, L. E., . . . De Koninck, Y. (2013). Morphine hyperalgesia gated through microglia-mediated disruption of neuronal Cl(-) homeostasis. *Nat Neurosci, 16*(2), 183-192. doi:10.1038/nn.3295

Fields, R. D. (2008a). Oligodendrocytes changing the rules: action potentials in glia and oligodendrocytes controlling action potentials. *Neuroscientist, 14*(6), 540-543. doi:10.1177/1073858408320294

Fields, R. D. (2008b). White matter in learning, cognition and psychiatric disorders. *Trends Neurosci, 31*(7), 361-370. doi:10.1016/j.tins.2008.04.001

Filippi, M., & Rocca, M. A. (2011). MR imaging of multiple sclerosis. *Radiology, 259*(3), 659-681. doi:10.1148/radiol.11101362

Fillard, P., Descoteaux, M., Goh, A., Gouttard, S., Jeurissen, B., Malcolm, J., . . . Poupon, C. (2011). Quantitative evaluation of 10 tractography algorithms on a realistic diffusion MR phantom. *Neuroimage, 56*(1), 220-234. doi:10.1016/j.neuroimage.2011.01.032

Forstmann, B. U., Keuken, M. C., Schafer, A., Bazin, P. L., Alkemade, A., & Turner, R. (2014). Multi-modal ultra-high resolution structural 7-Tesla MRI data repository. *Sci Data, 1*, 140050. doi:10.1038/sdata.2014.50

Fox, M. D., Snyder, A. Z., Vincent, J. L., Corbetta, M., Van Essen, D. C., & Raichle, M. E. (2005). The human brain is intrinsically organized into dynamic, anticorrelated functional networks. *Proc Natl Acad Sci U S A, 102*(27), 9673-9678. doi:10.1073/pnas.0504136102

Frymoyer, J. W. (1988). Back pain and sciatica. *N Engl J Med, 318*(5), 291-300. doi:10.1056/NEJM198802043180506

Fuchs, P. N., Peng, Y. B., Boyette-Davis, J. A., & Uhelski, M. L. (2014). The anterior cingulate cortex and pain processing. *Front Integr Neurosci, 8*, 35. doi:10.3389/fnint.2014.00035

Ganguly, K., & Poo, M. M. (2013). Activity-dependent neural plasticity from bench to bedside. *Neuron, 80*(3), 729-741. doi:10.1016/j.neuron.2013.10.028

Gao, Y. J., & Ji, R. R. (2010). Targeting astrocyte signaling for chronic pain. *Neurotherapeutics, 7*(4), 482-493. doi:10.1016/j.nurt.2010.05.016

Garcia-Larrea, L., & Peyron, R. (2013). Pain matrices and neuropathic pain matrices: a review. *Pain, 154 Suppl 1*, S29-43. doi:10.1016/j.pain.2013.09.001

Geha, P. Y., Baliki, M. N., Harden, R. N., Bauer, W. R., Parrish, T. B., & Apkarian, A. V. (2008). The brain in chronic CRPS pain: abnormal gray-white matter interactions in emotional and autonomic regions. *Neuron, 60*(4), 570-581. doi:10.1016/j.neuron.2008.08.022

Gibson, E. M., Purger, D., Mount, C. W., Goldstein, A. K., Lin, G. L., Wood, L. S., . . . Monje, M. (2014). Neuronal activity promotes oligodendrogenesis and adaptive

myelination in the mammalian brain. *Science, 344*(6183), 1252304. doi:10.1126/science.1252304
Giguere, M., & Goldman-Rakic, P. S. (1988). Mediodorsal nucleus: areal, laminar, and tangential distribution of afferents and efferents in the frontal lobe of rhesus monkeys. *J Comp Neurol, 277*(2), 195-213. doi:10.1002/cne.902770204
Gomez-Beldarrain, M., Oroz, I., Zapirain, B. G., Ruanova, B. F., Garcia-Chimeno, Y., Cabrera, A., . . . Garcia-Monco, J. C. (2016). Erratum to: Right fronto-insular white matter tracts link cognitive reserve and pain in migraine patients. *J Headache Pain, 17*, 22. doi:10.1186/s10194-016-0617-x
Good, C. D., Johnsrude, I. S., Ashburner, J., Henson, R. N., Friston, K. J., & Frackowiak, R. S. (2001). A voxel-based morphometric study of ageing in 465 normal adult human brains. *Neuroimage, 14*(1 Pt 1), 21-36. doi:10.1006/nimg.2001.0786
Goubran, M., Rudko, D. A., Santyr, B., Gati, J., Szekeres, T., Peters, T. M., & Khan, A. R. (2014). In vivo normative atlas of the hippocampal subfields using multi-echo susceptibility imaging at 7 Tesla. *Hum Brain Mapp, 35*(8), 3588-3601. doi:10.1002/hbm.22423
Greve, D. N. (2011). *An absolute beginner's guide to surface- and voxel- based morphometric analysis.* Paper presented at the Proceedings of the International Society for Magnetic Resonance in Medicine.
Gustin, S. M., Wrigley, P. J., Siddall, P. J., & Henderson, L. A. (2010). Brain anatomy changes associated with persistent neuropathic pain following spinal cord injury. *Cereb Cortex, 20*(6), 1409-1419. doi:10.1093/cercor/bhp205
Guy, J. R., Sati, P., Leibovitch, E., Jacobson, S., Silva, A. C., & Reich, D. S. (2016). Custom fit 3D-printed brain holders for comparison of histology with MRI in marmosets. *J Neurosci Methods, 257*, 55-63. doi:10.1016/j.jneumeth.2015.09.002
Gwilym, S. E., Filippini, N., Douaud, G., Carr, A. J., & Tracey, I. (2010). Thalamic atrophy associated with painful osteoarthritis of the hip is reversible after arthroplasty: a longitudinal voxel-based morphometric study. *Arthritis Rheum, 62*(10), 2930-2940. doi:10.1002/art.27585
Haavik, H., & Murphy, B. (2012). The role of spinal manipulation in addressing disordered sensorimotor integration and altered motor control. *J Electromyogr Kinesiol, 22*(5), 768-776. doi:10.1016/j.jelekin.2012.02.012
Hagmann, P., Jonasson, L., Maeder, P., Thiran, J. P., Wedeen, V. J., & Meuli, R. (2006). Understanding diffusion MR imaging techniques: from scalar diffusion-weighted imaging to diffusion tensor imaging and beyond. *Radiographics, 26 Suppl 1*, S205-223. doi:10.1148/rg.26si065510
Hains, B. C., & Waxman, S. G. (2006). Activated microglia contribute to the maintenance of chronic pain after spinal cord injury. *J Neurosci, 26*(16), 4308-4317. doi:10.1523/JNEUROSCI.0003-06.2006
Hanscom, D. A., Brox, J. I., & Bunnage, R. (2015). Defining the Role of Cognitive Behavioral Therapy in Treating Chronic Low Back Pain: An Overview. *Global Spine J, 5*(6), 496-504. doi:10.1055/s-0035-1567836
Haroon, E., Miller, A. H., & Sanacora, G. (2017). Inflammation, Glutamate, and Glia: A Trio of Trouble in Mood Disorders. *Neuropsychopharmacology, 42*(1), 193-215. doi:10.1038/npp.2016.199

Hart, L. G., Deyo, R. A., & Cherkin, D. C. (1995). Physician office visits for low back pain. Frequency, clinical evaluation, and treatment patterns from a U.S. national survey. *Spine (Phila Pa 1976), 20*(1), 11-19.

Hart, R. P., Wade, J. B., & Martelli, M. F. (2003). Cognitive impairment in patients with chronic pain: the significance of stress. *Curr Pain Headache Rep, 7*(2), 116-126.

Hatchard, T., Lepage, C., Hutton, B., Skidmore, B., & Poulin, P. A. (2014). Comparative evaluation of group-based mindfulness-based stress reduction and cognitive behavioral therapy for the treatment and management of chronic pain disorders: protocol for a systematic review and meta-analysis with indirect comparisons. *Syst Rev, 3*(1), 134. doi:10.1186/2046-4053-3-134

Hawley, L. L., Padesky, C. A., Hollon, S. D., Mancuso, E., Laposa, J. M., Brozina, K., & Segal, Z. V. (2017). Cognitive-Behavioral Therapy for Depression Using Mind Over Mood: CBT Skill Use and Differential Symptom Alleviation. *Behav Ther, 48*(1), 29-44. doi:10.1016/j.beth.2016.09.003

Hedo, G., Laird, J. M., & Lopez-Garcia, J. A. (1999). Time-course of spinal sensitization following carrageenan-induced inflammation in the young rat: a comparative electrophysiological and behavioural study in vitro and in vivo. *Neuroscience, 92*(1), 309-318.

Henze, D. A., & Urban, M. O. (2010). *Translational Pain Research: From Mouse to Man.* (K. L. & L. A.R. Eds.): CRC Press/Taylor & Francis.

Hodges, P. W., & Tucker, K. (2011). Moving differently in pain: a new theory to explain the adaptation to pain. *Pain, 152*(3 Suppl), S90-98. doi:10.1016/j.pain.2010.10.020

Hofmann, S. G., & Smits, J. A. (2008). Cognitive-behavioral therapy for adult anxiety disorders: a meta-analysis of randomized placebo-controlled trials. *J Clin Psychiatry, 69*(4), 621-632.

Hotta, J., Zhou, G., Harno, H., Forss, N., & Hari, R. (2017). Complex regional pain syndrome: The matter of white matter? *Brain Behav, 7*(5), e00647. doi:10.1002/brb3.647

Hoza, D., Vlasak, A., Horinek, D., Sames, M., & Alfieri, A. (2015). DTI-MRI biomarkers in the search for normal pressure hydrocephalus aetiology: a review. *Neurosurg Rev, 38*(2), 239-244; discussion 244. doi:10.1007/s10143-014-0584-0

Hua, X. Y., Svensson, C. I., Matsui, T., Fitzsimmons, B., Yaksh, T. L., & Webb, M. (2005). Intrathecal minocycline attenuates peripheral inflammation-induced hyperalgesia by inhibiting p38 MAPK in spinal microglia. *Eur J Neurosci, 22*(10), 2431-2440. doi:10.1111/j.1460-9568.2005.04451.x

Hubbard, C. S., Khan, S. A., Keaser, M. L., Mathur, V. A., Goyal, M., & Seminowicz, D. A. (2014). Altered Brain Structure and Function Correlate with Disease Severity and Pain Catastrophizing in Migraine Patients. *eNeuro, 1*(1), e20 14. doi:10.1523/ENEURO.0006-14.2014

Hubbard, P. L., Zhou, F. L., Eichhorn, S. J., & Parker, G. J. (2015). Biomimetic phantom for the validation of diffusion magnetic resonance imaging. *Magn Reson Med, 73*(1), 299-305. doi:10.1002/mrm.25107

Iannetti, G. D., & Mouraux, A. (2010). From the neuromatrix to the pain matrix (and back). *Exp Brain Res, 205*(1), 1-12. doi:10.1007/s00221-010-2340-1

Iannitti, T., Graham, A., & Dolan, S. (2012). Increased central and peripheral inflammation and inflammatory hyperalgesia in Zucker rat model of leptin receptor deficiency and genetic obesity. *Exp Physiol, 97*(11), 1236-1245. doi:10.1113/expphysiol.2011.064220

Ishibashi, T., Dakin, K. A., Stevens, B., Lee, P. R., Kozlov, S. V., Stewart, C. L., & Fields, R. D. (2006). Astrocytes promote myelination in response to electrical impulses. *Neuron, 49*(6), 823-832. doi:10.1016/j.neuron.2006.02.006

Jelsing, J., Nielsen, R., Olsen, A. K., Grand, N., Hemmingsen, R., & Pakkenberg, B. (2006). The postnatal development of neocortical neurons and glial cells in the Gottingen minipig and the domestic pig brain. *J Exp Biol, 209*(Pt 8), 1454-1462. doi:10.1242/jeb.02141

Jenkinson, M., Beckmann, C. F., Behrens, T. E., Woolrich, M. W., & Smith, S. M. (2012). Fsl. *Neuroimage, 62*(2), 782-790. doi:10.1016/j.neuroimage.2011.09.015

Jensen, J. H., Helpern, J. A., Ramani, A., Lu, H., & Kaczynski, K. (2005). Diffusional kurtosis imaging: the quantification of non-gaussian water diffusion by means of magnetic resonance imaging. *Magn Reson Med, 53*(6), 1432-1440. doi:10.1002/mrm.20508

Jeurissen, B., Leemans, A., Tournier, J. D., Jones, D. K., & Sijbers, J. (2013). Investigating the prevalence of complex fiber configurations in white matter tissue with diffusion magnetic resonance imaging. *Hum Brain Mapp, 34*(11), 2747-2766. doi:10.1002/hbm.22099

Ji, R. R., Berta, T., & Nedergaard, M. (2013). Glia and pain: is chronic pain a gliopathy? *Pain, 154 Suppl 1*, S10-28. doi:10.1016/j.pain.2013.06.022

Ji, R. R., Kohno, T., Moore, K. A., & Woolf, C. J. (2003). Central sensitization and LTP: do pain and memory share similar mechanisms? *Trends Neurosci, 26*(12), 696-705. doi:10.1016/j.tins.2003.09.017

Ji, R. R., Xu, Z. Z., & Gao, Y. J. (2014). Emerging targets in neuroinflammation-driven chronic pain. *Nat Rev Drug Discov, 13*(7), 533-548. doi:10.1038/nrd4334

Johannes, C. B., Le, T. K., Zhou, X., Johnston, J. A., & Dworkin, R. H. (2010). The prevalence of chronic pain in United States adults: results of an Internet-based survey. *J Pain, 11*(11), 1230-1239. doi:10.1016/j.jpain.2010.07.002

Johanson, E., Brumagne, S., Janssens, L., Pijnenburg, M., Claeys, K., & Paasuke, M. (2011). The effect of acute back muscle fatigue on postural control strategy in people with and without recurrent low back pain. *Eur Spine J, 20*(12), 2152-2159. doi:10.1007/s00586-011-1825-3

Jones, D. K. (2008). Studying connections in the living human brain with diffusion MRI. *Cortex, 44*(8), 936-952. doi:10.1016/j.cortex.2008.05.002

Jones, D. K., Knosche, T. R., & Turner, R. (2013). White matter integrity, fiber count, and other fallacies: the do's and don'ts of diffusion MRI. *Neuroimage, 73*, 239-254. doi:10.1016/j.neuroimage.2012.06.081

Jones, S. L., & Gebhart, G. F. (1986). Quantitative characterization of ceruleospinal inhibition of nociceptive transmission in the rat. *J Neurophysiol, 56*(5), 1397-1410.

Jutzeler, C. R., Huber, E., Callaghan, M. F., Luechinger, R., Curt, A., Kramer, J. L., & Freund, P. (2016). Association of pain and CNS structural changes after spinal cord injury. *Sci Rep, 6*, 18534. doi:10.1038/srep18534

Kairys, A. E., Schmidt-Wilcke, T., Puiu, T., Ichesco, E., Labus, J. S., Martucci, K., . . . Harris, R. E. (2015). Increased brain gray matter in the primary somatosensory cortex is associated with increased pain and mood disturbance in patients with interstitial cystitis/painful bladder syndrome. *J Urol, 193*(1), 131-137. doi:10.1016/j.juro.2014.08.042

Kang, X., Herron, T. J., Turken, A. U., & Woods, D. L. (2012). Diffusion properties of cortical and pericortical tissue: regional variations, reliability and methodological issues. *Magn Reson Imaging, 30*(8), 1111-1122. doi:10.1016/j.mri.2012.04.004

Kerrigan, C. L., Zelt, R. G., Thomson, J. G., & Diano, E. (1986). The pig as an experimental animal in plastic surgery research for the study of skin flaps, myocutaneous flaps and fasciocutaneous flaps. *Lab Anim Sci, 36*(4), 408-412.

Kettenmann, H., Kirchhoff, F., & Verkhratsky, A. (2013). Microglia: new roles for the synaptic stripper. *Neuron, 77*(1), 10-18. doi:10.1016/j.neuron.2012.12.023

Kim, D. J., Lim, M., Kim, J. S., Son, K. M., Kim, H. A., & Chung, C. K. (2014). Altered white matter integrity in the corpus callosum in fibromyalgia patients identified by tract-based spatial statistical analysis. *Arthritis Rheumatol, 66*(11), 3190-3199. doi:10.1002/art.38771

Kim, H. J., Kim, S. J., Kim, H. S., Choi, C. G., Kim, N., Han, S., . . . Lee, C. S. (2013). Alterations of mean diffusivity in brain white matter and deep gray matter in Parkinson's disease. *Neurosci Lett, 550*, 64-68. doi:10.1016/j.neulet.2013.06.050

Kim, S. H., Stoicea, N., Soghomonyan, S., & Bergese, S. D. (2014). Intraoperative use of remifentanil and opioid induced hyperalgesia/acute opioid tolerance: systematic review. *Front Pharmacol, 5*, 108. doi:10.3389/fphar.2014.00108

Kinnunen, K. M., Greenwood, R., Powell, J. H., Leech, R., Hawkins, P. C., Bonnelle, V., . . . Sharp, D. J. (2011). White matter damage and cognitive impairment after traumatic brain injury. *Brain, 134*(Pt 2), 449-463. doi:10.1093/brain/awq347

Knoerl, R., Lavoie Smith, E. M., & Weisberg, J. (2016). Chronic Pain and Cognitive Behavioral Therapy: An Integrative Review. *West J Nurs Res, 38*(5), 596-628. doi:10.1177/0193945915615869

Knyazeva, M. G. (2013). Splenium of corpus callosum: patterns of interhemispheric interaction in children and adults. *Neural Plast, 2013*, 639430. doi:10.1155/2013/639430

Kong, J., Spaeth, R. B., Wey, H. Y., Cheetham, A., Cook, A. H., Jensen, K., . . . Gollub, R. L. (2013). S1 is associated with chronic low back pain: a functional and structural MRI study. *Mol Pain, 9*, 43. doi:10.1186/1744-8069-9-43

Kregel, J., Meeus, M., Malfliet, A., Dolphens, M., Danneels, L., Nijs, J., & Cagnie, B. (2015). Structural and functional brain abnormalities in chronic low back pain: A systematic review. *Semin Arthritis Rheum, 45*(2), 229-237. doi:10.1016/j.semarthrit.2015.05.002

Krzyzak, A., Klodowski, K., & Raszewski, Z. (2015). Anisotropic phantoms in Magnetic Resonance Imaging. *Conf Proc IEEE Eng Med Biol Soc, 2015*, 414-417. doi:10.1109/EMBC.2015.7318387

Krzyzak, A. T., & Klodowski, K. (2015). The b matrix calculation using the anisotropic phantoms for DWI and DTI experiments. *Conf Proc IEEE Eng Med Biol Soc, 2015*, 418-421. doi:10.1109/EMBC.2015.7318388

Kuchinad, A., Schweinhardt, P., Seminowicz, D. A., Wood, P. B., Chizh, B. A., & Bushnell, M. C. (2007). Accelerated brain gray matter loss in fibromyalgia patients: premature aging of the brain? *J Neurosci, 27*(15), 4004-4007. doi:10.1523/JNEUROSCI.0098-07.2007

Kucyi, A., Salomons, T. V., & Davis, K. D. (2016). Cognitive behavioral training reverses the effect of pain exposure on brain network activity. *Pain, 157*(9), 1895-1904. doi:10.1097/j.pain.0000000000000592

Kutch, J. J., Labus, J. S., Harris, R. E., Martucci, K. T., Farmer, M. A., Fenske, S., . . . Network, M. R. (2017). Resting-state functional connectivity predicts longitudinal pain symptom change in urologic chronic pelvic pain syndrome: a MAPP network study. *Pain, 158*(6), 1069-1082. doi:10.1097/j.pain.0000000000000886

Kwon, O. H., Park, H., Seo, S. W., Na, D. L., & Lee, J. M. (2015). A framework to analyze cerebral mean diffusivity using surface guided diffusion mapping in diffusion tensor imaging. *Front Neurosci, 9*, 236. doi:10.3389/fnins.2015.00236

Landman, B. A., Huang, H., Prince, J. L., & Ying, S. H. (2007). *A Window for High-Resolution Post-Mortem DTI: Mapping Contrast Changes in Neural Degeneration.* Paper presented at the ISMRM Berlin, Germany.

Langevin, H. M., Fox, J. R., Koptiuch, C., Badger, G. J., Greenan-Naumann, A. C., Bouffard, N. A., . . . Henry, S. M. (2011). Reduced thoracolumbar fascia shear strain in human chronic low back pain. *BMC Musculoskelet Disord, 12*, 203. doi:10.1186/1471-2474-12-203

Langevin, H. M., & Sherman, K. J. (2007). Pathophysiological model for chronic low back pain integrating connective tissue and nervous system mechanisms. *Med Hypotheses, 68*(1), 74-80. doi:10.1016/j.mehy.2006.06.033

Langevin, H. M., Stevens-Tuttle, D., Fox, J. R., Badger, G. J., Bouffard, N. A., Krag, M. H., . . . Henry, S. M. (2009). Ultrasound evidence of altered lumbar connective tissue structure in human subjects with chronic low back pain. *BMC Musculoskelet Disord, 10*, 151. doi:10.1186/1471-2474-10-151

Latremoliere, A., & Woolf, C. J. (2009). Central sensitization: a generator of pain hypersensitivity by central neural plasticity. *J Pain, 10*(9), 895-926. doi:10.1016/j.jpain.2009.06.012

Lazaridou, A., Kim, J., Cahalan, C. M., Loggia, M. L., Franceschelli, O., Berna, C., . . . Edwards, R. R. (2017). Effects of Cognitive-Behavioral Therapy (CBT) on Brain Connectivity Supporting Catastrophizing in Fibromyalgia. *Clin J Pain, 33*(3), 215-221. doi:10.1097/AJP.0000000000000422

Lee, P. R., & Fields, R. D. (2009). Regulation of myelin genes implicated in psychiatric disorders by functional activity in axons. *Front Neuroanat, 3*, 4. doi:10.3389/neuro.05.004.2009

Legrain, V., Iannetti, G. D., Plaghki, L., & Mouraux, A. (2011). The pain matrix reloaded: a salience detection system for the body. *Prog Neurobiol, 93*(1), 111-124. doi:10.1016/j.pneurobio.2010.10.005

Lichenstein, S. D., Bishop, J. H., Verstynen, T. D., & Yeh, F. C. (2016). Diffusion Capillary Phantom vs. Human Data: Outcomes for Reconstruction Methods Depend on Evaluation Medium. *Front Neurosci, 10*, 407. doi:10.3389/fnins.2016.00407

Lieberman, G., Shpaner, M., Watts, R., Andrews, T., Filippi, C. G., Davis, M., & Naylor, M. R. (2014). White matter involvement in chronic musculoskeletal pain. *J Pain*. doi:10.1016/j.jpain.2014.08.002

Lin, J. C., Chu, L. F., Stringer, E. A., Baker, K. S., Sayyid, Z. N., Sun, J., . . . Younger, J. W. (2016). One Month of Oral Morphine Decreases Gray Matter Volume in the Right Amygdala of Individuals with Low Back Pain: Confirmation of Previously Reported Magnetic Resonance Imaging Results. *Pain Med, 17*(8), 1497-1504. doi:10.1093/pm/pnv047

Lind, N. M., Moustgaard, A., Jelsing, J., Vajta, G., Cumming, P., & Hansen, A. K. (2007a). The use of pigs in neuroscience: Modeling brain disorders. *Neuroscience and Biobehavioral Reviews, 31*(5), 728-751. doi:Doi 10.1016/J.Neubiorev.2007.02.003

Lind, N. M., Moustgaard, A., Jelsing, J., Vajta, G., Cumming, P., & Hansen, A. K. (2007b). The use of pigs in neuroscience: modeling brain disorders. *Neurosci Biobehav Rev, 31*(5), 728-751. doi:10.1016/j.neubiorev.2007.02.003

Liu, J., Dietz, K., DeLoyht, J. M., Pedre, X., Kelkar, D., Kaur, J., . . . Casaccia, P. (2012). Impaired adult myelination in the prefrontal cortex of socially isolated mice. *Nat Neurosci, 15*(12), 1621-1623. doi:10.1038/nn.3263

Liu, J., Dupree, J. L., Gacias, M., Frawley, R., Sikder, T., Naik, P., & Casaccia, P. (2016). Clemastine Enhances Myelination in the Prefrontal Cortex and Rescues Behavioral Changes in Socially Isolated Mice. *J Neurosci, 36*(3), 957-962. doi:10.1523/JNEUROSCI.3608-15.2016

Liu, P., Wang, G., Liu, Y., Yu, Q., Yang, F., Jin, L., . . . Calhoun, V. D. (2016). White matter microstructure alterations in primary dysmenorrhea assessed by diffusion tensor imaging. *Sci Rep, 6*, 25836. doi:10.1038/srep25836

Loggia, M. L., Chonde, D. B., Akeju, O., Arabasz, G., Catana, C., Edwards, R. R., . . . Hooker, J. M. (2015). Evidence for brain glial activation in chronic pain patients. *Brain, 138*(Pt 3), 604-615. doi:10.1093/brain/awu377

Lu, C., Yang, T., Zhao, H., Zhang, M., Meng, F., Fu, H., . . . Xu, H. (2016). Insular Cortex is Critical for the Perception, Modulation, and Chronification of Pain. *Neurosci Bull, 32*(2), 191-201. doi:10.1007/s12264-016-0016-y

Luchtmann, M., Baecke, S., Steinecke, Y., Bernarding, J., Tempelmann, C., Ragert, P., & Firsching, R. (2015). Changes in gray matter volume after microsurgical lumbar discectomy: a longitudinal analysis. *Front Hum Neurosci, 9*, 12. doi:10.3389/fnhum.2015.00012

Lund, J. P., Donga, R., Widmer, C. G., & Stohler, C. S. (1991). The pain-adaptation model: a discussion of the relationship between chronic musculoskeletal pain and motor activity. *Can J Physiol Pharmacol, 69*(5), 683-694.

Lutz, J., Jager, L., de Quervain, D., Krauseneck, T., Padberg, F., Wichnalek, M., . . . Schelling, G. (2008). White and gray matter abnormalities in the brain of patients with fibromyalgia: a diffusion-tensor and volumetric imaging study. *Arthritis Rheum, 58*(12), 3960-3969. doi:10.1002/art.24070

Mackey, A. P., Whitaker, K. J., & Bunge, S. A. (2012). Experience-dependent plasticity in white matter microstructure: reasoning training alters structural connectivity. *Front Neuroanat, 6*, 32. doi:10.3389/fnana.2012.00032

Maeda, Y., Kim, H., Kettner, N., Kim, J., Cina, S., Malatesta, C., . . . Napadow, V. (2017). Rewiring the primary somatosensory cortex in carpal tunnel syndrome with acupuncture. *Brain, 140*(4), 914-927. doi:10.1093/brain/awx015

Maher, C., Underwood, M., & Buchbinder, R. (2017). Non-specific low back pain. *Lancet, 389*(10070), 736-747. doi:10.1016/S0140-6736(16)30970-9

Makin, T. R., Filippini, N., Duff, E. P., Henderson Slater, D., Tracey, I., & Johansen-Berg, H. (2015). Network-level reorganisation of functional connectivity following arm amputation. *Neuroimage, 114*, 217-225. doi:10.1016/j.neuroimage.2015.02.067

Malanga, G. A., & Cruz Colon, E. J. Myofascial low back pain: a review. *Phys Med Rehabil Clin N Am, 21*(4), 711-724. doi:S1047-9651(10)00039-2 [pii]
10.1016/j.pmr.2010.07.003

Maleki, N., Becerra, L., Brawn, J., McEwen, B., Burstein, R., & Borsook, D. (2013). Common hippocampal structural and functional changes in migraine. *Brain Struct Funct, 218*(4), 903-912. doi:10.1007/s00429-012-0437-y

Malfliet, A., Coppieters, I., Van Wilgen, P., Kregel, J., De Pauw, R., Dolphens, M., & Ickmans, K. (2017). Brain changes associated with cognitive and emotional factors in chronic pain: A systematic review. *Eur J Pain, 21*(5), 769-786. doi:10.1002/ejp.1003

Mansour, A. R., Baliki, M. N., Huang, L., Torbey, S., Herrmann, K. M., Schnitzer, T. J., & Apkarian, A. V. (2013). Brain white matter structural properties predict transition to chronic pain. *Pain, 154*(10), 2160-2168. doi:10.1016/j.pain.2013.06.044

Mao, C., Wei, L., Zhang, Q., Liao, X., Yang, X., & Zhang, M. (2013). Differences in brain structure in patients with distinct sites of chronic pain: A voxel-based morphometric analysis. *Neural Regen Res, 8*(32), 2981-2990. doi:10.3969/j.issn.1673-5374.2013.32.001

Marcarian, H. Q., & Calhoun, M. L. (1966). Microscopic anatomy of the integument of adult swine. *Am J Vet Res, 27*(118), 765-772.

Markov, N. T., Ercsey-Ravasz, M., Van Essen, D. C., Knoblauch, K., Toroczkai, Z., & Kennedy, H. (2013). Cortical high-density counterstream architectures. *Science, 342*(6158), 1238406. doi:10.1126/science.1238406

Martino, J., Brogna, C., Robles, S. G., Vergani, F., & Duffau, H. (2010). Anatomic dissection of the inferior fronto-occipital fasciculus revisited in the lights of brain stimulation data. *Cortex, 46*(5), 691-699. doi:10.1016/j.cortex.2009.07.015

Martucci, K. T., & Mackey, S. C. (2016). Imaging Pain. *Anesthesiol Clin, 34*(2), 255-269. doi:10.1016/j.anclin.2016.01.001

Martucci, K. T., Ng, P., & Mackey, S. (2014). Neuroimaging chronic pain: what have we learned and where are we going? *Future Neurol, 9*(6), 615-626. doi:10.2217/FNL.14.57

Mazzola, L., Isnard, J., & Mauguiere, F. (2006). Somatosensory and pain responses to stimulation of the second somatosensory area (SII) in humans. A comparison with SI and insular responses. *Cereb Cortex, 16*(7), 960-968. doi:10.1093/cercor/bhj038

Mazzola, L., Isnard, J., Peyron, R., & Mauguiere, F. (2012). Stimulation of the human cortex and the experience of pain: Wilder Penfield's observations revisited. *Brain, 135*(Pt 2), 631-640. doi:10.1093/brain/awr265

McFarquhar, M., McKie, S., Emsley, R., Suckling, J., Elliott, R., & Williams, S. (2016). Multivariate and repeated measures (MRM): A new toolbox for dependent and multimodal group-level neuroimaging data. *Neuroimage, 132*, 373-389. doi:10.1016/j.neuroimage.2016.02.053

McKenzie, I. A., Ohayon, D., Li, H., de Faria, J. P., Emery, B., Tohyama, K., & Richardson, W. D. (2014). Motor skill learning requires active central myelination. *Science, 346*(6207), 318-322. doi:10.1126/science.1254960

Medina, D., DeToledo-Morrell, L., Urresta, F., Gabrieli, J. D., Moseley, M., Fleischman, D., . . . Stebbins, G. T. (2006). White matter changes in mild cognitive impairment and AD: A diffusion tensor imaging study. *Neurobiol Aging, 27*(5), 663-672. doi:10.1016/j.neurobiolaging.2005.03.026

Melzack, R. (1999). From the gate to the neuromatrix. *Pain, Suppl 6*, S121-126.

Melzack, R., & Wall, P. D. (1965). Pain mechanisms: a new theory. *Science, 150*(3699), 971-979.

Meurens, F., Summerfield, A., Nauwynck, H., Saif, L., & Gerdts, V. (2012). The pig: a model for human infectious diseases. *Trends Microbiol, 20*(1), 50-57. doi:10.1016/j.tim.2011.11.002

Meyer, W., Neurand, K., & Radke, B. (1981). Elastic fibre arrangement in the skin of the pig. *Arch Dermatol Res, 270*(4), 391-401.

Meyer, W., Schwarz, R., & Neurand, K. (1978). The skin of domestic mammals as a model for the human skin, with special reference to the domestic pig. *Current problems in dermatology, 7*, 39-52.

Millan, M. J. (2002). Descending control of pain. *Prog Neurobiol, 66*(6), 355-474.

Miller, K. L. (2012). FMRI using balanced steady-state free precession (SSFP). *Neuroimage, 62*(2), 713-719. doi:10.1016/j.neuroimage.2011.10.040

Mistry, C. J., Bawor, M., Desai, D., Marsh, D. C., & Samaan, Z. (2014). Genetics of Opioid Dependence: A Review of the Genetic Contribution to Opioid Dependence. *Curr Psychiatry Rev, 10*(2), 156-167. doi:10.2174/1573400510666140320000928

Moayedi, M., Desouza, D., & Erpelding, N. (2011). Making sense of gray matter abnormalities in chronic orofacial pain--synthesizing divergent findings. *J Neurosci, 31*(35), 12396-12397. doi:10.1523/JNEUROSCI.3103-11.2011

Moayedi, M., Weissman-Fogel, I., Salomons, T. V., Crawley, A. P., Goldberg, M. B., Freeman, B. V., . . . Davis, K. D. (2012a). Abnormal gray matter aging in chronic pain patients. *Brain Res, 1456*, 82-93. doi:10.1016/j.brainres.2012.03.040

Moayedi, M., Weissman-Fogel, I., Salomons, T. V., Crawley, A. P., Goldberg, M. B., Freeman, B. V., . . . Davis, K. D. (2012b). White matter brain and trigeminal nerve abnormalities in temporomandibular disorder. *Pain, 153*(7), 1467-1477. doi:10.1016/j.pain.2012.04.003

Mogil, J. S. (2009). Animal models of pain: progress and challenges. *Nat Rev Neurosci, 10*(4), 283-294. doi:10.1038/nrn2606

Moriarty, O., McGuire, B. E., & Finn, D. P. (2011). The effect of pain on cognitive function: a review of clinical and preclinical research. *Prog Neurobiol, 93*(3), 385-404. doi:10.1016/j.pneurobio.2011.01.002

Moseley, M. E., Nishimura, M. C., Pitts, L. H., Bartkowski, H. M., & James, T. L. (1984). Proton nuclear magnetic resonance spectroscopy of normal and edematous brain tissue in vitro: changes in relaxation during tissue storage. *Magn Reson Imaging, 2*(3), 205-209.

Muraskin, J., Dodhia, S., Lieberman, G., Garcia, J. O., Verstynen, T., Vettel, J. M., . . . Sajda, P. (2016). Brain dynamics of post-task resting state are influenced by expertise: Insights from baseball players. *Hum Brain Mapp, 37*(12), 4454-4471. doi:10.1002/hbm.23321

Mutso, A. A., Radzicki, D., Baliki, M. N., Huang, L., Banisadr, G., Centeno, M. V., . . . Apkarian, A. V. (2012). Abnormalities in hippocampal functioning with persistent pain. *J Neurosci, 32*(17), 5747-5756. doi:10.1523/JNEUROSCI.0587-12.2012

Napadow, V., LaCount, L., Park, K., As-Sanie, S., Clauw, D. J., & Harris, R. E. (2010). Intrinsic brain connectivity in fibromyalgia is associated with chronic pain intensity. *Arthritis Rheum, 62*(8), 2545-2555. doi:10.1002/art.27497

Naylor, M. R., Helzer, J. E., Naud, S., & Keefe, F. J. (2002). Automated telephone as an adjunct for the treatment of chronic pain: a pilot study. *J Pain, 3*(6), 429-438.

Naylor, M. R., Keefe, F. J., Brigidi, B., Naud, S., & Helzer, J. E. (2008). Therapeutic Interactive Voice Response for chronic pain reduction and relapse prevention. *Pain, 134*(3), 335-345. doi:10.1016/j.pain.2007.11.001

Olvet, D. M., Delaparte, L., Yeh, F. C., DeLorenzo, C., McGrath, P. J., Weissman, M. M., . . . Parsey, R. V. (2016). A Comprehensive Examination of White Matter Tracts and Connectometry in Major Depressive Disorder. *Depress Anxiety, 33*(1), 56-65. doi:10.1002/da.22445

Ongur, D., Bechtholt, A. J., Carlezon, W. A., Jr., & Cohen, B. M. (2014). Glial abnormalities in mood disorders. *Harv Rev Psychiatry, 22*(6), 334-337. doi:10.1097/HRP.0000000000000060

Otsu, N. (1979). A threshold selection method from gray-level histograms. *IEEE Trans Sys Man Cyber, 9*(1), 62-66. doi:10.1109/TSMC.1979.4310076

Pajevic, S., Basser, P. J., & Fields, R. D. (2014). Role of myelin plasticity in oscillations and synchrony of neuronal activity. *Neuroscience, 276*, 135-147. doi:10.1016/j.neuroscience.2013.11.007

Park, S. K., Solomon, D., & Vartanian, T. (2001). Growth factor control of CNS myelination. *Dev Neurosci, 23*(4-5), 327-337.

Patenaude, B., Smith, S. M., Kennedy, D. N., & Jenkinson, M. (2011). A Bayesian model of shape and appearance for subcortical brain segmentation. *Neuroimage, 56*(3), 907-922. doi:10.1016/j.neuroimage.2011.02.046

Perl, E. R. (2007). Ideas about pain, a historical view. *Nat Rev Neurosci, 8*(1), 71-80. doi:10.1038/nrn2042

Peters, A., McEwen, B. S., & Friston, K. (2017). Uncertainty and stress: Why it causes diseases and how it is mastered by the brain. *Prog Neurobiol*. doi:10.1016/j.pneurobio.2017.05.004

Pomares, F. B., Funck, T., Feier, N. A., Roy, S., Daigle-Martel, A., Ceko, M., . . . Schweinhardt, P. (2016). Histological Underpinnings of Grey Matter Changes in

Fibromyalgia Investigated Using Multimodal Brain Imaging. *J Neurosci, 37*(5), 1090-1101. doi:10.1523/JNEUROSCI.2619-16.2016

Pomares, F. B., Funck, T., Feier, N. A., Roy, S., Daigle-Martel, A., Ceko, M., . . . Schweinhardt, P. (2017). Histological Underpinnings of Grey Matter Changes in Fibromyalgia Investigated Using Multimodal Brain Imaging. *J Neurosci, 37*(5), 1090-1101. doi:10.1523/JNEUROSCI.2619-16.2016

Porreca, F., Ossipov, M. H., & Gebhart, G. F. (2002). Chronic pain and medullary descending facilitation. *Trends Neurosci, 25*(6), 319-325.

Poupon, C., Rieul, B., Kezele, I., Perrin, M., Poupon, F., & Mangin, J. F. (2008). New diffusion phantoms dedicated to the study and validation of high-angular-resolution diffusion imaging (HARDI) models. *Magn Reson Med, 60*(6), 1276-1283. doi:10.1002/mrm.21789

Pullens, P., Roebroeck, A., & Goebel, R. (2010). Ground truth hardware phantoms for validation of diffusion-weighted MRI applications. *J Magn Reson Imaging, 32*(2), 482-488. doi:10.1002/jmri.22243

Quartana, P. J., Campbell, C. M., & Edwards, R. R. (2009). Pain catastrophizing: a critical review. *Expert Rev Neurother, 9*(5), 745-758. doi:10.1586/ern.09.34

Quesson, B., de Zwart, J. A., & Moonen, C. T. (2000). Magnetic resonance temperature imaging for guidance of thermotherapy. *J Magn Reson Imaging, 12*(4), 525-533.

Raffelt, D. A., Smith, R. E., Ridgway, G. R., Tournier, J. D., Vaughan, D. N., Rose, S., . . . Connelly, A. (2015). Connectivity-based fixel enhancement: Whole-brain statistical analysis of diffusion MRI measures in the presence of crossing fibres. *Neuroimage, 117*, 40-55. doi:10.1016/j.neuroimage.2015.05.039

Raffelt, D. A., Tournier, J. D., Smith, R. E., Vaughan, D. N., Jackson, G., Ridgway, G. R., & Connelly, A. (2017). Investigating white matter fibre density and morphology using fixel-based analysis. *Neuroimage, 144*(Pt A), 58-73. doi:10.1016/j.neuroimage.2016.09.029

Rayhan, R. U., Stevens, B. W., Timbol, C. R., Adewuyi, O., Walitt, B., VanMeter, J. W., & Baraniuk, J. N. (2013). Increased brain white matter axial diffusivity associated with fatigue, pain and hyperalgesia in Gulf War illness. *PLoS One, 8*(3), e58493. doi:10.1371/journal.pone.0058493

Ren, K., & Dubner, R. (2008). Neuron-glia crosstalk gets serious: role in pain hypersensitivity. *Curr Opin Anaesthesiol, 21*(5), 570-579. doi:10.1097/ACO.0b013e32830edbdf

Reveley, C., Seth, A. K., Pierpaoli, C., Silva, A. C., Yu, D., Saunders, R. C., . . . Ye, F. Q. (2015). Superficial white matter fiber systems impede detection of long-range cortical connections in diffusion MR tractography. *Proc Natl Acad Sci U S A, 112*(21), E2820-2828. doi:10.1073/pnas.1418198112

Rodriguez-Raecke, R., Niemeier, A., Ihle, K., Ruether, W., & May, A. (2009). Brain gray matter decrease in chronic pain is the consequence and not the cause of pain. *J Neurosci, 29*(44), 13746-13750. doi:10.1523/JNEUROSCI.3687-09.2009

Rodriguez-Raecke, R., Niemeier, A., Ihle, K., Ruether, W., & May, A. (2013). Structural brain changes in chronic pain reflect probably neither damage nor atrophy. *PLoS One, 8*(2), e54475. doi:10.1371/journal.pone.0054475

Rogers, W. H., Wittink, H. M., Ashburn, M. A., Cynn, D., & Carr, D. B. (2000). Using the "TOPS," an outcomes instrument for multidisciplinary outpatient pain treatment. *Pain Med, 1*(1), 55-67. doi:10.1046/j.1526-4637.2000.99101.x

Roland, M. O. (1986). A critical review of the evidence for a pain-spasm-pain cycle in spinal disorders. *Clin Biomech (Bristol, Avon), 1*(2), 102-109. doi:10.1016/0268-0033(86)90085-9

Rorden, C., & Brett, M. (2000). Stereotaxic display of brain lesions. *Behav Neurol, 12*(4), 191-200.

Rose, E. H., Vistnes, L. M., & Ksander, G. A. (1978). A microarchitectural model of regional variations in hypodermal mobility in porcine and human skin. *Ann Plast Surg, 1*(3), 252-266.

Rose, S. E., Janke, A. L., & Chalk, J. B. (2008). Gray and white matter changes in Alzheimer's disease: a diffusion tensor imaging study. *J Magn Reson Imaging, 27*(1), 20-26. doi:10.1002/jmri.21231

Salminen, L. E., Schofield, P. R., Pierce, K. D., Zhao, Y., Luo, X., Wang, Y., . . . Paul, R. H. (2016). Neuromarkers of the common angiotensinogen polymorphism in healthy older adults: A comprehensive assessment of white matter integrity and cognition. *Behav Brain Res, 296*, 85-93. doi:10.1016/j.bbr.2015.08.028

Samad, T. A., Moore, K. A., Sapirstein, A., Billet, S., Allchorne, A., Poole, S., . . . Woolf, C. J. (2001). Interleukin-1beta-mediated induction of Cox-2 in the CNS contributes to inflammatory pain hypersensitivity. *Nature, 410*(6827), 471-475. doi:10.1038/35068566

Sarubbo, S., De Benedictis, A., Maldonado, I. L., Basso, G., & Duffau, H. (2013). Frontal terminations for the inferior fronto-occipital fascicle: anatomical dissection, DTI study and functional considerations on a multi-component bundle. *Brain Struct Funct, 218*(1), 21-37. doi:10.1007/s00429-011-0372-3

Sasaki, T., Tsuda, S., Riemer, R. K., Ramamoorthy, C., Reddy, V. M., & Hanley, F. L. (2010). Optimal flow rate for antegrade cerebral perfusion. *The Journal of Thoracic and Cardiovascular Surgery, 139*(3), 530-535. doi:http://dx.doi.org/10.1016/j.jtcvs.2009.12.005

Satpute, A. B., Wager, T. D., Cohen-Adad, J., Bianciardi, M., Choi, J. K., Buhle, J. T., . . . Barrett, L. F. (2013). Identification of discrete functional subregions of the human periaqueductal gray. *Proc Natl Acad Sci U S A, 110*(42), 17101-17106. doi:10.1073/pnas.1306095110

Scheurer, E., Lovblad, K. O., Kreis, R., Maier, S. E., Boesch, C., Dirnhofer, R., & Yen, K. (2011). Forensic application of postmortem diffusion-weighted and diffusion tensor MR imaging of the human brain in situ. *AJNR Am J Neuroradiol, 32*(8), 1518-1524. doi:10.3174/ajnr.A2508

Schilling, N., Arnold, D., Wagner, H., & Fischer, M. S. (2005). Evolutionary aspects and muscular properties of the trunk--implications for human low back pain. *Pathophysiology, 12*(4), 233-242. doi:10.1016/j.pathophys.2005.09.005

Schmahmann, J. D., & Pandya, D. N. (2006). *Fiber Pathways of the Brain*. New York: Oxford University Press.

Schmidt-Wilcke, T., Leinisch, E., Ganssbauer, S., Draganski, B., Bogdahn, U., Altmeppen, J., & May, A. (2006). Affective components and intensity of pain

correlate with structural differences in gray matter in chronic back pain patients. *Pain, 125*(1-2), 89-97. doi:10.1016/j.pain.2006.05.004

Schmidt-Wilcke, T., Leinisch, E., Straube, A., Kampfe, N., Draganski, B., Diener, H. C., . . . May, A. (2005). Gray matter decrease in patients with chronic tension type headache. *Neurology, 65*(9), 1483-1486. doi:10.1212/01.wnl.0000183067.94400.80

Schmidt-Wilcke, T., Luerding, R., Weigand, T., Jurgens, T., Schuierer, G., Leinisch, E., & Bogdahn, U. (2007). Striatal grey matter increase in patients suffering from fibromyalgia--a voxel-based morphometry study. *Pain, 132 Suppl 1*, S109-116. doi:10.1016/j.pain.2007.05.010

Schmierer, K., Thavarajah, J. R., An, S. F., Brandner, S., Miller, D. H., & Tozer, D. J. (2010). Effects of formalin fixation on magnetic resonance indices in multiple sclerosis cortical gray matter. *J Magn Reson Imaging, 32*(5), 1054-1060. doi:10.1002/jmri.22381

Schnakers, C., Chatelle, C., Demertzi, A., Majerus, S., & Laureys, S. (2012). What about pain in disorders of consciousness? *AAPS J, 14*(3), 437-444. doi:10.1208/s12248-012-9346-5

Scholz, J., Klein, M. C., Behrens, T. E., & Johansen-Berg, H. (2009). Training induces changes in white-matter architecture. *Nat Neurosci, 12*(11), 1370-1371. doi:10.1038/nn.2412

Schroeter, M. L., Abdul-Khaliq, H., Sacher, J., Steiner, J., Blasig, I. E., & Mueller, K. (2010). Mood disorders are glial disorders: evidence from in vivo studies. *Cardiovasc Psychiatry Neurol, 2010*, 780645. doi:10.1155/2010/780645

Seizeur, R., Wiest-Daessle, N., Prima, S., Maumet, C., Ferre, J. C., & Morandi, X. (2012). Corticospinal tractography with morphological, functional and diffusion tensor MRI: a comparative study of four deterministic algorithms used in clinical routine. *Surg Radiol Anat*. doi:10.1007/s00276-012-0951-x

Seminowicz, D. A., & Moayedi, M. (2017). The Dorsolateral Prefrontal Cortex in Acute and Chronic Pain. *J Pain*. doi:10.1016/j.jpain.2017.03.008

Seminowicz, D. A., Shpaner, M., Keaser, M. L., Krauthamer, G. M., Mantegna, J., Dumas, J. A., . . . Naylor, M. R. (2013). Cognitive-behavioral therapy increases prefrontal cortex gray matter in patients with chronic pain. *J Pain, 14*(12), 1573-1584. doi:10.1016/j.jpain.2013.07.020

Seminowicz, D. A., Wideman, T. H., Naso, L., Hatami-Khoroushahi, Z., Fallatah, S., Ware, M. A., . . . Stone, L. S. (2011). Effective treatment of chronic low back pain in humans reverses abnormal brain anatomy and function. *J Neurosci, 31*(20), 7540-7550. doi:10.1523/JNEUROSCI.5280-10.2011

Shepherd, T. M., Thelwall, P. E., Stanisz, G. J., & Blackband, S. J. (2009). Aldehyde fixative solutions alter the water relaxation and diffusion properties of nervous tissue. *Magn Reson Med, 62*(1), 26-34. doi:10.1002/mrm.21977

Shpaner, M., Kelly, C., Lieberman, G., Perelman, H., Davis, M., Keefe, F. J., & Naylor, M. R. (2014). Unlearning chronic pain: A randomized controlled trial to investigate changes in intrinsic brain connectivity following Cognitive Behavioral Therapy. *Neuroimage Clin, 5*, 365-376. doi:10.1016/j.nicl.2014.07.008

Skaper, S. D., Facci, L., & Giusti, P. (2014). Neuroinflammation, microglia and mast cells in the pathophysiology of neurocognitive disorders: a review. *CNS Neurol Disord Drug Targets, 13*(10), 1654-1666.

Smallwood, R. F., Laird, A. R., Ramage, A. E., Parkinson, A. L., Lewis, J., Clauw, D. J., . . . Robin, D. A. (2013). Structural brain anomalies and chronic pain: a quantitative meta-analysis of gray matter volume. *J Pain, 14*(7), 663-675. doi:10.1016/j.jpain.2013.03.001

Smith, R. E., Tournier, J. D., Calamante, F., & Connelly, A. (2013). SIFT: Spherical-deconvolution informed filtering of tractograms. *Neuroimage, 67*, 298-312. doi:10.1016/j.neuroimage.2012.11.049

Smith, S. M., Jenkinson, M., Woolrich, M. W., Beckmann, C. F., Behrens, T. E., Johansen-Berg, H., . . . Matthews, P. M. (2004). Advances in functional and structural MR image analysis and implementation as FSL. *Neuroimage, 23 Suppl 1*, S208-219. doi:10.1016/j.neuroimage.2004.07.051

Sofroniew, M. V., & Vinters, H. V. (2010). Astrocytes: biology and pathology. *Acta Neuropathol, 119*(1), 7-35. doi:10.1007/s00401-009-0619-8

Solomonow, M. (2012). Neuromuscular manifestations of viscoelastic tissue degradation following high and low risk repetitive lumbar flexion. *J Electromyogr Kinesiol, 22*(2), 155-175. doi:10.1016/j.jelekin.2011.11.008

Sotak, C. H. (2002). The role of diffusion tensor imaging in the evaluation of ischemic brain injury - a review. *NMR Biomed, 15*(7-8), 561-569. doi:10.1002/nbm.786

Sotiropoulos, S. N., Jbabdi, S., Andersson, J. L., Woolrich, M. W., Ugurbil, K., & Behrens, T. E. (2013). RubiX: combining spatial resolutions for Bayesian inference of crossing fibers in diffusion MRI. *IEEE Trans Med Imaging, 32*(6), 969-982. doi:10.1109/TMI.2012.2231873

Spooner, J., Yu, H., Kao, C., Sillay, K., & Konrad, P. (2007). Neuromodulation of the cingulum for neuropathic pain after spinal cord injury. Case report. *J Neurosurg, 107*(1), 169-172. doi:10.3171/JNS-07/07/0169

Starr, C. J., Sawaki, L., Wittenberg, G. F., Burdette, J. H., Oshiro, Y., Quevedo, A. S., & Coghill, R. C. (2009). Roles of the insular cortex in the modulation of pain: insights from brain lesions. *J Neurosci, 29*(9), 2684-2694. doi:10.1523/JNEUROSCI.5173-08.2009

Sullivan, M., Bishop, S., & Pivak, J. (1995). The pain catastrophizing scale: development and validation. *Psychological Assessment, 7* 524-532

.

Sullivan, M. D., Edlund, M. J., Fan, M. Y., Devries, A., Brennan Braden, J., & Martin, B. C. (2008). Trends in use of opioids for non-cancer pain conditions 2000-2005 in commercial and Medicaid insurance plans: the TROUP study. *Pain, 138*(2), 440-449. doi:10.1016/j.pain.2008.04.027

Sullivan, M. D., Edlund, M. J., Steffick, D., & Unutzer, J. (2005). Regular use of prescribed opioids: association with common psychiatric disorders. *Pain, 119*(1-3), 95-103. doi:10.1016/j.pain.2005.09.020

Sullivan, T. P., Eaglstein, W. H., Davis, S. C., & Mertz, P. (2001). The pig as a model for human wound healing. *Wound Repair Regen, 9*(2), 66-76.

Sullivan, T. P., Eaglstein, W. H., Davis, S. C., & Mertz, P. (2001). The pig as a model for human wound healing. *Wound Repair and Regeneration, 9*(2), 66-76.

Summerfield, A., Meurens, F., & Ricklin, M. E. (2015). The immunology of the porcine skin and its value as a model for human skin. *Mol Immunol, 66*(1), 14-21. doi:10.1016/j.molimm.2014.10.023

Sun, S. W., Neil, J. J., Liang, H. F., He, Y. Y., Schmidt, R. E., Hsu, C. Y., & Song, S. K. (2005). Formalin fixation alters water diffusion coefficient magnitude but not anisotropy in infarcted brain. *Magn Reson Med, 53*(6), 1447-1451. doi:10.1002/mrm.20488

Sun, S. W., Neil, J. J., & Song, S. K. (2003). Relative indices of water diffusion anisotropy are equivalent in live and formalin-fixed mouse brains. *Magn Reson Med, 50*(4), 743-748. doi:10.1002/mrm.10605

Swindle, M. M., Makin, A., Herron, A. J., Clubb, F. J., & Frazier, K. S. (2012). Swine as Models in Biomedical Research and Toxicology Testing. *Veterinary Pathology, 49*(2), 344-356. doi:Doi 10.1177/0300985811402846

Swindle, M. M., Makin, A., Herron, A. J., Clubb, F. J., Jr., & Frazier, K. S. (2012). Swine as models in biomedical research and toxicology testing. *Vet Pathol, 49*(2), 344-356. doi:10.1177/0300985811402846

Szabo, N., Kincses, Z. T., Pardutz, A., Tajti, J., Szok, D., Tuka, B., . . . Vecsei, L. (2012). White matter microstructural alterations in migraine: a diffusion-weighted MRI study. *Pain, 153*(3), 651-656. doi:10.1016/j.pain.2011.11.029

Taguchi, T., Hoheisel, U., & Mense, S. (2008). Dorsal horn neurons having input from low back structures in rats. *Pain, 138*(1), 119-129.

Tang, Y. Y., Lu, Q., Fan, M., Yang, Y., & Posner, M. I. (2012). Mechanisms of white matter changes induced by meditation. *Proc Natl Acad Sci U S A, 109*(26), 10570-10574. doi:10.1073/pnas.1207817109

Tang, Y. Y., Lu, Q., Geng, X., Stein, E. A., Yang, Y., & Posner, M. I. (2010). Short-term meditation induces white matter changes in the anterior cingulate. *Proc Natl Acad Sci U S A, 107*(35), 15649-15652. doi:10.1073/pnas.1011043107

Tesarz, J., Hoheisel, U., Wiedenhofer, B., & Mense, S. (2011). Sensory innervation of the thoracolumbar fascia in rats and humans. *Neuroscience, 194*, 302-308. doi:10.1016/j.neuroscience.2011.07.066

The Centers for Disease Control and Prevention. (2014). Therapeutic Drug Use. https://www.cdc.gov/nchs/fastats/drug-use-therapeutic.htm

Thomas, C., Ye, F. Q., Irfanoglu, M. O., Modi, P., Saleem, K. S., Leopold, D. A., & Pierpaoli, C. (2014). Anatomical accuracy of brain connections derived from diffusion MRI tractography is inherently limited. *Proc Natl Acad Sci U S A, 111*(46), 16574-16579. doi:10.1073/pnas.1405672111

1405672111 [pii]

Tian, T., Guo, L., Xu, J., Zhang, S., Shi, J., Liu, C., . . . Zhu, W. (2016). Brain white matter plasticity and functional reorganization underlying the central pathogenesis of trigeminal neuralgia. *Sci Rep, 6*, 36030. doi:10.1038/srep36030

Tillman, L. J., & Cummings, G. S. (1992). Biologic mechanisms of connective tissue mutability. In D. P. Currier & R. M. Nelson (Eds.), *Dynamics of human biologic tissues*

Contemporary perspectives in rehabilitation. Philadelphia: F.A. Davis.

Torres-Platas, S. G., Comeau, S., Rachalski, A., Bo, G. D., Cruceanu, C., Turecki, G., . . . Mechawar, N. (2014). Morphometric characterization of microglial phenotypes in

human cerebral cortex. *J Neuroinflammation, 11*, 12. doi:10.1186/1742-2094-11-12

Torrisi, S., O'Connell, K., Davis, A., Reynolds, R., Balderston, N., Fudge, J. L., . . . Ernst, M. (2015). Resting state connectivity of the bed nucleus of the stria terminalis at ultra-high field. *Hum Brain Mapp, 36*(10), 4076-4088. doi:10.1002/hbm.22899

Tournier, J.-D., Calamante, F., & Connelly, A. (2012). MRtrix: Diffusion tractography in crossing fiber regions. *International Journal of Imaging Systems and Technology*.

Tournier, J. D., Calamante, F., King, M. D., Gadian, D. G., & Connelly, A. (2002). Limitations and requirements of diffusion tensor fiber tracking: an assessment using simulations. *Magn Reson Med, 47*(4), 701-708.

Tournier, J. D., Yeh, C. H., Calamante, F., Cho, K. H., Connelly, A., & Lin, C. P. (2008). Resolving crossing fibres using constrained spherical deconvolution: validation using diffusion-weighted imaging phantom data. *Neuroimage, 42*(2), 617-625. doi:10.1016/j.neuroimage.2008.05.002

Tracey, I., & Bushnell, M. C. (2009). How neuroimaging studies have challenged us to rethink: is chronic pain a disease? *J Pain, 10*(11), 1113-1120. doi:10.1016/j.jpain.2009.09.001

Tracey, I., & Mantyh, P. W. (2007). The cerebral signature for pain perception and its modulation. *Neuron, 55*(3), 377-391. doi:10.1016/j.neuron.2007.07.012

Tremblay, M. E., Stevens, B., Sierra, A., Wake, H., Bessis, A., & Nimmerjahn, A. (2011). The role of microglia in the healthy brain. *J Neurosci, 31*(45), 16064-16069. doi:10.1523/JNEUROSCI.4158-11.2011

Tromp, D. P., Grupe, D. W., Oathes, D. J., McFarlin, D. R., Hernandez, P. J., Kral, T. R., . . . Nitschke, J. B. (2012). Reduced structural connectivity of a major frontolimbic pathway in generalized anxiety disorder. *Arch Gen Psychiatry, 69*(9), 925-934. doi:10.1001/archgenpsychiatry.2011.2178

Tsuang, M. T., Lyons, M. J., Meyer, J. M., Doyle, T., Eisen, S. A., Goldberg, J., . . . Eaves, L. (1998). Co-occurrence of abuse of different drugs in men: the role of drug-specific and shared vulnerabilities. *Arch Gen Psychiatry, 55*(11), 967-972.

Tuch, D. S. (2004). Q-ball imaging. *Magn Reson Med, 52*(6), 1358-1372. doi:10.1002/mrm.20279

Tuch, D. S., Wisco, J. J., Khachaturian, M. H., Ekstrom, L. B., Kotter, R., & Vanduffel, W. (2005). Q-ball imaging of macaque white matter architecture. *Philos Trans R Soc Lond B Biol Sci, 360*(1457), 869-879. doi:10.1098/rstb.2005.1651

Tzourio-Mazoyer, N., Landeau, B., Papathanassiou, D., Crivello, F., Etard, O., Delcroix, N., . . . Joliot, M. (2002). Automated anatomical labeling of activations in SPM using a macroscopic anatomical parcellation of the MNI MRI single-subject brain. *Neuroimage, 15*(1), 273-289. doi:10.1006/nimg.2001.0978

Uddin, L. Q. (2015). Salience processing and insular cortical function and dysfunction. *Nat Rev Neurosci, 16*(1), 55-61. doi:10.1038/nrn3857

Vardaxis, N. J., Brans, T. A., Boon, M. E., Kreis, R. W., & Marres, L. M. (1997). Confocal laser scanning microscopy of porcine skin: implications for human wound healing studies. *Journal of Anatomy, 190*(4), 601-611.

Vasic, V., & Schmidt, M. H. (2017). Resilience and Vulnerability to Pain and Inflammation in the Hippocampus. *Int J Mol Sci, 18*(4). doi:10.3390/ijms18040739

Vleeming A, P.-G. A., Stoeckart R, van Wingerden JP, Snijders CJ. (1995). The posterior layer of the thoracolumbar fascia. Its function in load transfer from spine to legs. *Spine, 20*(7), 753-758.

Vrana, A., Hotz-Boendermaker, S., Stampfli, P., Hanggi, J., Seifritz, E., Humphreys, B. K., & Meier, M. L. (2015). Differential Neural Processing during Motor Imagery of Daily Activities in Chronic Low Back Pain Patients. *PLoS One, 10*(11), e0142391. doi:10.1371/journal.pone.0142391

Waldvogel, H. J., Curtis, M. A., Baer, K., Rees, M. I., & Faull, R. L. (2006). Immunohistochemical staining of post-mortem adult human brain sections. *Nat Protoc, 1*(6), 2719-2732. doi:10.1038/nprot.2006.354

Waldvogel, H. J., Curtis, M. A., Baer, K., Rees, M. I., & Faull, R. L. M. (2007). Immunohistochemical staining of post-mortem adult human brain sections. *Nat. Protocols, 1*(6), 2719-2732.

Walhovd, K. B., Johansen-Berg, H., & Karadottir, R. T. (2014). Unraveling the secrets of white matter--bridging the gap between cellular, animal and human imaging studies. *Neuroscience, 276*, 2-13. doi:10.1016/j.neuroscience.2014.06.058

Wang, T., Shi, F., Jin, Y., Yap, P. T., Wee, C. Y., Zhang, J., . . . Shen, D. (2016). Multilevel Deficiency of White Matter Connectivity Networks in Alzheimer's Disease: A Diffusion MRI Study with DTI and HARDI Models. *Neural Plast, 2016*, 2947136. doi:10.1155/2016/2947136

Wang, X., Pathak, S., Stefaneanu, L., Yeh, F. C., Li, S., & Fernandez-Miranda, J. C. (2016). Subcomponents and connectivity of the superior longitudinal fasciculus in the human brain. *Brain Struct Funct, 221*(4), 2075-2092. doi:10.1007/s00429-015-1028-5

Wasan, A. D., Loggia, M. L., Chen, L. Q., Napadow, V., Kong, J., & Gollub, R. L. (2011). Neural correlates of chronic low back pain measured by arterial spin labeling. *Anesthesiology, 115*(2), 364-374. doi:10.1097/ALN.0b013e318220e880

Wedeen, V. J., Hagmann, P., Tseng, W. Y., Reese, T. G., & Weisskoff, R. M. (2005). Mapping complex tissue architecture with diffusion spectrum magnetic resonance imaging. *Magn Reson Med, 54*(6), 1377-1386. doi:10.1002/mrm.20642

Wedeen, V. J., Rosene, D. L., Wang, R., Dai, G., Mortazavi, F., Hagmann, P., . . . Tseng, W. Y. (2012). The geometric structure of the brain fiber pathways. *Science, 335*(6076), 1628-1634. doi:335/6076/1628 [pii]
10.1126/science.1215280

Wedeen, V. J., Wang, R. P., Schmahmann, J. D., Benner, T., Tseng, W. Y., Dai, G., . . . de Crespigny, A. J. (2008). Diffusion spectrum magnetic resonance imaging (DSI) tractography of crossing fibers. *Neuroimage, 41*(4), 1267-1277. doi:10.1016/j.neuroimage.2008.03.036

Weinstein Stuart M, H. S., and Standaert CJ Low back pain (2005). In D. Lisa (Ed.), *Physical Medicine and Rehabilitaiton 4th ed.* New York: Lipincott Williams and Wilkins.

Weston, P. S., Simpson, I. J., Ryan, N. S., Ourselin, S., & Fox, N. C. (2015). Diffusion imaging changes in grey matter in Alzheimer's disease: a potential marker of early neurodegeneration. *Alzheimers Res Ther, 7*(1), 47. doi:10.1186/s13195-015-0132-3

Wheeler-Kingshott, C. A., & Cercignani, M. (2009). About "axial" and "radial" diffusivities. *Magn Reson Med, 61*(5), 1255-1260. doi:10.1002/mrm.21965
White, T., Nelson, M., & Lim, K. O. (2008). Diffusion tensor imaging in psychiatric disorders. *Top Magn Reson Imaging, 19*(2), 97-109. doi:10.1097/RMR.0b013e3181809f1e
Willard, F. H., Vleeming, A., Schuenke, M. D., Danneels, L., & Schleip, R. (2012). The thoracolumbar fascia: anatomy, function and clinical considerations. *Journal of Anatomy, 221*(6), 507-536. doi:Doi 10.1111/J.1469-7580.2012.01511.X
Willemen, H. L., Eijkelkamp, N., Wang, H., Dantzer, R., Dorn, G. W., 2nd, Kelley, K. W., . . . Kavelaars, A. (2010). Microglial/macrophage GRK2 determines duration of peripheral IL-1beta-induced hyperalgesia: contribution of spinal cord CX3CR1, p38 and IL-1 signaling. *Pain, 150*(3), 550-560. doi:10.1016/j.pain.2010.06.015
Williams, A. C., Eccleston, C., & Morley, S. (2012). Psychological therapies for the management of chronic pain (excluding headache) in adults. *Cochrane Database Syst Rev, 11*, Cd007407. doi:10.1002/14651858.CD007407.pub3
Woodworth, D., Mayer, E., Leu, K., Ashe-McNalley, C., Naliboff, B. D., Labus, J. S., . . . Network, M. R. (2015). Unique Microstructural Changes in the Brain Associated with Urological Chronic Pelvic Pain Syndrome (UCPPS) Revealed by Diffusion Tensor MRI, Super-Resolution Track Density Imaging, and Statistical Parameter Mapping: A MAPP Network Neuroimaging Study. *PLoS One, 10*(10), e0140250. doi:10.1371/journal.pone.0140250
Woolf, C. J. (2011). Central sensitization: implications for the diagnosis and treatment of pain. *Pain, 152*(3 Suppl), S2-15. doi:10.1016/j.pain.2010.09.030
Woolf, C. J., & Costigan, M. (1999). Transcriptional and posttranslational plasticity and the generation of inflammatory pain. *Proc Natl Acad Sci U S A, 96*(14), 7723-7730.
Woolf, C. J., & Salter, M. W. (2000). Neuronal plasticity: increasing the gain in pain. *Science, 288*(5472), 1765-1769.
Woolrich, M. W., Jbabdi, S., Patenaude, B., Chappell, M., Makni, S., Behrens, T., . . . Smith, S. M. (2009). Bayesian analysis of neuroimaging data in FSL. *Neuroimage, 45*(1 Suppl), S173-186. doi:10.1016/j.neuroimage.2008.10.055
Woolsey, C. N., & Fairman, D. (1946). Contralateral, ipsilateral, and bilateral representation of cutaneous receptors in somatic areas I and II of the cerebral cortex of pig, sheep, and other mammals. *Surgery, 19*, 684-702.
Wu, W., Liang, J., Chen, Y., Chen, A., Wu, Y., & Yang, Z. (2017). Microstructural changes are coincident with the improvement of clinical symptoms in surgically treated compressed nerve roots. *Sci Rep, 7*, 44678. doi:10.1038/srep44678
Wu, Y., Sun, D., Wang, Y., & Wang, Y. (2016). Subcomponents and Connectivity of the Inferior Fronto-Occipital Fasciculus Revealed by Diffusion Spectrum Imaging Fiber Tracking. *Front Neuroanat, 10*, 88. doi:10.3389/fnana.2016.00088
Xanthos, D. N., & Sandkuhler, J. (2014). Neurogenic neuroinflammation: inflammatory CNS reactions in response to neuronal activity. *Nat Rev Neurosci, 15*(1), 43-53. doi:10.1038/nrn3617
Xian, H., Chantarujikapong, S. I., Scherrer, J. F., Eisen, S. A., Lyons, M. J., Goldberg, J., . . . True, W. R. (2000). Genetic and environmental influences on posttraumatic

stress disorder, alcohol and drug dependence in twin pairs. *Drug Alcohol Depend, 61*(1), 95-102.

Yahia, L., Rhalmi, S., Newman, N., & Isler, M. (1992). Sensory innervation of human thoracolumbar fascia. An immunohistochemical study. *Acta Orthop Scand, 63*(2), 195-197.

Yanasak, N., & Allison, J. (2006). Use of capillaries in the construction of an MRI phantom for the assessment of diffusion tensor imaging: demonstration of performance. *Magn Reson Imaging, 24*(10), 1349-1361. doi:10.1016/j.mri.2006.08.001

Yarkoni, T., Poldrack, R. A., Nichols, T. E., Van Essen, D. C., & Wager, T. D. (2011). Large-scale automated synthesis of human functional neuroimaging data. *Nat Methods, 8*(8), 665-670. doi:10.1038/nmeth.1635

Yeh, F. C., Tang, P. F., & Tseng, W. Y. (2013). Diffusion MRI connectometry automatically reveals affected fiber pathways in individuals with chronic stroke. *Neuroimage Clin, 2*, 912-921. doi:10.1016/j.nicl.2013.06.014

Yeh, F. C., & Tseng, W. Y. (2011). NTU-90: a high angular resolution brain atlas constructed by q-space diffeomorphic reconstruction. *Neuroimage, 58*(1), 91-99. doi:10.1016/j.neuroimage.2011.06.021

Yeh, F. C., Verstynen, T. D., Wang, Y., Fernandez-Miranda, J. C., & Tseng, W. Y. (2013). Deterministic diffusion fiber tracking improved by quantitative anisotropy. *PLoS One, 8*(11), e80713. doi:10.1371/journal.pone.0080713

Yeh, F. C., Wedeen, V. J., & Tseng, W. Y. (2010). Generalized q-sampling imaging. *IEEE Trans Med Imaging, 29*(9), 1626-1635. doi:10.1109/TMI.2010.2045126

Yeh, F. C., Wedeen, V. J., & Tseng, W. Y. (2011). Estimation of fiber orientation and spin density distribution by diffusion deconvolution. *Neuroimage, 55*(3), 1054-1062. doi:10.1016/j.neuroimage.2010.11.087

Younger, J. W., Chu, L. F., D'Arcy, N. T., Trott, K. E., Jastrzab, L. E., & Mackey, S. C. (2011). Prescription opioid analgesics rapidly change the human brain. *Pain, 152*(8), 1803-1810. doi:10.1016/j.pain.2011.03.028

Yu, D., Yuan, K., Qin, W., Zhao, L., Dong, M., Liu, P., . . . Tian, J. (2013). Axonal loss of white matter in migraine without aura: a tract-based spatial statistics study. *Cephalalgia, 33*(1), 34-42. doi:10.1177/0333102412466964

Yuan, K., Qin, W., Liu, P., Zhao, L., Yu, D., Zhao, L., . . . Tian, J. (2012). Reduced fractional anisotropy of corpus callosum modulates inter-hemispheric resting state functional connectivity in migraine patients without aura. *PLoS One, 7*(9), e45476. doi:10.1371/journal.pone.0045476

Yuan, K., Qin, W., Wang, G., Zeng, F., Zhao, L., Yang, X., . . . Tian, J. (2011). Microstructure abnormalities in adolescents with internet addiction disorder. *PLoS One, 6*(6), e20708. doi:10.1371/journal.pone.0020708

Zalesky, A., Fornito, A., & Bullmore, E. T. (2010). Network-based statistic: identifying differences in brain networks. *Neuroimage, 53*(4), 1197-1207. doi:10.1016/j.neuroimage.2010.06.041

Zatorre, R. J., Fields, R. D., & Johansen-Berg, H. (2012). Plasticity in gray and white: neuroimaging changes in brain structure during learning. *Nat Neurosci, 15*(4), 528-536. doi:10.1038/nn.3045

Zerr, I., Kallenberg, K., Summers, D. M., Romero, C., Taratuto, A., Heinemann, U., . . . Sanchez-Juan, P. (2009). Updated clinical diagnostic criteria for sporadic Creutzfeldt-Jakob disease. *Brain, 132*(Pt 10), 2659-2668. doi:10.1093/brain/awp191